DTU Library

Coordinated control of wind power plants in offshore HVDC grids

Sakamuri, Jayachandra N.

Coordinated control of wind power plants in offshore HVDC grids

Jayachandra Naidu Sakamuri

March 2017

DTU Wind Energy
Department of Wind Energy

Summary:

During the recent years, there has been a significant penetration of offshore wind power into the power system and this trend is expected to continue in the future. The North Sea in Europe has higher potential for offshore wind power; therefore, the North Seas Countries' Offshore Grid initiative was formed among nine North Sea countries. They agreed on closer energy cooperation to enable development of an efficient and economic offshore grid infrastructure for integration of offshore wind energy. Due to its several advantages, interconnectors based on the voltage source converter based high voltage DC (HVDC) transmission system is being used to exchange power between different countries, and different synchronous areas. It is very likely that they will then be combined with offshore wind power plant (OWPP) connections in the North Sea, transforming it in a multi terminal DC (MTDC) grid and, therefore, in a fully meshed offshore DC grid in near future. However, increased penetration of offshore wind power into the power system poses several challenges to its security.

This thesis deals with two main research challenges, (1) Develop, and analyze the coordinated control strategies for AC voltage and reactive power control in the cluster of OWPPs connected to common offshore HVDC station, (2). Develop, analyze, and test the control strategies for ancillary services from OWPPs to the AC grid, mainly fast primary frequency control from OWPPs. Moreover, the impact of wind speed on the frequency control from OWPPs is also studied in this thesis.

The main results of this research work show that the OWPPs in the HVDC grid can participate in fast primary frequency control of the power system by using the proposed frequency control methods. Also, wind speed has a significant impact on the frequency control, particularly at below rated wind speeds. The proposed methods for AC voltage and reactive power control can improve the steady state and dynamic AC voltage profile of the offshore AC grid with cluster of OWPPs connected to common HVDC station, while minimizing the active power losses in the offshore AC grid. The research work is carried at the Technical University of Denmark (DTU) in the Department of Wind Energy and it is funded by the People Programme (Marie Curie Actions) of the EU FP7/2007-2013/ under REA grants agreement no. 317221, project title MEDOW.

DTU Wind Energy is a department of the Technical University of Denmark with a unique integration of research, education, innovation and public/private sector consulting in the field of wind energy. Our activities develop new opportunities and technology for the global and Danish exploitation of wind energy. Research focuses on key technical-scientific fields, which are central for the development, innovation and use of wind energy and provides the basis for advanced education.

DTU Wind Energy has a staff of approximately 240 and a further 35 PhD-students, spread across 38 different nationalities. The variety of research, education, innovation, testing and consultancy is reflected in the employment profile which includes faculty with research and teaching responsibilities, researchers and technical academic staff, highly skilled technicians and administrative staff.

Our facilities are situated at DTU Risø Campus and at DTU Lyngby Campus. Furthermore the department is running the national test stations in Høvsøre and Østerild.

This page would be intentionally left blank if we would not wish to inform about that.

This thesis is dedicated to:

My beloved parents,

My lovely wife, Divya,

And my daughter, Keerthisri.

This page would be intentionally left blank if we would not wish to inform about that.

Abstract

During the recent years, there has been a significant penetration of offshore wind power into the power system and this trend is expected to continue in the future. The North Sea in Europe has higher potential for offshore wind power; therefore, the North Seas Countries' Offshore Grid initiative was formed among nine North Sea countries. They agreed on closer energy cooperation to enable development of an efficient and economic offshore grid infrastructure for integration of offshore wind energy. Due to its several advantages, interconnectors based on the voltage source converter based high voltage DC (HVDC) transmission system are being used to exchange power between different countries, and different synchronous areas. It is very likely that these interconnectors will then be combined with offshore wind power plant (OWPP) connections in the North Sea, transforming to a multi terminal DC (MTDC) grid, thus a fully meshed offshore DC grid in near future. However, increased penetration of offshore wind power into the power system poses several challenges to its security.

This thesis deals with two main research challenges, (1) Develop and analyze the coordinated control strategies for AC voltage and reactive power control in the cluster of OWPPs connected to common offshore HVDC station, (2). Develop, analyze, and test the control strategies for ancillary services from OWPPs to the AC grid, mainly fast primary frequency control from OWPPs. Moreover, the impact of wind speed on the frequency control from OWPPs is also studied in this thesis.

The main results of this research work show that the OWPPs in the HVDC grid can participate in fast primary frequency control of the power system by using the proposed frequency control methods. Also, wind speed has a significant impact on the frequency control, particularly at below rated wind speeds. The proposed methods for AC voltage and reactive power control can improve the steady state and dynamic AC voltage profile of the offshore AC grid with cluster of OWPPs connected to common HVDC station, while minimizing the active power losses in the offshore AC grid.

This page would be intentionally left blank if we would not wish to inform about that.

Dansk Resume

Udbygningen af offshore vindkraft har været kraftigt stigende gennem det sidste årti, og denne udvikling forventes at fortsætte med øget styrke i fremtiden. Specielt Nordsøen er attraktiv for vindkraftudbygning med en kombination af fremragende vindforhold og forholdsvis små havdybder. Disse gode betingelser har medvirket til dannelsen af North Seas Countries' Offshore Grid Initiative (NSCOGI), som er et samarbejde mellem 9 lande om at udvikle elforbindelserne i Nordsøen. Disse udlandsforbindelser er normalt jævnstrømsforbindelser (HVDC – High Voltage Direct Current). Mens de første HVDC forbindelser benyttede den såkaldte LCC (line commutated converter) teknologi så er den mere moderne VSC (voltage source converter) teknolgi foretrukket i dag. Selv om VSC teknologien i dag anvendes til simple forbindelser mellem to lande, så er VSC teknologien velegnet til mere komplekse såkaldt multiterminale (MT) elektriske netværk som også kan anvendes til at tilslutte vindkraftværker offshore. På lang sigt tales om et formasket MT HVDC netværk som i kompleksitet minder om vekselstrømstransmissionsnettet (HVAC – High Voltage Alternating Current) på land. Et sådant formasket offshore MT HVDC netværk vil imidlertid medføre nye tekniske udfordringer for også fremover at bevare en sikker og stabil elforsyning.

Denne PhD afhandling beskæftiger sig med to forskningsmæssige udfordringer, som begge er afgørende for at sikre stabiliteten i elforsyningen. Den første udfordring handler om at udvikle en koordineret strategi for spændingsreguleringen i en klynge af flere store offshore vindkraftværker som alle er forbundet til den samme offshore HVDC station. Formålet er at undgå at hele klyngen lukker ned på grund af en fejl i offshore netværket. Den anden udfordring handler om at levere såkaldte systemydelser til HVAC nettet på land. Dette arbejde fokuserer på hvordan offshore vindkraftværker kan medvirke til at stabilisere frekvensreguleringen som er udtryk for balancen mellem produktion og forbrug.

Det vigtigste bidrag fra afhandlingen er udviklingen og verificeringen af en metode til hvordan offshore vindkraftværker forbundet til MT HVDC offshore netværk bidrager til frekvensreguleringen i de AC systemer som HVDC netværket er forbundet til. Her er der speciel fokus på mulighederne når møllerne producerer mindre end maksimum fordi vindhastigheden er under den nominelle. Et andet bidrag er den foreslåede metode til spændingsregulering i en klynge af offshore vindmølleparker. Det er vist at den foreslåede metode kan bidrage til at stabilisere spændingen og på samme tid reducere de elektriske tab i offshore netværket. PhD arbejdet er udført i Instituttet for Vindenergi på Danmarks Tekniske Universitet. Det er finansieret af MEDOW projektet kontrakt no. REA 317221, som er en del af People Programme (Marie Curie Actions) under EU FP7/2007-2013.

This page would be intentionally left blank if we would not wish to inform about that.

Acknowledgements

This thesis represents not only my work of the past three years; it also symbolizes one of my biggest achievements of my life. Many people have supported me to accomplish this.

I specially thank my thesis supervisors, Dr. Nicolaos Antonio Cutululis, Dr. Anca Daniela Hansen and Prof. Poul Ejnar Sørensen. I thank Nikos wholeheartedly, not only for his tremendous academic support, but also standing for me when I faced tough times during the past three years. I specially thank Anca for her detailed review on the articles, conference papers, and thesis. I am sure, all these publications wouldn't have possible without your review, Anca. I would like to express my special appreciation and thanks to Poul, you have been a tremendous mentor for me. Your suggestions on my yearly performance review (MUS), have helped me to shape my developing plan, Poul. I also would like to thank Jens Carsten Hansen, our head of the section, for his support and encouragement both on professional, personal, or other initiatives (guidance for graduates).

I will forever be thankful to Dr. Zakir Hussain Rather, my external unofficial thesis supervisor. I thank you, Zakir for all the weekends you spent on skype discussing voltage and reactive power control and the confidence you gave me in the form of first article of my research career. I also specially thank my mentor, Double Dr. John Yesuraj, for his guidance on my career path selection.

My special words of thanks should also go to Müfit Altin and Ömer Göksu , my unofficial thesis supervisors for providing guidance on PowerFactory simulation challenges and shaping ideas into implementations. I thank all my colleagues at Department of Wind Energy of DTU for creating the friendliest working environment. I greatly appreciate the support received through the collaborative work undertaken with Elia, KU Leuven, University of Porto, and UPC Barcelona. Thank you to Prof. Dirk, Pieter, Robert, Johan, Prof. Helder, Prof. Adriano, Prof. Oriol, Joan, Edu, and all other friends I met during my stay at these institutions.

I gratefully acknowledge the funding received for my PhD work from Marie Curie's MEDOW project and EU. I specially thank Dr. Jun Liang and Cath, for their support. I have acquired many skills (presentation, writing, research) with the help of MEDOW trainings.

I specially thank my brother, uncle and aunt for their encouragement and moral support. I thank my wife and my little one for travelling with me all these 3 years to different countries, taking the pain of packing and unpacking stuff every 3 months and supporting me in best possible ways.

This page would be intentionally left blank if we would not wish to inform about that.

Table of contents

List of Abbreviations

Abbreviation/Symbol	Definition
AC	Alternating current
ADC	Analog to Digital Converter
CAN	Controller Area Network
CC	Coordinated Control
CRPC	Coordinated Reactive Power Control Scheme
CVCS	Coordinated Voltage Control Scheme
DAC	Digital to Analog Converter
DC	Direct Current
DSP	Digital Signal Processor
EU	European Union
EWEA	European Wind Energy Association
ENTSO-E	European Network of Transmission System Operators for Electricity
FPFC	Fast Primary Frequency Control
FRT	Fault Ride Through
HVDC	High Voltage Direct Current
IGBT	Insulated Gate Bipolar Transistor
LVRT	Low Voltage Ride Through
MEDOW	Multi-Terminal DC Grid for Offshore Wind
MTDC	Multi-Terminal Direct Current
MV	Medium Voltage
NSCOGI	North Seas Countries' Offshore Grid initiative
OLTC	On Load Tap Changer

OWPP	Offshore Wind Power Plant
PCC	Point of Common Coupling
PF	Participation Factor
POC	Point of Connection
PSO	Particle Swarm Optimization
RMS	Root Mean Square
RL	Ramp Rate Limiter
ROCOF	Rate of Change of Frequency
SVC	Static Var Compensators (SVC)
TSO	Transmission System Operator
VSC	Voltage Source Converter
WPP	Wind Power Plant
WT	Wind Turbine

Chapter 1

Introduction

This chapter starts with short background knowledge on the importance and need for renewable energy generation to meet the present electrical energy demands and the motivations for offshore wind energy are presented. The challenges for integration and power transmission from offshore wind power plants to the onshore AC grid and the corresponding problem definition for this thesis are given in Section 1.2. The objectives of this thesis are given in Section 1.3. A short description of each chapter of the thesis is given in Section 1.4 followed by the related list of publications given in Section 1.5.

1.1 General Background and Motivation

Due to the depletion of fossil fuels, increased concerns for environmental impact by fossil fuels, and technology developments have encouraged the use renewable sources for electrical power production. The European Union's (EU) Renewable Energy Directive created an overall policy for the generation and promotion of energy from renewable sources in the EU [1]. According to this directive, EU targets to fulfil at least 27% of its total energy needs with renewables by 2030. This shall be achieved through the execution of individual national targets of its member countries. According to the Renewable Energy Projections as published in the National Renewable Energy Action Plans, wind energy has the potential to supply 40.6% of all renewable electricity; whereas offshore wind energy will account for 27% of the total wind energy share [2], [3], which is equal to a total of 40 GW of installed offshore wind energy throughout Europe by 2020. The European Wind Energy Association (EWEA)'s new central scenario expects 320 GW of the wind energy capacity to be installed in the EU in 2030, of which 254 GW of onshore wind and 66 GW of offshore wind [4]. To meet the EU action plan targets, The North Seas Countries' Offshore Grid initiative (NSCOGI) was formed among nine North Sea countries and agreed on closer energy cooperation to enable development of an efficient and economic offshore grid infrastructure for integration of offshore wind energy [5], [6], which also involves selection of technology to transmit offshore wind power: AC or DC.

Due to their distance from the shore and higher installed capacity, the power from the offshore wind power plants (OWPPs) in the North Sea can be transmitted to the shore using voltage source converter (VSC) based high voltage DC (HVDC) transmission systems [7]. Also, Multi-Terminal DC (MTDC) transmission system seems to be a promising solution for interconnecting offshore wind power plants with different onshore AC grids and to lay foundation for future European super grid [8],[9]. Several research projects and researchers have already focused on finding solutions for key challenges for integration of offshore wind power to MTDC grids, for example, TWENTIES, OffshoreDC, Multi-terminal DC grid for offshore wind (MEDOW), to name few projects [10]-[12].

This PhD project is a part of the research project funded by EU and it is in a consortium organized by Cardiff University with a project title MEDOW [12], which is a consortium, formed by eleven partners (five universities and six industries). MEDOW has mainly 12 key research objectives under 4 work packages:

WP1 - Connection of Offshore Wind power to DC grids

WP2 - Investigation of voltage source converters for DC grids

WP3 - Relaying protection

WP4 - Interactive AC/DC grids

One of the objectives of MEDOW is to develop coordinated control schemes for effective delivery of ancillary services from OWPPs to AC and DC grids. This has motivated to study the challenges on the control and coordination of OWPPs and MTDC grid for effective operation of the onshore AC grid. Nowadays, the trend is increasing for integrating multiple OWPPs to a common HVDC station [13]-[15], where the offshore AC grid voltage control and reactive power sharing between OWPPs are major concerns. These challenges have composed the main motivation of the present thesis:

"*Coordinated Control of Wind Power Plants in Offshore HVDC grids*"

1.2 Problem Definition

Traditionally power from OWPPs is transmitted to the main land AC grid through AC cables and the AC cable connections are normally feasible for a transmission distance up to 60 km [16]. AC transmission is not a viable option for increased transmission distance from the shore due to the higher charging current requirement because of cable capacitance which results in higher losses with AC cable. Therefore, VSC-HVDC technology becomes suitable option for grid integration of large OWPPs located far from the shore (>80 km).

The HVDC decoupling from the mainland AC grid makes the offshore AC grid weak and vulnerable to dynamical voltage events due to the limited short circuit power contribution from the HVDC converter and OWPP [17]-[19]. This leads to significant concern for voltage ride through (VRT) capability of OWPPs in the offshore AC grid. Moreover, due to the large available wind resource in the North Sea, many OWPPs are being planned in the close vicinity as clusters and are being connected and considered to be connected to a common HVDC station [13],[15]. The steady state voltage/reactive power control and dispatch strategy of the OWPP cluster connected to the offshore HVDC converter is also important as several OWPPs in close proximity may be connected to the same HVDC converter station, particularly in the growing offshore grid. This requires coordination between them for reactive power and AC voltage control between the clusters of OWPPs in the offshore AC grid.

HVDC Interconnectors to interconnect two synchronous areas are already existing today or being built and since they are, almost all, based on VSC technology. It is very likely that they will then be combined with OWPP connections, transforming it in a MTDC and, why not, in a fully meshed offshore DC grid. The increased penetration of wind power plants (WPPs) into the power system postures several challenges to its operation and stability [8], [9]. Among them, frequency control is one of the important concerns for the transmission system operators (TSOs) along with other system services, for example, fault ride through (FRT) support, reactive power and voltage control [20]. In particular, increased penetration of WPPs replacing conventional synchronous machines leads to the reduced effective inertia of the power systems and that may lead to a lower frequency nadir point, or load shedding, for a large infeed/generation loss in power systems. The primary frequency control today might be too slow for the future power system with much less inertia and then a faster response is needed, creating the need for fast primary frequency control (FPFC) [11]. Therefore, WPPs including OWPPs are required participate in frequency control to limit the frequency nadir [11] i.e. FPFC of the power system. Moreover, the impact of wind speed on the OWPPs power output and the corresponding impact on frequency control also have to be analyzed.

The primary frequency control today might be too slow for the future power system with much less inertia and then a faster response is needed, creating the need for fast primary frequency control (FPFC) [11].

Another challenge with the OWPPs in the HVDC/MTDC system is that they do not respond to the frequency events in the associated onshore AC grid due to the power electronic interfaces in the form of converters inside the WTs and HVDC transmission system. Therefore suitable methods have to be developed to make sure that onshore AC grid frequency events are available to the OWPPs controllers so that they can participate in frequency control.

Considering the above points, the attention in this thesis is directed towards two main research challenges resulted due to OWPPs integration to HVDC /MTDC transmission systems.

- Coordinated AC voltage/reactive power control in cluster of OWPPs connected through common HVDC station.

- Onshore AC grid frequency control from OWPPs in MTDC grid: Methods for frequency control, Impact of wind speed on the frequency control.

The state of art of the above two research problems is given in later chapters.

1.3 Thesis Objectives and Limitations

The main objectives of this PhD work can be described as:

- To better understand the AC voltage and reactive power control in the offshore AC grid with the cluster of OWPPs connected to common offshore VSC-HVDC station, and study the reactive power contribution from WTs within the cluster for symmetrical faults at different locations of the offshore AC grid.

- To develop coordinated control schemes for reactive power and AC voltage control in the offshore AC grid composed of cluster of OWPPs connected to common offshore VSC-HVDC station to improve the steady state and dynamical performance of the offshore AC grid.

- To analyze the different methods for frequency control from OWPPs connected through MTDC grids, with and without depending on the communication channels to replicate the onshore AC grid frequency events at offshore AC grid. To study other possible active power balance control services from OWPPs to AC and DC grids (DC voltage control, fault ride through support)

- To study the impact of wind speed on the OWPPs active power output and the corresponding impact on frequency control from OWPPs in MTDC grid.

- To demonstrate the proof of concept of frequency control methods for OWPPs in MTDC grid and the impact of wind speed on the frequency control using a laboratory scaled 3-terminal DC grid test set up.

The main limitations of the study are:

- The study is focused on using root-mean-square (RMS) simulation models; therefore the electromagnetic transient phenomena are discarded.

- Only impact of symmetrical faults in the offshore AC grid is considered. The asymmetrical faults and their impact on the offshore AC grid voltage profile and on the coordinated voltage control schemes are not considered.

- In the laboratory scaled DC grid platform, only simulation model for OWPP is considered for the study instead of prototype OWPP/WT implementation.

- The protection issues related to HVDC converters and WPPs are not considered in this thesis. For FRT study, only the control of DC choppers is being considered.

1.4 Thesis Outline

This thesis is written based on the collection of papers given in section 1.5 and is organized as 7 chapters as given below.

- Chapter 1 provides a General background and motivation for the study, problem definition and objectives of thesis, and list of the publications related to the study.

- Chapter 2 presents the three different methods for reactive power and AC voltage in the offshore AC grid with cluster of OWPPs connected to common in HVDC station control are proposed. The three methods are voltage control with a droop, coordinated reactive power control scheme, and coordinated voltage control scheme. These three methods are compared and the suitable best method is proposed based on steady state and dynamic performances.

- The kinetic energy of the WTs in the OWPPs is used to provide active power support for frequency control. Different possible methods for WT overloading to extract kinetic energy are discussed in Chapter 3. The results from this chapter are used as an input for active power balance control from OWPPs discussed in Chapter 4 and 5.

- The active power control from OWPPs in MTDC grid to provide ancillary services for AC grid (frequency control and FRT support) and DC grid (DC voltage control) is the topic of discussion in Chapter 4. The two methods for frequency control from OWPPs (communication based and coordinated frequency control) are presented and the impacts of wind speed on the frequency control are also discussed.

- Chapter 5 describes the laboratory scaled 3-terminal DC grid test set up. The comparisons between the two frequency control methods are made with the help of time domain simulations using DIgSILENT PowerFactory and the corresponding experimental validations. The impact of wind speed on the frequency control is also verified experimentally.

- Chapter 6 presents the overall contributions of this thesis by mentioning the contribution of each technical paper related to this thesis.

- Finally, Chapter 7 summarizes the conclusions of this study and highlights the potential future work.

1.5 List of Publications

The following lists of conference and journal publications are the major contributions to make this report. These papers are included in the appendices and are referenced at appropriate places in the report as needed.

Journal Publications:

J1 Ömer Göksu, Jayachandra N. Sakamuri, C. Andrea Rapp, Poul Sørensen, Kamran Sharifabadi, "Cluster Control of Offshore Wind Power Plants Connected to a Common HVDC Station", Energy Procedia, Volume 94, Sep 2016, Pages 232-240, ISSN 1876-6102

J2 Jayachandra N. Sakamuri. Rather Z.H., Cutululis N.A., Rimez J., "Coordinated Voltage Control in Offshore HVDC Connected Cluster of Wind Power Plants ", *IEEE Trans. on Sustainable Energy*, vol.7, pp.1592-1601, Oct 2016.

J3 Jayachandra N. Sakamuri., Altin M, Hansen A.D., Cutululis N.A., "Coordinated Frequency Control from Offshore Wind Power Plants Connected to multi terminal DC System Considering Wind Speed Variation ", *IET Rene. Power Generation, Special Issue: Active Power Control of Renewable Energy Generation Systems,* Available Online Aug 2016

J4 Jayachandra N. Sakamuri, Joan Sau, Eduardo Prieto, Oriol Gomis, Altin M, Hansen A.D., Cutululis N.A., "Experimental Validation of Frequency Control from Offshore Wind Power Plants in Multi Terminal DC Grid", *Under Review at CIGRE Science & Engineering*.

J5 Jayachandra N. Sakamuri, Joan Sau, Eduardo Prieto, Oriol Gomis, Altin M, Hansen A.D., Cutululis N.A., "Impact of Release of OWPP Kinetic Energy Support on DC voltage in MTDC Grids", *Under Review at IEEE Trans of Power Delivery*.

Conference Publications:

C1 Jayachandra N. Sakamuri, Rather Z.H., Cutululis N.A., Rimez J., "Dynamic Reactive Power Control in Offshore HVDC Connected Wind Power Plants ", *Proc.t 14th Wind Integration Workshop*, Brussels, 2015.

C2 Jayachandra N. Sakamuri, Rather Z.H., Cutululis N.A., Rimez J., "A New Coordinated Voltage Control Scheme for Offshore AC Grid of HVDC Connected Offshore Wind Power Plants ", *Proc. CIGRE Canada Conference*, Winnipeg, Canada, 2015.

C3 Jayachandra N. Sakamuri, Das K, Altin M., Hansen A.D., Cutululis N.A., Tielens P. Dirk Van Herterm, "Improved Frequency Control from Wind Power Plants Considering Wind Speed Variation", *Proc. 19th Power System Computation Conference*, Genoa, Italy, 2016.

C4 Jayachandra N. Sakamuri., Hansen A.D., Cutululis N.A., Altin M., Sørensen P.E., "Coordinated Fast Primary Frequency Control from Offshore Wind Power Plants in MTDC System ", *Proc. IEEE Energycon Conference*, Leuven, Belgium, 2016

C5 Jayachandra N. Sakamuri, Altin M, Hansen A.D., Cutululis N.A., Rather Z.H.,, "Coordinated Control Scheme for Ancillary Services from Offshore Wind Power Plants to AC and DC Grids ", *Proc. IEEE PES General Meeting 2016*. (selected as best conference paper)

C6 Jayachandra N. Sakamuri, Joan Sau, Eduardo Prieto, Oriol Gomis, Altin M, Hansen A.D., Cutululis N.A., "Suitable Method of Overloading for Fast Primary Frequency Control from Offshore Wind Power Plants in Multi-Terminal DC Grid", *Accepted for IEEE PowerTech Conference*

This page would be intentionally left blank if we would not wish to inform about that.

Chapter 2
Reactive Power and Voltage Control in Cluster of OWPPs

In this chapter, the main results for the first research topic in this PhD project i.e. the reactive power and AC voltage control in the cluster of OWPPs connected to common HVDC station are presented. The results pertaining to this chapter have been published in the papers C1, C2, J1, and J2, included in the appendices. The chapter begins with short back ground knowledge and motivation for reactive power and voltage control in OWPPs. In section 2.2, a voltage control method for the cluster of OWPPs with reactive power sharing based on droop control is presented and the corresponding details are documented in paper J1. In section 2.3, a coordinated reactive power control scheme for the cluster of OWPPs is presented with the corresponding details of investigation presented in paper C1. Finally, the coordinated voltage control scheme with reactive power sharing between clusters of OWPPs based on participation factors is presented in section 2.4, whose details are given in papers J2 and C2.

2.1 Motivation and State of the Art

Traditionally, in case of WPPs connected to AC grid, the transmission system operators (TSOs) sends active/reactive power reference to the wind power plant operators, where they are further dispatched to WPPs and their wind turbines (WT) [23]-[25]. The generic reactive power control part of the WPP and WT control is shown in Fig. 2.1. In steady state conditions, WPPs and WTs operate in one of the three modes; (1) reactive power control, (2) voltage control, and (3) power factor control. During transient conditions, particularly during and after faults, the WTs have to fulfill the low voltage ride through (LVRT) requirement and inject the reactive current into the electrical network [26]-[31]. This is achieved by incorporating additional LVRT controls at WT level as shown in Fig.2.1, which generate dynamic reactive current reference based on the voltage measurement at WT terminals. It is well proven by many researchers [32]-[33] that the WPPs having WTs equipped with power electronic converters, i.e. Type 3 and Type 4 can control the reactive power/voltage during normal operation and also meet the LVRT

requirements. Moreover, the WPPs are also equipped with different reactive power or voltage regulation devices, such as fixed capacitor, shunt reactors, static Var compensators (SVCs), on load tap changing (OLTC) transformers, to meet the required grid codes [27],[29]-[31].
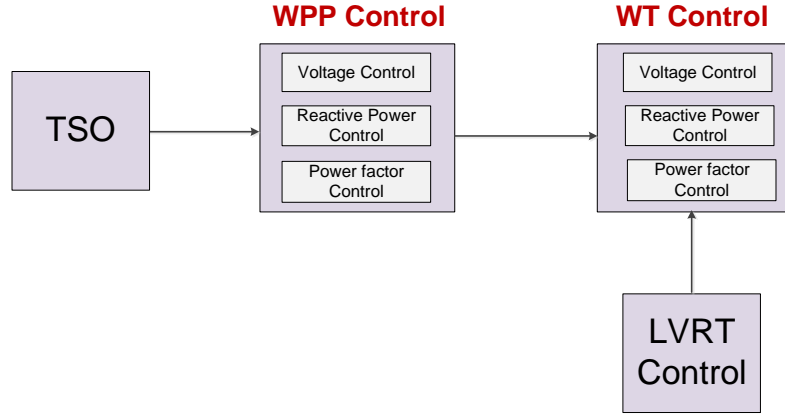
Fig. 2.1 Generic reactive power control structure for WPP and WTs

For the connection of large OWPPs, over long distances from the shore, to the onshore power system, HVDC technology seems to be feasible option [35]. In many cases, multiple OWPPs are being connected to same offshore HVDC station as a cluster; for instance, the offshore grid of Dolwin-1 consists of Borkum Riffgrund 1, Trianel wind farm Borkum, and Merkur offshore wind farm with 800 MW of total capacity [13]. The Borkum Riffgrund WPP is of 277 MW and 11.4 km from the Dolwin-Alpha collector substation, whereas Trianel wind farm Borkum is 200 MW, 7.3 km and Merkur offshore wind farm is 400 MW, 13 km, respectively [13]. However, the decoupling between OWPPs and mainland AC grid because of HVDC interface makes the offshore grid weak and vulnerable to dynamic voltage events due to lower short circuit power contribution from the power electronic interfaced variable speed WTs and HVDC converter [18]. Even though the offshore HVDC converter controls the voltage at its terminals, due its limited capacity, it is necessary that the OWPPs also control the reactive power/voltage at their terminal [19]. Moreover, coordination among OWPPs is needed for effective utilization of reactive power capacity of WPPs and for efficient sharing of reactive power within the cluster so as to minimize active power losses in the offshore AC grid. Also, coordination between the WPPs is required to improve offshore AC grid dynamic voltage profile in case of faults within the offshore AC network.

Three different coordinated reactive power/voltage control methods for the cluster of OWPPs connected to common HVDC station for efficient operation of the offshore AC grid are proposed and developed in this PhD work as given below and explained in the subsequent sections of this chapter.

10

- o   Voltage control with a droop for sharing of reactive power

- o   Coordinated reactive power control scheme

- o   Coordinated voltage control scheme

In this work, IEC type-4 WTs (full scale power converter based variable speed WTs) are considered for simulation [36].

2.2 *Voltage Control with a Droop for Sharing of Reactive Power*

In this method, each OWPP in the cluster operates in voltage control mode, but its voltage reference is modulated according to the measured reactive power flow at its terminal using a droop, similar to the governor droop for sharing of active power support among synchronous generators for frequency control. The details of the proposed method are given in paper [J1] in the Appendix.

2.2.1   *Power System Model under Study*

Fig. 2.2 depicts the benchmark layout for the power system model where a two terminal HVDC link with three OWPPs (A- 400 MW, B- 400 MW, and C- 200 MW) is connected to common offshore HVDC station. Each WPP is represented as aggregated single WTs [37], since the focus of the study is limited to reactive power sharing between WPPs and excludes internal dynamics between the WTs in the WPPs. In this work, WT is modeled according to the electrical simulation models for WT given in IEC 61400-27-1[36]. The main role of offshore HVDC station is to exchange the power generated by OWPPs to the DC grid by controlling the AC voltage and frequency. In this work, the offshore HVDC station is modeled as a VSC with constant DC voltage; acting thus as an ideal voltage source. The onshore HVDC terminal and DC link is not modelled since the focus of the study is coordination of reactive power between the OWPPs within the cluster.
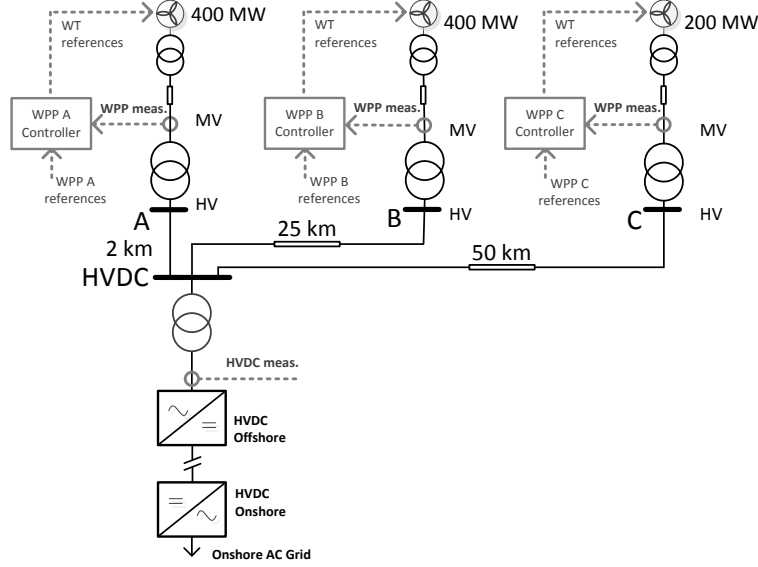
Fig. 2.2 Benchmark layout of cluster of 3 OWPPs connected to common HVDC station

2.2.2 Voltage Control with a Droop Method

The proposed voltage control with a droop for the cluster of OWPPs is inspired from the coordinated reactive power and voltage control for a multi machine power plant proposed in [38], where the bus bar voltage is regulated by coordinating the reactive power outputs of participating synchronous generators. The voltage control method for the cluster of OWPPs is developed in this work based on [38]. The simplified block diagram of the proposed voltage control part of the WPP and WT is shown in Fig. 2.3. Please refer section 3 of paper [J1] for further details. The initial voltage references to the WPP and WT are generated based on the load flow calculation. In normal condition, the WTs inside the WPP receives the voltage reference from the corresponding WPP controller by controlling the voltage at medium voltage (MV) side of WPP transformer, as depicted in Fig. 2.1. The WPPs within the cluster share the reactive power according to their voltage droop gain (k_{qdroop}). Each WPP controller modifies its voltage reference (V_{ref}^{wpp}) according to the measured reactive power (Q_{meas}^{wpp}) at its terminals and the corresponding voltage droop gain (k_{qdroop}) as given in (1).

$$V_{ref}^{wpp} = V_{set}^{wpp} - Q_{meas}^{wpp} k_{qdroop} \tag{1}$$
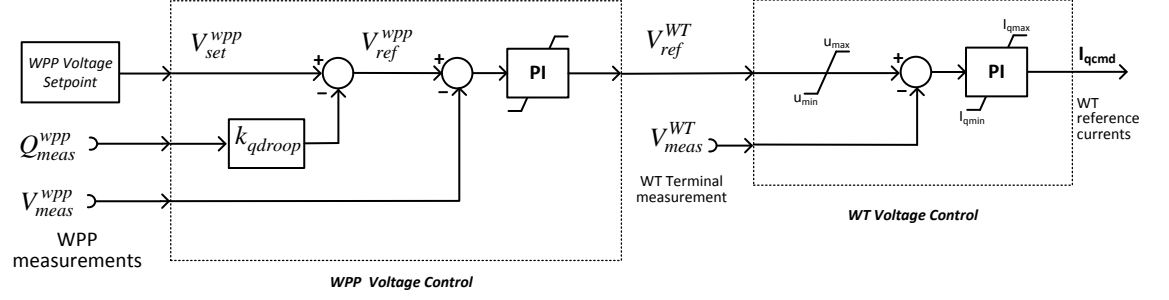
Fig. 2.3 Simplified block diagram for WT and WPP voltage controller.

2.2.3 Analysis of Simulation Results for Voltage Control with a Droop

The reactive power dispatch within the WPP cluster with respect to their active power output for the two study cases; (1) without voltage droop (2) with voltage droop is shown in Fig. 2.4. The results shows that droop ensures harmonized reactive power sharing between WPPs (A, B, C in Fig. 2.4) and HVDC converters for the full range of active power output of WPPs. Please refer section 4 of paper [J1] for more details on the results.
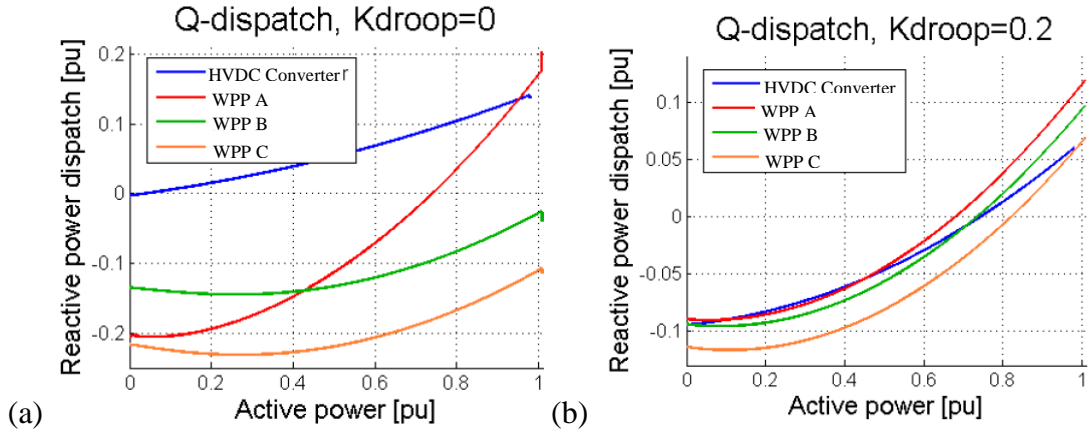
Fig. 2.4 (a) Reactive power flow without droop (b) Reactive power flow with droop

2.2.4 Conclusions on Voltage Control with a Droop Method

The proposed method ensures harmonized reactive power sharing between WPPs in cluster without depending on communication. In this work, the WPP is modeled as single aggregated WT, without a detailed layout of WPPs. The selection of voltage droop value has been done arbitrary, however, in a potential future work it could be furthermore selected based on an optimization algorithm aiming for minimum losses /cost as an objective function.

2.3 Coordinated Reactive Power Control Scheme

An overview of possible combinations of reactive power and voltage control for AC grid connected WPPs and WTs are given in [39]. However, there is no published research on the

13

reactive power control in the cluster of OWPPs connected to common HVDC station. Therefore, a coordinated reactive power control (CRPC) in a cluster of OWPPs is presented in this section. This method is applied to a cluster of four OWPPs, each with 200 MW and total capacity of 800 MW, connected to common offshore HVDC station, as shown in Fig. 2.5. Each 200 MW WPP is comprised of four parallel WT strings. Each string is of 50 MW capacities, with each string that consists of 8 series connected 6.25 MW WTs. Though a detailed modelling of WPP can provide more insight into the system, its consideration however, increases the computational burden. Hence, one string of the WPP-A1B1 is modelled in detail and the rest of the WPPs are represented by aggregated models without compromising the accuracy of results. A WT collector cable (8 machines, 50 MW total capacity) in WPP-A1B,1 in Fig. 2.5, is modeled in detail and the remaining WTs of the same WPP are represented by an aggregated 50MW model for the A1 (9-16) feeder and an 100 MW model for the B1 (1-16) feeders according to [37]. The rest of the WPPs are aggregated with each having 100 MW capacity. The proposed model complexity is sufficient to study the response of WTs within collector cable and WPP for the symmetrical faults at WT terminal, collector cable, and export cable. In CRPC method, the reactive power reference to the cluster is defined based on an optimization algorithm aiming at minimum active power losses in the offshore AC grid, considering the different operating points of the WPPs. The reactive power references to each WPP within the cluster and to each WT in a WPP are dispatched according to their available reactive power margin. Using the proposed method, the response of the WTs in different WPPs and their reactive power contribution for the symmetrical faults at different locations of the offshore grid is studied. In the following, a short summary of the findings is presented, while the method and the results are explained in detail in paper [C1]. A brief description of test system, the proposed CRPC scheme, and discussion on simulation results are given in the following sub sections.

The detailed model of the two terminal HVDC link with the cluster of four OWPPs is given in section II of paper [C1]. The main role of onshore HVDC converter is to maintain the power balance in the DC link by controlling the DC voltage at it terminals and also controls reactive power or AC voltage at its terminals. The offshore HVDC converter transfers the power generated by OWPPs cluster to the DC link by controlling the AC voltage and frequency at its terminals.
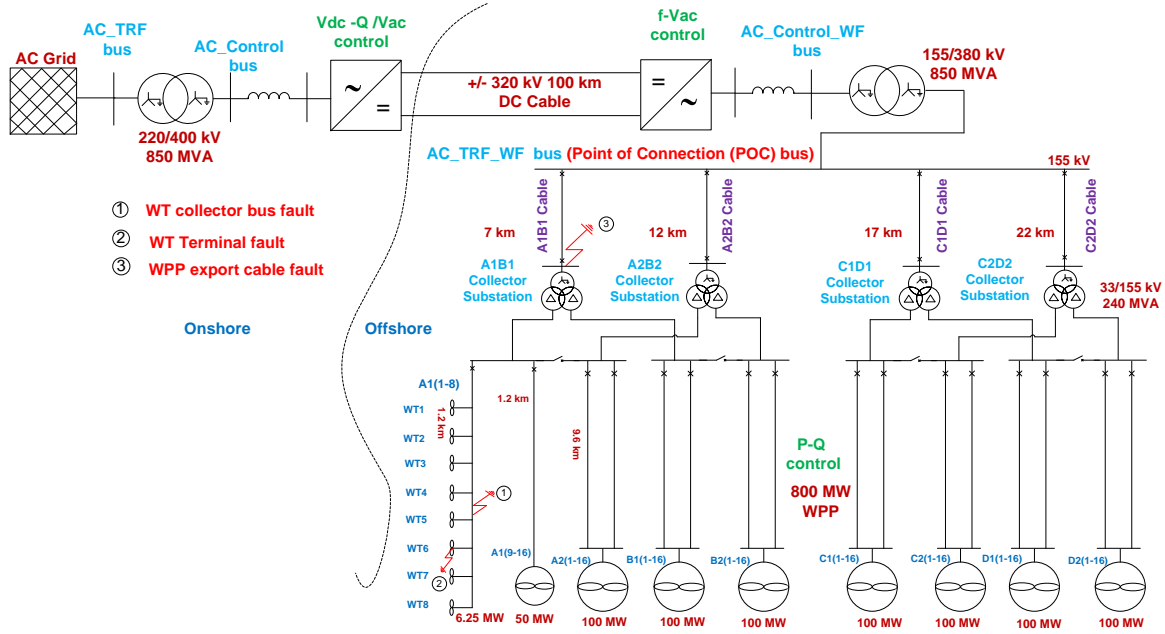
Fig. 2.5 Offshore HVDC connected cluster of WPPs

2.3.1 *Proposed Coordinated Reactive Power Control Scheme.*

The detailed description of the proposed CRPC scheme is given in section III of paper [C1] and only briefly presented here, as shown in Fig. 2.6. It consists of three control levels; (1) Cluster control (2) WPP control, and (3) WT Control. The cluster controller generates the reactive power references to each WPP within the cluster by controlling the reactive power at point of connection (POC) for WPP cluster (see Fig. 2.5). The reference at POC is generated by an optimization algorithm aiming at minimum active power losses in the offshore AC grid at all wind speeds, as explained in section III.A of the paper [C1]. Each WPP within the cluster controls the reactive power at its terminals and dispatches the reactive power or voltage reference to WTs within the respective WPP based on their available reactive power margin. The 'WPP AC Voltage Droop Controller' of the WPP controller ensures sharing of reactive power within the cluster in case of loss of communication with the cluster controller. This droop controller also helps controlling the reactive power in case of disturbances in the offshore AC grid so as to improve the dynamic performance. The 'WT VRT Controller' generates additional reactive current reference when the voltage at WT terminals deviates from its dead band so as to improve the dynamic voltage profile, in case of faults within the offshore AC grid.
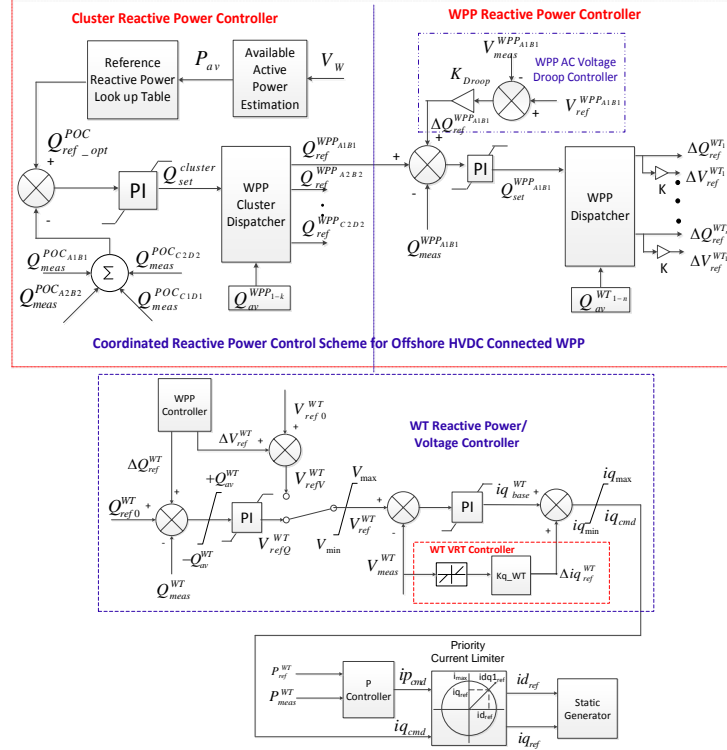
Fig. 2.6 Coordinated reactive power control scheme for cluster of OWPPs

2.3.2 Analysis of Simulation Results for CRPC Scheme.

The proposed CRPC scheme for the cluster of OWPPs has been validated in simulations on the test system given in Fig. 2.5. The voltage profile of the offshore AC grid and the reactive power output of the WTs are investigated for symmetrical faults in the offshore AC grid depicted in Fig. 2.5:

   (1) Collector cable fault

   (2) WT terminal fault

   (3) Export cable fault

The corresponding simulation results are given in section IV of the paper C1. From these results, also illustrated in Fig. 2.7, it can be observed that, in steady state conditions, the proposed CRPC ensures reactive power control in the offshore AC grid and sharing among the WPP by dispatching the references to the WTs as per their available reactive powers. In case of faults inside the offshore grid, the WTs generate additional reactive power if the voltage at their terminals violates the deadband limits (10% in this case). For collector cable fault at WTA1(5) depicted in Fig. 2.5, the voltage profile of the WTs under the faulted cable and faulted WPP

16

violates the deadband as shown in Fig. 2.7, therefore they only contribute to the fault by providing reactive power. However, it is observed that there is a scope to utilize the available reactive power margin of the WTs under the non- faulted WPPs to improve the voltage of the offshore AC grid. This can be achieved by the coordinated voltage control scheme, explained in the next section.

For fault at WT terminal , the WTs in that string only violate the allowed voltage deadband and the voltage profile of the offshore grid does not get affected, therefor the WTs under faulted WPP only provides additional reactive power during the fault. For export cable fault at one of the WPP, voltage of the offshore AC grid gets affected; therefore, all the WTs under the cluster contribute maximum possible reactive power to improve the voltage profile.
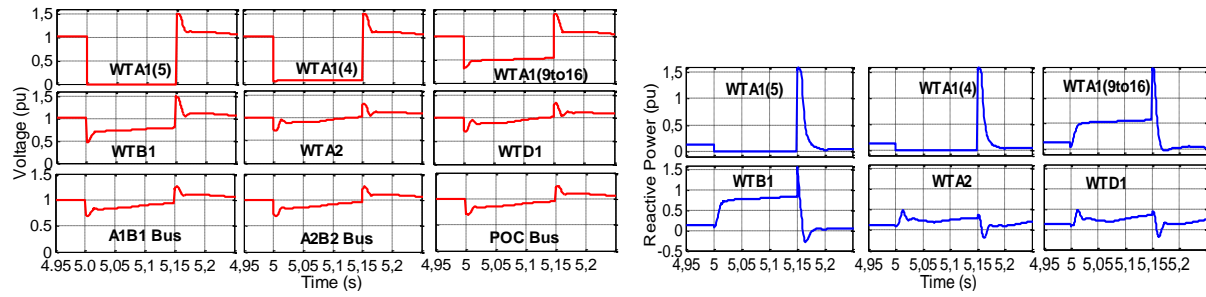
Fig. 2.7 .Collector cable fault at WTA1 (5) (a) Voltage at WT terminals and WP (b) Reactive Power at WT terminals

2.3.3 Conclusions on CRPC Scheme.

In this work, the elaborated model of the cluster of four OWPPs connected to common HVDC station is considered for the study. The effect of faults within one WPP on the other non-faulted WPPs and the offshore AC grid has been investigated. The CRPC scheme comprehends an optimization algorithm aiming for minimum active power losses which generate the reactive power reference at cluster level. The proposed CRPC scheme ensures better reactive power sharing between the WPPs in the cluster compared to the voltage control with a droop method because the dispatch is based on the WPP's available reactive power. However, this method may lead to over voltages at the WTs located far away from the collector substation, i.e. those lying at the end of collector cable, especially if equal reactive power references are sent to all the WTs in a collector cable. The dependency on communication for reactive power dispatch may impact the overall reliability of the CRPC scheme. The AC voltage droop controller at WPP control helps the sharing of reactive power between the WPPs, similar to the voltage control with a droop method explained in section 2.2, in case of loss of communication with the cluster controller.

2.4 Coordinated Voltage Control Scheme

The CRPC scheme, explained in last section is an effective method for reactive power control within the cluster of WPPs in the offshore AC grid. However, AC voltage control may be preferred over reactive power control for the offshore WPPs, due to the limited reactive power capacity of the offshore HVDC converter to control the AC voltage and weak grid nature of the offshore grid [19]. In case of faults/disturbances in the offshore AC grid, the WTs should supply the reactive power during and after the faults. However, as showed in the previous section, with CRPC the WTs in the non-faulted WPPs are not effectively utilized to provide dynamic reactive power support in order to improve the voltage profile of offshore AC grid. Also, an effective reactive power dispatch strategy is needed for the WTs in a WPP to avoid higher voltages at their terminals. To address these challenges, a coordinated voltage control scheme (CVCS) is proposed, which is initially described in paper [C2] and extended in paper [J2]. In this section, a brief description of CVCS and few important results are given.

The same cluster of four OWPPs layout, shown in Fig. 2.5, is used for the simulations. The onshore and offshore HVDC converters control is similar to what was explained in section 2.3.1. The only difference is the method of control of OWPP cluster, which is explained in next section.

2.4.1 Proposed Coordinated Voltage Control Scheme.

In traditional AC power system, for effective voltage control, AC buses with strong voltage coupling are grouped together to form a single voltage control zone [40]-[42]. Voltage control zones should be sufficiently decoupled from one another, each zone having sufficient reactive power resources to control the voltage within its boundaries with minimal reactive power influence from other neighboring voltage control zones. A secondary voltage controller is established for each zone which controls the voltage at one particular bus within that zone called Pilot bus and sends reference to the reactive power sources in that zone [42]. Since all the buses of a given zone are strongly coupled, the voltage profile of this zone can be smoothly maintained by controlling the voltage at the Pilot bus, hence reducing the control problem complexity. The Pilot bus can be selected on various factors such as its electrical distance based centrality, or having the highest short circuit capacity, or in some cases a selected load bus.

In this work, the Pilot bus concept, inherited from the control of mainland AC grid, is applied to the control of cluster OWPPs connected to the common HVDC station in the offshore AC grid. The Pilot bus is selected as the bus with highest short circuit capacity in the offshore AC grid. A complete short circuit analysis of the offshore AC grid has been carried out and the 155 KV bus (AC_TRF_WF), in Fig. 2.5, was identified as the bus with the highest short circuit capacity, hence, selected as Pilot bus for this study. Also, additional controls to enhance the voltage ride

18

through (VRT) capability of offshore AC grid by effectively utilizing the reactive power capability of the WTs in the cluster is also incorporated in this scheme. The schematic of the proposed CVCS for the cluster of OWPPs is given in Fig. 2.8. Section III of paper [J2] contains a detailed description of the proposed CVCS.
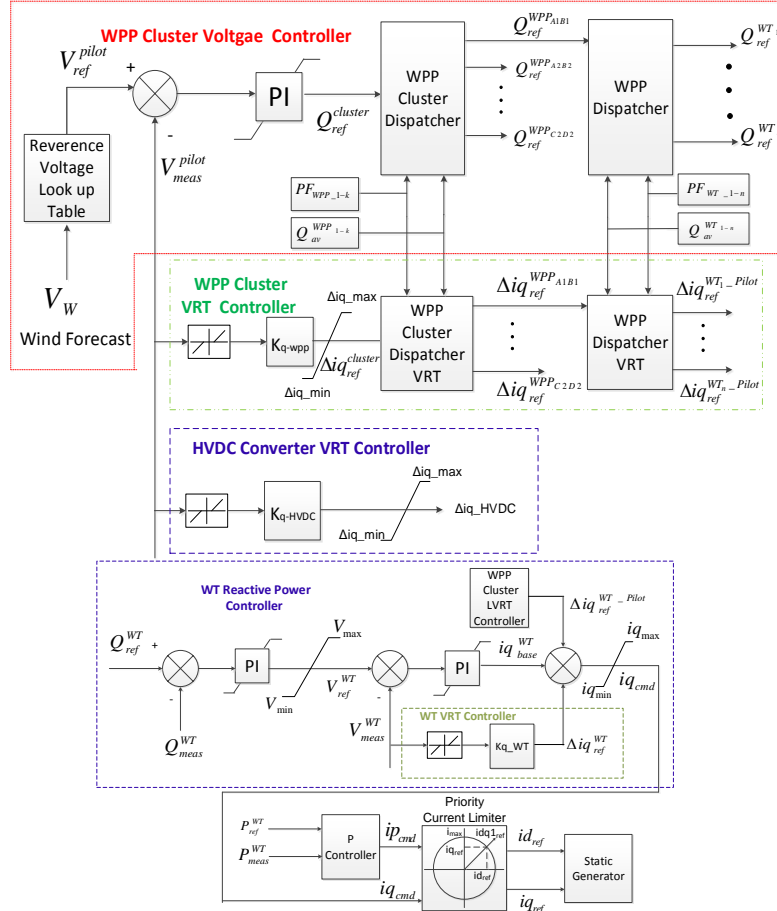
Fig. 2.8 Coordinated Voltage Control Scheme for the cluster of OWPPs

The proposed CVCS have mainly two control levels (1) Cluster voltage control (2) WT reactive power control. The primary control point of the cluster voltage control is at the Pilot bus. The voltage reference at the Pilot bus is generated by an optimization algorithm aimed at minimizing the active power losses in the offshore AC grid. During steady state conditions, the reactive power references to the WTs are dispatched, starting from the WPP cluster level and down according to their available reactive power margin and network sensitivity based participation factors (PFs), which are derived from the dV/dQ sensitivity of a WT bus w.r.t the Pilot bus. This method leads to minimization of the risk of undesired effects, particularly overvoltage at the terminals of the WT located far away from the AC collector substation, by dispatching lower reactive power references compared to the ones nearer to the substation. In addition, the cluster voltage controller includes a control strategy for improved voltage ride

through capability of WTs for faults in the offshore grid, thus leading to improved dynamic voltage profile in the offshore AC grid. The WT reactive power controller controls the reactive power reference received from the cluster voltage controller. It also incorporates the VRT controller at WT which generates additional reactive power for faults in the offshore grid based on the terminal voltage measurement.

2.4.2 *Analysis of Simulation Results for CVCS.*

A set of simulations performed on the test system, shown in Fig. 2.5, for steady state and dynamical events are well explained in section IV of paper [J2] and [C2]. The highlights of the results are given in this section. Active power losses in the offshore grid with and without CVCS are shown in Fig. 2.9. In the latter (without CVCS) it is assumed that each WPP is in voltage control mode controlling voltage at the low voltage side of the transformer at the WPP collector substation, while WTs are in reactive power control. It can be observed from Fig. 2.9 that losses are relatively low with the proposed CVCS with more visible difference for higher output power from the WPP cluster.
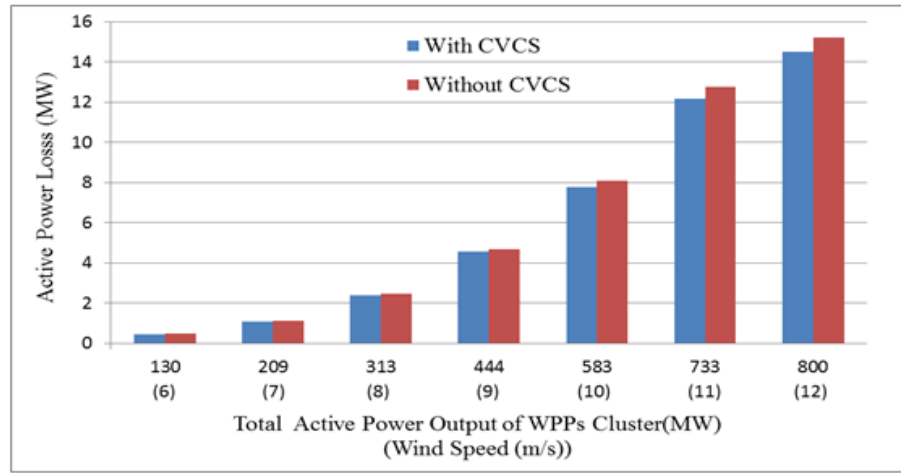
Fig. 2.9 Active power loss Vs active power output of WPP cluster

The reactive power output and voltage profile at the terminals WTA1 (1-8) under WPP A1B1, illustrated in Fig. 2.5, are given in Fig. 2.10, for reactive power dispatch within the WPP (1) with and (2) without considering participation factors. It can be observed that participation factors ensure lesser reactive power contribution from the WTs farther from the collector substation (WTA1 (8)) compared to the closer ones (WTA1 (1)); hence, the voltage at terminals of WTA1 (8) is less compared to the case without taking into account the participation factors. Thus, use of participation factors increases the effectiveness and efficiency of the proposed CVCS.
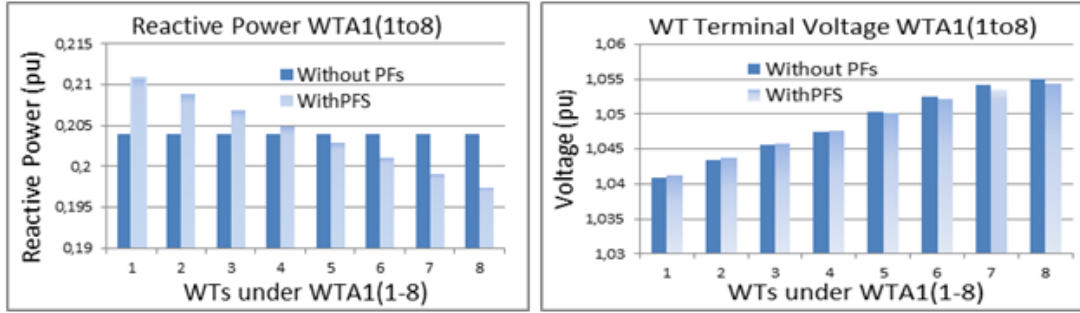
Fig. 2.10 Impact of participation factors on: (a). Reactive power (b). Terminal Voltage of WTs

The voltage of the Pilot bus for a symmetrical fault at collector cable near WTA1 (5) under WPP-A1B1 is given in Fig. 2.11. It shows the Pilot bus voltage for the following cases: (a) voltage control at WT alone (b) voltage control at WPP and WT level (c) proposed CVCS. It can be observed that the voltage profile is better with the proposed CVCS during the fault and also after the fault clearance compared to other traditional control methods. This is achieved by utilizing the reactive power capability of WTs under non-faulted WPPs.
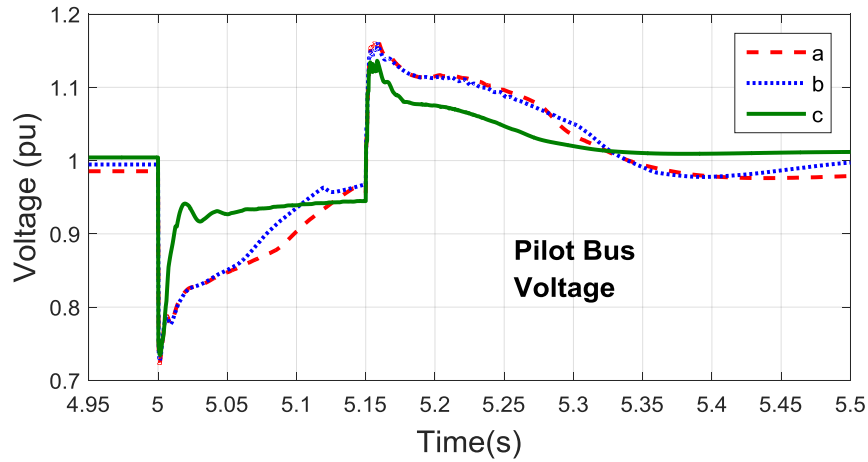
Fig. 211 Pilot bus voltage for collector cable fault at WTA1 (5)
a) voltage control at WT alone, b) voltage control at WT and WPP, c) proposed CVCS

2.4.3 Conclusions on Coordinated Voltage Control Scheme.

The proposed coordinated voltage control scheme for the cluster of offshore wind power plants improves the steady state and dynamic voltage profile of the offshore AC grid. This method has only two control levels for the cluster providing lesser control complexity than the coordinated reactive power control scheme. Reactive power distribution within the cluster based on network voltage sensitivity based participation factors avoids excessive voltage rise at WTs located far from the AC collector substation. It has also been shown that the proposed coordinated voltage control scheme improves the voltage stability margin of the offshore AC grid. However, the proposed method requires very fast and reliable communication within the offshore AC grid.

2.5 Chapter Conclusions

In this chapter, three new possible control methods for AC voltage and reactive power control in the cluster of offshore wind power plants connected to common HVDC station have been presented. Compared to other proposed methods, the voltage control with a droop method does not depend on communication infrastructure and ensures automatic sharing of reactive power among the WPPs according to their droops. The coordinated reactive power control scheme ensures optimized active power losses in the offshore AC grid by dispatching reactive power set-points to the WTs according to their available reactive power margin. Finally, the coordinated voltage control scheme uses the Pilot bus voltage control concept in an offshore wind power cluster environment, augmented by a reference point dispatch based on participation factors. Compared to the first two proposed and developed methods, coordinated voltage control scheme provides better steady state and dynamic voltage control and has less control complexity. Furthermore, reactive power dispatch based on participation factors relieves the risk of higher voltages at the WTs located away from the AC collector substation, making the coordinated voltage control scheme superior than the other two methods.

Chapter 3
Wind Turbine Overloading Methods for Frequency Control

In this chapter, two different WT overloading methods, for fast primary frequency control (FPFC) of the power system, are presented. The details of FPFC from OWPPs are presented in detail in chapter 4. The results in this chapter in the form of overloading the WTs for FPFC serves as inputs for the frequency control studies performed in chapter 4. The results pertaining to this chapter have been published in the papers C3, and J3, included in the appendices of this report. The results from this chapter serve as an input to fast frequency control from OWPPs in MTDC system. The chapter begins with motivation for the WT overloading to participate in frequency control. Two possible overloading methods are explained, whose details are elaborated in papers C3 and J3. Finally, different options for release of WT overload are discussed and the corresponding details are given in paper J3.

3.1 Motivation and state-of-the-art

Power system needs to balance the power production and the power consumption. If this balance is not maintained, it can lead to load shedding, generation trips, and eventually blackouts if there is a failure in preventing large frequency excursions [43]. Frequency is the global indicator of the system power balance and frequency control is one of the significant ancillary services in a power system. Traditionally, most of the transmission system operators (TSOs) use a two- or three-level frequency control strategy, categorized as primary control, secondary control and tertiary control according to UCTE operation handbook [20] as shown in Fig. 3.1. Among them, primary frequency control is the fastest, where the reserves start acting after few seconds (5 to 30s depending on grid code) of the frequency event. The secondary control reacts slower than primary control and brings the system frequency to the nominal frequency. Final the tertiary control replaces the secondary control reserves. The time frames for these controls are different for different grid codes. Apart from these frequency control strategies, synchronous machines natural inertia limits the rate of change of frequency (ROCOF) of the power system.

Traditionally synchronous generators offer inertia to the power system. Increased penetration of modern wind power into power system by replacing the conventional power from synchronous generators leads to reducing the system inertia due to the power electronic interfaces inside the WTs. This can result in higher ROCOF and thus leads to lower frequency nadir following a large contingency [44], [47]. In the past years, several research studies have focused on the control strategies to limit the frequency nadir by providing synthetic inertia from the WPPs [48]-[56], or fast primary frequency control as it is alternatively called by TSOs and in some research studies.[57]-[59]. Two methods to provide active power support for fast primary frequency control from WPPs are typically used [60], [62]. In first method, the wind turbines do operate in down regulation/deloaded mode, where they do not supply the maximum available power in normal conditions, so that some power margin available for frequency control [60]. Alternatively, the wind turbines can be overloaded above their maximum available power for certain duration (few seconds) utilizing the kinetic energy from the WT rotating mass [62]. However, such overloading method leads to reduction in the WT speed. Once the overload is released, the power output will drop until the WT reaches a new energy balance, particularly at below rated wind speeds. In this work, overloading option is chosen to provide active power support for fast primary frequency control and two different methods for WT overloading are presented.
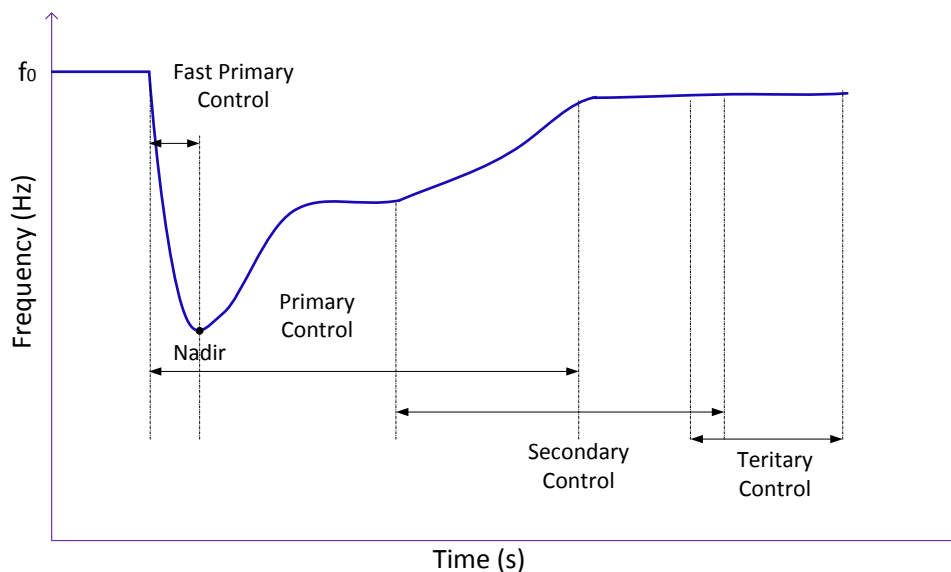
Fig. 3.1 Frequency control in power system

Two methods for WTs overloading with constant power over fixed duration have been proposed and tested in [61]. In both methods, an overloading power reference of fixed magnitude and duration is generated once the under frequency event is detected, irrespective of the magnitude of the frequency event. Hence, in this work, the overloading methods proposed in [61] and [62] are

24

modified to consider the magnitude of frequency event and suitable method for fast primary frequency control is suggested based on the overloading test results of the WT. The details of the proposed WT overloading methods are explained in the next section.

3.2 Proposed Overloading Methods for FPFC

The Fast Primary Frequency Controller model inside the WT, shown in Fig. 3.2, generates the active power reference to the WT in case of frequency events. The details of the two overloading methods are explained in section II.C of paper [C3] and section 3.3 of paper [J3]. They are categorized as External (Option 1) and Internal (Option 2) methods according to the base power reference (P_{base}) during the frequency control period. In general, when the WT is overloaded its rotation speed decreases, therefore the WT optimal power output also decreases. In External method, the effect of WT rotational speed on the base power reference is not considered. Hence, P_{base} is equal to the WT optimal power output before the frequency event, i.e. freezing the value of the output of the 'Optimal Operation' block. The Internal method does consider the impact of WT rotational speed on the base power reference. In case of Internal method, P_{base} is equal to the actual output power of the 'Optimal Operation' block (P_{opt}), which decreases with overloading during frequency control, particularly at below rated wind speeds.

A full scale converter based WT (Type-4) model is considered in this work. The Type-4 WT model is based on the generic approach for WT simulation models proposed by the IEC Committee in Part 1 of IEC 61400-27 [36] for the short term power system stability studies. Additionally, this model is extended to include the dynamic features, such as aerodynamic model, pitch control, mechanical model, relevant for the study of the frequency control from WPPs [62], [63]. The WPP model is based on aggregated WT model according to the method given in [37].
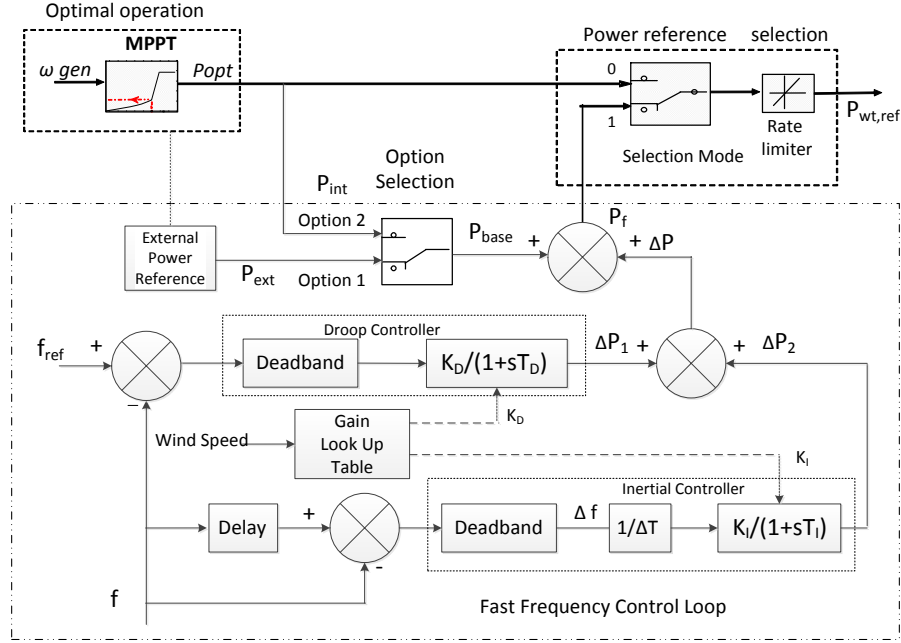
Fig. 3.2 Power Reference Selection for WT Active Power Controller

3.3 Important Simulation Results on WT Overloading Methods

In paper [C3], these two WT overloading methods are applied for fast primary frequency control from a WPP integrated to the AC power system. The gains of the fast frequency controller have been optimized over the whole wind speed range considering the limitations and dynamics of the WT and the corresponding results are shown in Fig. 3.3.

For both methods, the gains of the frequency controller, hence, the overloading power reference, vary with wind speed. However, higher gains are possible with Internal method (Option 2) for the whole wind speed range. These gains can be adapted in advance based on the very short term average wind speed forecast to improve the overloading of the WT without compromising system stability. One optimal gain can be chosen for each wind speed range, thereby limiting the gains to three or four values for the possible operating range of the wind turbine. To compensate for the inherent forecast errors, the gains could be set conservatively corresponding to the lower part of the considered range, i.e. corresponding to 0.5 pu wind speed for the lower medium average wind speed range (0.5-0.7 pu), for example.
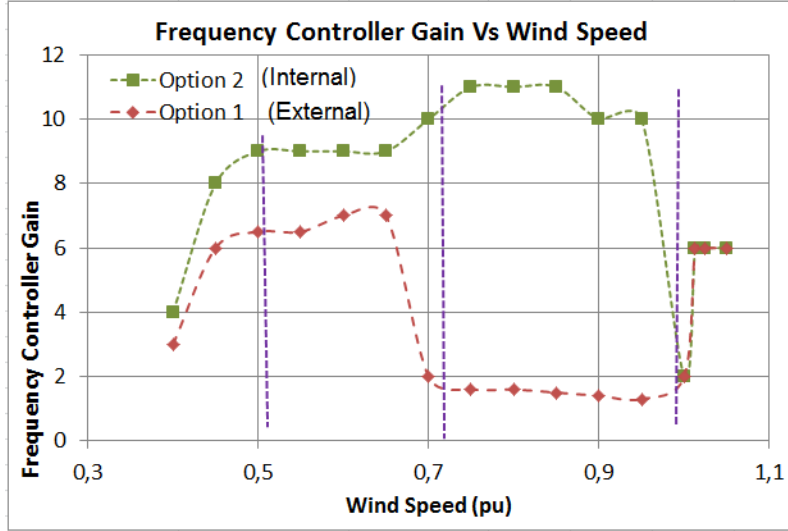
Fig. 3.3 Optimal Frequency Controller gains Vs Wind Speed

These two overloading methods are applied on a test system, where the WPP is integrated to AC power system and performed a frequency control test at below rated wind speeds (0.93 pu). The frequency of the test power system with and without the participation of WPP in frequency control is shown in Fig 3.4. It can be observed that the Internal overloading method (Option 2) provide better frequency control compared to External method (Option 1) due to higher optimal frequency controller gains with better dynamics of the WT at medium wind speeds. Please refer paper [C3] for detailed explanation. In paper [J3], the proposed overloading methods are applied for fast primary frequency control from OWPPs connected through a 3-terminal DC grid. The performance of External method is better during and after the frequency control period and the corresponding details are explained in Chapter 4.
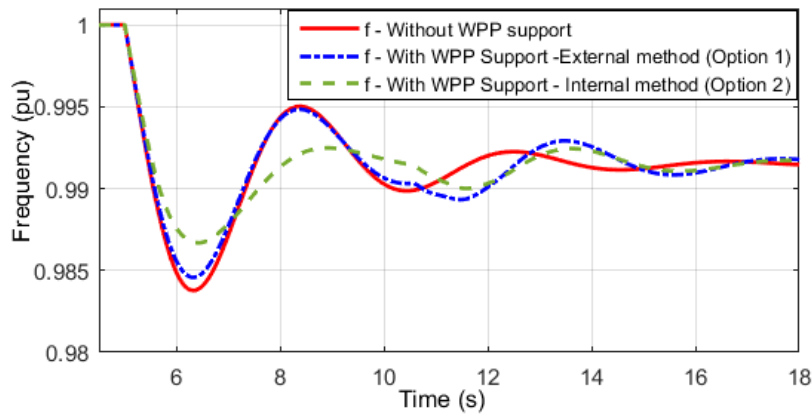
Fig. 3.4 Frequency of the power system considering contribution from WPPs

The challenge lies in the selection of an overloading method with the best possible results, which actually depends on the frequency control requirement and wind speeds. If the main objective of

27

the WPP is to participate in fast primary frequency control i.e. mainly limiting the frequency nadir, then the kinetic energy yield from the WTs can be increased to limit the frequency nadir by adapting appropriate gains of the frequency controller depending on the wind speed range. Thereafter, the primary control should take over the responsibility to stabilize system frequency be followed by secondary control. In that case, Internal method (Option 2) is preferred over External method (Option 1) due to its merits on higher kinetic energy yield from the WT and also better WT dynamics.

In case of extended frequency support (primary/secondary frequency control) and for application which involves guaranteed magnitude of power support from WT, selection of External method is suitable compared to Internal method. However, for this application, WT must have the reserve power at all wind speeds to avoid risk of the WT shutdown. Therefore, deloading /down regulating the WT with a certain percentage is required to ensure stable operation of the power system and WPP. This will, however, result in loss of revenue for the WPP owner. Setting up new markets accommodating remuneration for the WPPs participating in frequency control may compensate this loss.

3.4 WT Overloading Release Methods

WT must be relieved from overloading after few seconds to avoid the risk of stopping and to allow it for recovery, particularly at below rated wind speeds. There are different possibilities to release the overload, (1) instantaneous overloading release [62], (2) overloading release in a controller manner [64]. Instantaneous overloading release may result in abrupt reduction in WT power output, particularly at below rated wind speed, as explained in section IV of paper [0] and section 3 of [J3].Therefore it is recommended to release the overloading in a controller manner for smooth power transition and better WT dynamics. A method to optimally use WT kinetic energy by shaping the overloading power curve using a particle swarm optimization (PSO) has been discussed in [64]. Inspired by this paper, the WT overloading release using a ramp rate limiter (RL) for smoother power transition is proposed in this work as described in detail in paper [J3]. The 'RL' is used to limit the rate of rise of the power reference to the WT in case of normal and overloading conditions and also the rate of power decay after release of overload. The abrupt change in the WT output power after the overloading can be minimized by releasing the overload using a ramp rate limiter inside the 'Power Reference Selection' block of the WT active power controller shown in Fig. 3.2. The release of WT overloading with 'RL' results in smooth power transition and reduced magnitude of power reduction after release of overloading, as explained in section 3.2 of paper [J3]. The results considering the impact of 'RL' is presented for frequency control from OWPP in MTDC grid explained in chapter 4. In this work [J3], the rate of ramp rate limiter is chosen arbitrarily. However, the rate can be optimized using an

optimization method similar to [46] for effective utilization of WT kinetic energy and this is considered as future work.

3.5 Chapter Conclusions

In this chapter, two WT overloading methods, (1) External and (2) Internal methods, for fast primary frequency control from WPPs are presented. The External method, which does not consider the impact of WT rotational speed on the overloading power reference, leads to higher power drop after the release of overload compared to Internal method for the same frequency controller gains. However, the External method can guarantee the required overloading power reference for certain duration which is not possible with Internal method. Therefore, Internal method is recommended over External method for fast primary frequency control because of its merits on higher power support with minimal impact on WT dynamics. External method is recommended for extended power support for frequency control (such as primary or secondary frequency control), where it is required to provide guaranteed magnitude of power for longer duration (few minutes). In such cases, WPP should possess power reserve by operating the WTs in down regulation mode. The ramp rate limiter for the WT ensures smooth power transition after the overloading, creating the less impact on the associated grid. The impact of the WT overloading methods and overloading release methods on the fats primary frequency control from OWPPs in MTDC grid is studied in chapter 4.

This page would be intentionally left blank if we would not wish to inform about that.

Chapter 4
Active Power Control from OWPPs in MTDC Grid

In this chapter, the main results for the second research topic in this PhD project i.e. the frequency control from the OWPPs in the MTDC grid are presented. Mainly, active power control from OWPPs in MTDC grid to provide most important ancillary services for AC and DC grids, such as, frequency control, FRT, and DC grid voltage control are investigated. Among the ancillary services, FPFC is dealt in detail, whereas brief introduction of DC grid voltage control and onshore AC grid FRT are given. The chapter starts with the motivation for active power control of OWPPs to provide ancillary services. The methods for FPFC from OWPPs in MTDC grid are discussed in section 4.2 and the corresponding details are elaborated in papers J3, J4 and C4. The impacts of wind speed on the operating point of the OWPP, and thus, on the frequency control are highlighted in section 4.3 and the corresponding details are given in paper J3. The brief discussion on the other ancillary services from OWPPs, such as DC grid voltage control, AC grid FRT are given in section 4.4, and elaborated in paper C5.

4.1 Motivation and state-of-the-art

Active power balance is one of the main responsibilities of the system operator [31], [44], [57]. This is achieved by controlling the frequency in the AC grid and DC voltage in the DC grid. As discussed in chapter 3, increased penetration of WPPs replacing the power from the conventional synchronous machines, poses challenges to the TSOs to maintain system balance mainly due to reduced effective inertia [44],[57]. The OWPPs integrated through HVDC system further complicates the frequency control by not responding to the onshore AC grid frequency events because of the decoupling due to the power electronic interface [8]-[69]. In case of AC connected WPPs, the frequency signal is available at PCC of the OWPP whereas in case of HVDC connected WPPs, they add a second level of decoupling in the form of HVDC interface, which further increases the complexity in representing onshore AC grid frequency signal. These two challenges have motivated to investigate the FPFC from OWPPs connected through a HVDC system [57], [65], [68].

For an OWPP connected through a two terminal HVDC link, one solution to handle the decoupling is that the frequency of the onshore AC grid can be communicated to the OWPP through communication channels [69] as shown in Fig 4.1. However, the reliability depends on the reliability and speed of communication network. In case of MTDC systems, connecting more than one AC areas and OWPPs, the reliability becomes more concern because of the multiple communication channels between the AC areas. Therefore, a communication-less scheme to replicate onshore AC grid frequency, in a coordinated manner, at the offshore AC grid for an OWPP connected through a two terminal HVDC system is given in [67]. The coordinated frequency control method from an OWPP connected through an MTDC grid is given in [65], [66]. This method uses the DC grid voltage as an indicator for imbalance in the AC grid frequency. However, most of these studies [8]-[69] have considered OWPPs as constant power sources and none of these studies focused on the impact of wind speed on the FPFC from OWPPs and therefore on the DC grid voltage and AC grid frequency.
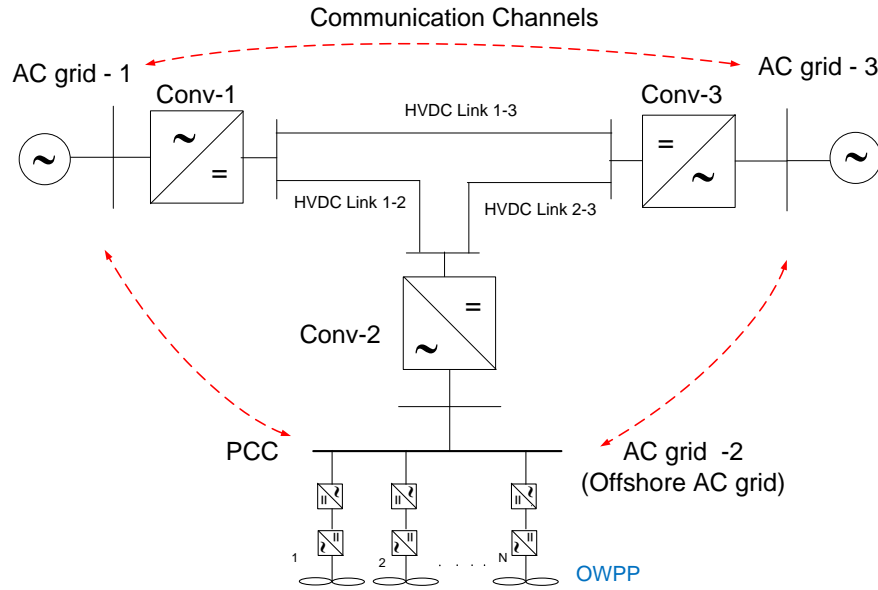
Fig. 4.1 3-terminal HVDC grid layout

Hence, in this thesis, the study is focused on the impact of OWPPs operating point, which depends on the wind speed, and thus on the frequency control and the DC grid voltage. The FPFC from OWPPs in a 3-terminal HVDC grid is studied. The OWPP is overloaded to produce additional power for frequency control by utilizing the kinetic energy of WTs. The impacts of release of kinetic energy support by releasing the WT overloading on the secondary dips in DC grid voltage and AC grid frequency are studied. Moreover, methods to mitigate these secondary effects due to release of kinetic energy from OWPPs are proposed.

Along with FPFC, DC grid voltage control, and AC grid fault ride through (FRT) support require fast active power control from OWPPs. The main concern for the FRT support from OWPPs

connected through HVDC system is the delay in detection and communication of onshore fault at the offshore station, which results in an unacceptable rise of DC voltage leading to trip of the HVDC link, thus blocking the power flow from OWPPs [70]. One of the possible solutions to avoid such type of issue is to use expensive DC chopper in the onshore HVDC station to dissipate the excess energy in the DC link [71]. A method of fast reduction of active power from the OWPPs in MTDC grid based on modulating the AC voltage or frequency in the offshore AC grid has been described in [72]. However, this approach will have detrimental impact during a voltage event in the offshore grid as such type of approach will be in contradiction to the requirement of additional reactive current injection during a fault in the offshore AC grid. Along with FRT support, for higher share of wind power in MTDC systems, it is imperative that OWPPs feeding into the DC grid shall also provide DC grid voltage support. However, to avail such type of voltage support service from OWPPs, high speed measurement and communication infrastructure will be required [73]. A coordinated control scheme for ancillary services for AC (frequency control, FRT support) and DC grids (DC voltage control) from MTDC connected OWPPs based on offshore frequency modulation approach is proposed in this thesis.

4.2 Frequency Control Methods

The brief description of the communication based and coordinated frequency control methods, applied to a 3-terminal HVDC grid shown in Fig. 4.1 is given here. The Conv-1 and Conv-3, in Fig. 4.1, are the onshore HVDC converters connected to AC grid-1 and grid-3, respectively and the Conv-2 is the offshore HVDC converter connected to offshore AC grid (i.e. AC grid-2). The onshore HVDC converters share the responsibility of maintaining the active power balance in the DC grid; therefore, Conv-1 and Conv-3 operate in droop control mode. The offshore HVDC converter exchanges the power generated by OWPP to the DC grid by controlling the offshore AC voltage and frequency.

In case of communication based frequency control, the converters of the MTDC grid exchange frequency information of their associated AC grid using the dedicated communication channels, as shown in Fig. 4.1. The communication based frequency control method is initially presented in [69]. However, the study is limited to two terminal HVDC system and to under frequency events; therefore the impact of frequency control on DC grid cannot be identified. Therefore, in paper [J4], the communication based frequency control method is applied to a three terminal HVDC system for frequency control in one of the associated AC grid and the impact on DC grid voltage is studied in detail. The experimental validation of the communication based frequency control has also been done in [J4] and the corresponding details are given in chapter 5.

The 'coordinated frequency control method' is based on a communication-less scheme, where the onshore frequency is replicated at the offshore grid through supplementary control blocks

implemented locally at the VSCs in the MTDC system[65]- [67], [C4], [J3], [J4]. The control scheme of supplementary control blocks at onshore HVDC converter depends on the method of droop control implemented at onshore HVDC converters. There are several possibilities to implement droop control [74], [75]. In this thesis, two droop control methods, (1) DC voltage control with an active power droop [C4] (2) Active power control with DC voltage droop [J3], [J4], are implemented as shown in Fig. 4.2. These two control methods have almost similar behavior in steady state and dynamic conditions by sharing the active power in the DC grid between the onshore HVDC converters according to $P-V_{dc}$ or $V_{dc}-P$ droop control gains [74],[75].

The additional control mechanism, namely $f_{on}-V_{dc}$ or $f_{on}-P$ droop control in Fig. 4.2 translates the onshore AC grid frequency (for example at AC grid-1) variations into DC grid voltage change or active power change and the later, anyway, result in DC grid voltage change. Therefore, the other onshore HVDC converters participating in droop control, inherently provides active power support. However, the OWPP doesn't detect the frequency event; hence mirroring onshore frequency deviation in the offshore AC network frequency is needed. The offshore HVDC converter performs this through the DC voltage variations using a droop controller, which modifies the offshore AC grid frequency proportional to the DC voltage variation measured at its terminals. Finally, the OWPP changes its power output according to the change in frequency measured at its point of connection. The further details on coordinate frequency control method have been explained in papers [C4], [J3], and [J4].
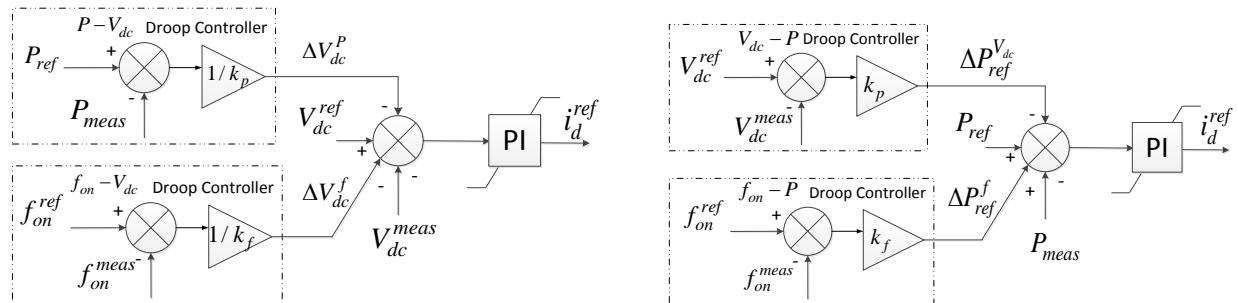
Fig 4.2. (a) DC Volatge Control with Active Power Droop   (b) Active power control with DC voltage droop

The simulation results for communication based frequency control for under and over frequency events at a test gird have been explained in paper [J4]. The simulation results for coordinated frequency control have been initially presented in paper [C4] and extended for under frequency events when OWPPs operating at above and just below rated wind speeds in [J3]. The simulation results for an under frequency event at AC grid-3 (Fig. 4.1), created at time t = 10s, using the coordinated frequency control method are shown in Fig. 4.3 [J3]. It is assumed that OWPP is operating at above rated wind speed (1.1 pu); hence there is enough additional power available from OWPP to participate in FPFC. It can be observed from Fig. 4.3 that the AC grid-3

34

frequency is improved with the coordinated control (CC) from AC grid-2 (dotted line) compared to without CC (dashed line). The frequency of AC grid-3 is further improved with the CC from both AC grid-2 and OWPP (solid line) These results show that OWPP in an MTDC grid can participate in the associated AC grid frequency control in a coordinated manner, without depending on the communications as it involves concerns for the reliability.

The simulation and experimental validation of communication and coordinated frequency control from OWPPs for under and over frequency events at above rated wind speeds are given in paper [J4] and they are explained in chapter 5. The impact of OWPP operating point on the FPFC at just below rated and the corresponding impact on DC and AC grids have been explained in papers [C4] and [J3] and the details are given in the next section.

Fig. 4.3 Frequency of AC grids, DC voltage and active power output of three HVDC converters for an under frequency event at AC grid-3 at wind speed Vw= 1.1 pu

4.3 Impact of Wind Speed on Frequency Control

The impact of wind speed on the FPFC from OWPPs in MTDC grid is explained in this section. The coordinated FPFC from offshore wind power plants (OWPPs) integrated to a 3-terminal HVDC grid, at below rated wind speeds has been presented in papers [C4] and [J3]. The impact of wind speed on the OWPP active power output and thus on the AC grid frequency and DC grid voltage is analyzed. The removal of active power support from OWPP after the FPFC action results in secondary DC grid voltage and frequency dips. A method based on releasing the active power support from OWPP with a ramp rate limiter to mitigate these secondary effects is proposed in [C4]. Along with this method, the other mitigation methods such as: Varying the

droop gains of the HVDC converter according to wind speed and An alternative method for the wind turbine overloading considering rotor speed, are also presented in paper [J3]. The WT overloading methods (External and Internal methods) and overloading release method with a ramp rate limiter, explained in chapter 3, have been utilized to mitigate the secondary effects on frequency and DC voltage.

The simulation results of FPFC from OWPP operating at just below rated wind speed (0.9 pu), for an under frequency event at AC grid-3, created at time t = 10 s, are shown in Fig. 4.4. In these results, External method has been used for WT overloading and the overloading is released without the application of a ramp rate limiter. The OWPP is overloaded for 10s (from t = 10s to 20s) to provide active power support for FPFC. The frequencies of three AC grids, DC voltage and active power output of three HVDC converters are also shown in Fig. 4.4. It can be observed from these results that the frequency of AC grid-3 is improved during the overloading period (up to t= 20s). However, the output power from OWPP decreases rapidly after the release of overload, causing sudden power imbalance in the AC and DC grids, which leads to second frequency and DC voltage dips. The reason for sudden power drop from WT (hence OWPP) can be understood by its dynamics given in Fig. 4.5. As the pitch of the WT blade is already at it optimal position, the decrease in WT speed due to overloading decreases the aerodynamic power and the optimal power output (P_{opt}).The explanations of these results are well documented in section 4 of paper [J3]. The impact of the proposed three methods to mitigate second frequency and DC voltage dips are investigated in the sections 4 of [J3] and the results show that all the three methods help to mitigate the impact. However, the reliability of varying the droop gains of the HVDC converter is dependent on the reliability and accuracy of wind speed forecast. Hence, an alternative method (Internal method) of overloading the WTs together with release of overload with a ramp rate limiter provides better results for FPFC from OWPPs during and after the release of overload.

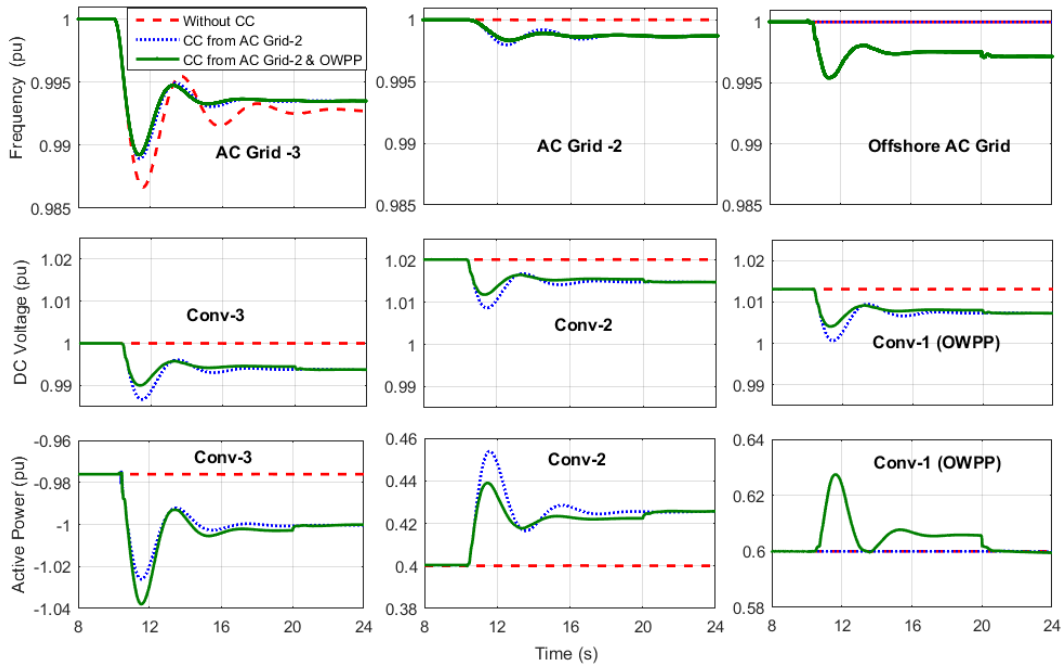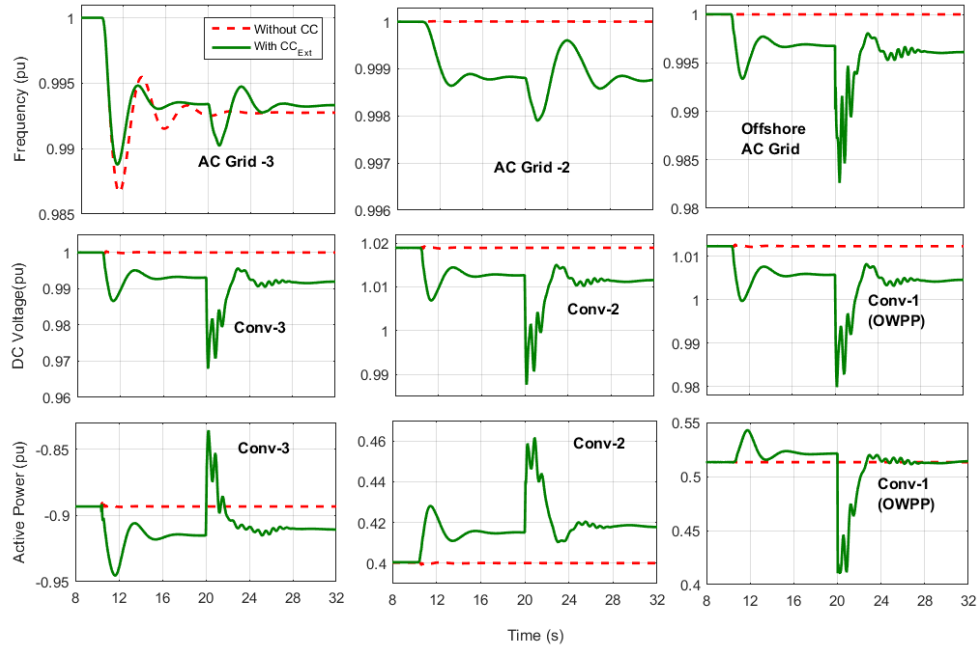Fig. 4.4 Frequency of AC grids, DC voltage and active power output of three HVDC converters for an under frequency event at AC grid-3 at wind speed Vw= 0.9 pu for OWPP with External overloading without rate limiter. Dotted: Without Coordinated Control (CC) Solid: With CC
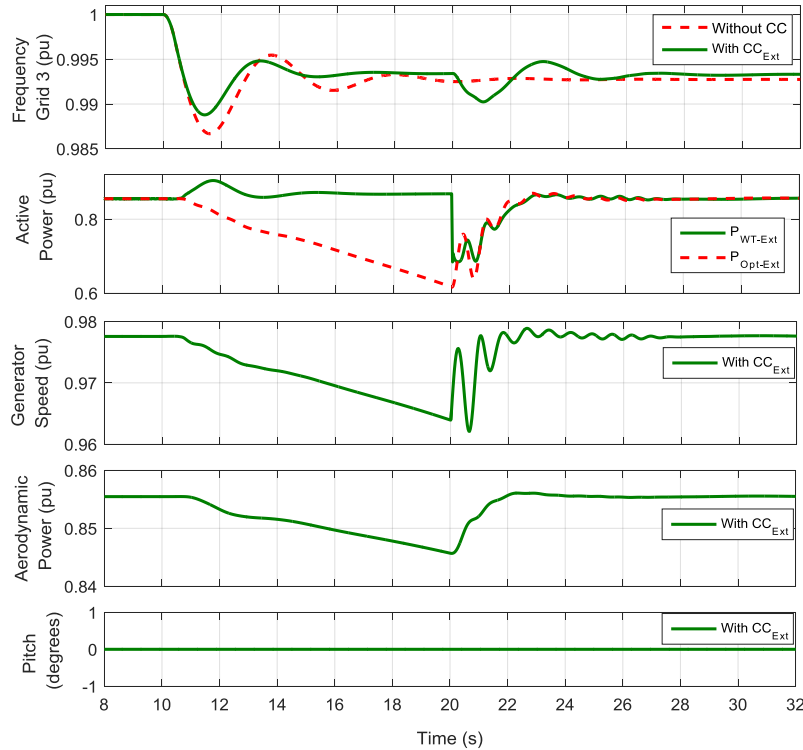

Fig. 4.5 AC grid-3 frequency and WT dynamics at Vw=0.9 pu- with CC from OWPP (External overloading without rate limiter).

4.4 Other System Services from OWPPs

Along with the frequency control, the coordinated control method can be used to avail other system services from OWPPs in MTDC grid, such as, FRT support in the onshore grid, and DC grid voltage control; the corresponding details are given in paper [C5]. As discussed in previous sections, for the onshore frequency control, the proposed control strategy involves a coordinated control mechanism based on active power or DC voltage regulation at the onshore converter and the frequency regulation at the offshore converter. For onshore AC fault ride through and DC Grid voltage control, the control strategy involves regulating the offshore AC grid frequency according to DC voltage variation. Based on detailed simulations on the 3-terminal HVDC system, it is shown that with the proposed coordinated control strategy, offshore wind power plants can effectively deliver the ancillary services to DC and AC grids with less dependency on communications. The possible limitations of the proposed control strategy are: (1) The accuracy and speed of the frequency measurement may influence the performance of the proposed method, (2) For onshore FRT support, the OWPP output should be reduced within few hundred milli-seconds and this is only possible by draining the energy from the OWPPs by DC chopper inside the WT converter, and (3). The faults in the DC grid may also lead to lower DC voltage. In that case, it may not advisable that OWPP contribute more power to DC grid. Hence, the proposed coordinated control scheme should be coordinated with DC grid protection settings. Reader is suggested to refer paper [C5] for further details.

4.5 Chapter Conclusions

The control strategies to avail active power support from OWPPs in MTDC grid for ancillary services to DC and AC grid have been presented in this chapter. For onshore AC grid frequency control, two methods have been proposed. If the size of the DC link is small (2 or 3 converters, for example), communication based frequency control may be preferred. However, for larger DC grids with more number of converters, coordinated control can be preferred over communication based method, considering the reliability and dynamics of DC grid voltage. The application of the coordinated control method for other system services, onshore FRT, DC grid voltage control have also been verified with time domain simulations. The impact of the wind speed on the operating point of OWPP and on the fast primary frequency control for the AC grid, are investigated. A secondary dip is observed in DC grid voltage and AC grid frequency after the release of active power support from OWPPs, particularly at below rated wind speeds. Three methods to mitigate these problems: (1) varying the droop gains of HVDC converter, (2) application of ramp rate limiter, (3) alternative method of overloading the wind turbine

considering rotor speed have been proposed and investigated. The combination of Internal overloading method and the ramp rate limiter further helps to minimize the secondary effects of frequency control from OWPPs and seems to be the best option to minimize the second frequency dip.

This page would be intentionally left blank if we would not wish to inform about that.

Chapter 5

Experimental Validation of Frequency Control from OWPPs

In this chapter, experimental validation of two frequency control methods from OWPPs in MTDC grid are presented, i.e. (1) Communication based Frequency Control (2) Coordinated Frequency Control, are presented. A laboratory scaled 3-terminal DC grid test set up has been used to validate these two frequency control methods. The chapter starts with motivation for experimental validation of frequency control from OWPPs. The brief description of laboratory scaled 3-terminal DC grid experimental test up is given in section 5.2 and implementation of two frequency control methods and their comparison are given in section 5.3 and are elaborated in paper J4. The impact of wind speed on the frequency control from OWPPs and the corresponding impact on DC grid voltage and frequency control are explained in section 5.4 and the corresponding results are given in papers J5 and C6.

5.1 Motivation

With an increased integration of WPPs and a growing interest in power transmission using HVDC, the transmission system operators will require services such as inertia provision and frequency control from VSC-HVDC connected power plants [31], [20], [44]. The MTDC transmission interconnecting different synchronous areas and OWPPs poses several challenges for frequency control due to power electronic decoupling between the associated energy sources. In this regard, several studies have been conducted to validate the frequency control from OWPPs connected through point to point (two-terminal) and multi-terminal HVDC system. Most of these studies are limited to time domain simulations; therefore a need arises to study the feasibility and impact of these methods on the AC and DC grids. The experimental verification of inertial response from WPP in a two terminal HVDC system has been performed a laboratory scale test set up in [76]. These tests are limited to under frequency events with only communication-less scheme in a point to point HVDC system. A simple droop test, verifying the sharing of active power between the converters in a 3-terminal HVDC system has been performed on an experimental test set up in [77]-[79]. However, these are limited to study of the performance of the droop-control in case of variation in power output from WPP and loss of a

converter and do not deal with frequency control from WPPs. Therefore, in this thesis, the two methods for frequency control (communication based and coordinated) from OWPPs and other converters in MTDC grid are verified on an laboratory scaled 3-terminal DC grid test set up. The main objective is to compare these two methods and to validate the use of DC voltage as an indicator for system imbalance in the AC grid [J4]. Moreover, the impact of wind speed on the FPFC from OWPPs in the 3-terminal DC grid and thus on the DC and AC grids are also validated and described in [J5], [C6].

5.2 *Laboratory Scaled 3-Terminal DC grid Test Set Up*

The differences between the simulation and laboratory scaled 3-Terminal DC grid test set up have been explained in the papers [J4] and [J5] and is briefly presented in this section. A frequency control test is performed on a 3-terminal DC grid laboratory scaled test set up whose single line diagram is shown in Fig. 5.1. The test set up is composed of three cabinets, as shown in Fig. 5.2, and a physical emulation of the DC cables. The DC lines (1-2, 1-3 and 2-3) are modelled using the PI equivalent cable, with the values of resistance (R) and inductance (L) illustrated in Table I of paper [J4]. The cable capacitance is included in the VSC capacitance. Each cabinet contains a three-phase 12.5 kVA transformer, the VSC, the control board and the measuring boards (as shown in Fig. 5.3). The VSCs are two-level converters based on insulated-gate bipolar transistors (IGBTs) with a nominal power of 5.7 kVA. The nominal AC RMS voltage is 230 V phase to phase. The switching frequency of each converter is 20 kHz and it is controlled using a control board based on a digital signal processor (DSP) F28M35 of Texas Instruments (TI). All the converters are connected to the same AC grid of 230 V phase to phase and the behavior of the OWPP in the AC side of Conv-2 and the frequency event in the AC grid of Conv-1 are emulated.
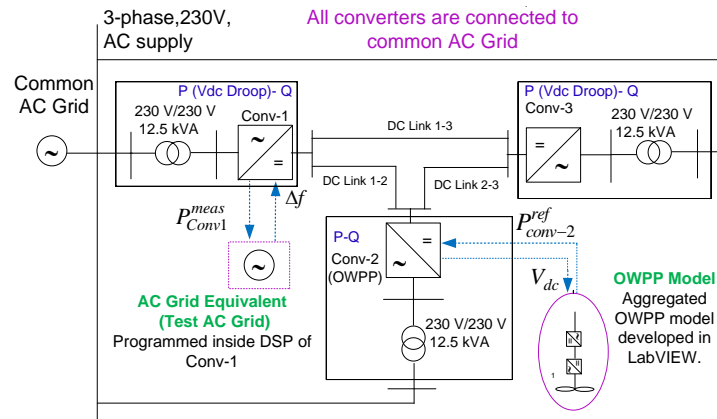
Fig. 5.1 3- terminal test set up to perform frequency control test

A SCADA system is implemented in LabVIEW using the cRIO 9024 controller of National Instruments (NI) to monitor the variables of the 3-terminal DC grid and it also includes the emulation of the OWPP of Conv 2, see Fig. 5.3. The OWPP emulation in the cRIO 9024 is communicated with Conv 2 via the Digital to Analog Converter (DAC) and the Analog to Digital Converter (ADC) of its control board and is described in section IV.B of paper [J4]. The emulation of the frequency event of AC grid of Conv 1 is implemented by software in the DSP of Conv. 1 and it is described in Section IV.A of paper [J4]. The communication between converters in the case of the communication based frequency control is implemented using a Controller Area Network (CAN) bus with period of 100 ms.
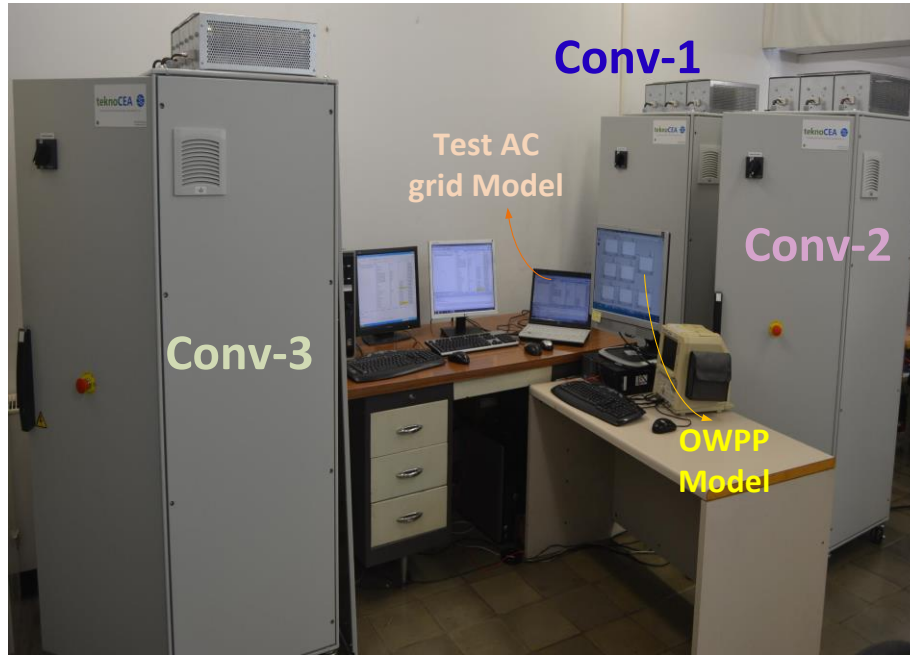
Fig. 5.2 Picture of three-terminal DC grid experimental test set up

As it is not possible to change the frequency of the laboratory AC grid, an AC grid equivalent with a dynamic frequency model (test AC grid) based on the swing equation [18], shown in Fig. 5.4, is implemented inside the DSP of Conv-1. The change in frequency (Δf) is zero as long as there is a balance between change in mechanical power input (ΔP_m) and electrical power output (ΔP_l) of the grid. A frequency event in the test AC grid can be created by perturbing the ΔP_l. In case of coordinated frequency control, Δf is sent to the onshore VSC (Conv-1) controller, which then provides the additional active power reference (ΔP_{ref}^f) to the corresponding onshore VSC (Conv-1). The change in power output from this onshore VSC (Conv-1) results in change in the

43

DC grid voltage, therefore, other onshore VSC (Conv-3) participates in frequency control by increasing/decreasing its active power output according to the magnitude of DC voltage droop constant. The OWPP model sends the new power reference to the offshore VSC (Conv-2) according to the measured change in DC voltage. In case of communication based control, Δf is communicated to Conv-3 and OWPP model with a communication delay of 100 ms and the power output from these converters (Conv-3 and Conv-2) are changed according to the change in Δf. In both methods, the measured change in active power output of Conv-1 due to the frequency control (ΔP_{Conv-1}) is sent to the test AC grid model, thereby participating in the frequency control of the test AC grid

Fig. 5.3 Picture of Measurement and control board inside a converter
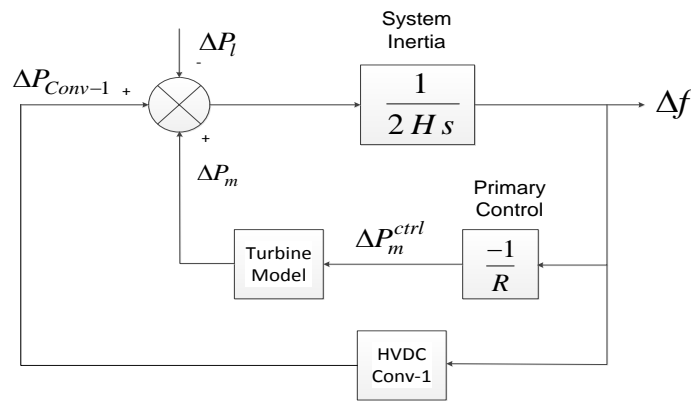
Fig. 5.4 AC Grid equivalent with dynamic frequency model

5.3 Discussion of Results for Frequency Control Methods

The detailed discussion of simulation and experimental results of communication based and coordinated frequency control methods are given in section V of paper [J4] and are briefly presented here.

The frequency control test is performed both for under and over frequency events created in the test AC grid, shown in Fig 5.4, by modifying its electrical power output (ΔP_l). The simulation results, performed using DIgSILENT PowerFactory, are validated with experimental results, where the tests are performed on a 3-terminal laboratory test set up shown Fig 5.2. The results of communication based frequency control the coordinated frequency control are presented in paper [J4]. In both cases, an under frequency event in the test AC grid is created by applying $\Delta P_l = 0.15$ pu and an over frequency event with $\Delta P_l = $ -0.15 pu at time t = 6s. The results for under frequency event are given here for both frequency control methods.

5.3.1 Communication based Frequency Control Method

 The frequency of the test AC grid is communicated to Conv-3 and OWPP with a communication delay of 100 ms. Participation of OWPP (therefore Conv-2) and Conv-3 in the MTDC grid in the frequency control is studied. The power flow and droop parameters of the 3-terminal DC grid test set up (Fig.5.2) used in this test are given in paper [J4]. In normal conditions, the OWPP, hence the offshore converter (Conv-2) transfers power to DC grid whereas the onshore converters (Conv-1 and Conv-3) receive power from DC grid. The positive sign of power flow indicates power flow from DC to AC grid and vice versa for negative sign.

The simulation results of communication based frequency control for an under frequency event at test AC grid, created at time t = 6 s, are shown in Fig 5.5 (a). The test AC grid frequency, the DC voltage and active power of all three converters are presented. The corresponding experimental results are given in Fig. 5.5 (b). It can be observed from these results that the participation of OWPP improves the frequency of test AC grid (light solid line) compared to No support from OWPP (Conv-2) and Conv-3 (dashed dotted line). The increased power supply into the DC grid also leads to an increase in the DC grid voltage. The participation of Conv-3 together with OWPP (dark solid line) further improves the frequency response of the test AC grid. In this case, Conv-3 participates in frequency control by reducing its power export from the DC grid. However, Conv-3 participation together with OWPP further increases the DC grid voltage. The simulation results are aligned with the experimental results.
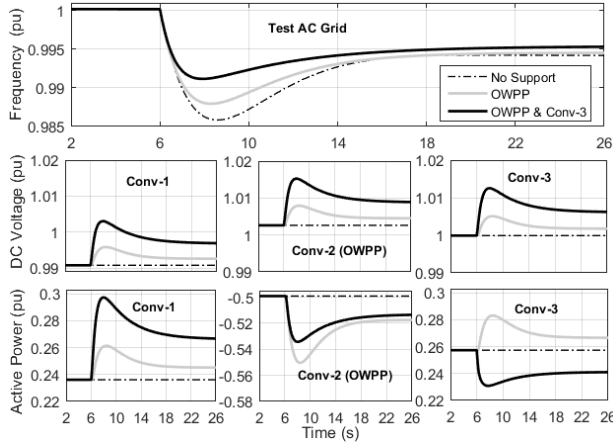
Fig. 5.5 Communication based frequency control Under frequency – (a). Simulation Results
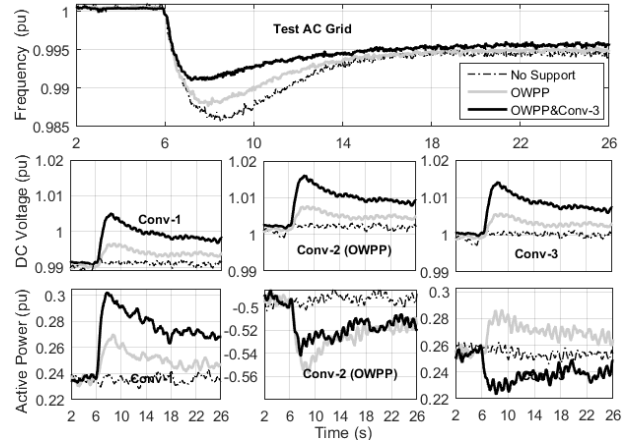
(b) Experimental validation of simulation results given Fig. 5.5 (a)

5.3.2 Coordinated Frequency Control Method

The converters and OWPP participate in frequency control without depending on the communication channels in the DC grid. The simulation and experimental results of the coordinated frequency control from OWPP (Conv-2) and Conv-3, for an under frequency event created at test AC grid, is shown in Fig. 5.6 (a) and (b), respectively.
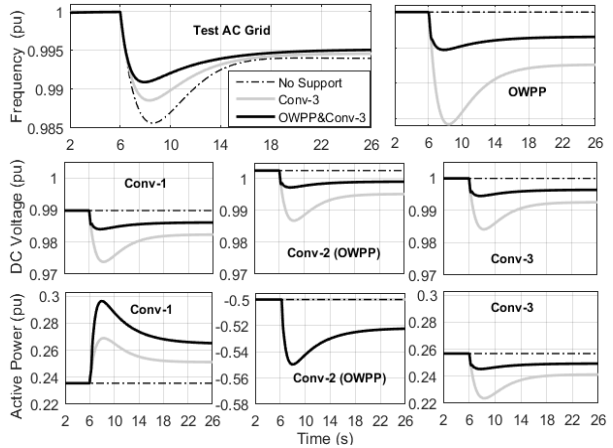
Fig. 5.6 Coordinated frequency control- Under frequency- (a). Simulation results
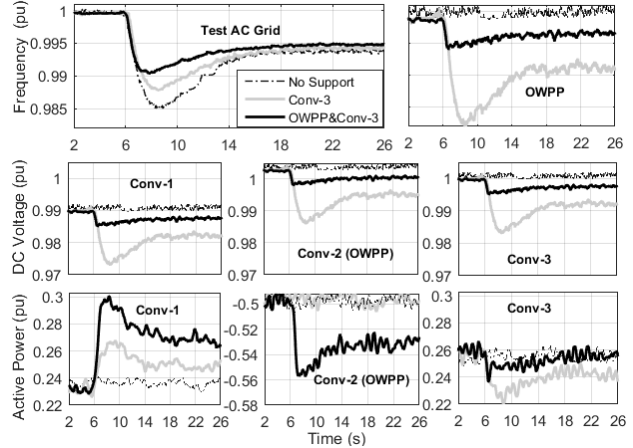
(b). Experimental validation of simulation results given in Fig. 5.6 a

The change in frequency at the test AC grid modifies the active power reference to Conv-1, and consequently also changes the DC grid voltage. The Conv-3 changes its power output due to natural action of DC voltage droop controller, participating in frequency control, whereas the OWPP modulates it power output based on the measured change in frequency at OWPP model, which is modified according to DC grid voltage received from Conv-2. It can be observed from

46

Fig. 5.6 that the frequency of the test AC grid is improved with the combined participation of Conv-3 and OWPP (dark solid line) compared to the other two cases, i.e. participation of Conv-3 (light solid line) alone and No support (dashed dotted line). Also, the participation of OWPP in the frequency control relieves the active power burden on Conv-3 by sharing the responsibility. It can also be observed that there is a slight decrease in the DC grid voltage due to the coordinated frequency control action for under frequency events. However, participation of the OWPP together with the Conv-3 in frequency control minimizes the reduction in DC grid voltage. In this case also, the simulations results are in align with experimental results.

Based on the results for the two frequency control methods, the following conclusions are drawn. For communication based frequency control, there must be dedicated communication channels between each converter in the DC grid, which raises concerns on the reliability. The coordinated control, which relies on communication-less scheme, minimizes this risk. However, coordinated control increases the control complexity, particularly for frequency control of the offshore wind power plants. Also, the converters operating in DC voltage droop control (Conv-3 in this case) naturally participates in frequency control with the coordinated control compared to communication based control. If the size of the DC link is small (2 or 3 converters, for example), the communication based frequency control can be preferred. However, for larger DC grids with more number of converters, the coordinated control can be preferred over communication based method, considering the reliability and dynamics of DC grid voltage.

5.4 Impact of Wind Speed on FPFC from OWPPs

In section 4.3 of chapter 4, the time domain simulations for impact of wind speed on the FPFC have been discussed. In this section, the experimental validation of the participation of OWPPs in FPFC considering the operation of the OWPP at different wind speeds, presented in papers [J5] and [C6], are explained. The kinetic energy of the OWPPs is utilized for FPFC by overloading the wind turbines (WTs). In paper [J5], the ability of the OWPPs participation in FPFC is tested at three different wind speeds: (1) above rated wind speed, (2). just below rated wind speed, and (3). low wind speeds. The impact of releasing the kinetic energy support from the OWPP on the DC voltage of the MTDC grid and frequency of the affected grid are studied in detail using time domain simulations and experimental validations on the laboratory scaled 3-terminal DC grid test set up. The simulation and experimental results (frequency, DC voltage,

and active power) of frequency control at just below rated wind speed (0.92 pu) are given in Fig. 5.7a and 5.7b, respectively. An under frequency event is created at test AC grid, in Fig. 5.1, by increasing its electrical power output $\Delta P_l = 0.15$ pu at time t = 6s. The kinetic energy of the OWPP is utilized by overloading the WT for 10 seconds after the initiation of frequency event, i.e. the kinetic energy support of the OWPP is released at time t = 16s. The frequency of the test AC grid is improved with the participation of OWPP and Conv-3 (Case c) compared to other two cases shown in Fig. 5.7 (Case a and b). However, at end of frequency control period, there is a considerable dip in the DC voltage of the DC grid and frequency of the test AC grid, in case c compared to a and b. However, the magnitude of secondary dips are lesser for Case d (overloading is released with a rate limiter) compared to Case c, because the WT dynamics are smoother with rate limiter. The reason for these secondary dips is due to the sudden drop in active power output after the release of kinetic energy support from the OWPP, which is well explained by simulation and experimental results of corresponding WT dynamics given in paper [J5].
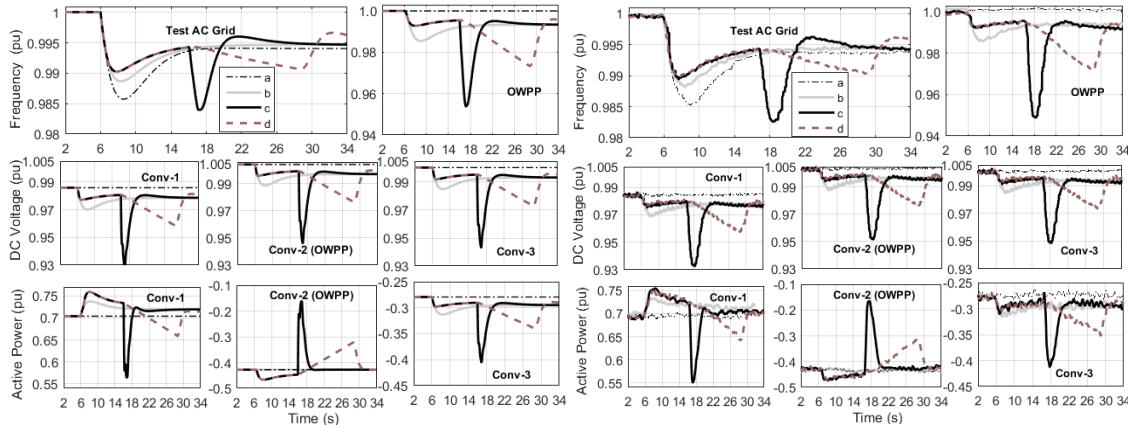
Fig. 5.7 Coordinated frequency control- at wind speed Vw_0.92 pu - (a) Simulation results   (b). Experimental Validations.

a). No Support, b). Support from Conv-3 alone c). Support from OWPP and Conv-3 d). Support from OWPP and Conv-3 with rate limiter at WT

In paper [C6], the two overloading methods for the wind turbine (WT) presented in chapter 3, i.e. Internal and External methods are utilized for FPFC from OWPPs connected through 3-terminal DC grid considering the operation of the WT at below rated wind speed. Finally, the suitable overloading method for FPFC from OWPPs in MTDC grid is proposed based on the simulation and experimental results.

Based on the results presented in paper [J5], in case of above rated wind speeds, the additional aerodynamic power can be utilized by changing the pitch angle to get the additional energy during the frequency control period. In this case, WT dynamics are smoother and secondary DC voltage and frequency dips due to the release of kinetic energy support from OWPP are reasonable. However, at just below rated wind speed, overloading the wind turbine results in a faster reduction in WT output power, causing significant secondary dips in frequency and DC voltage after releasing the WTs overloading (kinetic energy support), as shown in Fig. 5.7. Limiting the rate of power release with a ramp rate limiter can smoothen the WT dynamics to some extent and minimizes the secondary effects, as discussed in paper [J5]. Alternatively, use of overloading method which considers the WT dynamics during the overload (Internal method) can minimize the power drop after the overloading, creating less secondary impacts on DC grid voltage and AC grid frequency, compared to External method as discussed in paper [C6]. At lower wind speed, secondary DC voltage and frequency dips are minimal due to less share in the active power output from OWPP compared to the other converters in the DC grid as discussed in paper [J5]. However, the recovery time after releasing the overloading is longer, thus sufficient time has to be ensured to make the OWPP ready for another frequency event.

5.5 Chapter Conclusions

In this chapter, the experimental validation of two methods for onshore frequency control from OWPPs in a 3-terminal DC grid: (1) communication based and (2) coordinated frequency control methods is presented. In both methods, DC voltage acts a medium of imbalance in the associated AC grids. The impact of wind speed on the FPFC from OWPPs in MTDC grid is also validated experimentally and the corresponding secondary effects due to release of kinetic energy support from OWPPs on the DC and AC grids and their mitigation methods are also validated. In all the test cases, the simulation results are in align with experimental test results, proving that the frequency control is possible from OWPPs in MTDC grid with and without communicating the onshore AC grid frequency to the OWPP and other converters in the DC grid.

This page would be intentionally left blank if we would not wish to inform about that.

Chapter 6
Thesis Contributions

In this chapter, the contributions of this thesis for the two research problems defined in chapter 1: (1) Coordinated AC voltage/reactive power control in cluster of OWPPs connected through common HVDC station, (2). Onshore AC grid frequency controls from OWPPs in MTDC grid are presented. The contributions of each paper (C1 to C6 and J1 to J5) are also highlighted.

6.1 Main Contributions

The main contributions of the study performed in this thesis are given below.

1) Overview of the state of the art in the reactive power and AC voltage control in the WPPs, frequency control from WPPs and OWPPs connected through HVDC system have been given.

2) Three methods for reactive power and AC voltage control in the cluster of OWPPs connected to common HVDC station: (1) Voltage droop control method (2) Coordinated Reactive Power Control Scheme (3) Coordinated Voltage Control Scheme, have been proposed and compared.

3) Methods are proposed to improve steady state reactive power distribution to avoid excessive voltage at WTs and voltage ride through capability of the offshore AC grid with cluster of WPPs connected to common HVDC station.

4) Two overloading methods for active power control of WTs to utilize their kinetic energy for frequency control have been presented and the suitable method for fast primary frequency control from OWPPs in MTDC grid has been proposed based on the simulation and experimental results.

5) Two methods for frequency control: (1) Communication based, (2) Coordinated control, from OWPPs in MTDC grid have been presented. These methods are validated by time domain simulations using DIgSILENT PowerFactory and performing tests on a 3-terminal laboratory scaled test set up.

6) The impact of wind speed on the frequency control form OWPPs in MTDC grid have been verified with the time domain simulations and experimental tests.

7) The main results of the study have been disseminated in the form of presentations and publications international conference and reputed journals and they are given in next section.

6.2 Dissemination

Table 6.1: Short Description of the contributed papers

Paper ID	Main Idea	Contribution	Relation to other papers
C1	Reactive power control in a cluster of OWPPs connected to a common HVDC station.	Proposed a coordinated reactive power control scheme for a cluster of OWPPs connected to common HVDC station. Reactive power reference at the point of connection of WPPs is generated based on an optimization algorithm aiming at minimum active power losses in the offshore AC grid. Reactive power dispatch to each WT within WPP is based on their available reactive power margin. The reactive power contributions from different WTs for faults inside one of the WPP and their impact on offshore AC grid voltage profile have been addressed.	Unique Contribution
C2	Coordinated Voltage Control Scheme for a cluster of OWPPs connected to common HVDC station.	Proposed a coordinated voltage control scheme for a cluster of OWPPs connected to common HVDC station. This scheme improves the steady state voltage profile and voltage ride through performance (in case of faults within offshore AC grid) of offshore AC grid. Collector cable fault is analyzed. The concept presented in this paper is further extended in Journal J2, where, more details on optimization algorithm, Pilot bus concept, impact on voltage and reactive contribution of WTs other faults within the cluster have been explained.	Concept is further extended in 'J2'
C3	A fast frequency controller (FFC) for wind power plants (WPPs) connected to AC grid is proposed in this paper. The gains of the FFC are optimized for different wind speeds.	Contrary to standard controllers proposed in the literature, the gains of the FFC are optimized for different wind speeds ensuring an improved frequency control from WPPs over the whole wind speed range. Two options (with and without considering the dynamics of WT during overload) for fast frequency control from WPPs are analyzed and compared. In this paper, a simple system is analyzed, where an aggregated WPP is connected to an AC grid with aggregated synchronous machine. The outcome of this paper is applied to mitigation of secondary effects due to frequency control from HVDC connected OWPP , which	Unique Contribution. However, utilized the outcome of this paper as an input in 'J3'

		are explained in Journal 'J3'	
C4	Coordinated fast primary frequency control (FPFC) from offshore wind power plants (OWPPs) integrated to surrounding onshore AC power system through a 3-terminal VSC HVDC system is presented.	The impact of wind speed on the frequency control is presented. The problem of second frequency dip due to release of active power support from OWPP is highlighted. The concept proposed in this paper is further extended in Journal 'J3', where the different possible solutions to mitigate these secondary effects are presented.	Concept is further extended in 'J3'
C5	A new approach (changing the OWPP frequency in a coordinated manner) of providing ancillary services to AC (frequency, onshore FRT) and DC grids (DC voltage) from offshore wind power plants (OWPPs), connected through multi-terminal HVDC network is presented.	A coordinated control scheme where OWPP's AC grid frequency modulated according to DC grid voltage variations is used to detect and provide the ancillary service requirements of both AC and DC grids, is proposed in this paper. In particular, control strategies for onshore frequency control, fault ride-through for faults in the onshore AC grid, and DC grid voltage control are considered. The method is same as given in C3, however, extended to different ancillary services.	Unique Contribution
C6	In this paper, suitable overloading method among the two methods given in C4 are selected for fast primary frequency control (FPFC) from OWPPs connected through multi-terminal DC grid considering the operation of the WT at below rated wind speed. Proved the concept by simulation and experimental validations	Secondary effects on AC and DC grid due to release of overloading is predominant at just below rated wind speed. Two possible methods for WT overloading have been given in C4. In this paper, the methods presented in C4 are applied to OWPP connected through 3-terminal DC grid and suitable overloading method is proposed based on the simulations and experimental results. The recommendation is made considering the extended duration of overload (more than 10 s) as well.	Utilized methods given in C4 and applied to OWPP in MTDC grid. Both simulation and experimental validations are given.
J1	In this paper a coordinated droop voltage control for cluster of offshore	The study is done for two cases as; (1).Coordination of reactive power flow between HVDC converter and the WPP cluster using droop method while	Unique Contribution

		providing offshore AC grid voltage control, and (2). Coordinated closed loop control between the HVDC and the WPPs while the cluster is providing Power Oscillation Damping (POD) via active power modulation. It is shown that the coordinated cluster control helps to improve the steady-state and dynamic response of the offshore AC grid in case of offshore AC grid voltage control and onshore ancillary services provision, i.e. POD by the active power modulation of the cluster.	
	WPPs connected to the same HVDC connection is proposed. Power Oscillation damping provision by OWPP has also been analyzed.		
J2	Coordinated Voltage Control Scheme (CVCS) for cluster of OWPPs connected to common HVDC station which improves steady state and dynamic performance of offshore AC grid while minimizing losses is presented.	The developed CVCS comprehends an optimization algorithm, aiming for minimum active power losses in the offshore grid, to generate voltage reference to the Pilot bus. During the steady-state operation, the Pilot bus voltage is controlled by dispatching reactive power references to each wind turbine (WT) in the wind power plant cluster based on their available reactive power margin and network sensitivity-based participation factors, which are derived from the dV/dQ sensitivity of a WT bus w.r.t. the Pilot bus. This method leads to the minimization of the risk of overvoltage at the terminals of the WT located far away from the AC collector substation, by dispatching lower reactive power references compared with the ones nearer to the substation. In addition, this paper proposes a control strategy for improved voltage ride through (VRT) capability of WTs for faults in the offshore grid (3 faults are studied), thus leading to improved dynamic voltage profile in the offshore AC grid.	This paper is an extension to C2. In C2, only collector cable fault is considered, where as in this paper WT terminal fault, export cable faults have also been considered. Additionally, a method for dynamic reactive current dispatch to improve offshore AC grid VRT has been proposed.
J3	Coordinated fast primary frequency control scheme for OWPP in MTDC grid considering the overloading the WT at different wind speeds.	The impact of wind speed on the OWPP active power output and thus on the AC grid frequency and DC grid voltage is analyzed at (1) above rated (2) Just below rated wind speeds. The removal of active power support from OWPP after the frequency control action may result in second frequency and DC voltage dips. Three different methods to mitigate these secondary effects are proposed, such as, (i) Varying the droop gains of the HVDC converter (ii) Releasing the active power support from OWPP with a ramp rate limiter and (iii) An alternative method for the wind turbine overloading considering rotor speed.	This paper is extension of paper C4, where the secondary effects due to removal of active power support have been highlighted. In this paper (J3), three different secondary effect mitigation methods are proposed.
J4	Two methods for frequency control:	The proposed frequency control methods are verified through simulations on a	The communication based

	(1) Communication based method (2) Coordinated Control, from OWPPs in MTDC System are presented and experimentally validated.	test set up having OWPP connected to 3-terminal DC grid using DIgSILENT PowerFactory. Moreover, these methods are validated experimentally on a laboratory scaled 3-terminal HVDC grid. The simulation and experimental results prove that, with the proposed control strategies, OWPPs and other converters in the MTDC grid can participate in frequency control and improve the onshore grid frequency.	method validation is unique to this paper. Comparison between communication and coordinated control is also unique. Operation of OWPP at above rated wind speed is only considered. Experimental validation adds strength to the paper.
J5	The kinetic energy of the WTs is utilized by overloading them to extract additional active power support for FPFC of the AC grid. Impact of release of kinetic energy support from OWPPs at different wind speeds (above, below and low) on the AC and DC grids is validated using simulations and experimental test. .	The impact of overloading the wind turbine on the frequency control and impact of release of overloading on the AC and DC grids are studied considering the operation of the wind turbine at different wind speeds. The impact of overloading the WTs are validated with time domain simulations, using DIgSILENT PowerFactory, on an OWPP connected through a 3-terminal DC grid. Moreover, the simulation results are validated with experiment tests, performed on an OWPP connected through a laboratory scaled 3-terminal DC grid. This paper is experimental validation of paper J3. Frequency control from WPPs at low wind speeds is also addition contribution of this paper.	Experimental validation of J3 (except secondary effects mitigation methods) with the extension of low wind speed operation, as an additional contribution.

Chapter 7
Conclusions and Future Work

This chapter summarizes the overall conclusions of the PhD thesis and also provides the directions for future research.

7.1 Conclusions

Depletion of fossil fuels, increased concerns for environmental impact, and developed technology are encouraging the integration of wind power into electrical power system. Due to the available potential for the offshore wind in the North Sea and to interconnect different countries and synchronous areas, the North Sea countries are planning to install many large OWPPs in near future interconnected through MTDC grid. The integration of clusters of OWPPs to common HVDC station and the increased penetration of OWPPs replacing the conventional synchronous machines poses several challenges to the operation of offshore and onshore AC grids, respectively. Amon them, reactive power and voltage control in the offshore AC grid and frequency control in the onshore AC grid are the two important concerns. In this thesis, the control strategies for reactive power and voltage control in the offshore AC grid with the cluster of OWPPs connected to a common HVDC station have been developed. The methods for onshore AC grid frequency control from OWPPs connected though MTDC system has also been developed. Moreover, the impact of wind speed on the FPFC is also studied by considering the operation of the WTs at different wind speed. The conclusions of the study in this thesis are summarized as given below.

- Three methods for reactive power and AC voltage control in the cluster of OWPPs connected to common HVDC station are proposed in this study: (1) voltage control with a droop (29 coordinated reactive power control, and (3). coordinated voltage control.

- With individual voltage control at each OWPP, an uncontrolled reactive power flow occur, whereas, the voltage controller with a droop at OWPPs provides fair reactive

power share between the different OWPPs and HVDC converter, which leads to minimization of losses in the offshore AC grid compared to individual WPPs voltage control scheme. However, the voltage set points to individual WPPs are not optimized to minimize the losses.

- An alternative method for reactive power control and dispatch in the offshore AC grid, called coordinated reactive power control scheme, controls the reactive power at the point of connection of the OWPPs cluster, whose reference is generated by an optimization algorithm aimed at minimum active power losses in the offshore AC grid. In this method, the reactive power dispatch is performed according to the available reactive power margin of the WTs. This method ensures improved reactive power control and dispatch in the offshore AC grid with minimized losses compared to the voltage control with a droop method. However, this method sometimes may result in over voltages at the WTs located in the end of the collector cable, particularly when equal reactive power references are dispatched to all the WTs across the collector cable. To address these challenges, and to improve dynamic performance of the offshore AC grid, the third method, called coordinated voltage control scheme is recommended.

- In case of coordinated voltage control scheme, during the steady state operation, it generates reactive power references to each WT based dV/dQ sensitivity of the WT bus w.r.t the Pilot bus (the bust with higher short circuit capacity) along with their available reactive power margin. This method leads to minimise the risk of undesired over voltage at the WT terminals far from the substation while minimizing the active power losses in the offshore AC grid. Also, this method improves the dynamic voltage profile of the offshore AC grid in case of faults in the offshore AC gird by sending dynamic reactive current references to the WTs based on the voltage measurements at the pilot bus. In case of voltage control at each OWPP, the controller can observe only the terminal voltage of individual WPP/WT rather than the overall system voltage profile, and therefore would respond mainly on the basis of local voltage measurement. It is important to mention that in the coordinated voltage control scheme, the local reactive power/voltage controllers at WTs are still in place; however their response is controlled and coordinated by the overall cluster controller, providing better steady state and dynamic response of the offshore AC grid.

- Two methods for frequency control from OWPPs in MTDC grid: (1) communication based frequency control (2) coordinated frequency control are presented. The proposed frequency control methods are tested for both under and over frequency events with

different power flows in the DC grid. The time domain simulations using PowerFactory and experimental results on 3-terminal laboratory scaled DC grid test set up prove that the OWPPs in MTDC grid can participate in onshore AC grid frequency control by using the two methods. Moreover, with coordinated control, it is proved that the DC voltage can be used as medium of imbalance for the onshore AC grid frequency events, without depending on the communication methods to represent the onshore frequency events at offshore AC grid. If the size of the DC link is small (2 or 3 converters, for example), the communication based frequency control can be preferred. However, for larger DC grids with more number of converters, the coordinated control is advantageous compared to communication based method, considering the reliability and dynamics of DC grid voltage.

- The participation of OWPPs in fast primary frequency control of the power system by overloading the WTs for few seconds after the frequency event to utilize their kinetic energy has also been studied in this thesis. Two different methods for overloading have been proposed. It has been observed that the performance can be improved in case the frequency initiated power reference is based on the actual power output (Internal) instead of the constant pre-overloading power output of the WT (External). Moreover, a systematic approach to optimize the gains of the fast primary frequency controller over the whole wind speed range considering the limitations and dynamics of the WT have been proposed and analysed. Based on the simulation results, Internal method for overloading the WTs provides better performance for fast primary frequency control compared to external method.

- The possibility for fast primary frequency control from OWPPs in MTDC grid by overloading the WTs has also been studied in this thesis. The impact of wind speed on the frequency control and the corresponding impact on DC grid voltage during and after the frequency control period have also been studied. Secondary dips in DC voltage and frequency are resulted due to the release of WT overloading (hence the active power support for frequency control).Three methods to mitigate the impact of second frequency and DC grid voltage dips after the frequency support are proposed and analyzed. The first method is varying the droop gains of the HVDC converter based on the wind speed forecast whereas the second method is based on smooth release of active power support from WPPs with a ramp rate limiter. The final method is using an alternative way of overloading the wind turbine which considers the effect of rotor speed on the overloading power output. The effectiveness of the individual and combination of the proposed methods is investigated based on simulations and experimental tests on a 3-terminal DC

grid. The ramp rate limiter on the WT ensures smoother dynamics of the WT during the release of overloading which partially helps to mitigate the secondary effects on frequency and DC grid voltage. Smoother dynamics may result in reduced stress on the mechanical parts of the WT. The overloading method of the WT which considers the variation of rotor speed and hence the actual power output during the overload (Internal method), helps to minimize the secondary effects. The combination of this overloading method and the ramp rate limiter further helps to minimize the secondary effects of frequency control from offshore wind power plants and seems to be the best option for fast primary frequency control from OWPPs in MTDC grid.

7.2 Future Work

- The simulation model is being used in this thesis for OWPP to perform frequency control experiments. The test may be performed on an actual variable speed WT connected to MTDC grid to study the actual impact of overloading on the WT dynamics and therefore on the fast primary frequency control.

- In this study, the model of the test AC grid is also programmed inside the DSP of Conv-1, and measurement of change in frequency is used to implement the control, instead of actual frequency measurements. Therefore, alternative options to represent the test AC grid have to investigate where the controls are based on actual frequency measurements. In reality, the accurate frequency measurement requires few 100 ms.

- Variable wind speed time series can be used as input to study the effectiveness of the proposed frequency control methods for onshore AC grid and AC voltage control in the offshore AC grid with cluster of OWPPs connected to common HVDC station.

- More detailed investigation on the DC grid voltage control service from OWPPs can be performed considering the ramp rate limitation of the active power output of the WTs.

- The impact of DC grid protections including the fast DC breakers on the ancillary services for AC and DC grids shall be investigated.

References

[1] European Commission, "DIRECTIVE OF THE EUROPEAN PARLIAMENT AND OF THE COUNCIL on the promotion of the use of energy from renewable sources (recast)," November 2016, [Online]. Available: https://ec.europa.eu/energy/sites/ener/files/documents/1_en_act_part1_v7_1.pdf

[2] Energy Research Centre of the Netherlands (ECN), "Renewable Energy Projections as Published in the National Renewable Energy Action Plans of the European Member States Summary report," ECN, Technical Report Feb 2011, [Online]. Available: http://ledsgp.org/wp-content/uploads/2015/10/renewable-energy-projections.pdf

[3] European Wind Energy Association, "Wind Energy Scenarios for 2020," Technical Report July 2014, [Online]. Available: https://windeurope.org/fileadmin/files/library/publications/reports/EWEA-Wind-energy-scenarios-2020.pdf

[4] European Wind Energy Association, "Wind Energy Scenarios for 2030," Technical Report August 2015, [Online]. Available: https://windeurope.org/fileadmin/files/library/publications/reports/EWEA-Wind-energy-scenarios-2030.pdf

[5] Political Declaration on energy cooperation between the North Seas Countries, [Online]. Available: http://www.benelux.int/files/9014/6519/7677/Political_Declaration_on_Energy_Cooperation_between_the_North_Seas_Countries.pdf

[6] EWEA. Wind in power: 2014 European statistics. Technical Report. European Wind Energy Association (EWEA); 2015. [Online] Available: https://windeurope.org/wp-content/uploads/files/about-wind/statistics/EWEA-Annual-Statistics-2015.pdf

[7] ABB AB Grid Systems - HVDC, "HVDC Light - It's time to connect," ABB, Ludvika, Technical Report, December[Online] Available: https://library.e.abb.com/public/2742b98db321b5bfc1257b26003e7835/Pow0038%20R7%20LR.pdf

[8] D. Van Hertem, M. Ghandhari , "Multi-terminal VSC HVDC for the European Supergrid: Obstacles," Renewable and Sustainable Energy Reviews, vol 14, pp 3156–3163, Dec 2010

[9] D. Van Hertem, O. Gomis-Bellmunt and J. Liang, HVDC Grids: For Offshore and Supergrid of the Future, IEEE Press Series on Power Engineering, Ed. John Wiley & Sons, 2016.

[10] TWENTIES project, "Final report-short version, June 2013, [Online]. Available: http://www.ewea.org/fileadmin/files/library/publications/reports/Twenties_report_short.pdf

[11] N.A. Cutululis, L. Zeni, W.Z. El-Khatib, J, Holbøll, P.E. Sørensen, G. Stamatiou, O. Carlson, V.C. Tai, K. Uhlen, J. Kiviluoma, T., Lund, "Challenges Towards the Deployment of Offshore Grids: the OffshoreDC

Project". Proceedings of 13th International Workshop on Large-Scale Integration of Wind Power into Power Systems as well as on Transmission Networks for Offshore Wind Power (WIW 2014). Energynautics GmbH, 2014.

[12] Multi-terminal DC grid for offshore wind (MEDOW), [Online]. Available: http://sites.cardiff.ac.uk/medow/

[13] A. Abdalrahman, E. Isabegovic, " DolWin1 - Challenges of connecting offshore wind farms*", Proc.. IEEE International Energy Conference*, Apr 2016

[14] V. C. Tai and K. Uhlen, "Design and Optimisation of Offshore Grids in Baltic Sea for Scenario Year 2030," EERA DeepWind'2014, Energy Procedia, vol. 53, pp. 124–134, 2014

[15] Siemens SylWin1 Press Release, [online] Available: http://www.siemens.com/press/en/pressrelease/?press=/en/pressrelease/2015/energymanagement/pr2015040192emen.htm&content[]=EM

[16] D. M. Larruskain, I. Zamora1, A. J. Mazon, O. Abarrategui, J. Monasterio, "Transmission and Distribution Networks: AC versus DC", Proc. Solarec-2005, pp 1–6, 2005.

[17] R. Irnawan, K. Srivastava, M. Reza, "Fault detection in HVDC-connected wind farm with full converter generator", *Int. Jounrnal Elect. Power Energy Syst.*, vol. 64, pp. 833-838, Jan. 2015.

[18] E. Muljadi, N. Samaan, V. Gevorgian, J. Li, and S. Pasupulati, "Short circuit current contribution for different wind turbine generator types," in Power and Energy Society General Meeting, 2010 IEEE, pp. 1 - 8, july 2010.

[19] O. Gomis-Bellmunt, , F.Hassan, C.Barker, A. Egea-Alvarez, "Capability curves of a VSC-HVDC connected to a weak AC grid considering stability and power limits". *Proc. 11th IET International Conference on AC and DC Power Transmission*, ,2015

[20] UCTE, "Operation Handbook,", Union for the Co-ordination of Transmission of Electricity, Tech. Rep. June 2004.

[21] ENTSO-E. Entso-e network code for requirements for grid connection applicable to all generators, available online: ⟨https://www.entsoe.eu/⟩ [accessed 26.04.2013].

[22] EWEA. EU energy policy to 2050: Achieving 80–95% emission reductions. Technical Report. European Wind Energy Association (EWEA);2011. [online] Available: http://www.ewea.org/fileadmin/files/library/publications/reports/EWEA_EU_ nergy_Policy_to_2050.pdf.

[23] J. Fortmann, M. Wilch, F. W. Koch, I. Erlich, "A novel centralised wind farm controller utilising voltage control capability of wind turbines", *Proc. PSCC Power Syst. Comput. Conf.,* pp. 914-919, 2008

[24] A. D. Hansen, P. E. Sørensen, F. Iov, F. Blaabjerg, "Centralised power control of wind farm with doubly fed induction generators", Renewable Energy, vol. 31, no. 7, pp. 935-951, 2006

[25] B. Karthikeya, R. Schutt, "Overview of wind park control strategies", *IEEE Trans. Sustain. Energy*, vol. 5, no. 2, pp. 416-422, Apr. 2014.

[26] J. C. Boemer, A. A.van der Meer, B. G.Rawn, R. L.Hendriks, A. R. Ciupuliga, M. Gibescu, W. L. Kling, J. A. Ferreira, "Fault ride-through requirements for onshore wind power plants in Europe: The needs of the power system," *IEEE Power and Energy Society General Meeting,* pp.1-8, 24-29 July 2011.

[27] I. Erlich, U. Bachmann, "Grid code requirements concerning connection and operation of wind turbines in Germany," *IEEE Power Engineering Society General Meeting,* pp. 1253- 1257 Vol. 2, 12-16 June 2005.

[28] Ö. Göksu, R. Teodorescu, P. Rodriguez, and L. Helle, "A Review of the State of the Art in Control of Variable-Speed Wind Turbines," *9th International Workshop on Large-Scale Integration of Wind Power into Power systems as well as on Transmission Networks for Offshore Wind Power Plants*, Quebec, Canada, October 2010.

[29] M. Altin, O. Goksu, R. Teodorescu, P. Rodriguez, B.-B. Jensen, and L. Helle, "Overview of recent grid codes for wind power integration," in *12th Int. Conf. on Optimization of Electrical and Electronic Equipment,* pp. 1152–1160, May 2010.

[30] M. Tsili and S. Papathanassiou, "A review of grid code technical requirements for wind farms," *IET Renew. Power Gener.*, 3, (3), pp. 308–332, 2009.

[31] Eon Netz GmbH, "Grid code high and extra high voltage", online: http://www.eon-netz.com/, 2006.

[32] J. Fortmann, L. Cai, S. Engelhardt, J. Kretschmann, "Wind turbine modeling LVRT field test and certification", *Proc. IEEE Power Energy Soc. Gen. Meet.*, pp. 1-7, Jul. 2011.

[33] Babak Badrzadeh, Andrew Halley, "Challenges Associated With Assessment and Testing of Fault Ride-Through Compliance of Variable Power Generation in Australian National Electricity Market", *Sustainable Energy IEEE Transactions on*, vol. 6, pp. 1160-1168, 2015, ISSN 1949-3029.

[34] L. Faiella, N.A. Cutululis, F.Van Hulle, "Technical Capabilities and Challenges for Wind Power to provide Voltage Support Services" *Proc. 12th International Workshop on Large-Scale Integration of Wind Power into Power Systems as Well as on Transmission Networks for Offshore Wind Power ,* Sep 2013.

[35] D. Van Hertem, M. Ghandhari , "Multi-terminal VSC HVDC for the European Supergrid: Obstacles," *Renewable and Sustainable Energy Reviews*, vol 14, pp 3156–3163, Dec 2010

[36] Wind Turbines—Part 27-1: Electrical Simulation Models - Wind Turbines, IEC Standard 61400-27-1 ed. 1, Feb. 2015

[37] E. Muljadi et al. "Method of equivalencing for a large wind power plant with multiple turbine representation, "*in Proc. 2008 IEEE Power and Energy Society General Meeting*, pp-1-8.

[38] J. Dragosavac, Ž. Janda, J.V. Milanović,, "Coordinated Reactive Power-Voltage Controller for Multimachine Power Plant", *IEEE Transactions on Power Systems*, vol. 27, No. 3, pp 1540 - 1549, 2012.

[39] M. Altin, Teodorescu, R. Bak-jensen, P.Rodriguez, F.Iov, P. C. Kjær, "Wind Power Plant Control - An Overview", *Proc. 12th International Workshop on Large-Scale Integration of Wind Power into Power Systems as Well as on Transmission Networks for Offshore Wind Power ,* 2012.

[40] H. Lefebvre, D. Fragnier, J.Y. Boussion, P. Mallet, and M. Bulot, "Secondary coordinated voltage control system: feedback of EDF, " in *Proc. 2000 IEEE Power Engineering Society General Meeting*, pp. 290-295.

[41] A. Conejo, M. J. Aguilar, "Secondary voltage control: Nonlinear selection of pilot buses design of an optimal control law and simulation results", *Proc. IEE Gener. Trans. Distrib*., vol. 145, pp. 77-81, Jan. 1998.

[42] P. Lagonotte, J. C. Sabonnadiere, J. Y. Leost, and J. P. Paul, "Structural analysis of the electrical system: Application to secondary voltage control in France," IEEE Trans. Power Syst., vol. 4, pp. 479–486, May 1989.

[43] P. Kundur, "Power system stability and control," New York: McGraw? Hill, 1994.

[44] EirGrid. Eirgrid grid code version 4.0, available online: ⟨http://www.eirgrid. com⟩

[45] ENTSO-E. Operational handbook; policies; load-frequency control and performance, available online: ⟨https://www.entsoe.eu/⟩; 2009 [accessed 26.11.2016].

[46] Verb and der Netzbetreiber - VDN - e.V. beim VDEW. Transmission code 2007. Network and system rules of the German transmission system operators, available online: ⟨http://www.vde.com⟩; 2007 [accessed 26.11.2016]

[47] National Grid plc. The grid code, issue 4 revision 13, available online: ⟨http:// www.nationalgrid.com/uk/⟩; 2012 [accessed 26.11.2016].

[48] Brisebois, J., & Aubut, N., "Wind farm inertia emulation to fulfill Hydro-Quebec's specific need", *In Proc 2011 IEEE Power and Energy Society General Meeting, Pages 1–7.*

[49] Duckwitz, D., Shan, M., & Fischer, B., "Synchronous Inertia Control for Wind Turbines Contributions to Power System Inertia*". In Proc 13th Wind Integration Workshop, Nov 2014.*

[50] Fischer, M.,"Operational Experiences with Inertial Response Provided by Type 4 Wind Turbines", *In Proc.13th Wind Integration Workshop, Nov 2014*

[51] Muljadi, E., Gevorgian, V., Singh, M., & Santoso, S." Understanding inertial and frequency response of wind power plants", *In Proc. 2012 IEEE Power Electronics and Machines in Wind Applications, pp-1–8.*

[52] Martinez Sanz, I., Chaudhuri, B., & Strbac, G. "Inertial response from offshore wind farms connected through dc grids" *IEEE Transactions on Power Systems*", vol..30, pp.1518–1527, May 2015

[53] Morren, J., de Haan, S. W. H., Kling, W. L., & Ferreira, J. A." Wind Turbines Emulating Inertia and Supporting Primary Frequency Control", *IEEE Transactions on Power Systems*, vol.21, pp.433–434, Feb 2006.

[54] Wu, L., and Infield, D. G.,"Towards an assessment of power system frequency support from wind plant-modeling aggregate inertial response" *IEEE Transactions on Power Systems*, vol.28, pp.2283–2291, Aug.2013.

[55] Engelken, S., Mendonca, A., and Fischer, M., "Inertial Response with Improved Variable Recovery Behaviour Provided by Type 4 Wind Turbines", 14th Wind Integration Workshop" Oct 2015

[56] Asmine, M., & Langlois, C.-É,." Field measurements for the assessment of inertial response for wind power plants based on Hydro-Québec TransÉnergie requirements", IET Renewable Power Generation, vol. 10, pp.25–32, Oct 2016.

[57] National grid, System Operability Framework (SOF) 2014.

[58] Mufit Altin, "Dynamic frequency response of wind power plants", PhD Thesis, Aalborg University, may 2012

[59] Hansen, A. D., Altin, M., and Iov, F. "Provision of enhanced ancillary services from wind power plants – Examples and challenges. *Renewable Energy*", vol. 97, pp. 8–18, May 2016

[60] K.V. Vidyanandan, Nilanjan Senroy, Primary frequency regulation by deloaded wind turbines using variable droop, IEEE Trans. Power Syst. 28 (2) (MAY 2013) 837

[61] S. Wachtel, A. Beekman, " Contribution of Wind Energy Converters with Inertia Emulation to frequency control and frequency stability in power systems" in Proc. 2009 8th Wind Integration Workshop, pp. 1-6

[62] A. D. Hansen, M. Altin, et al, "Analysis of short-term over production capability of variable speed wind turbines," Renewable Energy, vol. 68, 2014

[63] A. D. Hansen, I. Margaris, G. C. Tarnowski and F. Iov,"Simplified type 4 wind turbine modeling for future ancillary services," in Proc. 2013 European Wind Energy Conference, pp. 768-774.

[64] Hafiz, F., and Abdennour, A. "Optimal use of kinetic energy for the inertial support from variable speed wind turbines". *Renewable Energy*, vol.80, pp.629–643

[65] B. Silva, C. L. Moreira, et al., "Provision of Inertial and Primary Frequency Control Services Using Offshore Multiterminal HVDC Network", IEEE Trans. on Sustainable Energy, vol. 3, pp. 800-808, Oct 2012.

[66] Inmaculada Martínez Sanz, Balarko Chaudhuri, et al., "Inertial Response From Offshore Wind Farms Connected Through DC Grids", IEEE Trans. on Power Systems, vol. 30, pp. 1518-1527, May 2015.

[67] Y. Phulpin,"Communication-free inertia and frequency control for wind generators connected by an HVDC link," IEEE Trans on Power Systems, vol. 27, pp. 1136-1137, May 2012.

[68] Adrià Junyent-Ferré, Yousef Pipelzadeh, Tim C. Green, "Blending HVDC-Link Energy Storage and Offshore Wind Turbine Inertia for Fast Frequency Response", IEEE Trans. on Sustainable Energy, vol. 6, pp. 1059-1066, July 2015.

[69] L. Zeni, I. Margaris, A. Hansen, P. Sørensen and P. Kjær, "Generic Models of Wind Turbine Generators for Advanced Applications in a VSC-based Offshore HVDC Network," in Proc. 2012 10th IET Conference on AC/DC Transmission, Birmingham..

[70] S. Nanou, S. Papathanassiou,"Evaluation of a communication-based fault ride-through scheme for offshore wind farms connected through high-voltage DC links based on voltage source converter," IET Rene. Power Generation, , pp. 1-10, Jan 2015.

[71] L. Zeni, B. Hesselnæk, P.E.Sørensen, A.D.Hansen, P.C.Kjær,"Power System Services from VSC-HVDC Connected WPPs: an Overview" in Proc. 2015 14th Wind Integration Workshop, pp. 1-5.

[72] B. Silva,C. L. Moreira, et al,"Control strategies for AC Fault Ride Through in Multiterminal HVDC Grids" IEEE Trans. Power Delivery, vol. 29, Feb 2014

[73] L. Zeni, "Power System Integration of VSC-HVDC connected Offshore Wind Power Plants " Ph.D thesis, DTU, Denmark, 2015.

[74] F. Tham , J. A. Suul, S. D'Arco, M Molinas, and F. W. Fuchs, "Stability of DC voltage droop controllers in VSC HVDC systems" In Proc. 2015 IEEE PowerTech conference, Eindhoven, pp:1-6

[75] F. Tham , R. Eriksson,and M Molinas," Interaction of Droop Control Structures and its inherent effect on the power transfer limits in multi-terminal VSC-HVDC ". In Proc. IEEE Transactions on Power Delivery, To be published.

[76] H.Støylen, K.Uhlen, A. R. Årdal , "Laboratory Demonstration of Inertial Response from VSC-HVDC connected Wind Farms,", in Proc. 2015 11th IET Conference on AC/DC Transmission,

[77] R.E Torres-Olguin, A.R.Ardal, H.Støylen, K.Uhlen, et. al , "Experimental verification of a voltage droop control for grid integration of offshore wind farms using multi-terminal HVDC ,"Energy Procedia, vol.53, 2014

[78] H. Stylen, K. Uhlen, A.R. rdal, K. Sharifabadi, "Laboratory demonstration of an offshore grid in the North Sea with DC droop control", Ecological Vehicles and Renewable Energies (EVER) 2014 Ninth International Conference on, pp. 1-8, 25-27 March 2014.

[79] Y.Li, X.Shi, B.Lio, et al , "Hardware Implementation of a Four-Terminal HVDC Test-Bed ," in Proc. 2015 IEEE Energy Conv. Congress and Exposition pp.5363-5370

Appendix: Publications

C1 Jayachandra N. Sakamuri, Rather Z.H., Cutululis N.A., Rimez J., "Dynamic Reactive Power Control in Offshore HVDC Connected Wind Power Plants ", Presented at 14th Wind Integration Workshop, Brussels,2015

This page would be intentionally left blank if we would not wish to inform about that.

Dynamic Reactive Power Control in Offshore HVDC Connected Wind Power Plants

Jayachandra N. Sakamuri,
Nicolaos A. Cutululis
Department of Wind Energy
Technical University of Denmark
e-mail: jays@dtu.dk

Zakir Hussain Rather
Electricity Research Centre
University College Dublin
Ireland
e-mail: zakirrather@gmail.com

Johan Rimez
Elia System Operator
Belgium
e-mail:Johan.Rimez@elia- engineering.com

Abstract—**This paper presents a coordinated reactive power control for a HVDC connected cluster of offshore wind power plants (WPPs). The reactive power reference for the WPP cluster is estimated by an optimization algorithm aiming at minimum active power losses in the offshore AC Grid. For each optimal reactive power set point, the OWPP cluster controller generates reactive power references for each WPP which further sends the AC voltage/ reactive power references to the associated WTs based on their available reactive power margin. The impact of faults at different locations in the offshore grid, such as wind turbine (WT) terminal, collector cable, and export cable, on the dynamic voltage profile of the offshore grid is investigated. Furthermore, the dynamic reactive power contribution from WTs from different WPPs of the cluster for such faults has also been studied.**

Keywords- offshore wind power plant; reactive power control; HVDC; offshroe grid faults

I. INTRODUCTION

During the past decade, there has been a significant penetration of offshore wind power plants (OWPPs) into power systems and such a trend is expected to continue in the future [1]. Power from offshore wind power plants (OWPPs) is traditionally transported to the mainland grid through submarine high voltage AC (HVAC) cables [2]. However, due to increased power output from OWPP and long distances from the shore, voltage source converter based HVDC (VSC- HVDC) systems have become a more feasible and economical solution for bulk power transmission to the onshore grid [3]. Among available wind turbine technologies, full scale power converter-based variable speed wind turbines (WT) are becoming more prevalent due to their inherent flexible and independent control of active and reactive power and their adaptability to variable wind speeds [4]. Furthermore, due to the anticipated increase in offshore WPPs, it is likely that a cluster of WPPs may be connected to the mainland grid by a common HDVC transmission system for various techno-economic reasons, such as low capital cost, lower losses and more reliability, thereby forming a common interlinked AC offshore grid.

As the HVDC system decouples OWPPs from the onshore Grid, the offshore AC grid becomes more vulnerable to dynamic voltage events due to less short circuit power contribution from power electronic interfaced variable speed WTs and HVDC converter [5]-[6]. Therefore, it is imperative to investigate the impact of offshore AC grid faults on the dynamic voltage profile of WPP cluster, and therefore on the power flow to the onshore Grid. Furthermore, a significant number of studies have investigated the fault ride through capability for offshore HVDC connected wind power plants for faults in the onshore grid [7]-[9]; the fault current contribution from offshore WPPs for the faults in the offshore grid and its impacts on fault ride through capability of the offshore grid has received limited attention. Fault response and protection of a HVDC connected wind farm for internal wind farm faults and in the HVDC link has been studied in [10]. This study is only focusses on WT internal faults and a single aggregated WT model is considered to represent the complete WPP, and therefore the response of non-faulted WT inside the WPP has not been analyzed.

This paper models a WPP cluster to the level of detail required to analyze the impact of faults at different locations within a WPP on the dynamic behavior of WTs of the faulted and non-faulted WPPs of the cluster. A Coordinated Reactive Power Controller (CRPC) for the cluster is proposed in this paper, whose reference reactive power set points are generated by an optimization algorithm aimed at the minimization of losses in the offshore Grid. The CRPC generates reactive power references for each WPP within the cluster based on their available reactive power margin. An AC voltage droop controller is adopted in each WPP reactive power controller to limit/enhance the reactive power contribution based on the voltage profile at WPP collector substation, which improves the reactive power support during dynamical events. The remainder of the paper is organized as follows. Section – II describes modeling of offshore HVDC connected cluster of WPP. The proposed coordinated reactive power control scheme is presented in section III. Simulation and analysis of results for different offshore grid faults is presented in section IV and the concluding remarks along with the scope for the future work is presented in section V.

II. MODELING OF OFFSHORE HVDC CONNECTED WPP CLUSTERS

An OWPP cluster comprised of four WPPS with total capacity of 800 MW connected to the onshore grid through a VSC-HVDC link is considered in this study.

A. WPP Layout

The 800 MW offshore WPP cluster with four 200 MW

69

WPPs, connected to four AC collector substations marked as A1B1, A2B2, C1D1, and C2D2 respectively, is shown in Fig. 1. These substations are located at respective distances of 7 km, 12, km, 17 km, and 22 km from the offshore HVDC converter station. Each 200 MW WPP is composed of four parallel WT strings; each of 50 MW capacity, with each string consisting of 8 numbers of series connected 6.25 MW WTs. Wind turbines are placed with an inter-machine distance of 1.2 km which is approximately equal to seven times the rotor diameter.

Fig.1 Offshore HVDC Connected Cluster of WPPs

B. AC Collector Substation

Each AC collector substation is fed in by four 33 kV WT collector cables connected to a power transformer secondary side. The cables between WT5- WT8 (i.e. the farthest from the substation) have current rating of 0.5 kA, while the cables between WT5 and the collector bus are rated at 1 kA with each power transformer of 33/155 kV, 240 MVA capacity. Technical data for the cables has been taken from ABB's cable data handbook [11].

C. WPP Model

While a detailed modelling of WPP can provide more insight into the system , consideration of a detailed model of WPP however, increases the computational burden. Therefore, one string of the WPP-A1B1 is modelled in detail while the rest of the WPPs are represented by aggregate models without compromising the accuracy of results. One of the WT collector cable (8 machines, a total of 50 MW capacity) in WPP-A1B1 has been modeled in detail, while the remaining WTs in that WPP are represented by an aggregated model of 50 MW capacity for A1 (9-16) feeder and 100 MW for B1 (1-16) feeders. The rest of the WPPs are aggregated with each of 100 MW capacity. The aggregation method for WTs and export cables of a WPP has been adopted from [12], [13].

D. WT Model

A full scale converter based detailed WT (Type-4) model considered in this work has been adopted from IEC 61400-27 – Part 1 [14]. In order to precisely estimate the available active power output and reactive power margin of a WT for the given wind speed, the adopted WT model is extended to include aerodynamic and pitch controller models, the schematic of the overall model is shown in Fig.

2. Active and reactive power references, to WT (discussed in section-III) are obtained from the WPP controller.

Fig.2 Type IV wind turbine model structure

E. HVDC System Model

The HVDC system considered is a 850 MVA VSC-HVDC transmission link, the voltage levels are 380 kV line-to-line on the AC side and ±320 kV on the DC link. The standard pulse width modulation (PWM) based converter model has been adopted for the offshore and onshore HVDC converters. Power balance over the HVDC link to maintain the DC link voltage at its optimal value, is assigned to the onshore HVDC converter controller, as shown in Fig.3. It also controls reactive power/AC Voltage at the converter bus as per grid code regulations. The current references provided by the outer controllers are then handled by a standard inner current controller operating in the d-q reference frame. The offshore HVDC converter, shown in Fig.3, is assigned with the control of AC voltage at the offshore HVDC converter station (AC_Control_WF bus in Fig. 1), sets the frequency of the offshore AC network, and thus allows the active power transfer from the WPPs to the HVDC system. Similar to the onshore HVDC converter, the current references provided by the outer controllers are handled by a standard inner fast current controller operating in the d-q reference frame.

Fig.3 Onshore and Offshore HVDC Converter Control

III. COORDINATED REACTIVE POWER CONTROL SCHEME FOR OFFSHORE WPP CLUSTER

The schematic of the proposed coordinated reactive power control scheme for offshore HVDC connected 70

cluster of WPPs is shown in Fig.4. The reactive power is controlled at the WPP side of HVDC converter transformer, which can be considered as Point of Connection (POC) bus for the WPP cluster. The optimal reference reactive power set point at the POC bus, $Q_{ref\_opt}^{POC}$, is generated from an optimization algorithm with minimum active power losses in the offshore AC Grid as the objective function. This algorithm, the operation of the CRPC scheme is further described in the subsections to be followed.

A. Optimization considering wind speed variation

The optimal reactive power reference desired at the POC bus, $Q_{ref\_opt}^{POC}$, is dispatched at regular intervals from the optimization program. Based on wind forecast, real power output from each wind turbine is estimated and fed in to the optimization program and the optimization problem is in turn solved to estimate optimal reactive power reference for the POC bus. The optimization problem is formulated as a loss minimization problem as defined in (1-8).

$$\min f(x) \tag{1}$$

such that

$$h(x) = 0; \tag{2}$$
$$g^{\min} \le g(x) \le g^{\max} \tag{3}$$
$$y^{\min} \le y \le y^{\max} \tag{4}$$

Where,

$$f(x) = P_{loss}(x) \tag{5}$$

$h(x)$ and $g(x)$ are a set of equality and inequality constraints, and 'y' is a set of control parameters. Active and reactive power balance equations representing set of equality constrains, is given in (6), while (7) and (8) are inequality constraints of the system. Control variable parameter limits are given in (A)

$$h(x) = \begin{cases} P_g^j - P_l^j - \sum_{j=1}^{Nb} P_{inj}^j = 0 \\ Q_g^j - Q_l^j - \sum_{j=1}^{Nb} Q_{inj}^j = 0 \end{cases} \tag{6}$$

Where, P_g^j, P_l^j are active power generation and load at bus j. Q_g^j, Q_l^j are reactive power generation and load at bus j. P_{inj}^j, Q_{inj}^j are active and reactive power injection from adjacent nodes at bus j.

$$V_j^{\min} \le V_j \le V_j^{\max} \tag{7}$$

The power flow over a transmission line is not uniform due to its inductive and capacitive parameters. Therefore, in order to limit the actual design parameter of a branch, current limits have been considered instead of power flow limits.

$$\max\left(\left|I_{i1}\right|, \left|I_{i2}\right|\right) \le I_{\max}^i \tag{8}$$

where, I_{i1}, I_{i2} are current in branch i, measured at the two respective terminals of the branch.

$I_{\max}^i$; Maximum current allowed in i^{th} branch.

$$Q_{gj}^{\min} \le Q_{gj} \le Q_{gj}^{\max} \tag{9}$$

$Q_{gj}, Q_{gj}^{\min}, Q_{gj}^{\max}$ are actual reactive power generation, minimum and maximum allowed limit.

The optimisation problem (1-9) is solved through Interior Point Method (IPM). Due to its fast convergence and ease of handling inequality constraints using logarithmic barrier functions, IPM is considered as an efficient method [15].

B. Operation of the CRPC Scheme

Based on wind forecast, optimal reactive power set points at the POC bus can be obtained from the optimization algorithm for each operating condition and fed in as the reference value to the CRPC. Alternatively, for a range of operating conditions covering vast majority of possible operating states of the WPP cluster, optimal reference reactive power at the POC bus can be evaluated offline through optimization algorithm and stored in the 'Reference Reactive Power Look up Table' thus using interpolation approach, optimal reactive power for each operating condition is selected from the look up table in real time operation as shown in Fig. 4. Though the former approach is expected to be of higher accuracy as optimal reactive power reference can be calculated based on the latest wind forecast, the later approach can reduce computational burden required in real time operation to run the optimization algorithm continuously for each operating condition, with fairly good accuracy. For a given power output from a WPP, P_{av}, the corresponding optimal reactive power reference at the POC bus, $Q_{ref\_opt}^{POC}$, is communicated to the cluster reactive power controller, which generates required reactive power set point, $Q_{set}^{cluster}$, for the WPP cluster at the WPP collector substation. The 'WPP Cluster Reactive Power Dispatcher' distributes this reactive power references to each WPP within the cluster based on their available reactive power margin. The 'WPP Reactive Power Controller' maintains this reference value from the WPP cluster by sending the reactive power set point, $Q_{set}^{WPP_{A1B1}}$, to the 'WPP Dispatcher', where additional reactive power reference, ΔQ_{ref}^{WT}, and/or voltage reference, ΔV_{ref}^{WT}, are dispatched to all the WTs within the WPP. The additional reactive power reference generated by the AC voltage droop controller, $\Delta Q_{ref}^{WPP_{A1B1}}$, is added to WPP reactive power reference to limit/enhance the reactive power contribution from WPP depending on the voltage deviation observed at WPP collector substation from its base value. This will also ensure proper distribution of reactive power reference among the WPPs in case of communication failure within the cluster reactive power controller.

The mathematical model for the reactive power dispatch within the WPP level is given in (10).

$$\Delta Q_{ref}^{WT_i^j} = \frac{Q_{av}^{WT_i^j}}{Q_{av}^{WPP_j}} * Q_{set}^{WPP_j}$$

$$Q_{av}^{WPP_j} = \sum_{i=1}^{n} Q_{av}^{WT_i^j} \ with : Q_{av}^{WT_i^j} = \sqrt{(S_{Gen}^{WT_i^j})^2 - (P_{av}^{WT_i^j})^2} \tag{10}$$

The reactive power reference for i^{th} WT of jth WPP; $Q_{ref}^{WT_i^j}$, is formulated as a proportional distribution of the dispatched WPP reactive power set point, $Q_{set}^{WPP_j}$, based on the ratio of the available reactive power margin, where $P_{av}^{WT_i^j}$, $Q_{av}^{WT_i^j}$, and $S_{Gen}^{WT_i^j}$ are the available active and reactive powers and the MVA rating of the ith wind turbine, $Q_{av}^{WPP_j}$ is the total available reactive power of the jth WPP. Similarly, the
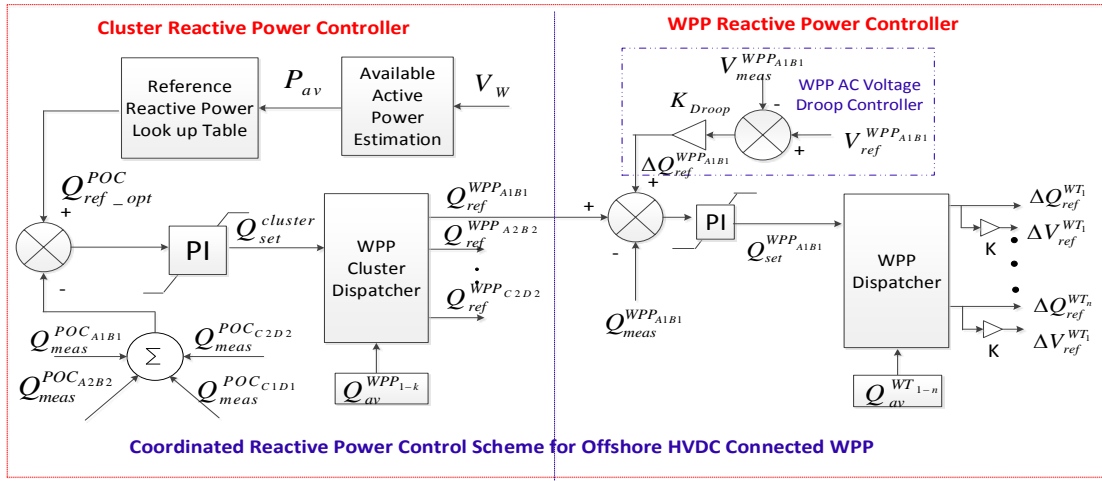
Fig. 4 WPP Cluster Coordinated Reactive Power Control Scheme

mathematical model for the reactive power dispatch at WPP cluster level is given in (11).

$$Q_{ref}^{WPP_j} = \frac{Q_{av}^{WPP_j}}{Q_{av}^{cluster}} * Q_{set}^{cluster}$$

$$Q_{av}^{cluster} = \sum_{j=1}^{k} Q_{av}^{WPP_j} \tag{11}$$

The reactive power reference for each WPP '$Q_{ref}^{WPP_j}$' is formulated as proportional distribution of the WPP cluster reactive power set point, $Q_{set}^{cluster}$, based on the ratio of available reactive power margin. $Q_{av}^{cluster}$ is the total available reactive power of the WPP cluster.

The reactive power / voltage controller at the WT level is shown in Fig. 5. For reactive power control mode of WT, the additional WT reactive power reference from the WPP controller, ΔQ_{ref}^{WT}, together with the initial reactive power reference of the WT, Q_{ref0}^{WT} (determined by the initial load flow), forms reactive power reference for the WT reactive power controller. The outer WT reactive power controller generates voltage reference, V_{refQ}^{WT}, to the WT inner voltage controller. For the voltage control mode of, the additional WT voltage reference from the WPP controller, ΔV_{ref}^{WT}, together with the initial voltage reference of the WT, V_{ref0}^{WT} (determined by the initial load flow), forms the voltage reference 'V_{refV}^{WT}',for the WT voltage controller. The voltage controller in turn generates corresponding base reactive current reference signal, iq_{base}^{WT}, for the WT.

A dynamic event like short circuit fault may result in voltage ride through issues in the offshore AC Grid. As per Grid code regulations [16], WPPs are expected to support the grid by contributing additional reactive power during and after dynamic events in the offshore AC Grid for better voltage recovery of the Grid. Therefore, a Voltage Ride Through (VRT) controller has been implemented at WT level, as shown in Fig. 5, which generates additional reactive current reference, Δiq_{ref}^{WT}, when the voltage at WT terminal deviates from the allowed deadband (normally 0.05 to 0.1 pu). The reactive current reference to the WT,

iq_{cmd}, is the combination of iq_{base}^{WT} and Δiq_{ref}^{WT}. Similarly, the Active power controller (P Controller) generates the active current reference, ip_{cmd}. The priority current limiter then sets the active/reactive current priority depending on the Transmission System Operators (TSO requirement and limits the total current reference to the WT as per the rating of the WT.
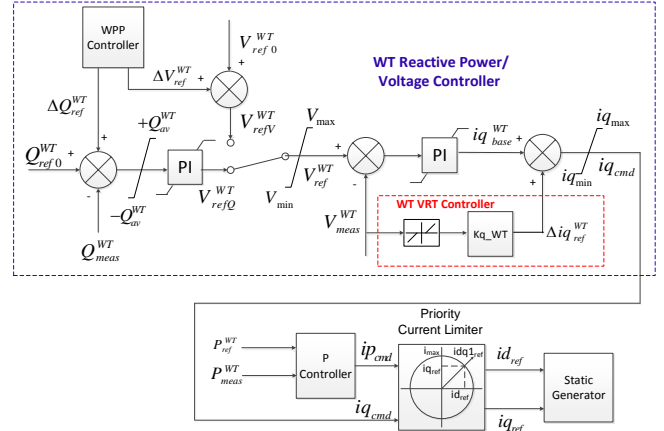

Fig. 5. WT Reactive Power/Voltage Controller

IV. RESULTS AND DISCUSSIONS

The voltage profile of the offshore AC Grid and the reactive power output from WTs of different WPPs of the cluster for short circuit faults at different locations in the offshore AC Grid, such as, collector cable , WT terminal and export cable are investigated here.

A. Collector Cable Fault

A fault at the collector cable is applied at the connection point of WTA1 (5) under WPP- A1B1 at time t=5s for 150 ms . The terminal voltage, reactive power output and reactive current measurements of a few representative WTs within the WPP cluster is shown in Fig.6, Fig.7, and Fig. 8 respectively. From Fig. 6, it can be observed that the voltage at the faulted WT terminal (WTA1 (5)) and at the terminals of the WT connected to the faulted collector cable, i.e. WTA1 (4) drops to significantly lower values (near to zero). The voltage at the WTs connected to the

non-faulted cables, however, connected to the same winding of the substation transformer, i.e. WTA1 (9 to 16) within the WPP –A1B1, drops to around 50% of its nominal value. The voltage at other WTs connected to the other secondary winding of the substation transformer within the same WPP- A1B1, i.e. WTB1, drops to around 75% of its nominal value. Therefore, low voltage at WTs terminals under faulted WPP-A1B1, triggers their VRT controllers to generate maximum allowed additional reactive current reference, Δiq_{ref}^{WT}, thereby increasing the total reactive current reference, iq_{cmd}, to the WT current controller, as shown in Fig. 8. This allows the WTs of the faulted WPP to generate/consume maximum possible reactive power during dynamic conditions as shown in Fig.7. However, the voltage at WTs of non-faulted WPPs, A2B2, C1D1, and C2D2, drops to around 90 % of it rated value and recovers fast. The voltage at WTA2 and WTD1 is shown here, representing the behavior of WTs in the non-faulted WPPs. The VRT controllers at these WTs does not generate additional reactive current set point due to low voltage dips at their terminals. However, such WTs have additional reactive current margin, hence, can generate additional reactive power. Therefore, the voltage profile of the offshore WPP cluster can be improved by generating/consuming additional reactive power from these WTs during the dynamic conditions.
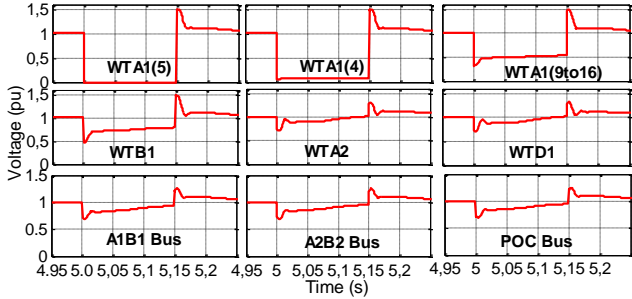

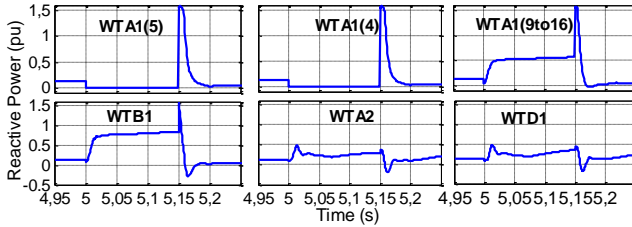Fig. 6. Voltage at WT terminals for collector cable fault at WTA1(5)

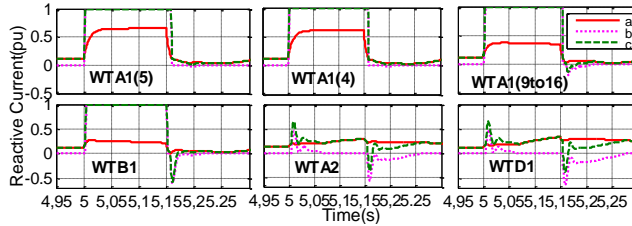Fig.7 .Reactive Power at WT terminals - collector cable fault at WTA1(5).

Fig.8. Reactive current at WT terminals for collector cable fault at WTA1 (5) including the FRT from WT a. iq_{base}^{WT} b. Δiq_{ref}^{WT} c. iq_{cmd}

A. WT Terminal Fault

A fault is applied at the WT terminal i.e. at the low voltage side of WT transformer of WTA1 (5) under WPP-A1B1 at t= 5 s for 150 ms. The WT terminal voltage, reactive power output and reactive current measurements of the WTs

within the WPP cluster are shown in Fig.9, Fig.10, and Fig. 11 respectively. It can be observed that the voltage at the faulted WTA1(5) drops to low values, while the voltage at WTA1(4), representing the WTs in the rest of the faulted collector cable, drops to 80 % of its nominal value. The low voltage at WTs terminals under faulted cable of WPP-A1B1, i.e. WTA1(1-8), triggers their VRT controllers to generate additional reactive current reference, Δiq_{ref}^{WT}, thereby increasing the total reactive current reference, iq_{cmd}, for the WT current controller, as shown in Fig.11. This strategy allows such WTs to generate additional reactive power during dynamic conditions, as shown in Fig. 10. However, the voltage at WTA1(9-16) drops to around 92 % of its nominal value and also the rest of the WTs in the faulted WPP-A1B1, i,e, WTB1, and all other WTs under non-faulted WPPs are not affected much, hence the voltage dip at their terminals is insignificantly small (less than 0.1 pu) and they recover fast. The VRT controllers at such WTs do not generate additional reactive current set point due to less voltage dip observed at their terminals. However, there is slight increase in the reactive power output of the WTs during the fault, as shown in Fig.10, which is due to the increase in base reactive reference current, iq_{base}^{WT}, from the WPP reactive power controller.
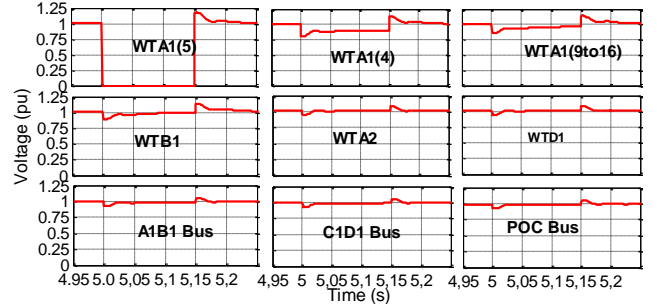

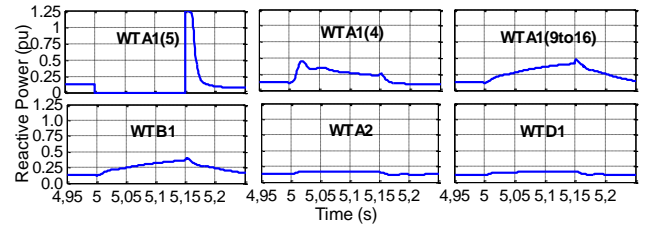Fig 9. Voltage at WT terminals for WT Terminal fault at WTA1 (5)

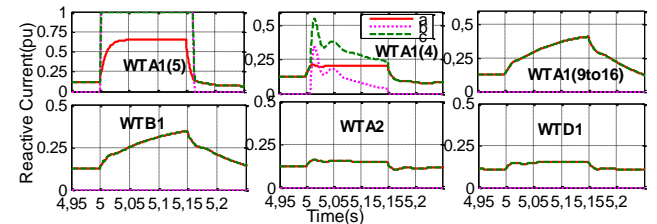Fig.10. Reactive Power output of WTs for WT Terminal fault at WTA1(5)

Fig. 11 WT Reactive Current for WT Terminal fault at WTA1 (5) including the VRT from WT and WPP cluster . a. iq_{base}^{WT} b. Δiq_{ref}^{WT} , c. iq_{cmd}

B. Export Cable Fault

A fault at the export cable A1B1 is applied near to A1B1 collector substation with a fault impedance of 2 Ω at t= 5 s for a duration of 150 ms. As seen from Fig 12, voltage at the WPP collector substation buses, A1B1 and C2D2, representing the faulted and non-faulted WPPSs, and the Pilot bus falls to a lower value, hence, the voltage at all WT

non-faulted cables, however, connected to the same winding of the substation transformer, i.e. WTA1 (9 to 16) within the WPP –A1B1, drops to around 50% of its nominal value. The voltage at other WTs connected to the other secondary winding of the substation transformer within the same WPP- A1B1, i.e. WTB1, drops to around 75% of its nominal value. Therefore, low voltage at WTs terminals under faulted WPP-A1B1, triggers their VRT controllers to generate maximum allowed additional reactive current reference, Δiq_{ref}^{WT}, thereby increasing the total reactive current reference, iq_{cmd}, to the WT current controller, as shown in Fig. 8. This allows the WTs of the faulted WPP to generate/consume maximum possible reactive power during dynamic conditions as shown in Fig.7. However, the voltage at WTs of non-faulted WPPs, A2B2, C1D1, and C2D2, drops to around 90 % of it rated value and recovers fast. The voltage at WTA2 and WTD1 is shown here, representing the behavior of WTs in the non-faulted WPPs. The VRT controllers at these WTs does not generate additional reactive current set point due to low voltage dips at their terminals. However, such WTs have additional reactive current margin, hence, can generate additional reactive power. Therefore, the voltage profile of the offshore WPP cluster can be improved by generating/consuming additional reactive power from these WTs during the dynamic conditions.
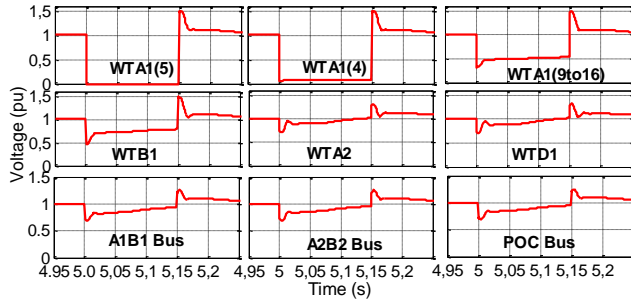

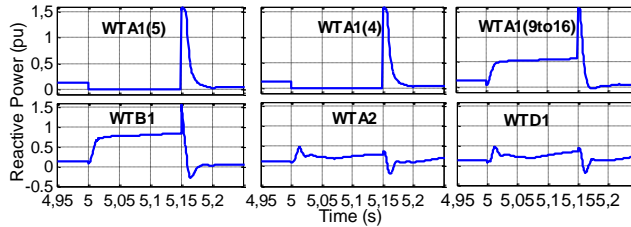Fig. 6. Voltage at WT terminals for collector cable fault at WTA1(5)

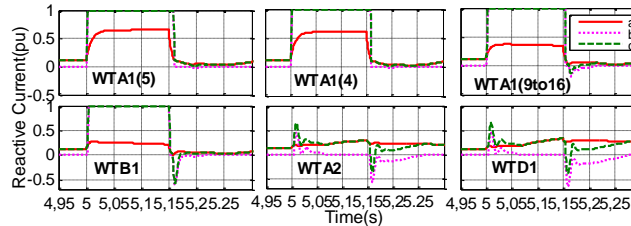Fig.7 .Reactive Power at WT terminals - collector cable fault at WTA1(5).

Fig.8. Reactive current at WT terminals for collector cable fault at WTA1 (5) including the FRT from WT a. iq_{base}^{WT} b. Δiq_{ref}^{WT} c. iq_{cmd}

B. WT Terminal Fault

A fault is applied at the WT terminal i.e. at the low voltage side of WT transformer of WTA1 (5) under WPP-A1B1 at t= 5 s for 150 ms. The WT terminal voltage, reactive power output and reactive current measurements of the WTs

within the WPP cluster are shown in Fig.9, Fig.10, and Fig. 11 respectively. It can be observed that the voltage at the faulted WTA1(5) drops to low values, while the voltage at WTA1(4), representing the WTs in the rest of the faulted collector cable, drops to 80 % of its nominal value. The low voltage at WTs terminals under faulted cable of WPP-A1B1, i.e. WTA1(1-8), triggers their VRT controllers to generate additional reactive current reference, Δiq_{ref}^{WT}, thereby increasing the total reactive current reference, iq_{cmd}, for the WT current controller, as shown in Fig.11. This strategy allows such WTs to generate additional reactive power during dynamic conditions, as shown in Fig. 10. However, the voltage at WTA1(9-16) drops to around 92 % of its nominal value and also the rest of the WTs in the faulted WPP-A1B1, i,e, WTB1, and all other WTs under non-faulted WPPs are not affected much, hence the voltage dip at their terminals is insignificantly small (less than 0.1 pu) and they recover fast. The VRT controllers at such WTs do not generate additional reactive current set point due to less voltage dip observed at their terminals. However, there is slight increase in the reactive power output of the WTs during the fault, as shown in Fig.10, which is due to the increase in base reactive reference current, iq_{base}^{WT}, from the WPP reactive power controller.
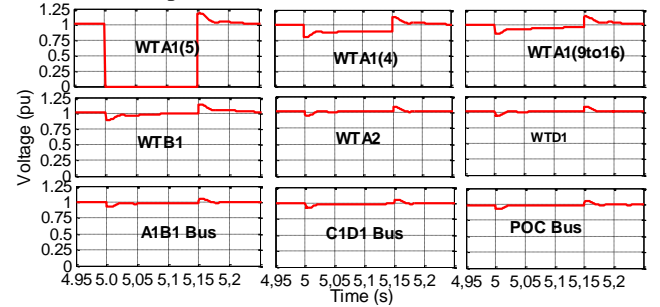

Fig 9. Voltage at WT terminals for WT Terminal fault at WTA1 (5)
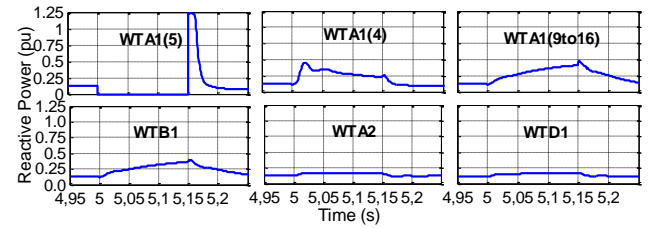

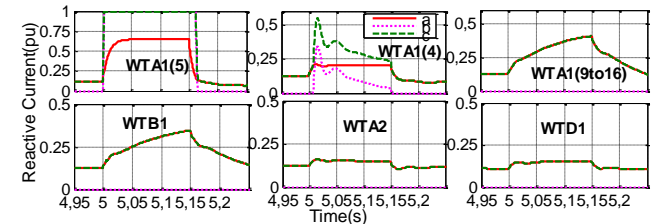Fig.10. Reactive Power output of WTs for WT Terminal fault at WTA1(5)

Fig. 11 WT Reactive Current for WT Terminal fault at WTA1 (5) including the VRT from WT and WPP cluster . a. iq_{base}^{WT} b. Δiq_{ref}^{WT}, c. iq_{cmd}

C. Export Cable Fault

A fault at the export cable A1B1 is applied near to A1B1 collector substation with a fault impedance of 2 Ω at t= 5 s for a duration of 150 ms. As seen from Fig 12, voltage at the WPP collector substation buses, A1B1 and C2D2, representing the faulted and non-faulted WPPSs, and the Pilot bus falls to a lower value, hence, the voltage at all WT

74

terminals in the WPP cluster also dropped. The reactive power and reactive current reference at WTA2 and WTD1 are increased to their maximum limits, as shown Fig. 13. The response of the other WTs is same, hence; only the results of two WTs are shown here. The base reactive current reference, iq_{base}^{WT}, and the additional current reference from the WT VRT controller, Δiq_{ref}^{WT}, further enhances the total reactive current reference, iq_{cmd}. The magnitude of Δiq_{ref}^{WT} is above 1 pu during the fault and less than -1 pu during post fault clearance. Hence, it may not be possible to get more reactive power from the WTs, therefore, the voltage profile of the offshore grid cannot be further improved.
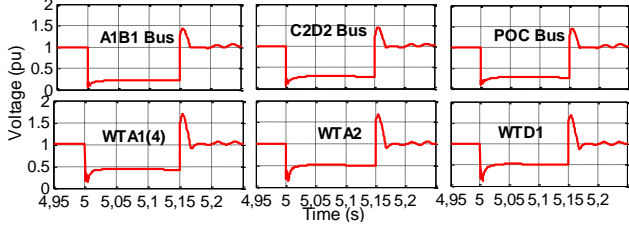

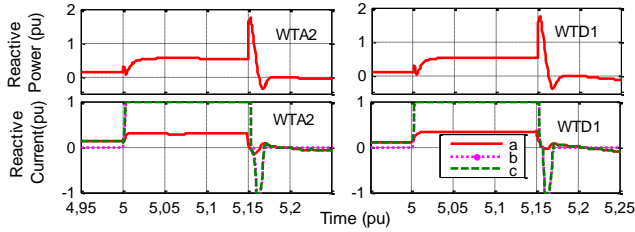Fig. 12. Voltage for export cable fault at A1B1 Collector Substation

Fig. 13 Reactive Power and Current for export cable fault a. iq_{base}^{WT} b. Δiq_{ref}^{WT}, c. iq_{cmd}

D. Effect on DC Voltage and Power Flow

The Active power and DC voltage at the offshore HVDC converter for different faults, collector cables (A), WT terminal (B) and export cable (C), are shown in Fig. 14. The active power and DC voltage are less affected by WT terminal fault (A). However instant active power is reduced to 0.4pu while DC voltage is reduced by 0.1 pu during the collector cable fault (B), and recovers within 200 ms after the fault. The active power and DC voltage are severely affected for an export cable fault; during the fault, however, the control system for WPP and HVDC converter ensures recovery within 400 ms after the fault.
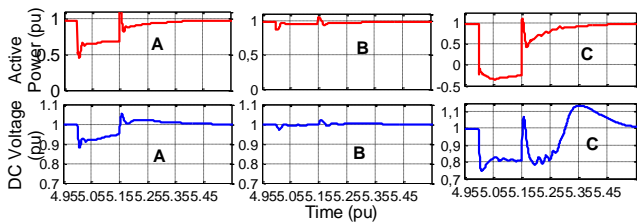

Fig. 14 Active Power and DC Voltage at HVDC Converter Terminals for fault cases A, B. C.

V. CONCLUSIONS

A coordinated reactive power control for cluster of offshore WPPs connected to a common HVDC link is presented in this paper. The reactive power reference for the WPP cluster is generated by an optimization algorithm aiming at minimum active power loss in the offshore Grid. The voltage profile and the reactive power output from the WTs of the cluster for a fault at different locations in one of the WPPs has been investigated in detail. It has been demonstrated that with the proposed CRPC, the WT terminal fault does not impact the voltage profile and power flow in the offshore grid, while only affecting the faulted cable voltage and its power flow. It has been shown that the WT collector cable fault can affect the voltage profile and power flow to some extent, however it may be improved by additional reactive power support from the non-faulted WPPs. It has also been demonstrated that the export cable fault affects the power flow and voltage profile of the offshore grid. The WT VRT controllers generate maximum possible reactive current as the voltage at their terminals deviate much from their nominal values. Hence, they contribute maximum possible reactive power during voltage dips and consume reactive power following the fault to limit the high voltage in the offshore AC Grid.

REFERENCES

[1] Windspeed.eu, 'Windspeed', 2015. [Online]. Available: http://www.windspeed.eu. [Accessed: 15- Jul- 2015].

[2] M. Aragues Penalba, O. Gomis-Bellmunt and M. Martins, "Coordinated Control for an Offshore Wind Power Plant to Provide Fault Ride Through Capability", *IEEE Transactions on Sustainable Energy*, vol. 5, no. 4, pp. 1253-1261, 2014.

[3] Oriol Gomis-Bellmunt, Jun Liang, Janaka Ekanayake, Rosemary King, Nicholas Jenkins, "Topologies of multiterminal HVDC-VSC transmission for large offshore wind farms," *Electric Power Systems Research*, vol.81,pp, 271-281 , Feb 2011.

[4] Z. Chen, J. Guerrero and F. Blaabjerg, 'A Review of the State of the Art of Power Electronics for Wind Turbines', *IEEE Transactions on Power Electronics*, vol. 24, no. 8, pp. 1859-1875, 2009.

[5] Muljadi E, Samaan N, Gevorgian V, Li J, Pasupulati S., "Different factors affecting short circuit behavior of a wind power plant.", *in Proc. 2010 IEEE Industry applications society annual meeting (IAS).*, p. 1–9.

[6] R. Irnawan, K. Srivastava and M. Reza, "Fault detection in HVDC-connected wind farm with full converter generator", *International Journal of Electrical Power & Energy Systems,* vol. 64, pp. 833-838, 2015.

[7] C. Feltes, H. Wrede, F. Koch and I. Erlich, 'Enhanced Fault Ride-Through Method for Wind Farms Connected to the Grid Through VSC-Based HVDC Transmission', *IEEE Transactions on Power Systems*, vol. 24, no. 3, pp. 1537-1546, 2009.

[8] M. Mohammadi, M. Avendano-Mora, M. Barnes, et al., "A study on fault ride-through of VSC-connected offshore wind farms", *in: Proc. 2013 IEEE Power andEnergy Soc. General Meeting (PES),* Vancouver, BC, pp. 1–5.

[9] B. Silva, C. Moreira, H. Leite, J.A. Peças Lopes, "Control Strategies for AC Fault Ride-Through in Multi-terminal HVDC Grids", IEEE Transactions on Power Delivery, vol.29, no.1, pp.395,405, Feb. 2014

[10] J. I. Marvik and H. G. Svendsen, "Analysis of Grid Faults in Offshore Wind Farm with HVDC Connection," Energy Procedia, vol. 35, no. 1876, pp. 81–90, Jan. 2013.

[11] ABB. XLPE Submarine Cable Systems Attachment to XLPE Land Cable Systems - User's Guide. 2010.

[12] E. Muljadi et al. "Equivalencing the collector system of a large wind power plant", *in Proc. 2006 IEEE Power Engineering Society General Meeting.*.

[13] E. Muljadi et al. "Method of equivalencing for a large wind power plant with multiple turbine representation".*in Proc. 2008 IEEE Power and Energy Society General Meeting: Conversion and Delivery of Electrical Energy in the 21st Century.*

[14] *IEC 61400-27 Committee Draft for Wind Turbines Part 27- 1: Electrical simulation models for wind power generation Wind turbine*, IEC Std. committee Draft (CD) 88/424/CD, Jan. 2012.

[15] X. F. Wang, Y. Song and I. Malcolm: Modern Power Systems Analysis, Springer Science, Business Media, LLC, 2008.

[16] Tennet TSO GmbH, Requirements for Offshore Grid Connections in the Grid of Tennet TSO GmbH, Germany, Dec. 2012, pp. 1–10.

This page would be intentionally left blank if we would not wish to inform about that.

C2 Jayachandra N. Sakamuri, Rather Z.H., Cutululis N.A., Rimez J., "A New Coordinated Voltage Control Scheme for Offshore AC Grid of HVDC Connected Offshore Wind Power Plants ", Presented at CIGRE Canada Conference, Winnipeg, Canada, 2015.

This page would be intentionally left blank if we would not wish to inform about that.

A New Coordinated Voltage Control Scheme for Offshore AC Grid of HVDC Connected Offshore Wind Power Plants

JAYACHANDRA N. SAKAMURI*, NICOLAOS A. CUTULULIS	ZAKIR HUSSAIN RATHER	JOHAN RIMEZ
Department of Wind Energy, Risø Technical University of Denmark Denmark	**Electricity Research Centre, University College Dublin Ireland**	**Elia System Operator Belgium**

SUMMARY

This paper proposes a coordinated voltage control scheme (CVCS) which enhances the voltage ride through (VRT) capability of an offshore AC grid comprised of a cluster of offshore wind power plants (WPP) connected through AC cables to the offshore voltage source converter based high voltage DC (VSC-HVDC) converter station. Due to limited short circuit power contribution from power electronic interfaced variable speed wind generators and with the onshore main grid decoupled by the HVDC link, the offshore AC grid becomes more vulnerable to dynamic voltage events. Therefore, a short circuit fault in the offshore AC Grid is likely to have significant implications on the voltage of the offshore AC grid, hence on the power flow to the onshore mainland grid. The proposed CVCS integrates individual local reactive power control of wind turbines and of the HVDC converter with the secondary voltage controller at offshore grid level. This secondary voltage controller controls the voltage at the pilot bus, the bus with the highest short circuit capacity in the offshore AC grid. By maintaining voltage at the pilot bus, reflecting the voltage variations of the entire offshore zone, the voltage profile of the offshore grid is indirectly maintained. During steady state operation, the secondary AC voltage controller generates reactive power references for individual wind turbines (WTs) based on their participation factors (PFs) and available reactive power margins, while during dynamic voltage events; the secondary voltage controller generates additional reactive power reference signals for WTs and the HVDC converter, to enhance VRT capability of the offshore AC network. The Participation Factor of each WT is calculated from their dV/dQ sensitivities w.r.t. the pilot bus. The WT and the HVDC converter control is modified to accommodate additional reactive power reference from the secondary controller, while maintaining their local VRT capability. A detailed model of 800 MW VSC-HVDC connected OWPP cluster developed in DigSILENT platform is considered in this study. VSC-HVDC transmission system operates at +/- 320 kV with active power balance (hence DC voltage) control assigned to the onshore converter, while frequency and AC voltage control at the offshore substation assigned to the offshore converter.

KEYWORDS

Coordinated Voltage Control - HVDC - LVRT - Offshore Wind Power Plant Control - Reactive Power

1. INTRODUCTION

Several large-scale offshore wind power plants (OWPPs) have been developed in recent years and this trend is likely to continue in the near future [1]. VSC-HVDC transmission system is considered as a feasible and economical solution for long distance bulk power transmission from OWPPs to the onshore grid [2]. Traditionally, a major part of the power production has been delivered by conventional power plants with large synchronous machines driven by hydro or thermal prime movers. These generators provide ancillary services including short circuit power during a fault to ensure secure recovery of power system within the desired time frame. Today, WPPs are expected to deliver services similar to those of conventional power plants; therefore, Transmission System Operators (TSOs) are developing stricter grid code regulations to ensure power system stability and reliability [3]-[5]. Grid codes require wind power plants to be capable of active and reactive power control, voltage regulation, fault ride-through, and limitation of power quality impacts. The main focus of the research work presented in this paper is (1) Improved reactive power and voltage control of offshore grid, and (2) Enhancement of Low Voltage Ride Through (LVRT) capability requirements [6].

Offshore grid of VSC-HVDC connected offshore WPPs tend to have low short circuit capacity due to limited short circuit power contribution from power electronic interfaced wind generators and decoupling from the onshore grid through HVDC link. Therefore, the offshore AC grid becomes more vulnerable to dynamic voltage events [7]. However, due to inherent control flexibility provided by HVDC converters and modern WTs with VSCs, additional reactive power can be supplied during short circuit events to aid grid voltage to comply with grid code regulations [4]. The voltage/reactive power control and dispatch strategy of the WPP cluster, integrated in the offshore HVDC converter, is also important because several large-scale offshore HVDC connected WPPS are planned in the near future. A possible control strategy for a single WPP, discussed in the literature [8]-[9], is that the TSO generates (1) power factor, (2) reactive power, or (3) voltage amplitude as set points to the WPP controller. The measured/estimated values of these set points are compared with the actual values by a PI controller to generate set points for the individual wind turbines. However, application of such control strategies to a WPP cluster may not be adequate for large-scale offshore WPP cluster and therefore, is worth investigating.

In this context, the voltage control of an 800 MW offshore WPP cluster having four 200 MW WPPs located at different locations within close proximity connected to an offshore HVDC converter is investigated in this paper. A novel CVCS is proposed for the offshore AC Grid using the offshore HVDC converter and the WPP control capabilities to enhance the LVRT capability of the offshore AC grid and to optimally control its voltage profile during steady state operation thereby improving the power flow to the onshore grid. During steady state operation, the CVCS generates reactive power reference for WPP cluster by controlling the voltage at the pilot bus, the voltage reference at the pilot bus being supplied by an optimization program aimed at minimizing active power losses in the offshore Grid. The generated reactive power reference values from CVCS are then dispatched to each WPP based on their PFs and available reactive power margin. For a fault at an offshore bus, while individual local reactive power controller controllers injects reactive current based on the voltage dip observed at its terminal bus, the CVCS supplements by forcing additional reactive power injection from WTs (or HVDC converter) that observe relatively lower voltage dip due to their farther location from the faulted location, thereby improving overall LVRT capability of the offshore grid. The performance of the proposed control scheme is demonstrated by applying symmetrical fault in the collector cable of the WPP in the offshore AC Grid.

2. MODELING OF HVDC CONNECTED OFFSHORE WPP CLUSTER

WPP Layout:

An 800 MW offshore WPP cluster comprised of four 200 MW WPPs, marked as A1B1, A2B2, C1D1, and C2D2, and located at a distance of 7 km, 12, km, 17 km, 22 km respectively from the offshore HVDC converter station has been developed in the PowerFactory simulation environment as shown in Fig. 1. Each 200 MW WPP is composed of four parallel WT strings, each of 50 MW

capacity composed of 8 numbers of series connected 6.25 MW WTs. The turbines are placed with an inter-machine distance of 1.2 km, approximately equal to seven times the rotor diameter.

Power Collector System:

The power collection system in each WPP consists of collector cables (feeders) and transformers. The 33 kV cables between WT5 and WT8 (i.e. the farthest from the collector bus) have current rating of 0.5 kA, while the 33 kV cables between WT5 and the collector bus are rated at 1 kA. Each WPP is connected to the collector bus through a 33/155 kV, 240 MVA step up transformer.

Aggregation of WPPs:

To study the impact of WPP on the power system, though it is preferable to consider the detailed WPP model instead of an aggregated WT model, the consideration of detailed model of WPP increases the computational burden. Therefore, most of the WPPs considered in this study are aggregated to simplify the WPP model without compromising the accuracy of the results. One of the WT strings (8 machines, 50 MW total capacity) in WPP-A1B1is modeled in detail. The remaining WTs in that WPP are represented by an aggregated model of 50 MW capacity for A1 (9-16) feeder. The rest of the strings in other WPPs are aggregated with each of 100 MW capacity. The WT aggregation method for WTs and export cables of a WPP has been adopted from [10], [11]; the overall WPP model is shown in Fig. 1.

WT Model:

A full converter based "type 4" WT model considered in this work is adopted from IEC 61400-27-1 – Part 1 [12], which is modeled for the short term power system stability studies.
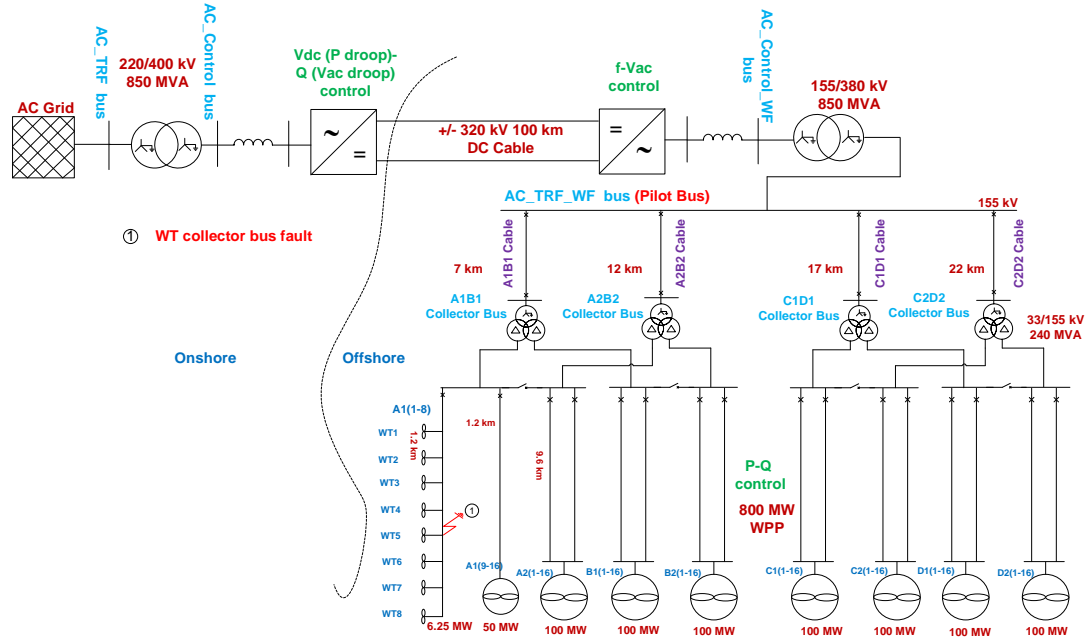

Fig. 1: Offshore HVDC Connected WPP Model

Onshore and offshore HVDC Converter Model:

The standard pulse width modulated (PWM) based converter model has been adopted for the offshore and onshore HVDC converters. The onshore HVDC converter is assigned with the power balance control of the HVDC link, by maintaining the DC voltage at the optimal value. It also controls the reactive power/AC Voltage at converter bus as per grid code regulations. The current references provided by the outer controllers are then handled by a standard inner current controller operating in the d-q reference frame [13]. The offshore HVDC converter is responsible for controlling the voltage magnitude at the offshore converter station (AC_Control_WF bus in Fig. 1), the frequency of the offshore AC network and allows the transfer of active power from the WPPs to the HVDC system. This is achieved by using a standard current control whose reference is provided by the outer converter controller [13].

81

3. PROPOSED COORDINATED VOLTAGE CONTROL SCHEME FOR VSC-HVDC BASED OFFSHORE WPP.

The principle of the proposed coordinated voltage control scheme at the WPP cluster and the HVDC converter for steady-state and dynamic operation to enhance the VRT capability of the offshore Grid is described in this section.

WPP Cluster Controller- Steady State operation:

The WPP cluster voltage controller is shown in Fig. 2. The reference voltage at the pilot bus, *V_pilot_Ref,* is provided by an optimization program, with minimum active power loss in the offshore grid as the objective function, for the available power output (*Pav*) from the WPP clusters. The available active power from all WPPs (*Pav)* is estimated from the forecasted wind speed, *Vw*. The optimal reference voltage at the pilot bus, *V_pilot_Ref*, is then fed to the WPP cluster voltage controller, which generates the required reactive power set point for the WPP cluster reactive power dispatcher, then these set points are dispatched to each individual WPP based on their PFs. The WPP dispatcher generates the reactive power references for each WT based on their available reactive power capacity and PFs. The mathematical model for the reactive power dispatch at the WPP level is given in (1).

$$Q_{ref}^{WT_i} = \frac{PF_{WT_i}}{PF_{WPP}} * \frac{Q_{av}^{WT_i}}{Q_{av}^{WPP}} * Q_{ref}^{WPP}$$

$$Q_{av}^{WPP} = \sum_{i=1}^{n} Q_{av}^{WT_i} \, with : Q_{av}^{WT_i} = \sqrt{(S_{Gen}^{WT_i})^2 - (P_{av}^{WT_i})^2} \tag{1}$$

$$PF_{WT_i} = \frac{dU_{pilotbus}}{dQ_i}, PF_{WPP} = \frac{\sum_{i=1}^{n} PF_{WT_i}}{n}$$
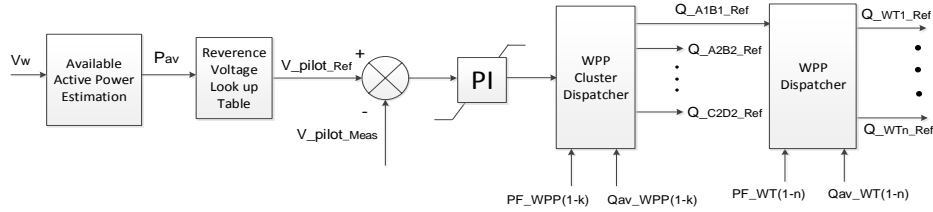

Fig. 2: WPP Cluster Voltage Controller

The reactive power reference for each WT, $Q_{ref}^{WT_i}$, is formulated as a proportional distribution of the WPP reactive power reference, Q_{ref}^{WPP}, based on the ratio of the participation factors and the available reactive power , where $P_{av}^{WT_i}$, $Q_{av}^{WT_i}$, and $S_{Gen}^{WT_i}$ are the available active and reactive powers and the MVA rating of the ith wind turbine, Q_{av}^{WPP} is the total available reactive power of the WPP, PF_{WT_i} is the participation factor of the ith wind turbine, and PF_{WPP} is the participation factor of the *WPP*.

Similarly, the mathematical model for the reactive power dispatch at WPP cluster level is given in (2).

$$Q_{ref}^{WPP_i} = \frac{PF_{WPP_i}}{PF_{cluster}} * \frac{Q_{av}^{WPP_i}}{Q_{av}^{cluster}} * Q_{ref}^{cluster}$$

$$Q_{av}^{cluster} = \sum_{i=1}^{k} Q_{av}^{WPP_i} \tag{2}$$

$$PF_{cluster} = \frac{\sum_{i=1}^{k} PF_{WPP_i}}{k}$$

The reactive power reference for each WPP, $Q_{ref}^{WPP_i}$, is formulated as the proportional distribution of the WPP cluster reactive power reference, $Q_{ref}^{cluster}$, based on the ratio of participation factors and available reactive power , where $PF_{cluster}$ is the participation factor of the WPP cluster, and

$Q_{av}^{cluster}$ is the total available reactive power of the WPP cluster. Therefore, during steady state operation, for any unacceptable voltage deviation at the pilot bus, WTs and HVDC converter are commanded to generated/absorb additional reactive power based on the generated set points.

WPP Cluster Controller- Dynamic Operation:

A short circuit fault or any other dynamic event may result in low voltages in the offshore AC Grid. To improve the voltage recovery of the Offshore Grid as per Grid code requirements, WTs are expected to increase their reactive power contribution during and after the short circuit event for better voltage recovery of the Grid. The schematic of the WT reactive power controller adopted in this research work is shown in Fig. 3. The WT reactive power controller generates a base reactive current reference, *Iq_base,* during normal operation. If the voltage at the WT terminals deviate from the allowed dead band (normally +/- 0.1 pu), additional reactive current reference, *Iqv1*, generated from the WT low voltage ride through (LVRT) controller, based on the WT terminal voltage, *V_WT_meas,* is sent to the WT inner current controller. However, the WT LVRT controller gets only local WT voltage measurements. For certain faults/disturbances, e.g. WT collector cable faults within a WPP, the WTs in that WPP observe a low voltage dip depending on their distance from the fault location, and accordingly their local LVRT controllers demand additional reactive power. However, WTs of other neighboring WPPs may not observe the same voltage dip, hence, such WTs are unlikely to generate additional adequate reactive power required for fast and effective voltage control. This may lead to a low voltage profile within the WPP cluster and also at the WPP point of connection (PCC), i.e. at the pilot bus. The proposed cluster controller utilizes the reactive power margin of such wind turbines in order to improve dynamic voltage recovery more effectively following a short circuit fault. The additional reactive current produced by this controller, *Iqv2*, based on the pilot bus voltage, *V_pilot_Meas*, is added to the *Iq_base*. The priority current limiter then sets the active/reactive current priority depending on the TSO requirement and limits the total current reference to the WT as per the rating of the WT.
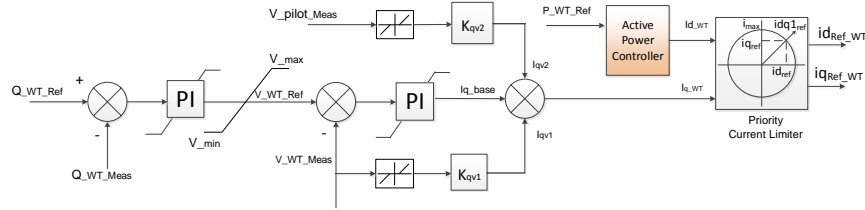

Fig. 3: WT Reactive Power Controller

HVDC Converter Control- Dynamic Operation:

Similar to the WTs, the LVRT controller is employed at the offshore HVDC converter, as shown in Fig. 4, which generates additional reactive current reference, *Iqv_H*, following a dip in AC voltage at the pilot bus of the offshore AC Grid due to a fault.
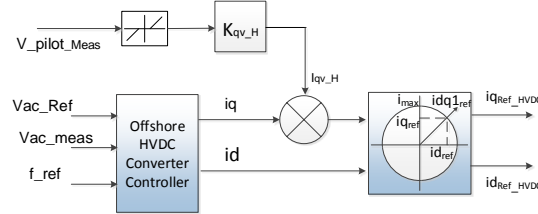

Fig. 4: Offshore HVDC Converter Control

4. SIMULATION AND ANALYSIS OF THE RESULTS

Steady State Operation:

The relation between the losses in the offshore Grid and the optimal pilot bus voltage for different active power output from WPP is shown in Fig. 5. It can be observed that there is a correlation between the optimal pilot bus voltage and the active power output from WPPs. With the proposed coordinated voltage control, the voltage at the pilot bus is maintained at its optimal value, depending on the power output from WPP, and thereby reducing the active power losses. To compare the active

power losses with the proposed WPP cluster coordinated voltage control (CVC) scheme with the traditional WPP control, it is assumed that each WPP is in voltage control mode controlling the voltage at the low voltage side of the transformer on the WPP collector bus. The comparison of active power losses for both methods is shown in Fig.6, and it is evident that losses are relatively low with the proposed CVC scheme.
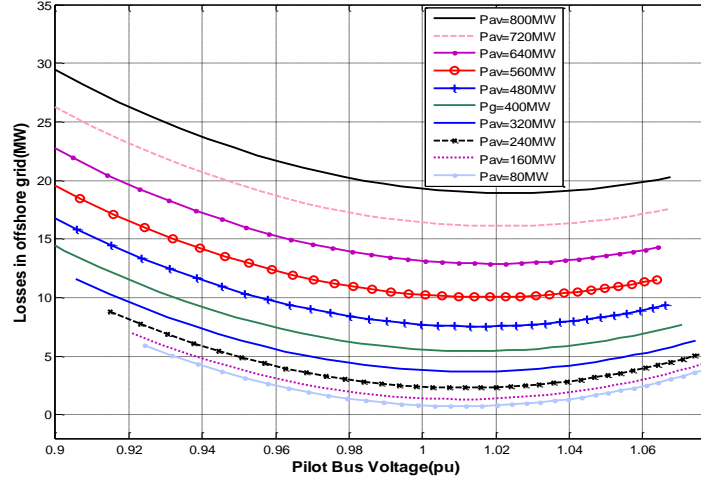

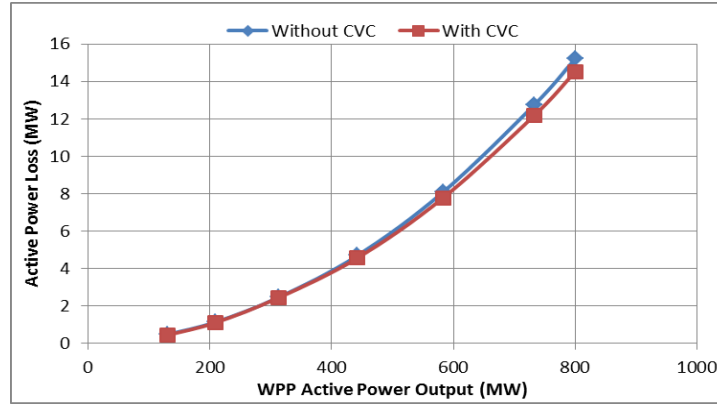**Fig. 5: Losses in the offshore grid Vs Pilot bus voltage**

Fig. 6: Active Power Loss Vs Active Power output of WPPs

Dynamic Operation:

The effectiveness of the proposed CVC scheme is studied for a 3 phase to ground fault at the WTGA1 (5), i.e. WT collector bus fault as shown in Fig. 1. It is worth to observe the reactive power contribution from the WTs of the faulted WPP and the other non-faulted WPPs of the WPP cluster. The wind turbines, WTB1 under the WPP-A1B1 and WTA2 under the WPP- A2B2 have been considered for the study. The AC voltage at the terminal of WTA1 (5), WTB1, and WTA2 with and without considering the effect of coordinated voltage control (CVC) from WPPs along with reactive power contribution from corresponding wind turbines is shown in Fig. 7. As WTB1 observes larger voltage dip at its terminal, its (local) LVRT controls are activated to provide additional reactive power. However, the voltage dip observed at the WTA2 terminal is not sufficient enough to trigger its LVRT controller for a adequate time as the voltage dip is not sustained for longer duration. In general, the local LVRT control is activated when the voltage at WT terminal falls below 0.95 p.u. and vice versa. The LVRT controller, based on the pilot bus voltage from the CVC, triggers the WTA2 to inject additional reactive power during and after the fault which results in the improvement of the voltage profile at its terminals. Similarly, the CVC scheme can trigger the LVRT controllers of all WTs from other WPPs with an available reactive power margin to produce the required additional reactive power during a dynamic event to improve the voltage profile of the offshore AC Grid. It can also be observed that the voltage overshoot at the WTA2 terminals after the fault clearance is less with the CVC scheme and this could be an advantage to limit the temporary short term over voltages at WT terminals.
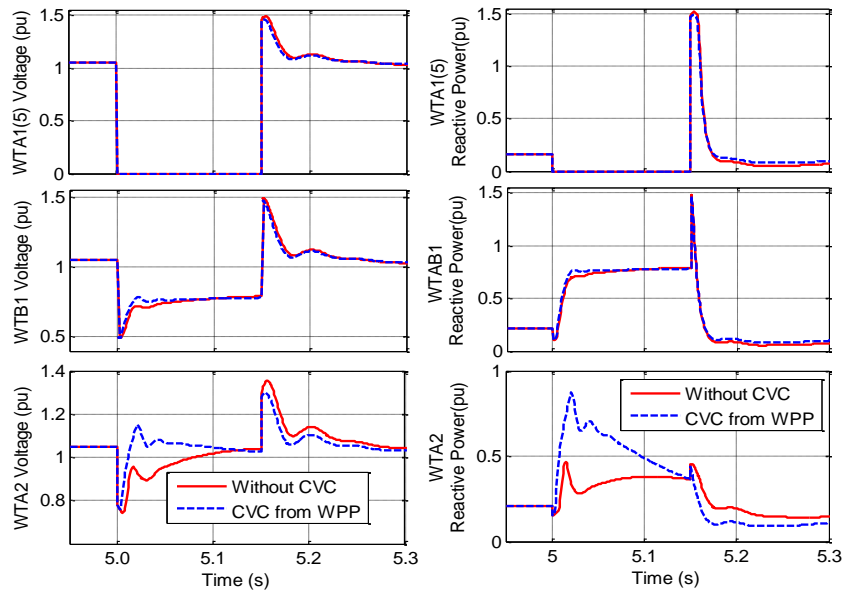
Fig. 7: Effect of CVC on the Terminal Voltage and reactive power output of WTs

The effectiveness of the proposed CVC scheme on the LVRT performance of the offshore AC grid, for a collector cable fault at WTGA1 (5), is shown in Fig.8. It can be observed that there is a considerable improvement in VRT capability using the CVC scheme. The active power flow at the offshore HVDC converter and DC voltage of the HVDC system is improved with the proposed CVC scheme as shown in Fig.8. It is also observed that during the fault clearance, the CVC from WPPs limits the peak of the temporary overvoltage at point of connection (PCC), i.e. at the pilot bus. This could be an advantage for the overvoltage protection under partial/full HVDC load rejection conditions as a result of the blocking of the converter (triggered by its internal protection system).
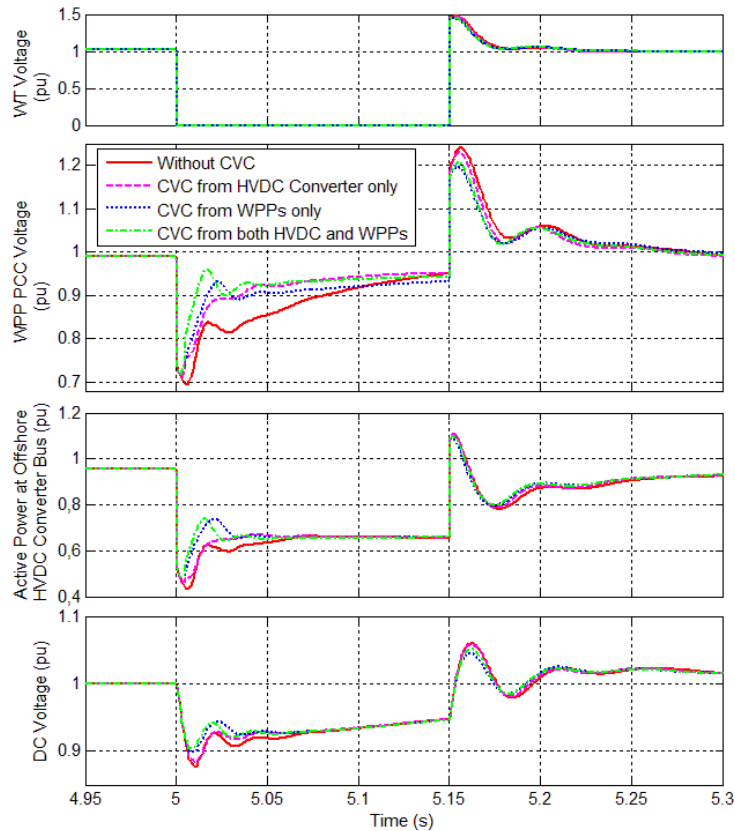

Fig. 8: Dynamics of Offshore HVDC Connecgted WPP for a collector cable fault at WTDA1 (5) with and without CVC (Coordinated Voltage Control)

85

5. CONCLUSIONS

A coordinated voltage control scheme for offshore HVDC connected WPP clusters, improving both the steady state and the voltage ride through performance of offshore AC Grid, is proposed in this paper. This control scheme integrates individual local voltage/reactive power control of wind turbines and the offshore HVDC converter, with the secondary voltage control at offshore grid level aimed to control voltage profile at the pilot bus. The proposed controller generates reactive power references which are distributed to the individual wind turbines and the HVDC offshore converter based on participation factors and the available reactive power margin of the WTs. The proposed coordinated voltage control scheme reduces the active power losses during steady state operation and improves low voltage ride through capability of the offshore AC Grid during faults. It is also observed that during fault clearance, CVC with WPPs limits the peak temporary overvoltage at the PCC, which will be beneficial for overvoltage protection under partial/full HVDC load rejections resulted by blocking of converter due to the action of protection system.. The proposed control scheme assumes fast communication channel within the WPP cluster. However, in case of communication failures, the individual WT operates in voltage/reactive control mode within their operational limits.

BIBLIOGRAPHY

[1]   Wind speed, "Roadmap to the deployment of offshore wind energy in Central and Southern North Sea to 2030, " final report, EU-IEE project Wind speed, March 2011. www.windspeed.eu [Online]. Available: www.windspeed.eu [Last Access 5 Jun. 2015].

[2]   Chaudhary SK, Teodorescu R, Rodriguez P., "Wind farm grid integration using VSC based HVDC transmission – an overview", (Energy 2030 conference,2008. Energy 2008. IEEE; 2008. p. 1–7).

[3]   Altın M, Go¨ksu O, Teodorescu R et al., "Overview of recent grid codes for wind power integration" (12th international conference on optimization of electrical and electronic equipment (OPTIM'10), Basov, Russia, 20–22 May 2010)

[4]   ENTSO- E, "Draft The Network Code on High Voltage Direct Current Connections (NC HVDC)", (ENTSO-E, Apr 2014)

[5]   Tennet TSO GmbH, "Grid Code High and Extra high voltage", Dec 2012, [Online]. Available: www.tennet.eu [Last Access 5 Jun. 2015]

[6]   Tennet TSO GmbH, " Requirements for Offshore Grid Connections in the Grid of TenneT TSO GmbH", Dec 2012, [Online]. Available: www.tennet.eu [Last Access 5 Jun. 2015]

[7]   R. Irnawan , K. Srivastava, M. Reza, "Fault detection in HVDC-connected wind farm with full converter generator",(Electrical Power and Energy Systems , vol 64, 2015)

[8]   J. Fortmann, Wilch, M., F. Koch and I. Erlich, "A novel centralised wind farm controller utilising voltage control capability of wind turbines",(PSCC Power System Computational Conference, UK, July 2008)

[9]   B. R. Karthikeya, Reiner Johannes Schütt, "Overview of Wind Park Control Strategies ", (Article in Press , IEEE Trans. Sustainable Energy)

[10] E. Muljadi et al. "Equivalencing the collector system of a large wind power plant". (IEEE Power Engineering Society General Meeting (2006)).

[11]   E. Muljadi et al. "Method of equivalencing for a large wind power plant with multiple turbine representation". (IEEE Power and Energy Society 2008 General Meeting: Conversion and Delivery of Electrical Energy in the 21st Century, PES (2008)).

[12] IEC 61400-27 Committee Draft, "Wind Turbines Part 27- 1: Electrical simulation models for wind power generation Wind turbines", (IEC Std. committee Draft (CD) 88/424/CD January 2012)

[13] L. Zeni, I. Margaris, A. Hansen, P. Sørensen and P. Kjær, "Generic Models of Wind Turbine Generators for Advanced Applications in a VSC-based Offshore HVDC Network", (10th IET Conference on AC/DC Transmission, Birmingham, 2012, DOI: 10.1049/cp.2012.1980).

C3 Jayachandra N. Sakamuri, Das K, Altin M.,Hansen A.D.,Cutululis N.A., Tielens P. Dirk Van Herterm, "Improved Frequency Control from Wind Power Plants Considering Wind Speed Variation", Proc. 19th Power System Computation Conference, Genoa,Italy, 2016.

This page would be intentionally left blank if we would not wish to inform about that.

Improved Frequency Control from Wind Power Plants Considering Wind Speed Variation

Jayachandra N. Sakamuri, Kaushik Das, Mufit Altin
Nicolaos A. Cutululis, Anca D. Hansen,
Department of Wind Energy,
Technical University of Denmark, Roskilde, Denmark
jays@dtu.dk

Pieter Tielens, Dirk Van Hertem
Department of Electrical Engineering
KU Leuven
Leuven, Belgium
pieter.tielens@esat.kuleuven.be

Abstract— **A fast frequency controller (FFC) for wind power plants (WPPs), which produces a temporary overloading power reference based on frequency deviation and rate of change of frequency, is proposed in this paper. Contrary to standard controllers proposed in the literature, the gains of the FFC are optimized for different wind speeds ensuring an improved frequency control from WPPs over the whole wind speed range. Two options for temporary frequency control implementations from WPPs are analyzed and compared. Moreover, the impact of mechanical, electrical and control limitations at different wind speeds and its effect on frequency control is discussed in the paper. Results show that by optimizing the gains, an improved frequency control can be obtained compared to standard controllers which apply a fixed gain over whole the wind speed range.**

Index Terms—**Frequency Control, Inertial Response, Temporary Overloading, Wind Power Plants**

I. INTRODUCTION

Frequency in a power system indicates the balance between generation and load. It is important to keep the frequency within a tight margin, otherwise generation or load shedding might be initiated to ensure system stability. Following an under frequency event, caused by a loss of generation or increased load demand, the initial frequency dynamics are dominated by the inertial response of the spinning generation units. Synchronous generators (SGs) naturally contribute with kinetic energy (KE) to reduce the frequency decline, following an under frequency event. However, the effective natural inertia of the system decreases with the expected increased penetration of wind power in power system replacing the SGs. The reason is that modern wind turbines (WTs) connected to the system through power electronics do not inherently contribute with inertia to the system. This may lead to an increased rate of change of frequency (ROCOF) following a frequency event triggering system protection devices. However, inertia is essential to limit the ROCOF and thus to ensure time for slower generation control (primary followed by secondary reserves) to stabilize the system frequency. Due to the large WPPs penetration into the system over the last few years,

transmission system operators (TSOs) are expecting WPPs to participate more and more in power system frequency control [1], [2]. However, there is no grid code specifying for how long the WPPs should contribute with additional power after under frequency events. Over the years, researchers have therefore proposed different frequency control methods for WPPs to support the system by injecting additional power into the system during an under frequency event [3]-[7].

One of these methods provides fast frequency control in order to emulate inertia from WPPs and thus to limit the ROCOF in case of frequency events. Different control concepts enabling the inertial response to produce additional power from WPPs have been proposed in the literature [8]-[14]. A method emulating the inertia based on ROCOF, referred as derivative control, is explained in [9], [10]. Due to the sensitivity of the derivative control towards noise, a low-pass filter is added to eliminate noise from the measurement. The other method, referred as proportional control, provides an additional active power reference proportional to the frequency deviation from nominal value [11], [12]. In [13]-[15], once the frequency event is detected, a fixed duration overloading method of the WT above its initial actual power output is implemented. Wind turbines capability to provide temporary overproduction depending on the initial pre-overproduction conditions, i.e. wind speed conditions, limits of the mechanical/electrical components and control strategy has been investigated in [16], by running case studies with different constant power overloading over fixed durations. In this light, it has been shown that at low wind speeds there might be a risk of stopping the WT during long overproduction periods.

Contrary to the above methods, where WPPs are assumed participating in temporary frequency control without reducing their power output during normal operation, in [17], a method to operate the WPPs at a deloaded power level under normal conditions is explained. This method is useful whenever extended frequency support from WPPs is necessary. Although this would potentially provide a more flexible, longer-term frequency support, from WPPs is necessary. Although this would potentially provide a more flexible

longer-term frequency support, it involves loss in energy yield.

Two different frequency control options for WTs assuming constant power overloading over fixed duration have been proposed and tested in [15]. In both options, an overloading power reference of fixed magnitude and duration is generated once the under frequency event is detected. In Option 1, this overloading power reference is added to the fixed pre-overloading power output value, while in Option 2, it is added to the actual power output of the WT. This may result in higher power output from WT during overloading period for Option 1 compared to Option 2, particularly for below rated wind speeds. The reason is that in Option 2, the actual power output value of WT decreases during overloading period due to the power unbalance between WT aerodynamic power and the electrical power output. However, Option 1 leads to larger reduction in WT electrical power output after the overloading period and therefore results in a longer recovery period compared to Option 2, which could be more stressing for the primary frequency control of the power system. However in [15], no solid conclusions on which option to choose is done as the study is limited to one particular wind speed and does not consider the effect of overloading on the dynamics of the WT.

In this paper, A FFC, which generates temporary overloading power reference to the WT based on the ROCOF and droop method is proposed. The WT operating conditions and the wind speed are considered in this paper to define the magnitude of the overloading power reference, and hence, the gains of the FFC. The procedure to calculate the optimal gains of the FFC at different wind speeds in the test power system is also discussed. The optimal gains of the FFC are calculated to yield maximum energy exchange from the WT at different wind speeds, considering the operating constraints of the wind turbine. This results in an improved support from WT at higher wind speeds or can prevent the turbine to reach an unstable operating point when wind speed is expected to drop. Similar to [15], two options to generate the power reference for frequency control from WPPs are considered. In Option 1, the fixed pre-overloading power output, while in Option 2, the actual power output of the WT are considered to generate power reference during under frequency events. The performance of these two options is analyzed and in addition to [15] optimal gains of the FFC are estimated for both the options based on WT dynamics at different wind speeds. This analysis provide guidelines on how to choose the most suitable option for temporary overloading of the WT during under frequency events considering WT dynamics and wind speed variations.

The paper is organized as follows. Section II describes the modeling of the test power system and WT's fast frequency controller. The methodology to calculate the optimal frequency controller gains is explained in section III. The simulation results along with the discussion of the two options for overloading the WT is presented in section IV. The concluding remarks along with the scope for future work are given in section V.

II. Model Description

A. Test Power System

A simple test system, shown in Fig.1, comprises of a lumped synchronous generator representing the power system, a WPP and a load, is considered for this study. This test system representation is an aggregated model of the test model of the transmission grid proposed in [18]. The ratings of the test system are given in Table I.
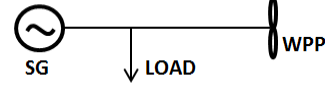

Figure 1. Model of the test system

TABLE I.   TEST SYSTEM PARAMETERS

Parameter	Value
Synchronous Generator Rating (MVA)	5000
WPP Rating (MW)	1000
Load (MW)	4000

Standard block diagrams and parameters for the turbine, governor and excitation system with AVR of the SG have been used [18],[19]. The parameters of the turbine and governing system are listed in Table II.

TABLE II.   PARAMETERS OF TURBINE AND GOVERNING SYSTEM
(S_{BASE} = 5000 MVA)

Parameter	Value
System Regulating Energy (pu)	10
Governor Time Constant (s)	0.1
Turbine Time Constant (s)	1
Inertia Constant (s)	8

B. WPP and WT Model

A WPP of 1000 MW is considered in this work. The WPP model is an aggregated wind turbine model based on the aggregation method given in [20]. The IEC Type IV wind turbine model has been used in this study. It is based on the generic approach proposed by the IEC Committee in Part 1 of IEC 61400-27 [21] for the short term power system stability studies. Additionally, the model includes the aerodynamic behavior of the rotor and wind speed variability, as this is of high relevance for the study as explained in [22]. The WT model also contains a FFC, as shown in Fig. 2, which generates the temporary overloading power reference to the WT.

C. Fast Frequency Controller from WT

The block diagram of the FFC from the WT is shown in Fig. 2. It consists of an 'Inertia and Droop' Controllers, a 'Gain Look Up Table' , an 'Option Selection' block which decides between the two options for frequency control, an 'Optimal Operation' block and 'Power Reference Selection' block, whose functions are explained below.

1) Inertia and Droop Controllers

This controller sends a temporary overloading power reference (ΔP), which is a combination of ΔP_1 and ΔP_2, to the WT during under frequency events.

ΔP_1 is proportional to the frequency deviation from steady state value (Δf), whereas ΔP_2 is proportional to the ROCOF ($\Delta f / \Delta T$). These controllers are inactive within certain frequency deviation and rate of change (dead band), with values depending on grid code requirements. The magnitude of overloading (ΔP) can be varied by changing the power references ΔP_1 and ΔP_2 through tuning of the gains K_D and K_I respectively. A low pass filter is used to remove the high frequency noise in order to protect the WPP from short spikes in its power references.

2) Optimal Operation Block

This block generates a power reference proportional to generator speed (ω_{gen}). In normal operating conditions, it generates maximum power reference as ω_{gen} is at its optimal value. During overloading it generates a reduced power reference as ω_{gen} decreases with overloading, particularly at below rated wind speeds.

3) Power Reference Selection Block

The 'Power reference selection' block selects between optimal power reference (P_{opt}) during normal operation and frequency initiated power reference (P_f) during a frequency event. The P_f is the sum of base power reference (P_{base}), which depends on the selected frequency control Option, and overloading power reference (ΔP) generated by the frequency controller.
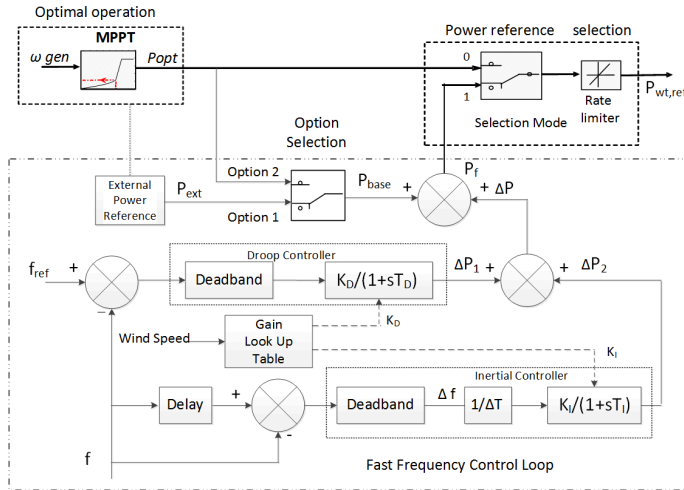

Figure 2. Improved fast frequency control from WPPs

4) Frequency Control Option Selection

There are two options to select the base power reference (P_{base}) for frequency control. In Option 1, P_{base} is equal to the WT output before the frequency event, freezing the output of the optimal operation block. In Option 2, P_{base} is equal to the actual output of the optimal operation block, which decreases with overloading during frequency support at below rated wind speeds. Option 1 does not consider the reduction in actual WT electrical power output during the

overload (due to reduction in ω_{gen} at below rated wind speeds) while Option 2 does. This results in a higher frequency initiated power reference (P_f) to the WT for Option 1 compared to Option 2 assuming constant and equal ΔP in both options. However, in this paper it is shown that ΔP can be varied by optimally changing the gains (K_D and K_I) of the FFC with the average wind speed. It is also shown that ΔP is different for the two Options. The principle of these two options can be better understood by the graphs given in Fig. 3 showing the P_f, P_{opt}, and rotor speed (ω) of the WT for the same under frequency event at below rated wind speed.
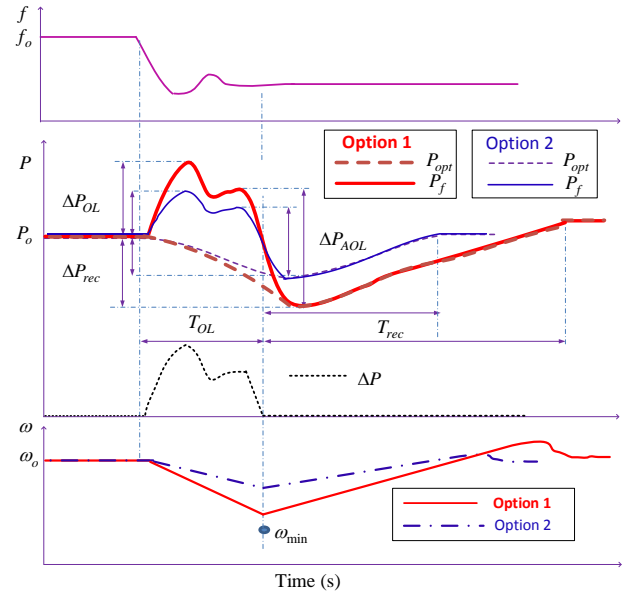

Figure 3. Overloading the WT with (Option 2) and without (Option 1) considering the variation of WT power output during the overload at below rated wind speed

Above the rated wind speeds, the additional energy from the WT can be released by changing the blade pitch angle during the overloading period, hence, ω and P_{opt} do not alter much. Hence, the study is more focused on the behavior of WT at below rated wind speeds. In Option 1, the effect of rotor speed on the WT aerodynamic power (hence the actual WT electrical power output) during the overloading period (T_{OL}) is ignored leading to an increased power support from the WT compared to Option 2 for the same operating conditions and gains of the FFC. However, this causes reduction of rotor speed and hence the actual power output of WT which leads to an increased recovery period (T_{rec}) after the overloading period with Option 1 compared to Option 2. It is hard to define which option is better. It mainly depends on the required performance, i.e. faster and higher initial power surge (ΔP) or shorter recovery period (T_{rec}) of the WTs speed, hence smaller power drop (ΔP_{AOL}). The answer to this may come from the characteristics of the specific power

system, e.g. for small, isolated power systems the emphasis will probably be on fast and high initial power surge.

5) Gain Look up Table

The gains of the FFC at different wind speeds are calculated by taking certain WT operational constraints and power system constraints into account. More details about these constraints are given in the next section. These gains are then stored in the *Gain Look Up Table*. Based on the estimated average wind speed, the FFC gains are dynamically updated to improve the frequency control from WPPs.

The capability of WTs for providing temporary overproduction strongly depends on the initial pre-overproduction conditions, i.e. wind speed conditions, limits of the mechanical/electrical components and control strategies. At wind speeds just below the rated, an imposed overproduction can stress the mechanical shaft drastically and causes a significant reduction in WT output power after overloading [16]. Similarly, at low wind speeds, the WT takes longer to recover to normal operation. However, at high wind speeds, the WT recovers quickly after overloading without causing reduction in power output. In general, the gains of the frequency controller are constant for all of the WTs operating points and usually set to protect the WT operation at low wind speeds. However, adapting optimally the FFC gains based on the average wind speed influences the temporary overloading and the dynamics of the WT. In the next section, the calculation of optimal FFC gains for both options depending on the average wind speed is presented.

III. CALCULATION OF OPTIMAL GAINS FOR THE FAST FREQUENCY CONTROLLER

The optimal frequency controller gains are estimated based on the assumption that WT is maximum overloaded during the frequency event. To calculate the capability of WPPs for temporary overloading, it is therefore important to test it under a critical power system frequency event which leads to maximum overloading of the WPP. The gains K_D and K_I of the WT's FFC determine the amount of temporary overloading power reference (ΔP) to the WT. The following steps are followed to estimate the optimal gains of the FFC.

A. Critical Frequency Event of the Test System

The largest infeed loss in a power system is an example of significant imbalance and is one of the (N-1) contingency criteria in transmission system planning. Therefore, a generation loss of 600 MW is considered as reference incident in the test power system (shown in Fig. 1) to create an under frequency event, shown Fig. 4.
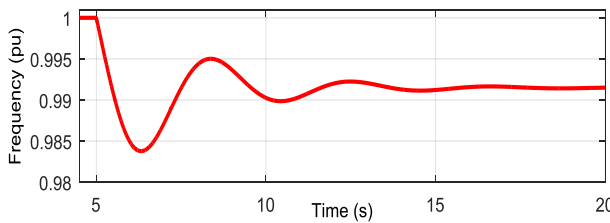

Figure 4. Critical frequency of the test system shown in Fig.1 for the generation loss of 600 MW

It is also considered that only synchronous machines are participating in frequency control. The frequency control from WPPs is disabled. This results in a critical frequency event as the overall power system inertia reduces because the WPP deliver maximum available power during normal conditions and do not participate in frequency control.

B. Calculation of optimal frequency controller gains

The objective of calculating optimal frequency controller gains is to determine the maximum possible temporary overloading of the WT during under frequency events. This necessitates the calculation of the maximum possible energy yield from the WT during under frequency events. The maximum energy yield test on the WT is more accurate if it is tested in open loop conditions, i.e. manipulating the WT power set point for temporary overloading, independently of the power system response and impact [16]. Therefore, the calculated critical frequency from section III A is fed as input to the FFC (which generates the temporary overload power reference) of the WT connected to the test system, as shown in Fig. 2. In order to simulate the impact of this under frequency event on the overloading of the WT, the test power system is replaced with a WPP feeding to a voltage source as shown in Fig. 5. This is called overloading test of the WT. The overloading of the WT can be varied by changing the gains of the fast frequency controller, K_D and K_I. The optimal gains are the ones leading to maximum energy yield from the WT without violating certain operating constraints of the WT and power system as explained below. The energy extracted from the WT depends upon the magnitude and duration of temporary overloading. Therefore the study is aimed at estimating the gains of the FFC of the WT participating in temporary frequency control during the first few seconds after the under frequency event. Based on the dynamics after the under frequency event, shown in Fig. 4, the duration of the WT overload is considered as 5.5s, after which the oscillations in the frequency are reduced.
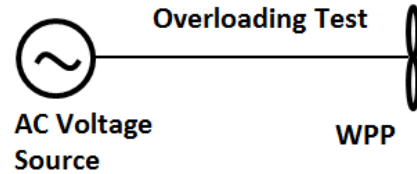

Figure 5. Test power system for calculation of FFC gains

The WT and power system operational constraints considered during the calculation of the optimal gains are:

- Minimum rotational speed: $\omega_{min} = 0.5$ pu
- Maximum power overload: P_{OLMax} $(= P_f / P_N)$: = 110% where P_N is nominal active power output of WT
- Maximum power drop after overloading period: $\Delta P_{AOLMax} = 10\%$
- Maximum recovery time: $T_{recMax} = 60$ s

The limit ω_{min} protects the WT from stalling caused by the overload. The P_{OLMax} is limited by the overall rating of the WT. Also, it limits the drive train torque value during the overload. The ΔP_{AOLMax} is the limitation set by the associate power system to avoid second frequency dip after the release of WT overload. The T_{recMax} ensures that the WT recovers fast enough to resume normal operation or even to participate in frequency control, if required, for any next event. These operational constraints ensure safe dynamical operation of WT during the overloading period and also at the recovery period after the overload. The optimal frequency controller gains are calculated for different wind speeds for both Option 1 and 2 meeting the above mentioned WT constraints. It is assumed that both the gains K_D and K_I are equal in each test case to simplify the analysis as the main objective is to calculate the maximum possible energy yield from the WT during under frequency event.

IV. SIMULATION AND ANALYSIS OF RESULTS

The variation of the optimal gains of the FFC with the average wind speed for both Option 1 and Option 2 is shown in Fig. 6. It can be observed that the optimal gains vary with wind speed for both options. Which constraint is limiting the optimal FFC gains at different wind speeds is also shown in Fig. 6. The maximum power overload (P_{OLMax}) is the constraint for overloading (hence optimal FFC gains) at high wind speeds (above 1 pu). At high wind speeds, the aerodynamic power is altered by changing the pitch angle, thereby producing more electrical power output during the overload. At medium wind speeds (between 0.7 and 1 pu), the maximum power drop after overloading period (ΔP_{AOLMax}) is the major constraint limiting the overloading. Similarly, at lower medium wind speed range (0.5 pu to 0.7 pu) is the recovery period (T_{recMax}), and at lower wind speeds (less than 0.5 pu) is the minimum rotational speed (ω_{min}) of the WT are limiting the optimal frequency controller gains. Therefore by dynamically adapting the gains of the FFC considering the average wind speed will result in an improved frequency support in case of increased wind speeds. Similarly, this prevents the turbine to reach an unstable operating point in the case that the average wind speed is evolving differently than expected, i.e. dropping. It can also be observed from Fig. 6 that the magnitude of these optimal gains is higher for Option 2 than for Option 1, especially at medium wind speed range. As mentioned above, Option 2 considers the variation of actual power output; hence, the recovery is faster leading to lower reduction in the power output after the overload encouraging higher FFC gains compared to Option 1. The difference between these two options can be understood in detail from the overloading test results of the WT at medium wind speed range (0.8 pu), shown in Fig. 7 and Fig. 8. The difference between the two options are more predominant at medium wind speed range, hence the results at 0.8 pu wind speed is discussed in detail.

In the next part, the dynamics of the WT for open loop overloading test are discussed in section A, the performance of the two options for frequency control in actual power system is discussed in section B. Finally, in section C, few recommendations are made for WPPs to participate in frequency control.
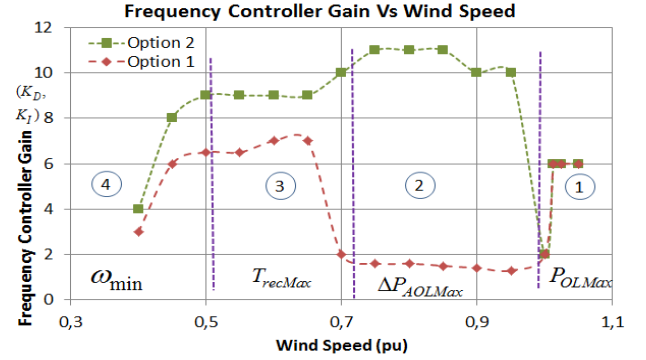

Figure 6. Optimal Frequency Controller gains Vs Wind Speed

A. Dynamics of WT with Option 1 and Option 2 for WT open loop overloading test at 0.8 pu wind speed

The overloading test provides information on the WT's limitations to support the grid during frequency dips. As shown in Fig. 7, in both options, the frequency input signal to the FFC, electrical power reference from optimal operation block (P_{opt}), WT electrical power output (P_{out}), WT rotor speed (ω), and the aerodynamic power (P_{aero}), are presented.
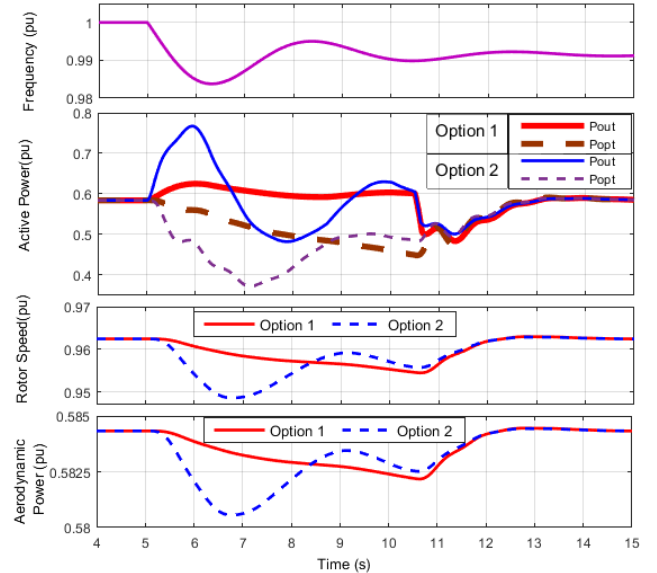

Figure 7. Dynamics of WT for temporary overloading test with Option 1 and Option 2 at wind speed – 0.8 pu

In Option 1, as the overloading power reference from FFC (ΔP) is added to the pre-overloading optimal power reference, P_{out} is always higher than P_{aero} during the whole overloading period (for 5.5 s). Hence, the rotor continues to

decelerate, which further decreases P_{aero}, until the release of overload. This leads to a higher power drop (P_{out} falls from 0.6 pu to 0.5 pu) after release of overload. Therefore, maximum power drop after overload (ΔP_{AOLMax}) is the limiting parameter for the gains ($K_D = K_I = 1.8$) of the FFC at medium wind speed range. For better understanding of the results P_{out} and P_{aero} are plotted together for both options in Fig. 8.

In case of Option 2, ΔP is added to the actual power output of the WT i.e. the output of optimal operation block (P_{opt}), which decreases when the rotor speed drops. Therefore P_{out} increases faster during the initial phase of overloading i.e. up to 6.1s due to the higher ΔP generated by higher estimated gains of the fast frequency controller. However, P_{out} decreases below its pre fault value during the mid-phase of overload (from 7 s to 9 s) because of the faster reduction in P_{opt}. During this period P_{out} is less than P_{aero}, which drives the rotor speed (ω) towards its pre-overloading value and leads to faster WT recovery. It can also be observed, from Fig. 7, that the frequency signal is rising (during 6.5 s to 9 s) after the first dip; hence reduction in WT power output does not deteriorate the overall frequency of the power system. In the last phase of overloading (from 9 s to 10.5 s), P_{out} becomes slightly higher than P_{aero}, due to fall in frequency, causing slight reduction in rotor speed until the release of overloading. For Option 2, ΔP_{AOLMax} is also the limiting parameter for the gains ($K_D = K_I = 11$) of the FFC, as P_{out} falls from 0.6 pu to 0.5 pu.
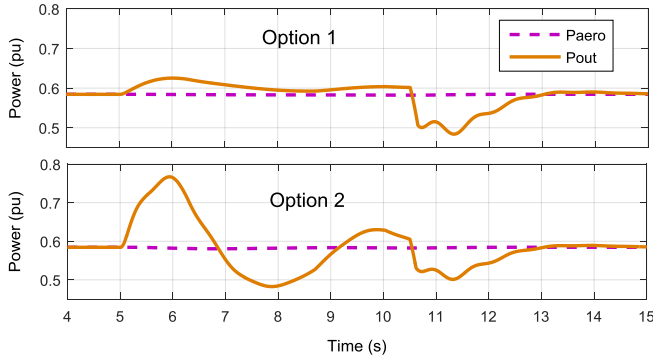

Figure 8. Active power output and aerodynamic power of WT for Option 1 and Option 2 (Extracted from Fig 7)

During medium wind speeds, a slight decrease in rotor speed leads to a higher reduction of active power output from WT. ΔP_{AOLMax} is the constraint for the temporary overloading and hence for the optimal gains of the frequency controller. In case of Option 2, it is possible to extract more energy from the WT during the first phase of frequency dip, thereby better utilizing the kinetic energy stored in the WT rotor to limit the ROCOF and frequency nadir, compared to Option 1. For Option 2, the recovery of the WT has started during the overload period itself as the overloading considers the actual WT power output. However, in case of Option 1, the recovery

is possible only after finishing the overloading period. Hence, higher FFC gains, therefore better frequency control, are possible with Option 2 compared to Option 1 for the same value of ΔP_{AOLMax}.

B. Testing of WPP to deliver frequency control in the test power system

The calculated fast frequency controller gains (K_D, K_I) and the conclusions drawn from the overloading test (Fig. 5) for both options are verified by applying these gains to the frequency controller of WPP connected to the test power system shown Fig.1. The same frequency event is created, as explained in section IIIA, by applying a generation loss of 600 MW. The test is performed for a wind speed of 0.8 pu so as to verify the conclusions drawn from the overloading test. The frequency of the test power system with and without the participation of WPP in frequency control is shown in Fig 9. It can be observed that overloading with Option 2 leads to a better performance compared to Option 1 due to higher optimal FFC gains at medium wind speeds. The dynamics of the WT for both options are given in Fig. 10.

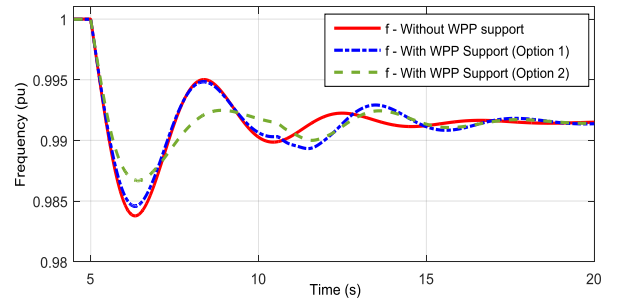Figure 9. Frequency of the power system considering contribution from WPPs (Option1 and Option 2) at wind speed - 0.8 pu
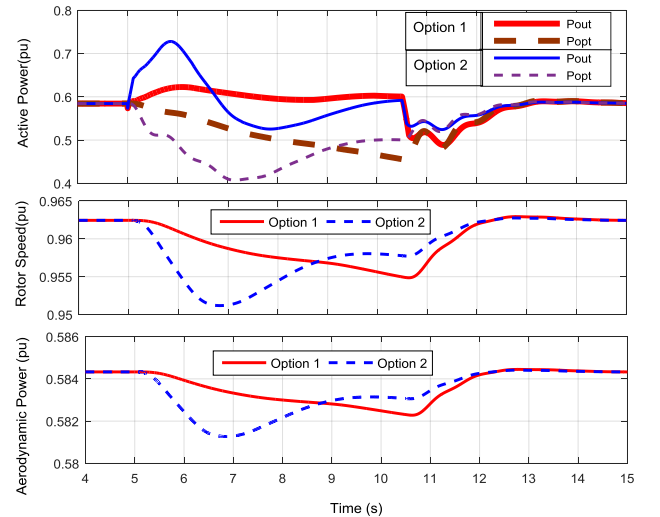

Figure 10. Dynamics of the WT for Option 1 and 2 for the case in Fig. 9.

The results shown in this Fig. 10 resemble the results drawn from the open loop overloading test shown Fig. 7. The estimated optimal gains of the FFC from the proposed method (WT overloading test) have thus been validated by

applying these gains to a WPP connected to a test power system.

C. *Recommendation for participation of WPPs in power system frequency control*

If the main objective of the WPP is to participate in temporary frequency control i.e. mainly inertial support, then the energy yield from the WTs can be increased to limit the ROCOF and frequency nadir by adapting appropriate gains of the FFC depending on the wind speed range. Thereafter, the primary control should take over the responsibility to stabilize system frequency be followed by secondary control. In that case, Option 2 is preferred over Option 1 due to its merits on higher temporary overloading with better WT dynamics. If the WPP are expected to participate in frequency control for an extended time period (for example more than 10s), then it may not possible to rely on overloading the WT. Therefore, deloading/down regulating the WT with a certain percentage is required to ensure stable operation of the power system and WPP. This will, however, result in loss of revenue for the WPP owner. Setting up new markets accommodating remuneration for the WPPs participating in frequency control may compensate this loss.

Another important conclusion from the results is that the temporary overloading of the WT and hence the gains of the FFC vary with wind speed. These gains can be adapted in advance based on the very short term average wind speed forecast to improve the temporary overloading of the WT without compromising system stability. One optimal gain can be chosen for each wind speed range, thereby limiting the gains to three or four values for the possible operating range of the wind turbine. To compensate for the inherent forecast errors, the gains could be set conservatively corresponding to the lower part of the considered range, i.e. corresponding to 0.5 pu wind speed for the lower medium average wind speed range (0.5-0.7 pu), for example.

V. CONCLUSIONS

In this paper an improved fast frequency controller for WPP is presented. This controller generates an additional temporary overloading power reference to the WT based on the frequency deviation and rate of change of frequency. Two different control options have been proposed and the dynamics of the WT have been analyzed at different wind speeds. It has been observed that the performance can be improved in case the frequency initiated power reference is based on the actual power output (Option 2) instead of the constant pre-overloading power output of the WT (Option 1). Moreover, the gains of the fast frequency controller have been optimized over the whole wind speed range considering the limitations and dynamics of the WT. This way the response is improved while stability is still ensured. These gains can e.g. be adapted in advance based on the very short term average wind speed forecast to improve the frequency response of the WT over the whole wind speed range.

REFERENCES

[1]   Tennet TSO GmbH, *Requirements for Offshore Grid Connections in the Grid pf Tennet TSO GmbH*, Germany, Dec. 2012. www.tennet.eu.

[2]   ENTSO-E, network code for requirements for grid connection Applicable to all Generators, Oct. 2013. www.entsoe.eu

[3]   L. Zeni, A. J. Rudolph, J. M. Swendesen, I. Margaris, A. D. Hansen and p. Sørensen "Virtual inertia for variable speed wind turbines," *Wind Energy*, vol. 16, pp. 1225-1239, Sep 2012.

[4]   M. Altin, R. Teodorescu, B. B. Jensen, U. D. Annakkage, F. Iov and P. C. Kjaer "Methodology for Assessment of inertial Response from Wind Power Plants," in *Proc. 2012 IEEE Power & Energy Society General Meeting*, pp. 1-8.

[5]   G. C. Tarnowski, P. C. Kjaer, S. Dalsgaard, and A. Nyborg, "Regulation and frequency response service capability of modem wind power plants," *in Proc. 2010 Power & Energy Society General Meeting,* pp.1-8.

[6]   F. D. Gonzalez, M. Hau, A. Sumper, O.G. Bellmunt, "Participation of wind power plants in system frequency control: Review of grid code requirements and control methods," *Renewable and Sust. Energy Reviews*, vol. 34, pp. 551-564, April 2014.

[7]   Abdul Basit, "Balancing modern power system with large scale wind power," Ph.D. dissertation, Dept. Wind Energy., DTU, Denmark, 2015.

[8]   P. W. Christensen, G. C. Tarnowski, "Inertia for Wind Power Plants-State of the Art Review ", *in Proc. 2011 10th International Workshop on Large-Scale Integration of Wind Power into Power Systems as well as on Transmission Network for Offshore Wind Power Plants*, pp. 457-463.

[9]   J. Morren, S. W.H. de Haan, W L. Kling, and J. A. Ferreira, "Wind turbine emulating inertia and supporting primary frequency control," *IEEE Transactions on Power Systems*, vol. 21, no. 1, pp. 433-434, 2006.

[10] J. F. Conroy and R. Watson, "Frequency response capability of full converter Wind turbine generators in comparison to conventional generation," *IEEE Transactions on Power Systems,* vol. 23, no. 2, pp. 649-656, May 2008.

[11] N. R. Ullah and T. Thiringer, "Temporary primary frequency control support by variable speed wind turbines-potential and applications," *IEEE Transactions on Power Systems*, vol.23, no.2, pp.601-612, May 2008.

[12] K. Ping-Kwan, L. Pei, H, Banakar, B. T. Ooi, "Kinetic Energy of Wind Turbine Generators for System Frequency Support," *IEEE Transactions on Power Systems*, vo1.24, no.1 , pp.279-287, Feb. 2009

[13] M. Fischer, S. Engelken, N. Mihov, A. Mendonka, " Temporary primary frequency control support by variable speed wind and applications," in *Proc. 2014 13th Wind Integration Workshop,* pp. 457-463.

[14] M. Asmine, C. E. Langlois, " Field Measurements for the Assessment of Inertial Response for Wind Power Plants based on Hydro Quebec TransEnergie Requirements," in *Proc. 2014 13th Wind Integration Workshop*, pp. 1-6

[15] S. Wachtel, A. Beekman, " Contribution of Wind Energy Converters with Inertia Emulation to frequency control and frequency stability in power systems" in *Proc. 2009 8th Wind Integration Workshop,* pp. 1-6

[16] A. D. Hansen, M. Altin, I. Margaris, F. Iov, and G. C. Tarnowski, "Analysis of short-term over production capability of variable speed wind turbines," *Renewable Energy*, vol. 68, , pp. 326-336, 2014

[17] K. V. Vidyanadhan and N. Senroy, " Primary Frequency Regulation by Deloaded Wind Turbines Using Variable Droop," IEEE Transactions on Power Systems, vol. 28, , pp. 837-846, May 2013..

[18] V. Akhmatov, A.H. Nielsen, "A small test model for the transmission grid with a large offshore wind farm for education and research at Technical University of Denmark", *in Proc. 2006 Power Systems Conference and Exposition*, pp. 650-654.

[19] P. Kundur, "Power system stability and control", 4th edition, New York: McGraw-Hill, 1994.

[20] E. Muljadi et al. "Method of equivalencing for a large wind power plant with multiple turbine representation".*in Proc. 2008 IEEE Power and Energy Society General Meeting, p*p.1-6

[21] *Electrical simulation models for wind power generation Wind turbine*, IEC 61400-27-1, 2015.

[22] A. D. Hansen, I. Margaris, G. C. Tarnowski and F. Iov,"Simplified type 4 wind turbine modeling for future ancillary services," in *Proc. 2013 European Wind Energy Conference*, pp. 768-774.

This page would be intentionally left blank if we would not wish to inform about that.

C4 Jayachandra N. Sakamuri., Hansen A.D., Cutululis N.A., Altin M., Sørensen P.E., "Coordinated Fast Primary Frequency Control from Offshore Wind Power Plants in MTDC System ", Proc. IEEE Energycon, Leuven, Belgium, 2016

This page would be intentionally left blank if we would not wish to inform about that.

Coordinated Fast Primary Frequency Control from Offshore Wind Power Plants in MTDC System

Jayachandra N. Sakamuri, Anca D. Hansen, Nicolaos A. Cutululis, Mufit Altin, Poul E.Sørensen

Department of Wind Energy
Technical University of Denmark
DTU Risø Campus, Denmark
e-mail: jays@dtu.dk

Abstract— **In this paper, coordinated fast primary frequency control (FPFC) from offshore wind power plants (OWPPs) integrated to surrounding onshore AC power system through a three terminal VSC HVDC system is presented. The onshore AC grid frequency variations are emulated at offshore AC grid through appropriate control blocks, based on modulation of the DC grid voltage. The proposed FPFC produces a power reference to the OWPP based on the frequency deviation and its rate of change measured in the offshore AC grid. Moreover, the impact of wind speed variations on the OWPP active power output and the dynamics of wind turbine are also discussed. The corresponding impact of OWPPs active power output variation at different wind speeds on the power system frequency control and DC grid voltage is also presented. The results show that the proposed coordinated fast primary frequency control from OWPPs improves the power system frequency while relieving the stress on the other AC grid participating in frequency control.**

Index Terms— coordinated frequency control, HVDC, offshore wind power plants, ramp rate limiter, RMS models.

I. INTRODUCTION

Many large-scale offshore wind power plants (OWPPs) are planned to be constructed in Europe in near future [1], [2]. Traditionally, the power from OWPPs is transmitted to the mainland grid through submarine high voltage AC (HVAC) cables [3]. However, the transmission of power from OWPPs using AC technology becomes challenging with the increase in magnitude of power and distance from the shore. Therefore, Voltage Source Converter (VSC) based High Voltage Direct Current (HVDC) transmission system is a feasible and economical solution to long distance bulk power transmission [4]. Accordingly, Multi-Terminal DC (MTDC) grids based on VSCs may become reality in a future European offshore super grid [1],[5].

However, the OWPPs connected through HVDC transmission network will not contribute to the power system effective inertia due to the decoupling from the AC power system. On the other hand, with the anticipated increase of offshore wind power, there are ascending requirements for OWPPs to participate in frequency regulation of surrounding onshore AC system [6], [8].

The possibilities of using onshore WPPs for inertial and primary frequency regulation of power system have been investigated in [9]-[13]. A common approach consists of operating the WPP below its possible power (down regulation), hence creating a spinning reserve margin. Another method is to temporarily overload the WPP for limited period during the frequency events [12]. In case of DC transmission since the HVDC system decouples the OWPPs from the mainland AC grid, they are unable to detect and respond to onshore grid disturbances based on their local offshore measurements. In the literature [14]-[17], there are two methods to replicate the onshore frequency at the offshore grid; (1) Communication based method (2) Coordinated control method. The former is based on transmitting the onshore frequency to the offshore converter station through appropriate communication channels, while the latter aims at emulating the onshore frequency variations into the offshore grid through appropriate control blocks. Communication based control requires sophisticated communication network between each OWPP converter station to the onshore AC grid. The coordinated frequency control is based on a cascaded reproduction of onshore frequency at the offshore AC grid through supplementary droop control loops at onshore and offshore converter stations regulating the DC voltage in the HVDC grid to mirror the frequency changes. According to [15], the coordinated control approach should be considered for OWPPs connected through an MTDC system, due to the reliability issues with the communication links between each WPP and associated AC grids. The coordinated frequency control from OWPPs connected through VSC-HVDC system based on DC voltage regulation method is investigated in [14], [15]. These studies are however limited to a point to point HVDC system. Frequency control from OWPPs connected to MTDC networks has been introduced in [16], [17]. However, none of these studies addressed the OWPP dynamics and its limitations on the power system frequency control and DC grid voltage at different wind speeds.

According to the grid codes [8], the generators participating in primary frequency control should supply 100% % of the agreed power within 30s and maintain the

response until the secondary control is activated, which can be up to 15 min. However, with the anticipated decrease in system inertia due to the penetration of HVDC connected OWPPs into the power system may lead to higher rate of change of frequency (ROCOF) following a loss of large infeed or step increase in load demand. High ROCOF causes the frequency to change very quickly and in the case when a large infeed is lost, the frequency may drop to the lower limit of nadir before a sufficient level of primary reserves has had time to start responding to the event. Therefore, to avoid the lower frequency nadir, it is important that the frequency control reserves deliver response quickly. However, primary reserves may take few seconds to start responding. Hence, a need for fast primary control reserves, which can act faster than primary reserves, has been highlighted by National Grid in its 2014 system operability framework report [18].

Hence, a coordinated fast primary frequency control (FPFC), which generates an additional active power for few seconds after the frequency event, from OWPPs connected through a 3 terminal HVDC system is proposed in this paper. This FPFC from OWPPs generates a temporary active power reference based on (1) frequency deviation from steady state value and (2) rate of change of frequency measured at offshore AC grid. Also, the coordinated frequency control from OWPPs takes into account the limitations imposed by the wind speed on the dynamic behavior of the wind turbines (WTs). The impact of release of fast primary frequency control from OWPPs on the power system frequency and DC grid voltage is also investigated. Root mean square (RMS) models for the OWPPs, HVDC system, and AC grid with aggregated synchronous machines have been used for the investigation and implemented in DIgSILENT PowerFactory.

The paper is organized as follows. Section II briefly presents the WPP, MTDC system modeling and control, and the proposed coordinated fast primary frequency control from WPPs. Section III presents the simulation and analysis of results, illustrating the proposed control methods, WPP capability to participate in fast primary frequency regulation and WPP behaviour at different wind speeds, and the impact of release of frequency support from WPPs on the power system frequency and DC grid voltage. Finally, conclusive remarks are reported in section IV.

II. MODEL DESCRIPTION

The grid layout considered in this paper consists of 2 onshore AC grids and one offshore grid with OWPPs connected all together through a 3-terminal HVDC system as shown in Fig. 1. A brief description of the simulation models for the onshore AC grid, OWPP, and the HVDC interconnection is given below.

A. Onshore AC Grid Model:

The onshore AC grid-2 is modelled as a lumped synchronous machine with rated power of 1200 MVA while that of AC grid-3 with 5000 MVA. Standard models and parameters for the Governor, Automatic Voltage Regulator and Power System Stabilizer have been developed [19].

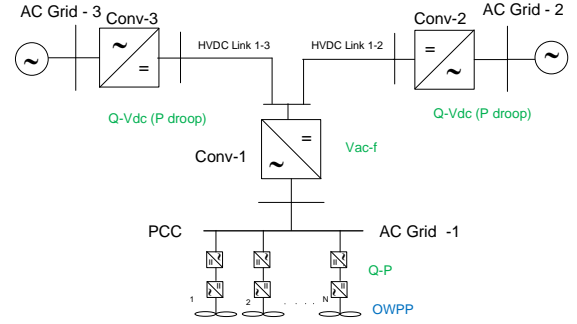Relevant parameters of the synchronous machine used in this study are summarised in Table 1.

Fig. 1 WPP integrated to 3 Terminal HVDC system

TABLE I : SYNCHRONOUS MACHINE PARAMETERS

Parameter	Value	Unit
System regulating energy, K_{sys}	10	pu
Governor time constant ,T_P	0.1	s
Turbine time constant ,T_1	1.0	s
Inertia constant ,H	8.5	s

B. HVDC System Model:

A 3-terminal HVDC interconnection based on three VSCs, modelled as ideal voltage sources behind reactance is shown in Fig. 1. It is based on symmetrical monopole configuration having same voltage with opposite polarity at the converter terminals. The given MTDC system is operated based on power-voltage ($P-V_{dc}$) droop control method due to its superiority in power sharing and reliability of MTDC system as explained in [20]. Data for the grid layout are summarised in Table II.

TABLE II : DESCRIPTION OF THE GRID LAYOUT IN FIG. 1

Parameter	Value	Unit
Onshore AC Voltage	380	kV
Offshore AC Voltage	155	kV
DC grid Voltage	320	kV
Converter MVA (Base)	1200	MVA
WPP Active Power Output	1000	MW

1) Onshore HVDC Converters

The Conv-2 and Conv-3 in Fig 1 are the onshore HVDC converter stations connected to AC grid-2 and AC grid-3 respectively. These converters are responsible for maintaining the power balance in the DC system, by keeping the DC voltage within the acceptable limits. The control block diagram for onshore HVDC converter is shown in Fig. 2. The onshore HVDC converter control consists of two main controllers: one for active power balance control (DC voltage –active power droop) and other for reactive power control. The sharing of active power imbalance between the onshore converters depends on the active power droop constant (k_p) of the $P-V_{dc}$ droop controller. The converter also controls the reactive power at converter bus through AC voltage droop ($Q-V_{ac}$) so as to maintain the AC voltage within specified range.
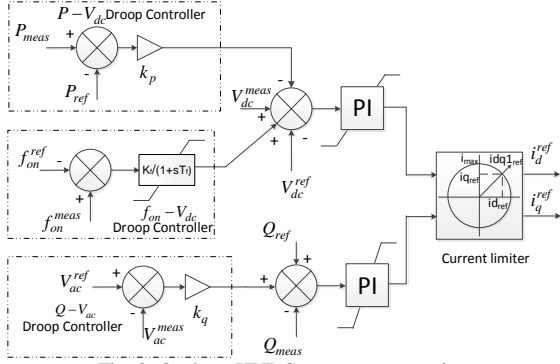
Fig. 2. Onshore HVDC converter control

The current references provided by the outer controllers are then handled by an inner current controller operating in $d-q$ reference frame. A supplementary frequency-DC voltage droop ($f_{on}-V_{dc}$) controller in the outer loop d-axis is responsible for modulating the DC voltage reference (V_{dc}^{ref}) proportional to the onshore frequency deviation. This controller allows exchange of frequency support between the onshore AC systems as well as the participation of WPPs in frequency control. This control loop contributes to the power system frequency control in coordination with a DC voltage-frequency droop controller ($V_{dc}-f_{off}$) at offshore HVDC converter, as depicted in Fig. 3, and active power controller of OWPP. However, it is recommended that the coordinated frequency control action should not cause significant deviation in the DC grid voltage as it may trigger DC gird protection systems and also the performance of the other associated AC system may get affected. Hence, proper measures have to be taken to limit the DC voltage within acceptable limits (within 2% deviation) during and after fast primary frequency control.
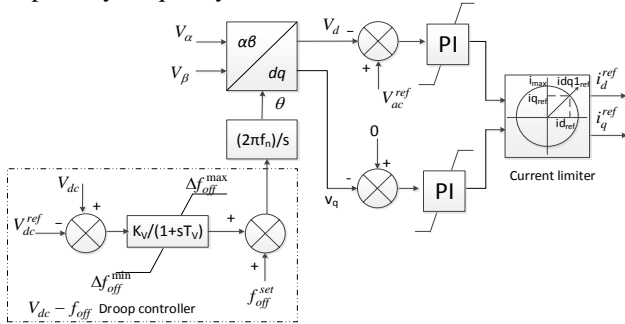

Fig. 3. Offshore HVDC converter control

2) Offshore HVDC Converter

The Conv-1 in Fig. 1 i.e. the offshore HVDC converter station connecting the OWPP to the MTDC system is responsible for controlling the AC voltage magnitude and frequency of the offshore AC network at the point of common connection (PCC) of the WPP and allows transferring the wind power output to the MTDC system. The converter's control consists of two inner current controllers whose references are provided by the outer controller, as illustrated in Fig 3. A DC voltage-frequency droop controller ($V_{dc}-f_{off}$) at the outer control loop changes the offshore AC

grid frequency reference proportionally to the DC voltage deviation. This controller in coordination with active power controller of OWPP provides the active power support required for the power system frequency control.

C. Offshore Wind Power Plant Model:

The OWPP considered in this paper is an aggregated IEC Type 4 wind turbine (WT) model based on the aggregation method described in [21]. The Type 4 WT model used in this study is based on generic approach proposed by the IEC Committee in Part 1 of IEC 61400-27 [22] for the short term power system stability studies. Additionally, this model is extended to include the dynamic features relevant for active power and frequency studies [23].

D. Coordinated Fast Primary Frequency Control from OWPP

For coordinated fast primary frequency control from OWPPs, the DC voltage reference is changed by the onshore HVDC converter according to the onshore frequency variations. The offshore HVDC converter then modifies the offshore AC grid frequency proportional to the DC voltage variation measured at its terminals. Based on the frequency deviation and rate of change of frequency at offshore AC grid, the OWPP frequency controller generates an additional power reference to WT active power controller. The relation between offshore AC grid frequency and the DC voltage is given in (1),(2), where f_{off}^{set} is the offshore frequency during normal conditions and f_{off}^{ref} is the reference offshore frequency according to DC grid voltage variation.

$$f_{off}^{ref} = f_{off}^{set} + \Delta f_{off} \tag{1}$$

$$\Delta f_{off} = k_v \Delta V_{dc} \tag{2}$$

An additional control mechanism, namely $f_{on}-V_{dc}$ droop as shown in Fig. 2, is necessary for OWPP to provide AC grid frequency control service. This translates the onshore AC grid frequency variations into DC voltage variations of MTDC system as given in (3). Notice however that the $f_{on}-V_{dc}$ droop control is only activated when the variation in the onshore frequency is above a certain dead band to avoid conflict with the $P-V_{dc}$ droop control of the onshore converter [15].

$$\Delta V_{dc} = k_f (f_{on}^{meas} - f_{on}^{ref}) \tag{3}$$

Where f_{on}^{ref} and f_{on}^{meas} are the reference and actual frequencies of the onshore AC grid respectively.

The frequency variation at the offshore AC grid modifies the WT active power reference (P_{wt}^{ref}) as given in (4).

$$P_{wt}^{ref} = P_{base} + \Delta P_1 + \Delta P_2$$
$$\Delta P_1 = k_d (f_{off}^{set} - f_{off}), \Delta P_2 = k_{in}(\Delta f_{off} / \Delta T) \tag{4}$$

The offshore AC grid frequency at PCC is communicated to the WPP controller which then produces the additional power reference to individual WT depending on frequency deviation. However, as the WPP is based on an aggregated

WT model, the frequency controller at WT level is shown in Fig. 4. The additional power ΔP from the 'frequency controller' is a combination of ΔP_1 and ΔP_2, where ΔP_1 is the power reference proportional to the frequency deviation from steady state value and ΔP_2 is proportional to the rate of change of frequency. The magnitude of ΔP_1 and ΔP_2 can be varied by changing the gains k_d and k_{in} respectively. The frequency controller is inactive for certain dead band in frequency deviation and rate of change, whose values depend on grid code requirements [6]. A low pass filter is used to remove the high frequency noise in order to protect the WT from short spikes in its power references.
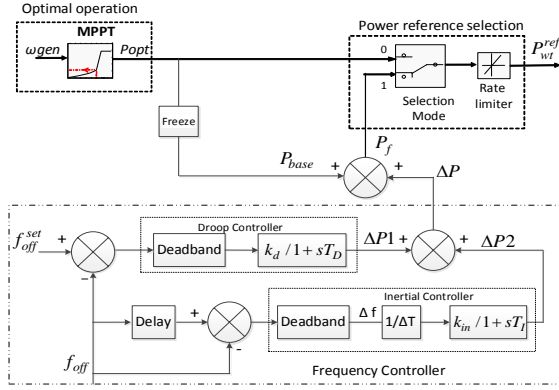

Fig. 4. WPP fast primary frequency controller

The 'Power reference selection' block in Fig. 4, selects between optimal power reference (P_{opt}) during normal operation and frequency initiated power reference (P_f) during a frequency event. P_f is the sum of base power reference (P_{base}), and overloading power reference (ΔP) generated by the frequency controller. P_{base} is the WT output before the frequency event i.e. the freezed value of the output of the 'optimal operation' block. In this paper a fast primary frequency control from OWPPs is considered. Hence, the WTs are allowed to produce additional power for few seconds after the frequency event, called as frequency support period (T_{OL}). After completion of T_{OL}, the minimum out of P_f ($P_f = P_{base}$ as $\Delta P = 0$ after T_{OL}) and P_{opt} will be selected for the fast recovery of the WT. However, during T_{OL}, if the WT rotational speed becomes lower than minimum value (i.e. $\omega < \omega_{min}$), then also the minimum out of P_f and P_{opt} is selected to protect the WT from stalling. The rate of change of WT power output is limited by the ramp rate limiter.

III. SIMULATION AND ANALYSIS OF RESULTS

In this section, the performance of coordinated fast primary frequency control from OWPPs connected through a 3-terminal HVDC system is demonstrated. A 10% load increase at AC grid-2 (in Fig. 1) is initiated at time t=10s to create an under frequency event. The OWPPs participate in frequency control by producing an additional power for a duration of frequency support period (T_{OL} = 10s) after the under frequency event. The impact of ramp rate limiter during the release of power support from OWPP, after T_{OL}, on the power system frequency and the DC grid voltage is also presented. The study is performed at above (1.1 pu) and below (0.9) rated wind speeds, where the simulation results at above rated wind speed are given in section A while the results at below rated wind speeds are given in section B. In both cases, the amount of power taken by AC grid-2 from DC grid is 1150 MW, where OWPP supplies a maximum power of 1000 MW while the rest of the power is supplied by AC grid-3.

A. Frequency Control at Above Rated Wind Speed (1.1 pu)

The frequency of AC grid-2 for three different study cases: (1).Without coordinated control (2).With coordinated control from AC grid-3 alone (3).With coordinated control from OWPP and AC grid-3, is shown in Fig. 5. The corresponding frequencies of offshore AC grid and AC grid-3 are also given in Fig. 5. The DC voltage, active power output of the three converters of the DC grid for the three study cases are given in Fig. 6.
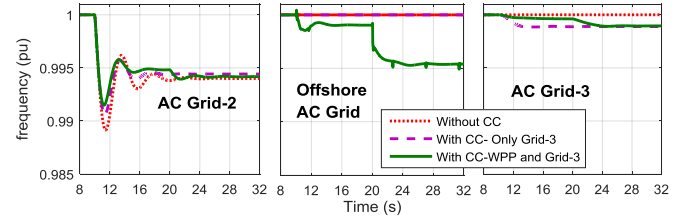

Fig. 5. Frequency of different AC grids at above rated wind speed 1.1 pu – With and Without Coordinated Control (CC)
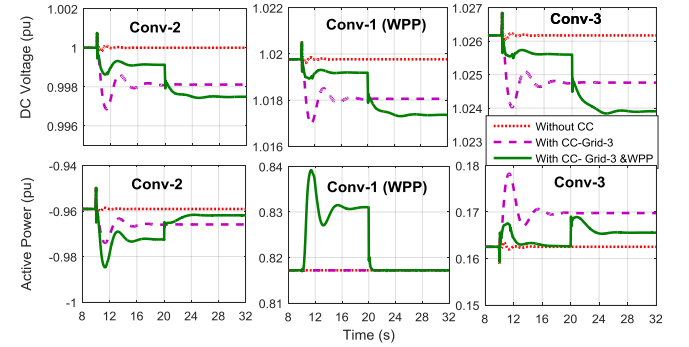

Fig. 6. DC Voltage and Active power at different converters at wind speed 1.1 pu -With and Without Coordinated Control (CC)

From these results, it can be observed that the frequency of AC grid-2 is improved with the coordinated control from AC grid-3(dashed line) compared to without coordinated control (dotted line). Once the under frequency event at AC grid-2 is detected, the $f - V_{dc}$ droop controller of Conv-2 reduces its voltage reference, thereby, reducing the voltage profile of the DC grid as a result of the coordinated frequency control action. Therefore Conv-3 increases the active power supply to the DC grid, due to its $P - V_{dc}$ droop control, allowing the increase of active power taken by Conv-2 from the DC grid. Similarly, the offshore AC grid frequency is

altered according to measured DC voltage at Conv-1 which triggers the OWPP fast primary frequency controller to generate additional power reference to the WT. Therefore, the AC grid-2 frequency is improved further with the coordinated control from OWPP together with the AC grid-3 (solid line) as shown in Fig. 5. However, the additional active power input from Conv-3 due to coordinated frequency control action results into a slightly reduced frequency of AC grid-3 as shown in Fig. 5. It can also be observed from Fig. 5 and Fig. 6 that the participation of OWPP in AC grid-2 frequency control reduces the burden on the AC grid-3 alone and improves the DC voltage profile of the DC grid.

At the end of frequency support period, i.e. at t= 20s, the OWPP stops delivering power support (a step change) for frequency control, reducing power injection to the DC grid. This in turn leads to a small second frequency dip in both the AC grids at 20s. Preferably, the second frequency dip should be avoided as it may trigger the primary reserves again. Moreover, the voltage of the DC grid is also slightly reduced at 20s due to the power imbalance in the DC grid and also the $f - V_{dc}$ droop controller at Conv-2 and Conv-3 changes their DC voltage reference due to the reduction of their corresponding AC grid frequencies. However, this second frequency and DC voltage dips of limited magnitude since it is proportional to the power reduction from the WTs . The magnitude and rate of second frequency and DC voltage dip can be decreased by limiting the rate of release of power support from WPPs i.e. opting power ramp down instead of step change. The impact of power ramp rate limiter (RL) of OWPP on the AC grid-2 frequency is shown in Fig. 7. The relevant dynamics of the WT during and after the frequency support is also highlighted in Fig. 7.
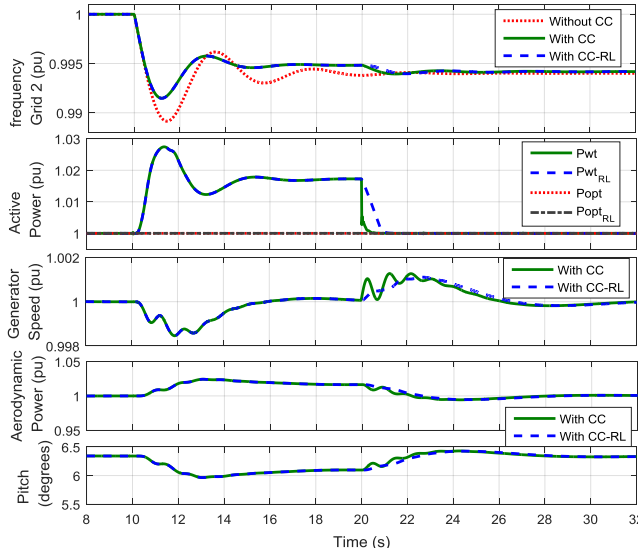

Fig. 7. AC grid-2 frequency and WT dynamics at above rated wind speeds (1.1 pu) - With and Without considering Ramp Rate Limiter (RL)

It can be observed from Fig. 7 that there is not much difference in the second frequency dip at AC grid-2 with and without power ramp rate limit of OWPP at above rated wind speeds as the magnitude power reduction after the frequency support is small. In both the cases, the WT generator speed decreases slightly during the initial phase of frequency

support. However, speed recovers quickly due to the increase in aerodynamic power of the WT due to the pitch control, as shown in the lower graph of Fig. 7. The dynamics of the WT are smoother with the 'power ramp rate limit' option compared to 'step change' option.

B. Frequency Control at Below Rated Wind Speed (0.9 pu)

The frequency of the three AC grids with and without considering the coordinated control from WPPs and AC grid-3, at a wind speed of 0.9 pu, is shown in Fig. 8. The results are shown for two cases: with and without the impact of ramp rate limit of WT during the release of active power support from OWPP. The corresponding DC voltage and active power outputs of the three converters is shown in Fig. 9.
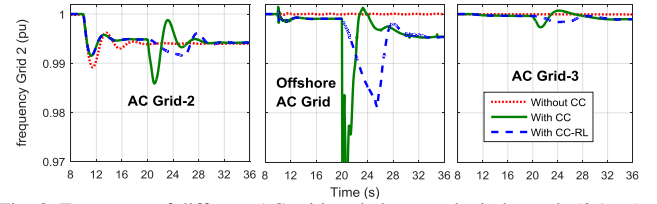

Fig. 8. Frequency of different AC grids at below rated wind speeds (0.9 pu) - With and Without Coordinated Control (CC) and Ramp Rate Limiter (RL)
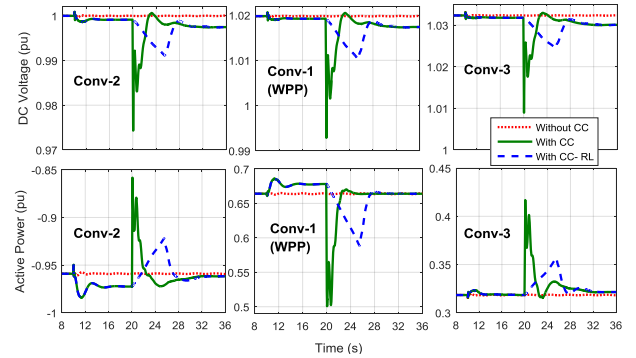

Fig. 9. DC Voltage and Active power at different converters at below rated wind speed 0.9 pu – With and Without Ramp Rate Limiter (RL)

From these results, it can be observed that the frequency of AC grid-2 is improved with the coordinated control from OWPP for both the cases. However, the magnitude and rate of second frequency and DC grid voltage dips after the frequency support from OWPP is significant at below rated wind speeds. In fact, the frequency nadir of AC grid-2 is higher than the initial one, due to the significant power reduction from the OWPP after the frequency support period. The introduction of the ramp rate limiter in the OWPP significantly improves the situation, being able to limit both the magnitude and rate of the DC grid voltage and second frequency dips. Also, the ramp rate limiter from OWPP reduces the stress on the Conv-3 by limiting the magnitude and time constant of the active power support from AC grid-3. The WT dynamics with and without considering effect of ramp rate limiter is shown in Fig. 10. At below rated wind speed, the WT active power output (P_{wt}) is always higher than the WT aerodynamic power output during the whole frequency support period (from t=10s until 20s). Also, the pitch angle is already at its optimal value (zero degrees) and does not contribute for the increase of aero dynamic power

103

during the frequency support period. Hence, the rotor continues to decelerate, until the completion of frequency support. The decrease in rotor speed leads to the reduction of WT optimal power output (P_{opt}) from 0.85 pu to 0.55 pu after completion of frequency support. It can be observed from Fig. 10 that the magnitude and rate of power reduction from OWPP after the frequency support is small with the ramp rate limiter option, resulting in smoother WT dynamics. This leads to reduced magnitude and rate of secondary frequency dip after the release of frequency support from OWPP.
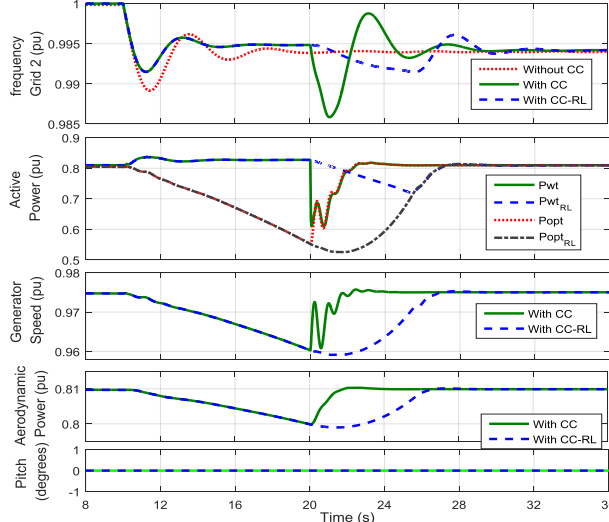

Fig. 10. AC grid-2 frequency and WT dynamics at below rated wind speeds (0.9 pu) - With and Without Ramp Rate Limiter (RL)

IV. CONCLUSIONS

In this paper, a coordinated fast primary frequency control from OWPPs connected through a 3 terminal HVDC grid has been investigated. The onshore grid frequency is replicated at the offshore grid through supplementary control blocks located at onshore and offshore HVDC converters. The impact of participation of OWPPs in power system frequency control and the associated dynamics of wind turbine has been studied at above and below rated wind speeds. Moreover, the impact of the active power ramp rate limiter of the OWPP on the power system frequency and DC grid voltage after completion of the fast frequency control from OWPPs is also presented. The results show that the power system frequency is significantly improved with the proposed coordinated fast primary frequency control from WPPs. However, a second frequency and, maybe more important for the stability of the offshore grid itself, DC voltage dips are observed once the OWPPs stop providing frequency control. This phenomenon is predominant at below rated wind speeds due to higher reduction of active power output from the wind turbines after the frequency support. The rate and magnitude of second frequency and DC grid voltage dips can be minimised with the help of active power ramp rate limiter. The coordinated frequency control from OWPPs, particularly with the ramp rate limiter, reduces the burden on the other converter and associated AC grid participating in frequency control.

V. REFERENCES

[1] Windspeed, "Roadmap to the deployment of offshore wind energy in Central and Southern North Sea to 2030, " final report, EU-IEE project Windspeed, March 2011. www.windspeed.eu

[2] ENTSOE, "Offshore grid Development in the North Seas: ENTSO-E views," 2011. www.entsoe.eu

[3] M. Aragues Penalba, O. Gomis-Bellmunt and M. Martins," Coordinated Control for an Offshore Wind Power Plant to Provide Fault Ride Through Capability", *IEEE Trans. Sustainable Energy*, vol. 5, pp. 1253-1261, Sep 2014.

[4] D. Van Hertem, M. Ghandhari , "Multi-terminal VSC HVDC for the European Supergrid: Obstacles," *Renewable and Sustainable Energy Reviews,* vol 14, pp 3156–3163, Dec 2010

[5] Oriol Gomis-Bellmunta, Jun Liang, Janaka Ekanayake, Rosemary King, Nicholas Jenkins, "Topologies of multiterminal HVDC-VSC transmission for large offshore wind farms," *Electric Power Systems Research,*vol.81,pp, 271-281 , Feb 2011.

[6] ENTSO- E, *Draft- The Network Code on High Voltage Direct Current Connections (NC HVDC)*, Apr 2014.

[7] Tennet TSO GmbH, *Requirements for Offshore grid Connections in the grid of Tennet TSO GmbH*, Germany, Dec. 2012, pp. 1–10.

[8] ENTSO-E, *Network code for requirements for grid connection applic able to all generators* ,March 2013

[9] S. M. Muyeen, R. Takahashi, T. Murata, and J. Tamura, "A variable speed wind turbine control strategy to meet wind farm grid code requirements*," IEEE Trans. Power Syst.,* vol. 25, pp. 331–340, Feb. 2010.

[10] Hansen, A. D., Altin, M. & Cutululis, N. A., Modelling of wind power plant controller, wind speed time series, aggregation and sample results,2013 DTU Wind Energy. 40 p. (DTU Wind Energy I; No. 0195).

[11] L. Zeni, A. J. Rudolph, J. Munster, I. Margaris, A. Hansen, and P. Sørensen,, "Virtual Inertia for Variable speed wind turbines, " *Wind Energy,* vol. 16, pp. 1225-1239. Nov 2013

[12] M. Fischer , S. Engelken, N. Mihov, and A. Mendonca, " Operational Experiences with Inertial Response Provided by Type 4 Wind Turbines ," *in 2014 Proc. 13th Wind Integration workshop, Berlin*.

[13] Altin M, Teodorescu R, Bak-Jensen B, Annakage UD, Iov F, Kjaer PC. Methodology for assessment of inertial response from wind power plants*, in 2012 Proc. IEEE power and energy society general meeting, pp 1-8*.

[14] Y. Phulpin,"Communication-free inertia and frequency control for wind generators connected by an HVDClink," *IEEE Trans on Power Systems,* vol. 27, pp. 1136-1137, May 2012

[15] L. Zeni, I. Margaris, A. Hansen, P. Sørensen and P. Kjær, "Generic Models of Wind Turbine Generators for Advanced Applications in a VSC-based Offshore HVDC Network, " *in 2012 Proc. 10th IET Conference on AC/DC Transmission, Birmingham.*.

[16] B. Silva, C. L. Moreira, L. Seca, Y. Phulpin, J. A. Peças Lopes, "Provision of Inertial and Primary Frequency Control Services Using Offshore Multiterminal HVDC Network," *IEEE Trans. on Sustainable Energy*, vol. 3, pp. 800-808, Oct 2012.

[17] Haileselassie, T.M Uhlen and K., "Primary frequency control of remote grids connected by multi-terminal HVDC, "*in 2010 Proc. Power and Energy General Meeting, Minneapolis* ,pp 1-6.

[18] National grid, *System Operability Framework (SOF) 2014.*

[19] P. Kundur, "Power system stability and control", 4th edition, McGraw-Hill 1994, New York.

[20] T. K. Vrana, J. Beerten, R. Belmans and O. B. Fosso, "A classification of DC node voltage control methods for HVDC grids*," Electric power systems research*, vol. 103, pp. 137-144, 2013.

[21] E. Muljadi et al. "Method of equivalencing for a large wind power plant with multiple turbine representation,"*in Proc. 2008 IEEE Power and Energy Society General Meeting,* pp-1-8.

[22] *Electrical simulation models for wind power generation Wind turbine*, IEC 61400-27-1, 2015.

[23] A. D. Hansen, I. Margaris, G. C. Tarnowski and F. Iov,"Simplified type 4 wind turbine modeling for future ancillary services," in *Proc. 2013 European Wind Energy Conference*, pp. 768-774.

C5 Jayachandra N. Sakamuri, Altin M, Hansen A.D., Cutululis N.A., Rather Z.H.,, "Coordinated Control Scheme for Ancillary Services from Offshore Wind Power Plants to AC and DC Grids ", Proc. IEEE PES General Meeting 2016. (selected as best conference paper)

This page would be intentionally left blank if we would not wish to inform about that.

Coordinated Control Scheme for Ancillary Services from Offshore Wind Power Plants to AC and DC Grids

Jayachandra N. Sakamuri, Mufit Altin,

Anca D. Hansen, Nicolaos A. Cutululis
Department of Wind Energy
Technical University of Denmark
Risø, Roskilde, Denmark
jays@dtu.dk

Zakir Hussain Rather
Department of Electronics and Electrical Engineering
Indian Institute of Technology Guwahati
Guwahati, India
zakir.rather@iitg.ac.in

Abstract— **This paper proposes a new approach of providing ancillary services to AC and DC grids from offshore wind power plants (OWPPs), connected through multi-terminal HVDC network. A coordinated control scheme where OWPP's AC grid frequency modulated according to DC grid voltage variations is used to detect and provide the ancillary service requirements of both AC and DC grids, is proposed in this paper. In particular, control strategies for onshore frequency control, fault ride-through support in the onshore grid, and DC grid voltage control are considered. The proposed control scheme involves only local measurements and therefore avoids the need of communication infrastructure otherwise required for communication based control, and thus increases the reliability of the control system. The effectiveness of the proposed control scheme is demonstrated on a MTDC connected wind power system developed in DIgSILIENT PowerFactory.**

Index Terms—**ancillary services, fault ride through, frequency control, HVDC grid voltage control, integration of wind power.**

I. INTRODUCTION

During recent years, there has been a significant penetration of offshore wind power plants (OWPPs) into power systems and this trend is expected to continue in the future [1]. Traditionally, active power from OWPPs is transmitted to the mainland grid through submarine high voltage AC (HVAC) cables [2]. However, increased active power from OWPPs combined with long distances to the shore has encouraged the use of the voltage source converter based high voltage direct current (VSC- HVDC) transmission system as a feasible and economical solution for bulk power transmission from OWPPs to the onshore grid [3]. Accordingly, increased penetration of wind power into power systems over past decades has introduced various technical challenges, such as onshore gird frequency control and fault ride through for AC grid faults, for secure and stable operation of the system. In order to counter such challenges, transmission system operators (TSOs)/system regulators have introduced new grid codes that are upgraded on regular basis [4],[5]. Among these grid codes, frequency support and Fault Ride-Through (FRT) capability are important for AC grids as these require the fast control of active power output from

HVDC connected offshore WPPs. Further, the active participation of offshore WPPs in DC grid voltage control is important especially when the share of wind power feeding the DC grid is significant [6]. The reason is the dynamic challenges imposed by DC grid voltage control are major; therefore, very fast active power control action is needed to ensure stable DC grid operation.

Since the HVDC system decouples the OWPPs from the mainland AC grid, OWPPs are unable to detect and respond to onshore grid disturbances based on their local measurements near the WTs. In the literature [7]-[9], two methods for frequency control to replicate the onshore frequency to offshore grid are typically described; (1) Communication based control (2) Coordinated control. The first method is based on the transmission of onshore frequency to the offshore converter station through appropriate communication channels, while the second method aims at emulating the onshore frequency variations onto the offshore grid through appropriate control blocks. Communication based control requires sophisticated communication network between each WPP converter station to the onshore AC grid. The coordinated frequency control is based on a cascaded reproduction of onshore frequency at offshore AC grid through supplementary droop control loops at onshore and offshore converter stations by regulating the DC voltage in the HVDC grid. For a two terminal HVDC system, communication based method might be sufficient while for a multi-terminal DC (MTDC) system coordinated control approach is necessary due to reliability issues with the communication links between each WPP and associated AC grids [8].

The main concern for the FRT support from OWPPs connected through HVDC system is the delay in detection and communication of onshore fault at the offshore station, which results in an unacceptable rise of DC voltage leading to trip of the HVDC link, thus blocking the power flow from OWPPs [10]. One of the possible solutions to avoid such type of issue is to use expensive DC chopper in the onshore HVDC station to dissipate the excess energy in the DC link [6]. To avoid the

requirements of DC chopper/reduce its size, a method of fast reduction of active power from the OWPPs in MTDC grid based on modulating the AC voltage or frequency in the offshore AC Grid has been described in [11]. However, as in this method, there is intentional voltage reduction in the offshore AC grid; the voltage dead band for dynamic reactive power controllers of the OWPPs should be adjusted to avoid offshore AC voltage support within the preset dead band during the event. However, this approach will have detrimental impact during a voltage event in the offshore grid as such type of approach will be in contradiction to the requirement of additional reactive current injection during a fault in the offshore AC grid. Therefore, frequency modulation approach, where instead of AC voltage modulation, the offshore AC grid frequency is increased while DC link voltage exceeds the threshold value, is considered in this paper.

For higher share of wind power in MTDC systems, it is imperative that such WPPs feeding into the DC grid shall also provide DC grid voltage support. However, to avail such type of voltage support service from WPPs, high speed measurement and communication infrastructure will be required [12]. Moreover, in the literature [6]-[12], different ancillary services from OWPPs (i.e. frequency support, FRT support from OWPPs) to AC grid have been studied individually and independently. However, this independent study approach may not be sufficient as the controllers designed for one type of service may not be effective for other type of service. For example, to provide onshore FRT support from OWPPs, the offshore AC voltage is intentionally reduced by blocking dynamic reactive current controllers from OWPPs which is not recommended for faults within the offshore AC grid itself as described earlier. Also, during disturbances in the DC gird, the response of WPPs should be fast enough to mitigate the DC grid voltage variations as the dynamics of DC grid is faster than AC grid. The controllers designed for onshore AC grid frequency control may therefore not be fast enough for DC grid voltage control. Hence, a coordinated control scheme for ancillary services for AC (frequency control, FRT support) and DC grids (DC voltage control) from MTDC connected OWPPs based on offshore frequency modulation approach is proposed in this paper. The limitation of this approach for each ancillary service is also discussed. Time domain simulations are carried out in the dedicated power system tool, PowerFactory platform, to verify the effectiveness of the proposed control scheme. The rest of the paper is organised as follows. Section II describes the modeling of the Multi-Terminal HVDC system and OWPPs. The proposed methodology for ancillary services from WPPs is discussed in section III. The simulation results for different ancillary services are presented in section IV, followed by concluding remarks provided in section V.

II. MODEL DESCRIPTION

The grid layout considered in this paper consists of 2 onshore AC grids and one offshore grid with OWPPs connected all together through a 3-terminal HVDC as shown in Fig. 1. A brief description of the simulation models for the onshore AC grid, WPP and the HVDC interconnection is given below.

A. Onshore AC Grid Model:

The onshore AC Grid is modelled as a lumped synchronous machine with rated power of 1200 MVA. Standard models and parameters for the Governor, Automatic Voltage Regulator and Power System Stabilizer have been developed [13]. Relevant parameters based on machine MVA base used in this research study are summarised in Table 1.

TABLE I : SYNCHRONOUS MACHINE PARAMETERS

Parameter	Value	Unit
System regulating energy, K_{sys}	10	pu
Governor time constant ,T_P	0.1	s
Turbine time constant ,T_1	1.0	s
Inertia constant ,H	8.5	s

B. HVDC System Model:

A 3-terminal HVDC interconnection based on three VSCs, modelled as ideal voltage sources behind reactance is shown in Fig. 1. It is based on symmetrical monopole configuration having same voltage with opposite polarity at the converter terminals. The given MTDC system is operated based on power-voltage ($P-V_{dc}$) droop control method due to its superiority in power sharing and reliability of MTDC system as explained in [14]. PowerFactory's built-in converter, pi-model of the cable, and standard transformer models [15] have been used in this study. A brief description of the grid layout is summarised in Table II.
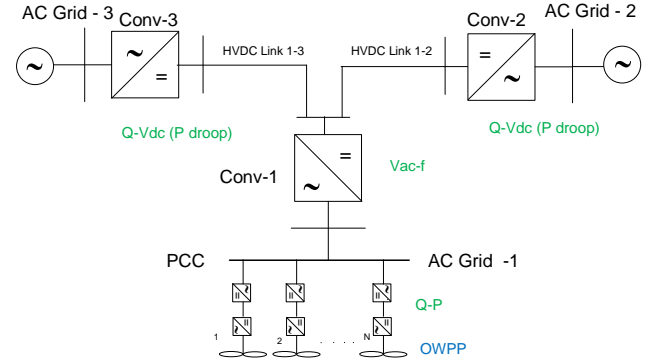

Fig. 1 Grid layout of the 3 terminal HVDC system

TABLE II : DESCRIPTION OF THE GRID LAYOUT IN FIG. 1

Parameter	Value	Unit
Onshore AC Voltage	380	kV
Offshore AC Voltage	155	kV
DC Grid Voltage	320	kV
Converter MVA	1060	MVA
WPP Active Power Output	1000	kW

1) Onshore HVDC Converters

The Conv-2 and Conv-3 in Fig 1 are the onshore HVDC converter stations connected to AC Grid-2 and AC Grid-3 respectively. They are responsible for maintaining the power balance in the DC system by keeping the DC voltage within the acceptable limits. The control block diagram for onshore HVDC converter is shown in Fig. 2.
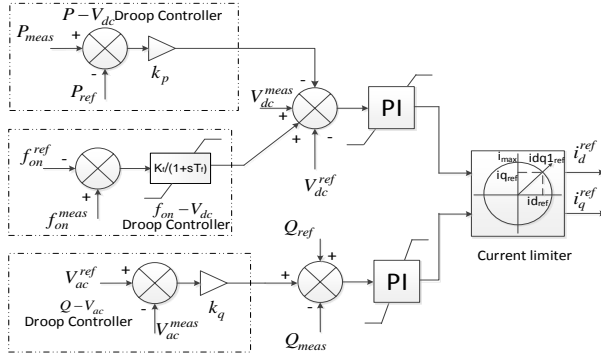
Fig. 2. Onshore HVDC converter control

The onshore HVDC converter control consists of two main controllers: one for active power balance control (DC voltage –active power droop) and other for reactive power control. The sharing of active power imbalance between the onshore converters depends on the active power droop constant (k_p) of the $P-V_{dc}$ droop controller. The converter also controls the reactive power at converter bus through AC voltage droop ($Q-V_{ac}$) so as to maintain the AC voltage within specified range. The current references provided by the outer controllers are then handled by an inner current controller operating in $d-q$ reference frame. A supplementary frequency-DC voltage droop ($f_{on}-V_{dc}$) controller in the outer loop d-axis is responsible for modulating the DC voltage reference (V_{dc}^{ref}) proportional to the onshore frequency deviation. This controller not only allows exchange of frequency support between the two onshore AC systems but also allows OWPPs to participate in frequency control. This loop contributes to the power system frequency regulation in coordination with a DC voltage- frequency droop controller ($V_{dc}-f_{off}$) at offshore HVDC converter, as depicted in Fig. 3, and active power controller of OWPP.
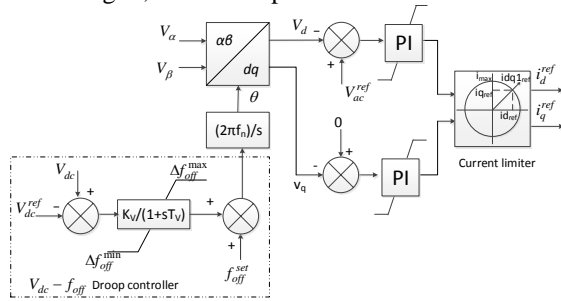

Fig. 3. Offshore HVDC converter control

2) Offshore HVDC Converter

The Conv-1 in Fig. 1 is the offshore HVDC converter station connecting the OWPP to the MTDC system. It is responsible for controlling the AC voltage magnitude and frequency of the offshore AC network at point of common connection (PCC) of the WPP and allows transferring the wind power output to the MTDC system. This is achieved through the use of a standard current controller whose references are provided by the outer controller illustrated in

Fig 3. A DC voltage-frequency droop controller ($V_{dc}-f_{off}$) at the outer control loop changes the offshore AC grid frequency reference proportionally to the DC voltage deviation. This controller in coordination with active power controller of OWPP provides the active power support required for the ancillary services to AC and DC grids.

C. Offshore Wind Power Plant Model:

The OWPP is an aggregated IEC Type 4 wind turbine (WT) model based on the aggregation method for WTs given in [16]. The Type 4 WT model used in this study is based on generic approach proposed by the IEC Committee in Part 1 of IEC 61400-27 [17] for the short term power system stability studies. Additionally, this model is extended to include the dynamic features relevant for the study of ancillary services (such as onshore frequency control and FRT for AC grid and DC voltage control for DC grid) from WPPs [18].

III. PROPOSED COORDINATED CONTROL SCHEME

In this paper, a coordinated offshore AC grid frequency modulation according to the DC grid voltage variation is proposed in order to represent the ancillary services requirements of AC and DC grids at offshore AC grid without depending on the dedicated communication links. The idea of this method is that the offshore HVDC converter modifies the offshore AC grid frequency proportional to the DC voltage variation measured at its terminals. The relation between offshore AC grid frequency and DC voltage is given in (1),(2), where f_{off}^{set} is the offshore frequency during normal conditions and f_{off}^{ref} is the reference offshore frequency according to DC grid voltage variation.

$$f_{off}^{ref} = f_{off}^{set} + \Delta f_{off} \tag{1}$$

$$\Delta f_{off} = k_v \Delta V_{dc} \tag{2}$$

The above relation in (1) and (2) is valid for the onshore FRT support and DC grid voltage support as the DC voltage variation is the result of the natural phenomenon caused by the respective ancillary service. For the WPP to provide the AC grid frequency control service, it requires an additional control mechanism ($f_{on}-V_{dc}$ droop as shown in Fig. 2) that translates the onshore AC grid frequency variations into DC voltage variations of MTDC system as given in (3). However, the $f_{on}-V_{dc}$ droop control is activated only when the variation in the onshore frequency is above a certain dead band to avoid conflict with the $P-V_{dc}$ droop control of the onshore converter [9].

$$\Delta V_{dc} = k_f (f_{on}^{meas} - f_{on}^{ref}) \tag{3}$$

Where f_{on}^{ref} and f_{on}^{meas} is the reference and actual frequencies of the onshore AC grid respectively. The frequency variation in the offshore AC grid modifies the WT active power reference as given in (4)

$$P_{WT}^{ref} = P_{opt} - \Delta P_1 - \Delta P_2$$
$$\Delta P_1 = k_d (f_{off} - f_{off}^{set}), \Delta P_2 = k_{in}(\Delta f_{off} / \Delta T) \tag{4}$$

109

P_{opt} is the optimal power output of WT as determined by its maximum power point tracking control. ΔP_1 is the power reference proportional to the frequency deviation from steady state value, whereas ΔP_2 is proportional to the rate of change of frequency. The WT, hence the WPP active power output is regulated as defined in (4) in coordination with DC and AC grids to provide the required ancillary service.

IV. SIMULATION AND DISCUSSION ON RESULTS

In this section, the effectiveness of the proposed coordinated control scheme to provide different ancillary services (frequency and FRT support for AC grid and DC voltage control for DC grid) from OWPP connected to MTDC system is discussed. The onshore AC grid frequency support is discussed in section A, while onshore FRT support and DC grid voltage support are discussed in section B and C respectively.

A. Onhore AC Grid Frequency Support

The power output from WPP (1000 MW) is shared between Grid-2 (500 MW) and Grid-3 (470 MW). A 10 % load increase at t=10s initiates an under frequency event in the AC Grid-2 of the test system shown in Fig.1. The effect of coordinated control on the frequency of AC Grid-2 and the corresponding offshore AC grid frequency is shown in Fig. 4 for different situations: A. Without coordinated control from WPP and Grid-3 B. With coordinated control from Grid-3 only, and C. With coordinated control from WPP and Grid-3.The corresponding DC voltage and the active power output of the three converters are given in Fig. 5.
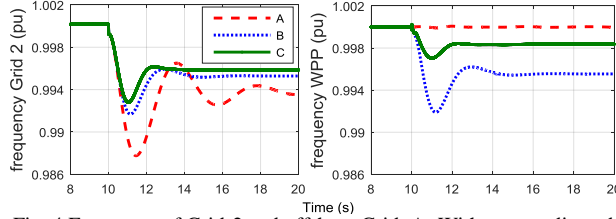

Fig. 4 Frequency of Grid-2 and offshore Grid. A -Without coordinated control B- Coordinated control from Grid-3 alone
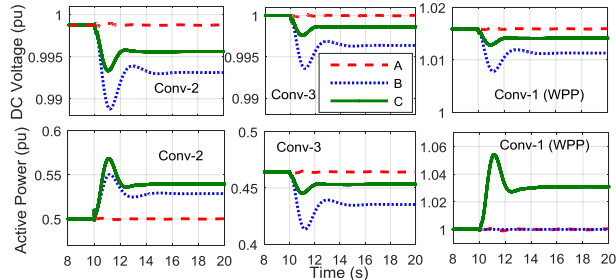C- With coordinated control from Grid-3 and WPP

Fig. 5. DC Voltage & Active Power of the converters for test case in Fig. 4

Due to coordinated frequency control action, the Conv-2 changes its DC voltage reference once it detects the frequency event; hence the overall DC Grid voltage profile is changed as shown in Fig. 5. This leads to the reduction of offshore AC grid frequency, as shown in Fig. 4, which initiates additional power output from WPP. Similarly, the

power taken by Conv-3 is also reduced due to $P-V_{dc}$ droop control action, helping the fast recovery of AC Grid-2 frequency. It can be observed from Fig. 4 that with the coordinated frequency control, the frequency of the AC Grid -2 is improved with the active power contribution from AC Grid-3 (dotted line) alone compared to without coordinated control (dashed line). With the coordinated control from WPP along with AC Grid-3, the frequency of AC grid-2 is significantly improved (solid line). Moreover, the WPP participation in frequency control relives the burden on the AC Grid-3 by sharing the active power contribution.

B. FRT support from OWPPs for Onshore Faults

A 3- phase to ground fault is applied (at t=10s for 200 ms) at the converter AC side of AC Grid-3. The AC voltage of the AC Grid-3, DC voltage, and active power output of the three converters are shown in Fig. 6. During the fault, active power output of Conv-3 becomes zero. In contrast, the Conv-2 in AC Grid-2 is able to increase the power transmission in about 0.2 pu. This behavior is due to the previously mentioned $P-V_{dc}$ droop control action which regulates the active power extraction as a function of DC voltage variation. Moreover, it can be observed that the active power dynamics of the Conv-2 is slower than the corresponding time constant observed in the active power reduction by Conv-3. This leads to additional energy stored in the DC grid, resulting in DC voltage rise. With the coordinated control; there is a rise in the offshore WPP AC grid frequency during the fault, as shown in Fig. 7, which reduces the WPP output power significantly. This results in reduced overvoltage in the DC grid and also relieves the stress on the Conv-2 by sharing active power contribution.
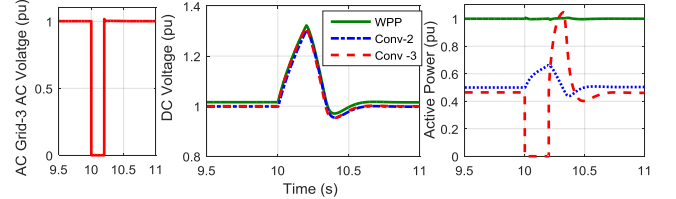

Fig. 6. AC Grid-3 AC Voltage, DC Voltage, Active Power of DC Grid without coordinated control from WPP
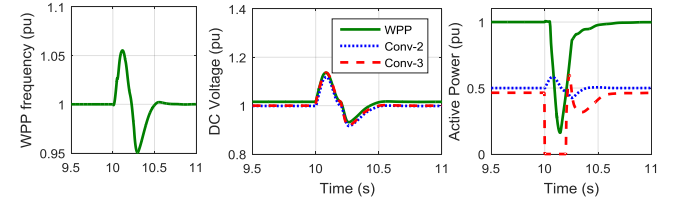

Fig. 7. WPP frequency, DC Voltage, Active Power of DC Grid with coordinated control from WPP

C. DC Grid Voltage Control Service

The dynamic challenges imposed by DC grid voltage control are critical and therefore a very fast control action is required to ensure stable operation. The increased connection of OWPPs to the DC grid requires OWPPs to participate in DC grid voltage control. To study the proposed coordinated control action, a disturbance is created in the DC Grid voltage by applying a step changes in power reference of Conv-2 at t=10s (from 0.5 pu to 0.55 pu) and t=15s (0.55 pu to 0.45 pu).

With the coordinated control, the frequency of the offshore AC grid is modulated, as shown in Fig. 8, according DC grid voltage variations, as shown in Fig. 9. The frequency triggers the active power control from WPP leading to reduced DC voltage variations. Without coordinated control, Conv-3 alone modulates its power output to control the DC voltage. However, with the coordinated control, participation of WPP reduces the burden on the Conv-3 and the DC voltage profile is also improved.
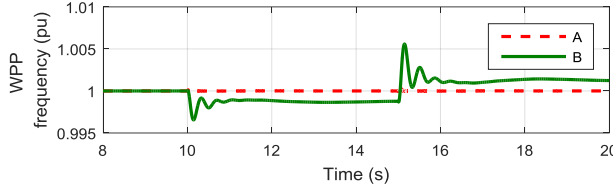

Fig. 8. Offshore AC grid frequency for active power disturbance at Conv- 2 Without (A) and With (B) coordinated control from WPP
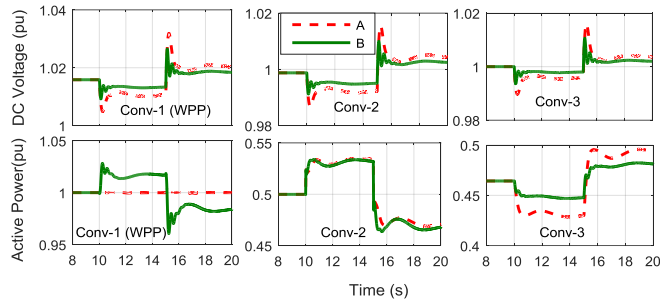

Fig. 9. DC Voltage & Active Power of 3 Converters for an active power disturbance at Conv-2 (for A and B refer Fig 8)

D. Possible limitations of the coordinated control method

As described previously, the proposed coordinated control method has good performance. However, it also presents some possible practical limitations, i.e. the accuracy and speed of the frequency measurement may influence the performance of the proposed method. Another limitation is the active power rate limiter of the WPPs which may influence the power output and hence the frequency control performance. For onshore FRT support, the OWPP output should be reduced within few 100 ms and this is only possible by draining the energy from the OWPPs by DC chopper inside the WT converter. The installation of DC chopper inside the WT is easy and less expensive option compared to the DC chopper at onshore HVDC terminals. For DC voltage control from WPPs, it is possible to reduce the WPP power output by increasing the rotor speed (i.e. storing kinetic energy) and then changing the pitch angle by the pitch control. However, to increase the active power output, it is not recommended to overload the WT for longer duration, therefore, it is recommended to down regulate the WPP to have some power reserves. The faults in the DC grid may also lead to low DC voltage. In that case, it may not advisable that WPP contribute more power to DC grid. Hence, the proposed coordinated control scheme should be coordinated with DC grid protection settings.

V. CONCLUSIONS

A coordinated control methodology for providing ancillary services for AC grid (frequency and FRT support) and DC grids (DC voltage control), from offshore wind power plants connected through multi-terminal HVDC network is described and demonstrated. For the onshore frequency control, the proposed control strategy involves a coordinated control mechanism based on DC voltage regulation at the onshore converter and the frequency regulation at the offshore converter. For onshore AC fault ride through, and DC Grid voltage control, the control strategy involves regulating the offshore AC grid frequency according to DC voltage variation. Based on detailed simulations on the 3-terminal HVDC system, it is shown that with the proposed coordinated control strategy, offshore wind power plants can effectively deliver the ancillary services to DC and AC grids without any conflict of interest between each service. Finally, the limitations of the proposed control strategy are addressed.

REFERENCES

[1]   Windspeed 2015. [Online]. Available: http://www.windspeed.eu. [Accessed: 25- Sep- 2015].

[2]   M. Aragues Penalba, O. Gomis-Bellmunt and M. Martins," Coordinated Control for an Offshore Wind Power Plant to Provide Fault Ride Through Capability", *IEEE Trans. Sustainable Energy*, vol. 5, pp. 1253-1261, Sep 2014.

[3]   Oriol Gomis-Bellmunta, J. Liang, J. Ekanayake, R. King, N. Jenkins, "Topologies of multiterminal HVDC-VSC transmission for large offshore wind farms," *Electric Power Systems Research,* vol. 81, pp, 271-281, Feb 2011.

[4]   ENTSO- E, *Draft- The Network Code on High Voltage Direct Current Connections (NC HVDC)*, Apr 2014.

[5]   Tennet TSO GmbH, *Requirements for Offshore grid Connections in the grid of Tennet TSO GmbH*, Germany, Dec. 2012, pp. 1–10.

[6]   L. Zeni, B. Hesselnæk, P.E.Sørensen, A.D.Hansen, P.C.Kjær,"Power System Services from VSC-HVDC Connected WPPs: an Overview" in *Proc. 2015 14th Wind Integration Workshop,* pp. 1-5.

[7]   Y. Phulpin,"Communication-free inertia and frequency control for wind generators connected by an HVDClink," *IEEE Trans on Power Systems,* vol. 27, pp. 1136-1137, May 2012

[8]   L. Zeni, I. Margaris, A. Hansen, P. Sørensen and P. Kjær, "Generic Models of Wind Turbine Generators for Advanced Applications in a VSC-based Offshore HVDC Network, " *in Proc. 2012 10th IET Conference on AC/DC Transmission, Birmingham..*

[9]   B. Silva,C. L. Moreira, et al,"Provision of Inertial and Primary Frequency Control Services Using Offshore Multiterminal HVDC Network," *IEEE Trans. on Sust. Energy*, vol. 3, pp. 800-808, Oct 2012.

[10]   S. Nanou, S. Papathanassiou,"Evaluation of a communication-based fault ride-through scheme for offshore wind farms connected through high-voltage DC links based on voltage source converter," *IET Rene. Power Generation*, , pp. 1-10, Jan 2015.

[11]   B. Silva,C. L. Moreira, et al,"Control strategies for AC Fault Ride Through in Multiterminal HVDC Grids" *IEEE Trans. Power Delivery*, vol. 29, Feb 2014

[12]   L. Zeni, "Power System Integration of VSC-HVDC connected Offshore Wind Power Plants " Ph.D thesis, DTU, Denmark, 2015.

[13]   P. Kundur, "Power system stability and control", 4th edition, McGraw-Hill 1994, New York.

[14]   T. K. Vrana, J. Beerten, R. Belmans and O. B. Fosso, "A classification of DC node voltage control methods for HVDC grids*," Electric power systems research*, vol. 103, pp. 137-144, 2013.

[15]   DIgSILENT GmbH, Technical Reference - PWM Converter.,2015.

[16]   E. Muljadi et al. "Method of equivalencing for a large wind power plant with multiple turbine representation,"*in Proc. 2008 IEEE Power and Energy Society General Meeting,* pp-1-8.

[17]   *Electrical simulation models for wind power generation Wind turbine*, IEC 61400-27-1, 2015.

[18]   A. D. Hansen, I. Margaris, G. C. Tarnowski and F. Iov,"Simplified type 4 wind turbine modeling for future ancillary services," in *Proc. 2013 European Wind Energy Conference*, pp. 768-774.

This page would be intentionally left blank if we would not wish to inform about that.

C6 Jayachandra N. Sakamuri, Joan Sau, Eduardo Prieto, Oriol Gomis, Altin M, Hansen A.D., Cutululis N.A., "Suitable Method of Overloading for Fast Primary Frequency Control from Offshore Wind Power Plants in Multi-Terminal DC Grid", Submitted to 2017 IEEE PowerTech Conference

This page would be intentionally left blank if we would not wish to inform about that.

Suitable Method of Overloading for Fast Primary Frequency Control from Offshore Wind Power Plants in Multi-Terminal DC Grid

Jayachandra N.Sakamuri, Anca D. Hansen

Mufit Altin, Nicolaos A. Cutululis
Department of Wind Energy
Technical University of Denmark, Roskilde, Denmark
jays@dtu.dk

Joan Sau- Bassols, Eduardo Prieto-Araujo

Oriol Gomis-Bellmunt
ETSEIB
UPC, Barcelona, Spain.
joan.sau@citcea.upc.edu

Abstract—**Increased penetration of offshore wind power plants (OWPPs) demands frequency control services from them. Overloading the wind turbine, for few seconds after the under frequency event, to utilize its kinetic energy seems promising option for fast primary frequency control. Two methods of overloading the wind turbine (WT), with and without considering the impact of WT dynamics and variation of WT output power during the overload, are proposed in the literature. In this paper, these two methods are applied for fast primary frequency control from OWPPs connected through multi-terminal DC grid considering the operation of the WT at below rated wind speed. Moreover, the impact of release of overload on the dynamics of the wind turbine, therefore on the associated AC and DC grids are studied in this paper. Finally, the suitable overloading method is proposed based on the simulation and experimental results. The time domain simulations for fast primary frequency control are performed on an OWPP connected through a 3-terminal DC grid using DIgSILENT PowerFactory. The experiments are performed on OWPP model integrated to a laboratory scale 3-terminal DC grid test set up. Based on the simulations and experimental results, overloading method which considers the variation of WT output power during the overload provides better performance during and after release of the overload.**

Index Terms— **Experimental Validation, Frequency Control, HVDC, MTDC, Offshore Wind Power Plants, Wind Speed**

I. INTRODUCTION

Installation of OWPPs in the power system is getting attention, especially in Europe. Multi-terminal DC grid with voltage source converters (VSCs) becomes a potential method to transmit power generated from OWPPs over long distance and to interconnect with different synchronous areas [1]. A major concern associated with MTDC connected OWPPs is their inability to respond to onshore AC grid frequency events due to the decoupling, when compared with frequency control by synchronous machines. With an increased penetration of OWPPs, assuming that they (at least a part of generation) replace conventional generation, the frequency control becomes increasingly difficult because of the reduced level of power system inertia. Lower the system inertia, the more the rate of change of frequency (ROCOF), after an abrupt change in generation or load. Therefore, a need for fast primary control from OWPPs connected through MTDC system, which provides active power support for few seconds following a frequency event, has been highlighted by transmission system operators (TSOs) [2]. Hence, this paper concentrates on fast primary frequency control from OWPPs connected through a 3-terminal DC grid.

There are two possible options for wind turbines to provide active power support for frequency control. In the first option, WT always operate in down regulation mode, creating some power reserve. This is suitable when frequency control is needed for extended durations (few minutes), i.e. for primary frequency control. In the second option, WT is overloaded above its optimal power output for few seconds, thereby utilizing its kinetic energy to participate in fast primary frequency control [3]. Two methods of overloading the WT, with and without considering the impact of WT rotational speed, are reported in [4]. However, in [4], WT is overloaded with constant power magnitude for fixed duration irrespective of the severity of the frequency event and wind speed. This may either over burden the WT at below rated wind speeds causing stalling of WT or less utilize it kinetic energy for above rated wind speeds. In [5], the methods given in [4] are modified to generate power reference proportional to the frequency deviation. Moreover, a procedure to optimize the gains of the frequency controller based on the wind speeds is given in [5]. However, the research is limited to WPP connected to an AC grid.

Considering the limited research on impact of WT overloading AC and DC grids, this paper investigates the WT overloading methods for frequency control proposed in [5] by applying to an OWPP connected through a 3-terminal DC grid. The study also investigates the impact of release of WT

6]. The time domain simulations on an OWPP connected through a 3-terminal DC grid is performed using DIgSILIENT PowerFactory. The simulation results are validated experimentally by performing the frequency control test on an OWPP model integrated to a laboratory scale DC grid test set up. Finally, the suitable method of overloading the WT for fast primary frequency control from OWPP in MTDC environment is proposed by analyzing the simulation and experimental results. The onshore AC grid frequency is replicated at offshore AC grid using supplementary control blocks implemented locally at each VSC in a coordinated manner, without depending on the communication channels [7].The rest of the paper is organized as follows. The model of the 3-terminal DC grid and the two WT overloading methods are given in section II. The details of experimental test set up are given in section III. The simulation and experimental test results of fast primary frequency control using the two overloading methods are given in section IV, while concluding remarks are given in section V.

II. MODELING OF THE TEST SYSTEM

A 3-terminal DC grid, shown in Fig.1, which interconnects an OWPP with two onshore AC grids (AC grid-1 and AC grid-2 is considered for this study. A brief description of the basic control schemes for onshore and offshore HVDC converters, communication-less scheme for frequency control, and the two overloading methods for the OWPP, are explained in the following sub sections.
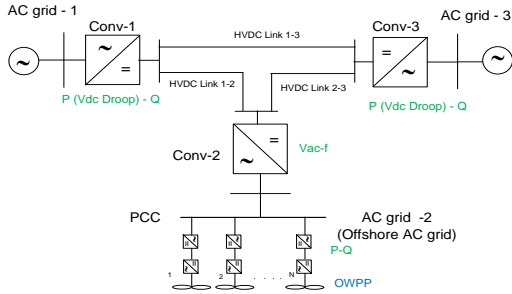

Fig. 1 3- terminal HVDC grid layout for the study

A. Onshore HVDC Converter Control

The main responsibility of onshore HVDC converters (Conv-1 and Conv-3) is to maintain active power balance in the DC grid whose control scheme is shown in Fig.2. The share of DC grid power balance is set by the $V_{dc} - P$ droop controller [8]. They are also responsible for controlling the reactive power using the 'Reactive Power Control loop' according to the corresponding AC grid requirements. The 'Frequency Control Loop' in Fig.2 generates additional power reference (ΔP_{ref}^f) to the converter based on the frequency deviation measured at the respective AC grid, so as to participate in frequency control (refer section II D).
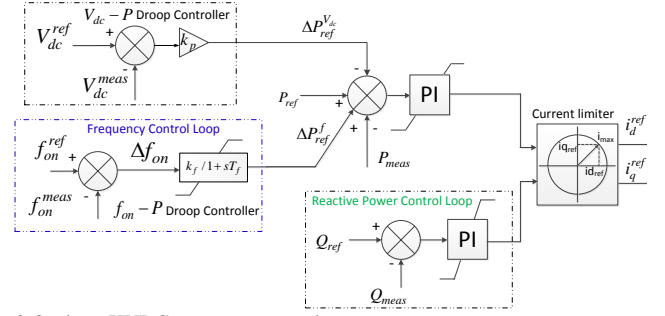

Fig.2 Onshore HVDC converter control

B. Offshore HVDC Converter Control

The offshore HVDC converter (Conv-2 in Fig.1) is responsible for transferring the power generated by OWPP to DC grid while controlling the AC voltage and frequency of offshore AC grid [9], as given in Fig.3. The 'Frequency Control Loop' modifies the offshore AC grid frequency reference according to the DC voltage deviations, measured at the terminals of Conv-2, to make the OWPP participate in frequency control. Further details of frequency control are given in section II D.
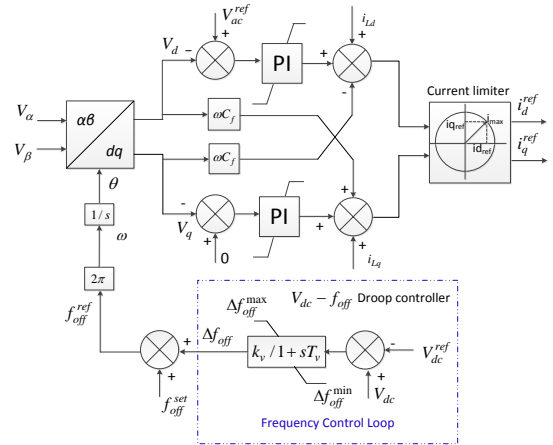

Fig.3 Offshore HVDC converter Control

C. Offshore Wind Power Plant Model and Methods of Overloading

The OWPP is modelled as an aggregated IEC Type-4 wind turbine (WT) based on the aggregation method given in [10]. The Type-4 WT model used in this study is based on generic approach proposed by the IEC Committee in Part 1 of IEC 61400-27 [11] for the short term power system stability studies. Additionally, this model is extended, as shown in Fig.4, to include the dynamic features, such as aerodynamic model, pitch control, and mechanical model, relevant for the study of the frequency control from WPPs [12]. The block diagram related to active power control of WT is shown in Fig.4. This model generates either optimal power reference (P_{mppt}) or frequency initiated power reference (P_{ref}^f) given in (1), depending on normal or frequency control operation.

$$P_{ref}^f = P_{base} + \Delta P_{ref-wpp}^f \qquad (1)$$

P_{base} is base power reference and its value depend on the

116

chosen method of WT overloading (External or Internal method) which is explained below. $\Delta P_{ref\_wpp}^{f}$ is modulated power reference generated by the 'Frequency control loop' based on the offshore AC grid frequency deviation resulted due to onshore AC grid frequency control (refer II D). The two methods for WT overloading can be understood by the WT dynamics given in fig.5.
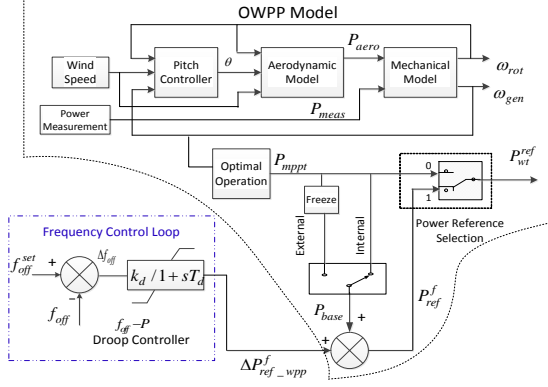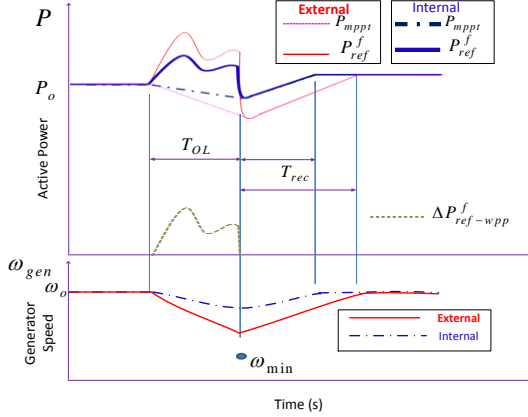

Fig. 4. OWPP active power controller.

Fig.5. External and Internal overloading methods for WT.

In the first method, called External method, the P_{base} is chosen as fixed value during the overload and is equal to the value of P_{mppt} just before the start of overloading. In general, the P_{mppt} value changes according to the WT generator speed (ω_{gen}). During the overload, ω_{gen} decreases because the WT electrical power output is more than its aerodynamic power input, particularly at just below rated wind speeds, hence, P_{mppt} also decreases. In the second method, called as Internal method, the P_{base} is equal to the actual value of P_{mppt}. Therefore, the magnitude of P_{ref}^{f} only depends on $\Delta P_{ref\_wpp}^{f}$ in case of external method as P_{base} is a fixed value. For Internal method, P_{ref}^{f} depends both on P_{base} and $\Delta P_{ref\_wpp}^{f}$ as both are variable during overloading period (T_{OL}). Hence, the magnitude of P_{ref}^{f} is more for External

method than Internal for the same magnitude of $\Delta P_{ref\_wpp}^{f}$. This results in lower magnitude of P_{mppt} for External method at the end of T_{OL} because of lower magnitude of ω_{gen} compared to Internal method, which adversely impacts the DC and AC grids. Also, it is important to observe that WT recovers faster, hence smaller recovery period (T_{rec}) in case of Internal method. The reason is, for an increase in magnitude of $\Delta P_{ref\_wpp}^{f}$, the P_{mppt} decreases, leading to faster decrease of P_{ref}^{f} and reaches near to the pre-overloading operating point during the progress of overloading period. The comparison of simulation and experimental results of External and Internal overloading methods for fast primary frequency control from OWPP in a 3-terminal DC grid are given in section IV.

D. Communication-less Scheme for Frequency Control

The communication-less scheme [7] for frequency control from an OWPP in MTDC grid is briefly explained in this section.

In this method, the onshore AC grid frequency is replicated at offshore AC grid according to the DC voltage variations. For example, the $f_{on} - P$ droop controller of the 'Frequency Control Loop', shown in Fig.2, modulates the active power reference (ΔP_{ref}^{f}) to the onshore HVDC converter according to the measured frequency deviation at the associated onshore AC grid. The corresponding relation between active power and frequency is given in (2), where f_{on}^{ref} and f_{on}^{meas} are the reference and measured frequency at the onshore AC grid.

$$\Delta P_{ref}^{f} = k_f (f_{on}^{ref} - f_{on}^{meas}) \qquad (2)$$

The change in active power output of the converter results in deviation in the DC grid voltage from its initial value. Therefore, the other onshore HVDC converters in the MTDC grid inherently modulate its active power reference ($\Delta P_{ref}^{V_{dc}}$) due to $V_{dc} - P$ droop control action, thereby participating in frequency control. However, the OWPP doesn't detect the frequency event; hence mirroring onshore frequency deviation in the offshore AC network frequency is needed. Therefore, the $V_{dc} - f_{off}$ droop controller at offshore HVDC converter, shown in Fig.3, modifies the offshore AC grid frequency proportional to the DC voltage variation measured at its terminals as given in (3),(4),where f_{off}^{set} is the offshore frequency during normal conditions and f_{off}^{ref} is the reference offshore frequency considering DC grid voltage variation.

$$f_{off}^{ref} = f_{off}^{set} + \Delta f_{off} \qquad (3)$$

117

$$\Delta f_{off} = k_v \Delta V_{dc} \qquad (4)$$

The power reference to the WT (P_{WT}^{ref}), hence OWPP, is then updated with the contribution $\Delta P_{ref\_wpp}^{f}$ from the 'Frequency Control Loop' shown in Fig.4, as given in (5).

$$P_{WT}^{ref} = P_{base} + \Delta P_{ref\_wpp}^{f} \qquad (5)$$
$$\Delta P_{ref\_wpp}^{f} = k_d (f_{off}^{set} - f_{off})$$

III. LABORATORY SCALE MTDC TEST SET UP

The frequency control test is performed on a 3-terminal DC grid laboratory test set up shown in Fig. 6 and its description is given in Table 1. The Conv-1, Conv-2 and Conv-3 in Fig.5 are laboratory scale 10 kVA converters with an inbuilt 3-phase, 400V/230V, and 10 kVA transformer. The DC lines (1-2, 1-3 and 2-3) are implemented with lumped resistances (R), and inductances (L) whose values are given in Table 1. The converter controllers are implemented in a digital signal processor (DSP) and executed at a speed of 20 kHz. The main difference between the experimental set up of 3 terminal DC grid in Fig 6 compared to its theoretical counterpart in Fig 1 lies in the AC grid connection for the test set up, AC grid equivalent model to create the frequency event, OWPP modeling, and control of offshore converter (Conv-2). These are explained in the following sub sections.
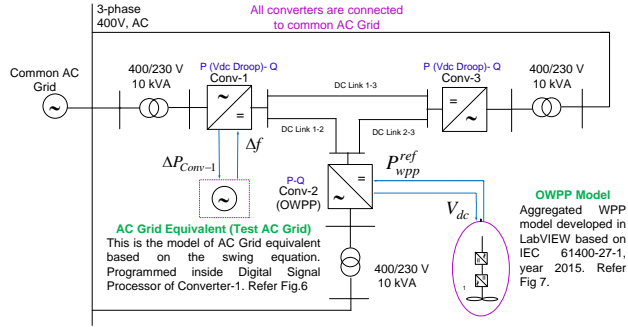

Fig. 6. 3 Terminal test set up to perform frequency control test

TABLE I : DESCRIPTION OF THE TEST LAYOUT IN FIG. 5

Parameter	Value	Unit
Common AC Voltage (L-L)	400	V
DC Voltage (Symmetrical Monopole)	+/- 250	V
Transformer rating (400V/230V)	10	kVA
Converter rating	10	kVA
DC line 1-2 Resistance, R12	0.22	ohms
Inductance, L12	1	mH
DC line 1-3 Resistance, R13	0.1	ohms
Inductance, L13	0.5	mH
DC line 2-3 Resistance, R23	0.44	ohms
Inductance, L23	1.5	mH
OWPP rating	2.85	kW

A. AC grid Connection for the Test Set up

In the laboratory, there is only one AC grid is available. Hence, all the converters are connected to same AC grid (3 phase, 400 V supply) instead of connecting to 3 separate AC grids.

B. AC Grid Equivalent to create Frequency Event

Power system frequency dynamics results from power imbalances. As it is not possible to change the frequency of the laboratory AC grid, an AC grid equivalent with a dynamic frequency model (test AC grid) based on swing equation [13], shown in Fig.7, is implemented inside the DSP of Conv-1. If there is a balance between change in mechanical power input (ΔP_m) and electrical power output (ΔP_l) of the grid, then change in frequency (Δf) is zero. A frequency event in the test AC grid can be created by perturbing the ΔP_l. The Δf is sent to the onshore HVDC Conv-1 controller (refer Fig.2), which then modulates its active power reference (ΔP_{ref}^{f}). The measured change in active power output of the Conv-1 due to frequency control (ΔP_{Conv-1}) is sent back to the test AC grid model, thereby participating in the frequency control of test AC grid.
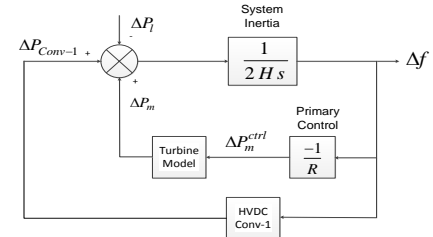

Fig 7. AC Grid equivalent with dynamic frequency model

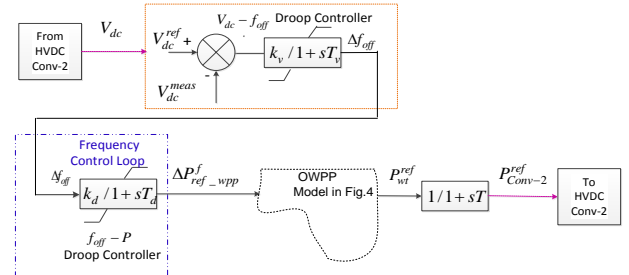### C. Implementation of OWPP Model and Control of HVDC Converters

Fig.8. OWPP model implemented in in LabVIEW (only active power controller is shown here)

The Conv-1 and Conv-3 operate in active power control with dc voltage droop, maintaining the power balance in the DC grid, as explained in section IIB. However, the Conv-2 connected to OWPP operates in active and reactive power ($P - Q$) control mode instead of AC voltage and frequency control mode ($V_{ac} - f$) as explained in section IIC. The main reason for $P - Q$ control is because OWPP is implemented as a simulation model programmed in LabVIEW instead of physical implementation as an isolated AC grid. However, the equivalent control delays which involved in '$V_{ac} - f$' control mode, in case of frequency control, are implemented in OWPP model as shown in Fig 8.

The HVDC Conv-2 sends dc voltage measurement,V_{dc} to the OWPP model. The $V_{ac} - f_{off}$ droop controller modulates

$\Delta P_{ref\_wpp}^f$ according to change in frequency. Finally, the OWPP model sends the active power reference to Conv-2, thereby, emulating the combined theoretical behavior of offshore HVDC converter and OWPP control, shown in Fig.3 and Fig.4. The picture of 3-terminal laboratory scale experimental test set up used in this study is shown in Fig.9.
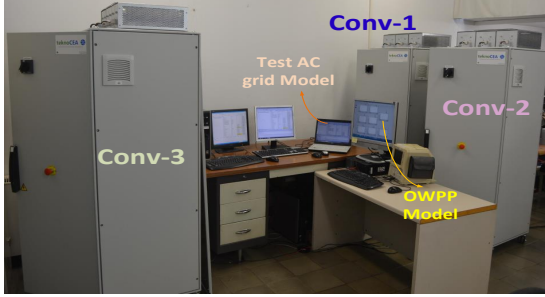

Fig.9. Picture of 3 terminal experimental test set up

D. Limitation of Experiment

The test is performed on a WPP simulation model; hence the dynamics of the actual WT and impact on mechanical loading could not be verified. Moreover, the time delays involved in actual frequency measurements are ignored.

IV. SIMULATON AND EXPERIMENTSL RESULTS

In this section, simulation and experimental results of frequency control from OWPPs utilizing the two overloading methods are presented. An under frequency event is created at test AC grid (in Fig.5) by applying 15% load change at time t=6s. The WT is overloaded for a duration (T_{OL}) of 10s, i.e. the overloading is removed at t=16s. It is assumed that wind speed is 0.92 pu and is constant throughout the simulation. In normal conditions, OWPP (Conv-2) and Conv-3 sends power to DC grid (-ve sign) and Conv-1 receives from DC grid (+ve sign). The parameters used in this test are given in Table II. The simulation and experimental results of frequency control test are given in Fig.10 and Fig.11 respectively. From these results, it can be observed that the frequency of the Test AC grid is improved with the participation of OWPP in frequency control,

TABLE II : PARAMETERS FOR FREQUENCY CONTROL

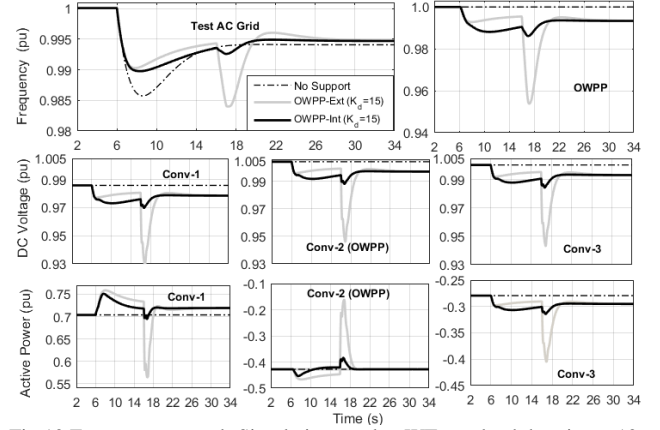| Parameter	Unit	Under Frequency
Conv Base kVA	kVA	5700
OWPP base kVA	kVA	2850
Base DC grid voltage	V	500
Base frequency	Hz	50
Power flow, Conv-1/2/3	pu	0.7/-0.42/-0.28
$V_{dc} - P$ droop gain (k_p) - Conv-1 /3	pu/pu	5/2.2
$f_{on} - P$ droop gain(Conv-1)	pu	10
$V_{dc} - f_{off}$ droop gain(Conv-3)	pu	1
$f_{off} - P$ gain (OWPP)	pu	15

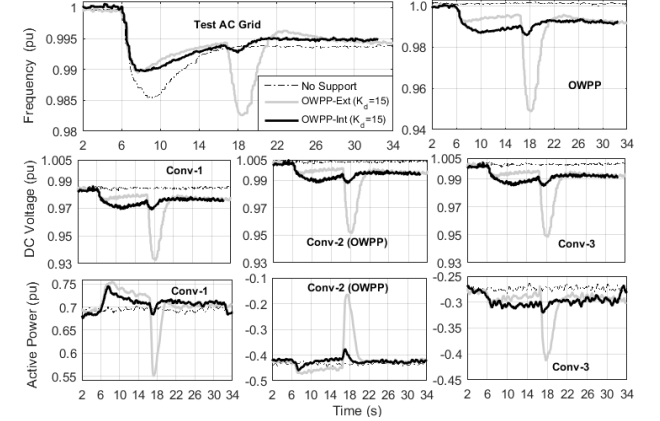Fig.10 Frequency control -Simulation results- WT overload duration = 10s

Fig.11 Frequency control- Experimental validation of results in Fig.12

during the overloading period (t=6s to 16s), for both overloading methods. Please note that Conv-3 also increases its active power output due to the natural action of the $V_{dc} - P$ droop controller, thereby, participating in frequency control. However, at the end of the overloading period, there is a sudden drop in power output of Conv-2, in case of External method. This leads to sudden drop in DC grid voltage and Test AC grid frequency and also Conv-3 gets overloaded so as to maintain power balance in the DC grid. These are called secondary effects of removal of WT overload. The reason for this behavior can be understood by the simulation and experimental results of WT dynamics given Fig.12 and 13 respectively. In case of External method, WT optimal power output (P_{mppt}) decreases significantly because of reduction in generator speed (O_{gen}) during the overload and results in sudden power drop in WT power output (P_{out}) at the end of overload. However, for Internal method, as it considers both P_{mppt} and $\Delta P_{ref\_wpp}^f$ to generate overloading power reference, they complement each other. Therefore the WT power output reaches almost near to pre-overloading operating point within few seconds after the frequency event (even though $\Delta P_{ref\_wpp}^f$ is higher in this case), before the end of overloading period, thus WT starts to recover during the overloading period.
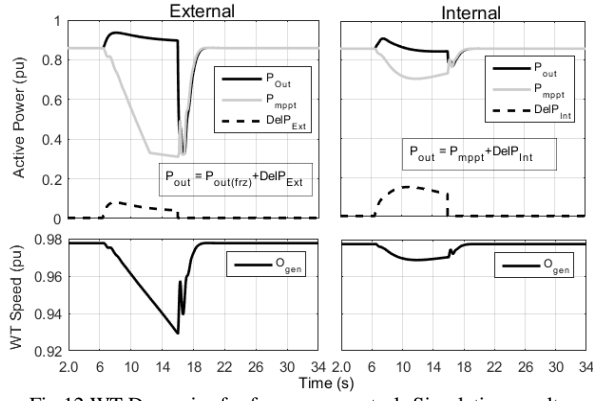
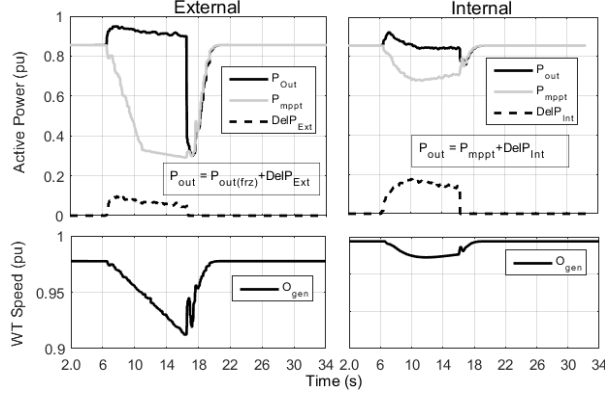Fig.12 WT Dynamics for frequency control -Simulation results

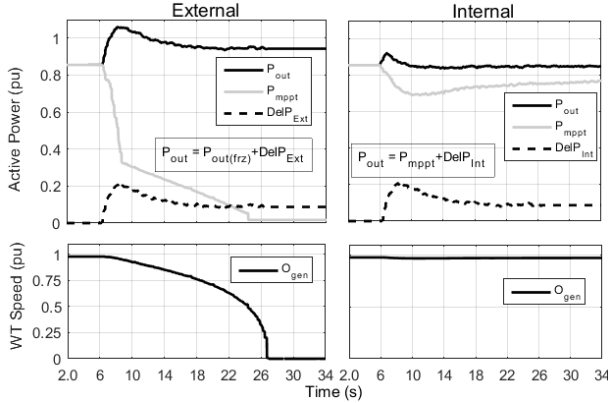Fig.13 WT dynamics for frequency control -Experimental results

Fig.14 WT dynamics for Frequency control _Extended overloading-
Experimental results

Hence, the drop in WT power output at the end of overloading period is less for Internal method compared to External method, thereby creating minimal secondary effects on DC and AC grids. It is interesting to know what happens if it is failed to remove the overloading at t= 16s and overloading continues for longer duration. The experimental results of WT dynamics for extended overloading are given in Fig.14. It is assumed equal $\Delta P_{ref\_wpp}^{f}$ for both overloading methods for fair comparison. In case of External method, the WT stalls at t= 26s (generator speed reached to zero). However, in case of Internal method, the WT recovered and its output power reached to pre-overloading operating point few seconds after the overloading. Therefore, Internal method

is best suited for fast primary frequency control of the power system where it is needed to provide power support for few seconds without stalling the WT. The External method is suitable when OWPP is required to provide assured power support, e.g. for primary or secondary frequency control. In that case, OWPP must be operated in downregulation mode to create the required power reserve.

V. CONCLUSIONS

In this paper, the capability of OWPP connected through a 3-terminal DC grid for fast primary frequency control of the AC grid is tested by performing time domain simulations and experimental tests. The wind turbine kinetic energy is utilized to provide active power support by overloading above its optimal power point using two types of overloading methods. Fixed power overloading method (External method) results in large power drop after the overloading, hence creates secondary effects on AC and DC grids. The second method which considers the WT dynamics during the overload (Internal method) is best suited for fast primary frequency control as the WT starts recovering during the overload and power drop after the overloading is less, creating less negative impact on DC and AC grids compared to External method.

VI. REFERENCES

[1] D. Van Hertem, M. Ghandhari , "Multi-terminal VSC HVDC for the European Supergrid: Obstacles," *Renewable and Sustainable Energy Reviews*, vol 14, pp 3156–3163, Dec 2010

[2] National grid, System Operability Framework (SOF) report, 2014.

[3] Altin M, Teodorescu R, Bak-Jensen B, Annakage UD, Iov F, Kjaer PC. Methodology for assessment of inertial response from wind power plants*, in 2012 Proc. IEEE power and energy society general meeting, pp 1-8.*

[4] S. Wachtel, A. Beekman, " Contribution of Wind Energy Converters with Inertia Emulation to frequency control and frequency stability in power systems" in *Proc. 2009 8th Wind Integration Workshop,* pp. 1-6

[5] J.N. Sakamuri, K.Das, P.Tielens,et al., "Improved Frequency Control from Wind Power Plants Considering Wind Speed Variation," In Proc. 2016 IEEE Power System Computation Conference, June 2016.

[6] A. D. Hansen, M. Altin, et al, "Analysis of short-term over production capability of variable speed wind turbines," Renewable Energy, vol. 68, 2014

[7] B. Silva, C. L. Moreira, et al., "Provision of Inertial and Primary Frequency Control Services Using Offshore Multiterminal HVDC Network", *IEEE Trans. on Sustainable Energy*, vol. 3, pp. 800-808, Oct 2012.

[8] J. Beerten and R. Belmans, "Analysis of Power Sharing and Voltage Deviations in Droop-Controlled DC Grids," IEEE Transactions on Power Systems, vol. 28, no. 4, pp. 4588-4597, 2013.

[9] A.Yazdani, R. Iravani, "Voltage source converters in power systems" (JohnWiley & Sons, 2010), ISBN: 978-0-470-52156-4

[10] E. Muljadi et al. "Method of equivalencing for a large wind power plant with multiple turbine representation," Proc. 2008 IEEE Power and Energy Society General Meeting, pp-1-8.

[11] Electrical simulation models for wind power generation- Wind turbine, IEC 61400-27-1, 2015.

[12] A. D. Hansen, I. Margaris, G. C. Tarnowski and F. Iov,"Simplified type 4 wind turbine modeling for future ancillary services," in *Proc. 2013 European Wind Energy Conference*, pp. 768-774.

[13] G. Anderson, Dynamics and Control of Electric Power Systems, Lecture Notes. Zurich: Feb 2012.

J1 Ömer Göksu, Jayachandra N. Sakamuri, C. Andrea Rapp, Poul Sørensen, Kamran Sharifabadi, "Cluster Control of Offshore Wind Power Plants Connected to a Common HVDC Station", Energy Procedia, Volume 94, Sep 2016, Pages 232-240, ISSN 1876-6102

This page would be intentionally left blank if we would not wish to inform about that.

Cluster Control of Offshore Wind Power Plants Connected to a Common HVDC Station

Ömer Göksu[a]1, Jayachandra N. Sakamuri[a], C. Andrea Rapp[b], Poul Sørensen[a], Kamran Sharifabadi[c]

a DTU Wind Energy, Roskilde, 4000, Denmark
b Halvorsen Power System AS, Norway
c Statoil ASA, Norway

Abstract

In this paper a coordinated control for cluster of offshore WPPs connected to the same HVDC connection is being implemented and analyzed. The study is targeting two cases as; coordination of reactive power flow between HVDC converter and the WPP cluster while providing offshore AC grid voltage control, and coordinated closed loop control between the HVDC and the WPPs while the cluster is providing Power Oscillation Damping (POD) via active power modulation. It is shown that the coordinated cluster control helps to improve the steady-state and dynamic response of the offshore AC grid in case of offshore AC grid voltage control and onshore ancillary services provision, i.e. POD by the active power modulation of the cluster. The two cases are simulated using DIgSILENT PowerFactory, where the IEC 61400-27-1 wind turbine and WPP control models and a generic offshore layout with cluster of three WPPs are utilized.

1. Introduction

Rich wind resources in the North Sea and the Baltic Sea region are being explored and utilized by the offshore wind power plants (WPPs) [1]-[2], where the HVDC is being the preferred solution to transfer the wind power from far offshore WPPs. In many cases, multiple (e.g. three) offshore WPPs are being connected to a single HVDC offshore station as a cluster; for instance the Butendiek, Dan Tysk, and Sandbank WPPs (each 288 MW) connected to the SylWind1 HVDC station (864 MW) [2].

Currently such installations are not known to be operated with separate WPP controllers in a coordinated way; however this is anticipated to be favored in the near future. In this paper, a coordinated control for cluster of offshore WPPs connected to the same HVDC connection is being implemented and analyzed. The study is aimed to coordinate the reactive power flow between the HVDC converter and WPPs' cluster, while staying within the steady-state operational limits of the WPPs. Additionally, WPPs are coordinated to improve the dynamic response of the offshore AC grid in case of onshore ancillary services provision, e.g. power oscillation damping (POD) [3]-[6] by active power modulation of the HVDC link and hence the WPPs. Aggregated model of WPPs and their controls used in this study are based on the IEC type 4B wind turbines (WTs) and the WPP control models in IEC 61400-27-1 [7], using a generic offshore layout with cluster of three WPPs [8]. The IEC type 4 WT model represents the latest generation WT type, where the generator is connected to the grid through a full scale power electronics based converter (hence decoupled from the grid). The generator can be either asynchronous (squirrel cage induction) generator or (permanent magnet or separately excited) synchronous generator; with or without gearbox (i.e. direct

---

drive). The full-scale power converter usually employs a chopper circuitry in the DC link, which helps for fault ride-through of the WT. Depending on the sizing of the chopper, post-fault power oscillations might be observed at the WT output, where the IEC type 4A represents an ideal WT with sufficient chopper neglecting aerodynamic and drivetrain parts thus without any post-fault oscillations and the IEC type 4B includes aerodynamic and drivetrain blocks replicating the post-fault oscillations.

It is shown that the objectives of coordinated flow and improved dynamic response can be reached via configuring and setting the WPP and WT controllers accordingly; and further improved by a coordinated cluster control. Analyzing the currently existing AC offshore hub concept, the paper aims to provide a benchmark case towards further meshed AC and/or DC network studies. Cluster control of WPPs connected to a common HVDC stands as a new research concept, where such a case is known to be studied only in few references, e.g. in the eighth chapter of [9] for frequency support and POD provision, in [11] for coordination of the cluster during offshore faults, in [12] for HVDC feasibility analysis for a cluster of WPPs.

In the next section the developed generic benchmark layout will be described. In the third section, a general overview of the IEC 61400-27-1 WT and WPP control model will be given. In the fourth and fifth sections, the offshore AC grid voltage regulation and POD cases will be studied, respectively, together with the simulation results. In the last section the concluding remarks will be provided.

2. Benchmark Layout – Cluster of Three WPPs

In order to study the phenomenon related to the cluster connected WPPs to a common HVDC station, a generic benchmark layout is created [8], as given in Fig. 1. However, in this study the onshore HVDC terminal and DC link is not modeled since the focus is coordination of reactive power (during offshore AC voltage control) and active power (during POD) between the WPPs and the HVDC offshore station. The offshore HVDC station is modeled as a voltage source converter with constant DC voltage; thus acts as an ideal voltage source. This simplification helps to focus on the main scope of this paper; cluster control of HVDC connected offshore WPPs and impact of communication delays within the offshore cluster, while eliminating the impact of external factors such as the non-linearity of the offshore HVDC converter, DC-link voltage control dynamics, etc. However, a complete analysis definitely requires the HVDC link to be included as in [10], where these external impacts are studied thoroughly. In the offshore cluster benchmark, the first WPP (A) is located very close (2 km) to the HVDC station, whereas the other WPPs (B and C) are located 25 km and 50 km away from the HVDC station, connected with separate submarine cables. Each WPP is represented as aggregated single WTs, since the focus of the study excludes internal dynamics between the WTs within the WPPs.
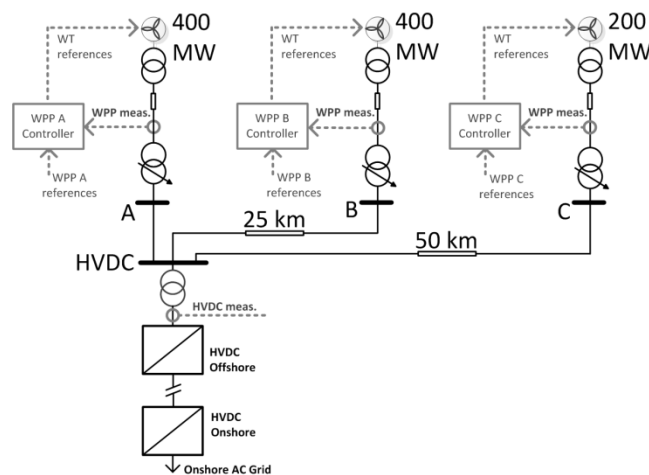

Fig. 1. The generic benchmark layout with cluster of three WPPs.

The parameters for the WPP and HVDC transformers are given in table 1 below, while the collector network and connection cable parameters are given in tables 2 and 3. The WT transformer values in Table 1 are given for the aggregated units which have ratings as the WPP ratings.

Table 1. WPPs' and HVDC's transformer specifications.

	WPP-A	WT-A	WPP-B	WT-B	WPP-C	WT-C	HVDC
Apparent power [MVA]	240	240	480	480	480	480	1160
Low voltage [kV]	33	0.69	33	0.69	33	0.69	150
High voltage [kV]	150	33	150	33	150	33	380
Transformer X [%]	13.77	5.935	13.77	5.935	13.77	5.935	15
Transformer R [%]	0.277	0.88	0.277	0.88	0.277	0.88	1

Table 2. WPPs' internal (aggregated) network cable impedance characteristics [Sbase].

	WPP-A [400 MVA]	WPP-B [400 MVA]	WPP-C [200 MVA]
X [%]	1.68	1.68	2.422
R [%]	0.51	0.51	0.812
B [%]	2.154	2.154	1.726

Table 3. WPPs' connection cable specifications [Sbase].

	WPP-A [400 MVA]	WPP-B [400 MVA]	WPP-C [200 MVA]
Length [km]	2	25	50
X [%]	0.2	2.5	5.02
R [%]	0.032	0.4	0.8
B [%]	1.62	20.3	40.6

The study is performed on the developed benchmark system having three offshore WPPs connected through a single HVDC system, shown in Fig. 1, using DIgSILENT PowerFactory rms simulations. The reactive power flow and the active power losses in the offshore AC grid are calculated by performing load flow at various generation levels from the WPPs.

AC cables generate high amount of reactive as seen by the stray capacitance values in Table 2 and 3, while the transformers are still large consumers of reactive power especially under high load. As will be seen in the fifth section, the cables totally produce 200 MVAr of reactive power when the WPPs' active power generation is close to minimum or zero. As a common practice, in order to absorb this excess reactive power, especially during low generation levels, shunt reactors are employed, whereas HVDC converter and the WPP (WT) converters have the capability to absorb or inject reactive power. In this study, in order to observe and compare pure converter responses, the WPP shunt reactors and OLTC (On Load Tap Changer) are not operated.

3. IEC 61400-27 WT and WPP Control Models

The international standard IEC 61400 from the International Electrotechnical Commission is a series of standards regarding WTs. This paper will use IEC 61400-27-1, which considers electrical simulation model of WTs [7]. As the penetration of wind energy in power systems is increasing system operators need to use dynamic models of wind power generation for studies regarding power system stability. As the models developed by the WT manufacturers are too detailed to assess power system stability and usually confidential, the IEC has developed the standard series 61400-27 to provide a frame for generic models. This specific standard consists of two parts, the first part provides WT models and validation procedures which can be applied in power system stability studies and the second part contains WPP models and their model validation procedure. These fundamental frequency positive sequence models are specified to represent the wind turbines' behavior in the large-disturbance short-term voltage stability, the rotor angle stability, frequency stability, and the small-disturbance voltage stability studies. The type 4B WTs, which are

125

used in this study, employ power-electronics converters, which are modelled by ideal current injection sources (e.g. static generators in PowerFactory) in the IEC models. The IEC WPP and WT active and reactive power control paths are shown as cascaded in Fig. 2, which is a simplified representation from [7].

3.1. Reactive Power Control Loop – Voltage Control with Droop Compensation

The WPP reactive power controller has four operating modes; it can perform reactive power control, power factor control, static voltage control, and voltage control. In case of reactive power control and the power factor control modes, the resultant reactive power reference is closed-loop regulated by a PI controller and also a feedforward path. In case of static voltage control mode, a reactive power reference is generated from a lookup table based on the voltage error and the reactive power reference is regulated by the same means as reactive power control mode. In case of voltage control mode, the voltage is closed-loop regulated by a PI controller, and additionally a droop gain (named as k_{qdroop} in Fig. 2), modifies the WPP voltage reference based on the measured reactive power value.
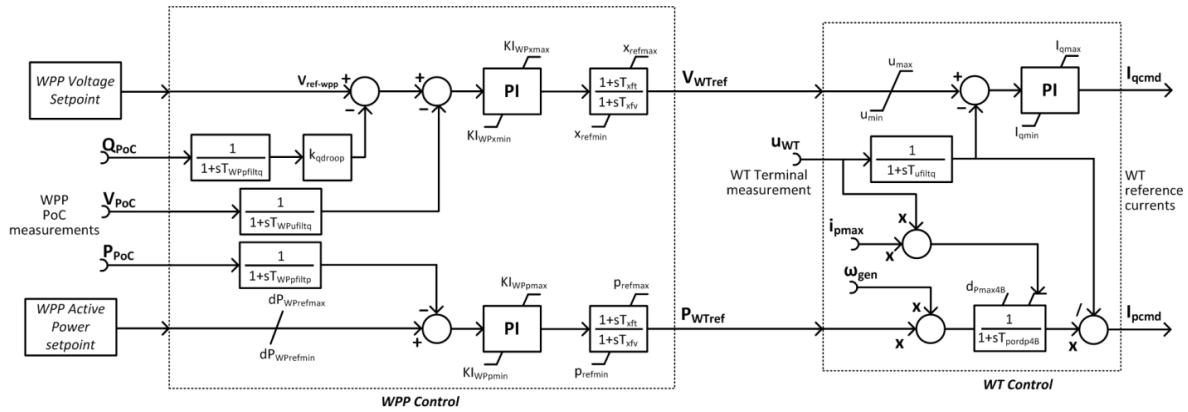

Fig. 2. Simplified block diagram for WT and WPP voltage and active power controller of IEC 61400-27-1.

As mentioned above and shown in Fig. 2 the IEC WPP voltage controller has the "Plant voltage control droop" gain which modifies the WPP voltage reference based on the WPP reactive power flow and the droop gain, as shown in (1). This function (1) will be utilized in the offshore AC grid voltage control section below, in order to share the reactive power between the WPPs and the HVDC station. The droop helps to decrease the reference voltage if there is a high reactive power injection from the WPP, and increase in a contrary case.

$$V_{WPP-compensated} = V_{WPP-ref} - Q_{WPP-actual} \times kq_{droop} \tag{1}$$

3.2. Active Power Control – Closed Loop Regulation and De-loaded Operation

As seen in Fig. 2, the active power control of the type 4B WT is assumed as an open loop implementation that the active power reference is divided to the voltage magnitude to generate active current reference. The outer WPP active power control performs closed loop control based on the feedback from the WPP PoC measurement, which provides possibility to operate the WPP as de-loaded (e.g. 80% of the initially available power). This active power control loop will be utilized to keep reserve (de-load) and to realize active power modulation signals referenced from the POD function at the HVDC link.

4. Offshore AC Grid Voltage Control

As mentioned in the second section, the large stray capacitance of the offshore cables generates a large amount of reactive power especially during low generation levels. However, it should also be remembered that the WPP-A is located very close to the HVDC station with almost no cable in between. Hence the WPP-A is observed to generate reactive power during high generation levels in order to compensate for the reactive losses at the WPP and WT

transformers. Another important point due to the close location of the HVDC station and the WPP-A, the voltage controllers at these two terminals start to impact each other and at the HVDC station starts injecting reactive power, in contrast to a general offshore case (where the shunt reactors and WT converters absorb the reactive power). This creates an unnecessary flow of reactive power such that the HVDC station is injecting reactive power while the WPP-B and WPP-C are absorbing (the excess reactive power of their cables) and WPP-A changing reactive power flow direction after 0.75 pu generation level, as seen in Fig. 3 (a).
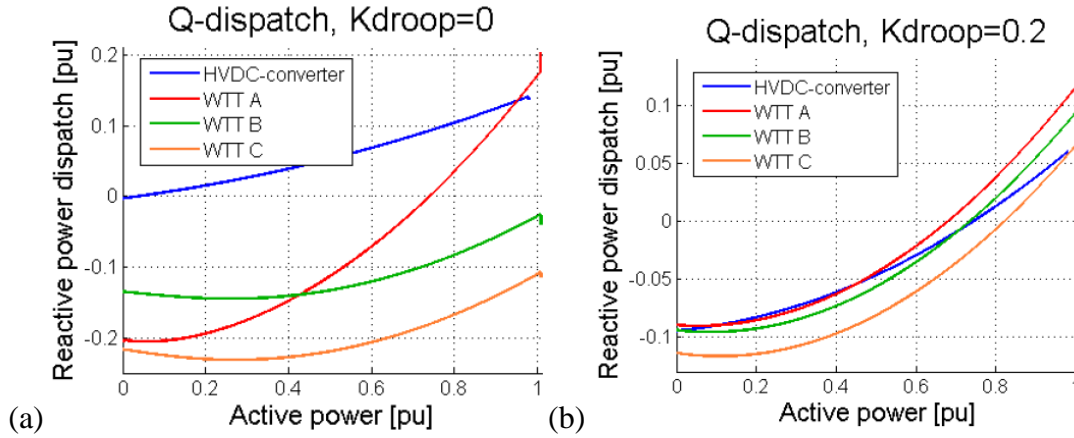

Fig. 3. (a) Reactive power flow without droop; (b) Reactive power flow with droop.

The voltage profiles are shown in Fig. 4 below, where a stiff 1 pu voltage is achieved for all control terminals when the droop gain is set as zero, however resulting in a reactive power flow as in Fig. 3 (a) above. In order to provide a coordinated response between the WPPs and the HVDC station, the droop function is utilized and the reactive power provision (absorbing and injecting) is shared fairly as seen in Fig. 3 (b). Here the reactive power values from the WT and HVDC converters are shown, which absorb the excess reactive power from the cables during low generation and inject reactive power to compensate the losses at the transformers during high generation in a harmonized way. As seen in Fig. 4, using the droop results in compromise of voltage as approximately 0.03 pu deviation from rated, which is considered to be acceptable.

5. Active Power Modulation by the WPPs for POD

The POD function requirement is being introduced for the converter based generation units in order to substitute the PSS function of the conventional synchronous generators, e.g. by the recent ENTSO-E "Network Code on High Voltage Direct Current Connections and DC-connected Power Park Modules" [4]. Though it is considered for the HVDC stations (of interconnectors) for the time being, the contribution of the DC-connected WPPs to the POD is anticipated in the literature [9]. An up-to-date survey of POD and implementation details can be found in [10]. The POD by the converter based renewables can be provided by active and/or reactive power modulation. In case the POD is realized by reactive power, it can easily be provided by the onshore HVDC converter without considerable impact on the offshore side [9]. However, provision of the POD by active power requires modulation of active power from the offshore WPPs.

In this study, the scenario is assumed as; the onshore HVDC station has the necessary feedback from the onshore AC grid (which experiences and senses the power system oscillation problem) and sends the necessary POD modulation signal to the HVDC offshore station, which tries to realize this POD modulation signal via sending references to the WPPs. The dynamic delay due to the DC voltage control at the HVDC link is not considered here, since this delay is known to be small and the main focus is on the offshore coordination. An artificial POD modulation signal is referenced as if it is coming from the HVDC onshore station, which is 0.1 Hz with 0.1 pu magnitude. Additionally, the same settings have been simulated for a case with 0.5 Hz modulation as well.

The realization of the POD active power modulation is implemented in two different ways in this paper; the first one as uncoordinated open loop reference dispatch to the WPPs and the second as the closed loop coordinated

control at the offshore HVDC station, which are shown in Fig. 5 and results compared in Fig. 6. In both cases the resultant references to each WPP are phase-gain compensated in order to account for the dynamics of the WPP and communication delays between the cluster controller at the HVDC station and the WPPs. The same compensation is applied in both cases. The communication delays between the cluster controller and the WPP controllers are modeled with time delay function of the DIgSILENT PowerFactory.
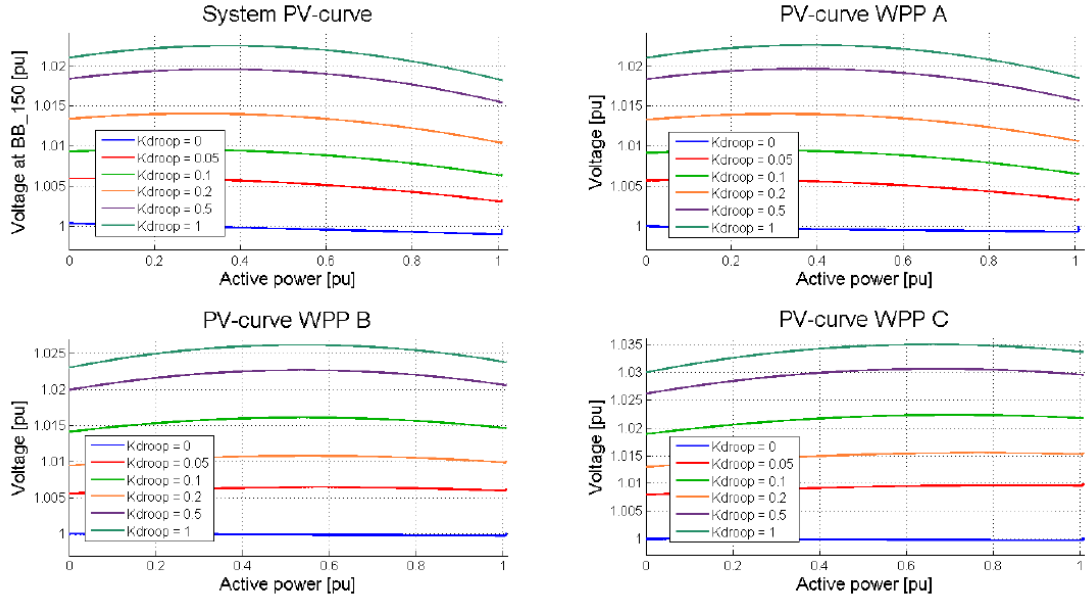

Fig. 4. Voltage profiles versus active power generation levels for various droop constants.

The results with the open loop dispatch method are shown in Fig. 6 (as dashed), where the WPP responses are unsynchronized (despite the phase-gain compensation) mainly due to non-deterministic dynamics of the WPPs and non-deterministic delay between the HVDC station and the WPPs. This results in ineffective overall active power response from the HVDC link to the onshore grid. However, the coordinated closed loop method results in synchronized response from the WPPs, since the mismatch between the reference and measured active power is regulated. It should be noted that the HVDC measured active power in Fig. 1 is used as the feedback, which is filtered to remove the steady-state generation from the WPPs. The power regulator here is implemented simply as a proportional-integral (PI-controller) structure, whereas more complicated methods (e.g. adaptive gain-scheduling) can be considered for improved response. In the coordinated closed loop method the WPPs' generation level is also taken into account. This is important considering the stability of the WT rotor speeds since a long and excess loading to a WPP with low generation level (e.g. due to low wind speed for that WPP) would cause problems [9]. As seen in Fig. 6 (b), the performance deteriorates for the increased modulation frequency (0.5 Hz), which implies a need for improvement for the regulator at the cluster controller and the WPP dynamic responses.
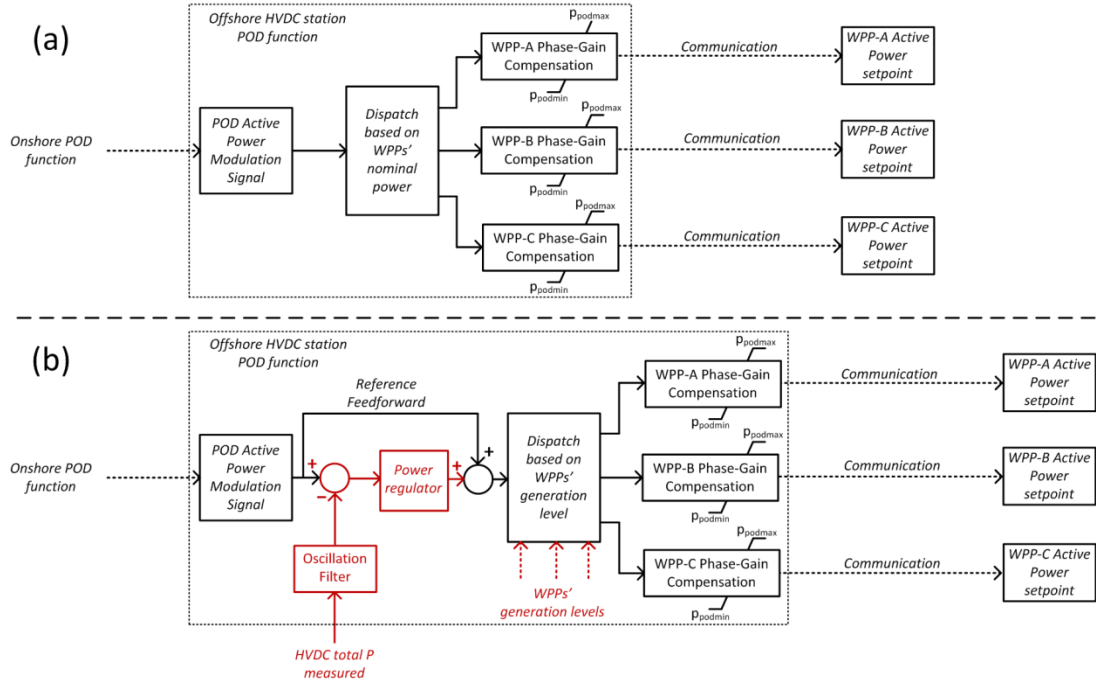
Fig. 5. (a) POD as open loop dispatch; (b) POD as closed loop coordinated regulation.
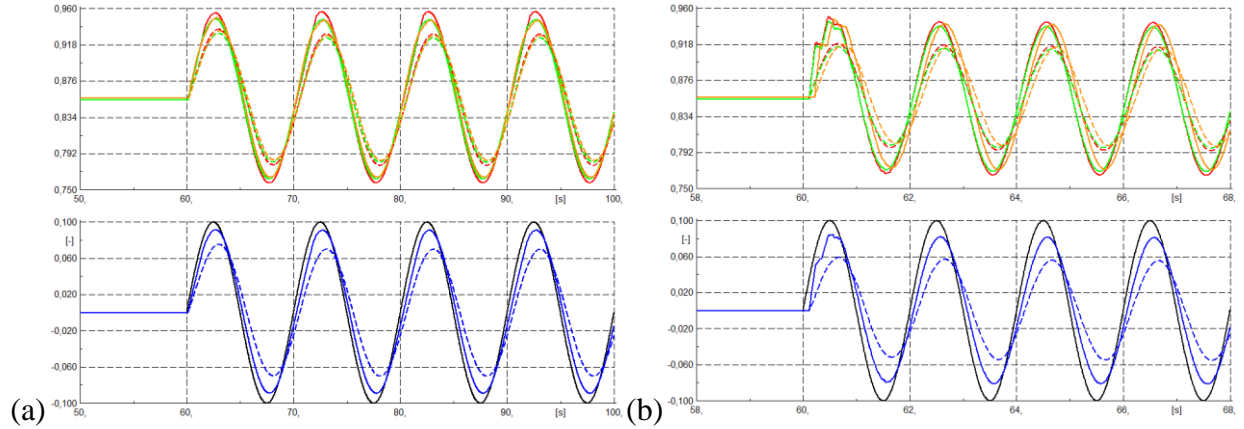

Fig. 6. POD results (a) 0.1 Hz (b) 0.5 Hz case. Black is the POD reference signal. Dashed red, green, orange, and blue are WPP A, B, C, and HVDC active power [pu] values, respectively with open loop dispatch. Solid red, green, orange, and blue are WPP A, B, C, and HVDC active power [pu] values, respectively with closed loop coordinated regulation.

6. Conclusion

In this paper the cluster control of HVDC connected offshore WPPs is studied on a generic benchmark layout of three WPPs with individual WPP controllers connected to a common offshore HVDC station, which is modeled with an ideal voltage source converter. The IEC 61400-27-1 models are shown to be utilized in DC-connected offshore WPP studies, where the offshore AC grid voltage is generated by the HVDC converter and the WPPs contribute to offshore grid voltage control. It is shown that when the WPPs are referenced with unity voltage, an uncontrolled reactive power flow occurs. The plant voltage droop compensation is shown to avoid this via providing fair share between the WPPs and the HVDC converter. This is considered to improve efficiency of the offshore grid via decreasing losses. Optimization of the voltage setpoints based on the active power losses stands as a future work. The POD function is performed by the active power modulation of the offshore WPPs with and without

coordination. It is shown that the closed loop control at the offshore HVDC station provides effective active power response, hence better potential support to the onshore AC grid, in case it is implemented. A potential application of the offshore cluster controller is shown, which may improve implementation of system services by DC-connected offshore WPPs, which is considered to be a demand in the near future. Implementation and analysis of other ancillary services, e.g. frequency support, with the DC-connected cluster of offshore WPPs worth to be a future work.

Acknowledgement and Disclaimer

References

[1] V. C. Tai and K. Uhlen, "Design and Optimisation of Offshore Grids in Baltic Sea for Scenario Year 2030," EERA DeepWind'2014, Energy Procedia, vol. 53, pp. 124–134, 2014

[2] Siemens SylWin1 Press Release, 25 April 2015 [online] Available:

http://www.siemens.com/press/en/pressrelease/?press=/en/pressrelease/2015/energymanagement/pr2015040192emen.htm&content[]=EM

[3] L. Harnefors, N. Johansson, Z. Lidong, and B. Berggren, "Interarea Oscillation Damping Using Active-Power Modulation of Multiterminal HVDC Transmissions," IEEE Transactions on Power Systems, vol.29, no.5, pp. 2529-2538, Sept. 2014

[4] ENTSO-E Draft Network Code on High Voltage Direct Current Connections and DC-connected Power Park Modules, 30 April 2014 [online] Available:

https://www.entsoe.eu/Documents/Network%20codes%20documents/NC%20HVDC/140430-NC%20HVDC.pdf

J2 Jayachandra N. Sakamuri. Rather Z.H., Cutululis N.A., Müfit Altin, Ömer Göksu, Rimez J., "Coordinated Voltage Control in Offshore HVDC Connected Cluster of Wind Power Plants ", IEEE Trans. on Sustainable Energy, vol.7, pp.1592-1601, Oct 2016.

This page would be intentionally left blank if we would not wish to inform about that.

Coordinated Voltage Control in Offshore HVDC Connected Cluster of Wind Power Plants

Jayachandra N. Sakamuri, *Graduate Student Member, IEEE*, Zakir Hussain Rather, *Member IEEE*, Johan Rimez, *Member IEEE,* Müfit Altin**,** *Member IEEE,* Ömer Göksu, *Member IEEE,* Nicolaos A. Cutululis, *Senior Member IEEE*

Abstract--**This paper presents a coordinated voltage control scheme (CVCS) for a cluster of offshore wind power plants (OWPPs) connected to a VSC HVDC system. The primary control point of the proposed voltage control scheme is the introduced Pilot bus, which is having the highest short circuit capacity in the offshore AC grid. The developed CVCS comprehends an optimization algorithm, aiming for minimum active power losses in the offshore grid, to generate voltage reference to the Pilot bus. During steady state operation, the Pilot bus voltage is controlled by dispatching reactive power references to each wind turbine (WT) in the WPP cluster based on their available reactive power margin and network sensitivity based participation factors, which are derived from the *dV/dQ* sensitivity of a WT bus w.r.t the Pilot bus. This method leads to minimization of the risk of undesired effects, particularly overvoltage at the terminals of the WT located far away from the AC collector substation, by dispatching lower reactive power references compared to the ones nearer to the substation. In addition, the paper proposes a control strategy for improved voltage ride through capability of WTs for faults in the offshore grid, thus leading to improved dynamic voltage profile in the offshore AC grid.**

Index Terms—**Cluster voltage controls, HVDC, power loss, offshore wind power plants, reactive power dispatch, voltage ride through.**

I. INTRODUCTION

During recent years, there has been significant penetration of offshore wind power plants into power systems and this trend is expected to continue in the future [1]. Traditionally, power from OWPPs is transported to the mainland grid through submarine high voltage AC (HVAC) cables [2]. However, increased power output from OWPPs combined with long distances to the shore has encouraged the use of voltage source converter based high voltage direct current (VSC- HVDC) system as a feasible and economical solution for bulk power transmission from OWPPs to the onshore grid [3]. Among the available wind turbine technologies, full scale power converter-based variable speed

wind turbines are becoming more popular due to their inherent flexible and independent control of active and reactive power and their adaptability to variable wind speeds [4]. Furthermore, owing to the anticipated increase in OWPPs, it is likely that a cluster of WPPs may be connected to the mainland grid through a common HDVC transmission system for various techno-economic reasons, such as low capital cost, lower transmission losses and higher reliability, thereby forming a common interlinked AC offshore grid.

Increased penetration of wind power into power systems over past decades has introduced various technical challenges towards secure and stable operation of the system. In order to counter such challenges, transmission system operators (TSOs)/system regulators have introduced new grid codes getting upgraded on regular basis [5]-[8]. Such wind integration related grid code regulations currently in place, are mainly applicable to AC connected wind power plants (WPPs), and very limited literature without any legally binding grid code addressing HVDC connected WPPs is presently available. Recently, ENTSO-E has prepared a draft Network Code on High Voltage Direct Current Connections and DC-Connected Power Park Modules (NC-HVDC), which has highlighted the grid code requirements for offshore HVDC connected WPPs [9].

Since the HVDC system decouples OWPPs from the mainland AC grid, the offshore AC grid becomes more vulnerable to dynamic voltage events due to lower short circuit power contribution from power electronic interfaced variable speed WTs and HVDC converter [10]-[11]. This leads to significant concern for voltage ride through (VRT) capability of WPPs in the offshore AC grid. A considerable number of research studies has undergone, investigating fault ride through capability (FRT) for offshore HVDC connected wind power plants for faults in the onshore mainland AC grid [12]-[14]. However, FRT capability and fault current contribution from offshore WPPs for faults in the offshore grid has received a limited attention. A method for controlling the negative sequence current injection into the offshore grid from the VSC-HVDC and WTs for asymmetrical faults in the offshore grid has been discussed in [15], however, this research is limited to control methods for a single WT and it has not considered the complete WPP cluster. Fault response and protection of a HVDC-connected WPP for faults in the HVDC-link has been studied in [16]; here, a single aggregated WT model is considered to represent the complete WPP, and therefore the response of each WT inside the WPP for faults

within the WPP has not been analyzed.

The steady state voltage/reactive power control and dispatch strategy of the WPP cluster connected to the offshore HVDC converter is also important as several offshore WPPs in close proximity may be connected to the same HVDC converter station, particularly in the growing offshore grid. The general control strategy for a single AC connected WPP is that the TSO dispatches (1) power factor, (2) reactive power, or (3) voltage magnitude, as set points to the WPP controller. At WPP level, based on the TSO dispatch set point, the WPP controller dispatches reactive power/voltage set points to individual WTs based on their available reactive powers [17]-[19]. However, such a control strategy does not recognize the network (offshore grid) voltage sensitivity. Therefore, application of such control and dispatch strategies may lead to undesirable and suboptimal operation, such as higher losses and undesirable voltage in the WTs located at the end of collector cable.

In this context, a new Coordinated Voltage Control Scheme (CVCS) for OWPP cluster based offshore AC grid connected to a HVDC transmission system is proposed in this paper. During steady state operation, the proposed CVCS generates reactive power references for the WPP cluster by controlling the voltage at the Pilot bus in the offshore grid. The procedure to select the Pilot bus is discussed in section III B. By controlling voltage at the Pilot bus, a stable and improved voltage profile is maintained in the offshore AC grid. The voltage reference for the Pilot bus is supplied by an optimization algorithm aimed at minimizing active power losses in the offshore grid, considering wind driven variability in the power output of WPPs. Based on the voltage reference at the Pilot bus, reactive power reference values generated by the CVCS are then dispatched to each WPP, based on their participations factors (PFs) and available reactive power margin in the corresponding WPP. The participations factor of a WT recognizes voltage sensitivity of the WT bus w.r.t the Pilot bus.

The proposed method thus eliminates the possible undesirable overvoltage at the WT terminals located at the farther end of the AC collector substation by commanding proportionally lower reactive power from it compared to the one nearer to the substation. For dynamic voltage control, while individual WT's local reactive power controller injects reactive current based on the voltage dip observed at its terminal bus, the proposed CVCS supplements with the additional reactive power injection from the WTs that observe relatively lower voltage dip due to their lower voltage sensitivity towards the faulted location, thereby improving the overall VRT capability of the offshore grid. Dynamic performance of the proposed CVCS is verified against various critical faults in the offshore AC grid, such as: WT terminal faults, collector cable faults and export cable faults.

The rest of the paper is organized as follows. Section – II describes the modeling of offshore HVDC connected clusters of WPP. The proposed CVCS is discussed in section-III. The simulation results along with discussions for steady state and dynamic operation is presented in section-IV, and concluding remarks along with scope for future work is given in section V.

II. MODELING OF OFFSHORE HVDC CONNECTED WPP CLUSTER

An OWPP cluster of 800 MW capacity comprising of four WPPs, connected to the main land grid through a VSC-HVDC link, is considered in this study. Further details of modelling are given below.

A. WPP Layout

The 800 MW offshore WPP cluster with four 200 MW WPPs, connected to four AC collector substations marked as A1B1, A2B2, C1D1, and C2D2 respectively, is shown in Fig. 1. These substations are located at respective distances of 7 km, 12, km, 17 km, and 22 km from the offshore HVDC

Fig. 1. Offshore HVDC connected cluster of WPPs

converter station. Each 200 MW WPP is comprised of four parallel WT strings. Each string is of 50 MW capacity, with each string that consists of 8 series connected 6.25 MW WTs. These wind turbines are placed with an inter-machine distance of 1.2 km, approximately equal to seven times their rotor diameter.

Each AC collector substation is fed by four 33 kV WT collector cables through a power transformer. The cables between WT5-WT8, and WT5-collector bus WTA1(1-8) have a current ratings of 0.5 kA and 1 KA respectively, while each 33/155 kV power transformer is of 240 MVA capacity. Technical data for cables adopted has been taken from the ABB cable data handbook [20].

Though a detailed modelling of WPP can provide more insight into the system, its consideration however, increases the computational burden. Hence, one string of the WPP-A1B1 is modelled in detail and the rest of the WPPs are represented by aggregated models without compromising the accuracy of results. A WT collector cable (8 machines, 50 MW total capacity) in WPP-A1B1is modeled in detail and the remaining WTs of the same WPP are represented by an aggregated 50MW model for the A1 (9-16) feeder and an 100 MW model for the B1 (1-16) feeders. The rest of the WPPs are aggregated with each having 100 MW capacity. The aggregation method for WTs and export cables of WPP has been adopted from [21], [22].

B. WT Model

A full power converter WT (Type-4) model considered for this work has been adopted from IEC 61400-27 – Part 1 [23]. To precisely estimate the available active power output and reactive power margin of each WT at a given wind speed, the adopted WT model, is extended with aerodynamic and pitch controller models. The active, reactive power references and control signals for the voltage ride through controls for WT (as discussed in section-III) are provided by the WPP controller.

C. HVDC System Model

The HVDC system considered is an 850 MVA VSC-HVDC transmission link, with voltage levels of 380 kV line-to-line on the AC side and ±320 kV on the DC link. The standard pulse width modulation (PWM) based converter model has been adopted for both offshore and onshore HVDC converter. The power balance control to maintain the DC link voltage at an optimal value is assigned to the onshore converter, as shown in Fig. 2. It also controls the reactive power/AC Voltage at the converter bus as per grid code regulations. The offshore HVDC converter, as shown in Fig. 2, is assigned with the AC voltage control of the offshore HVDC converter station ('AC_Control_WF' bus in Fig. 1), and also enforces the frequency of the offshore AC network. This allows the transfer of active power from the WPPs to the HVDC system. The current references provided by the outer controllers are handled by a standard inner fast current controller operating in the d-q reference frame. The offshore HVDC Converter also generates/consumes additional reactive power based on the additional reactive current reference

(Δiq_{HVDC}) from the WPP cluster controller during dynamic events upon improving the voltage recovery in the offshore AC grid.
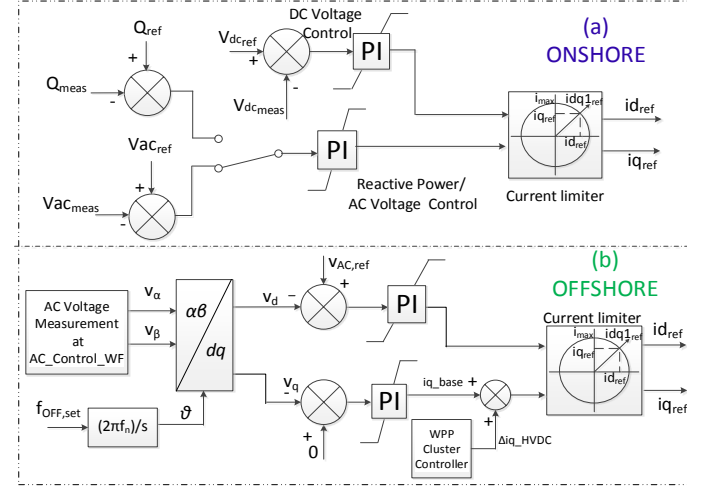

Fig. 2. (a). Onshore and (b.) Offshore HVDC converter controllers

III. COORDINATED VOLTAGE CONTROL SCHEME FOR HVDC CONNECTED OFFSHORE WPP CLUSTER

The proposed CVCS for an offshore HVDC connected cluster of WPPs is shown in Fig. 3. The voltage is controlled at the Pilot bus; the bus with the highest short circuit capacity in the offshore AC grid. The optimal reference voltage at the Pilot bus is supplied by the optimization algorithm aimed at minimizing active power losses in the offshore AC grid. The Pilot bus concept, the optimization and the operation (steady state and dynamic) of the CVCS is described in the following subsections.

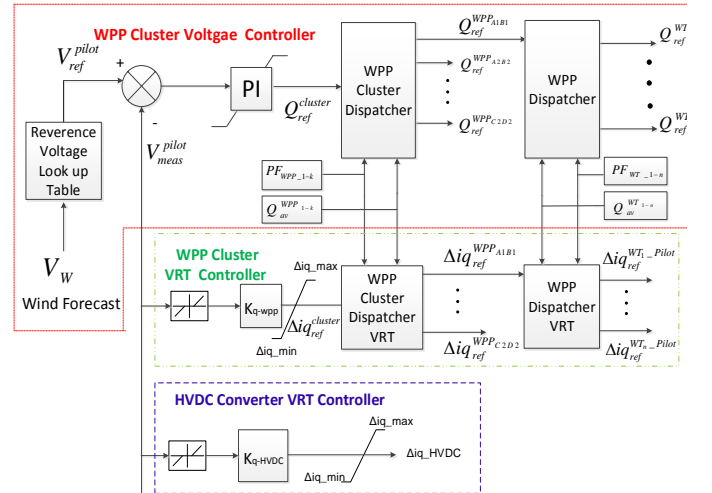Fig. 3. WPP cluster coordinated voltage control scheme

A. Optimization framework considering wind speed variation

The reference voltage for the Pilot bus is dispatched at regular intervals from the optimization algorithm depending on the availability of wind power forecast data and the operating conditions. In general, it should be updated following a significant change in the production level. To the

knowledge of the authors, most wind farm operators and/or TSOs (in systems with significant wind power capacity) can produce wind power forecasts every 5 min. The exact interval will have to be established based on operational experience and it could vary from case to case, or day to day (depending on weather conditions), possibly in the range of 5-30 min. Based on the wind forecast, the active power output from each wind turbine is estimated and the optimization routine is solved for optimal voltage reference at the Pilot bus. The proposed voltage controller in turn maintains the desired Pilot bus voltage profile. The optimization problem is formulated as a loss minimization problem as given in (1-9).

$$\min f(x) \tag{1}$$

with

$$h(x) = 0; \tag{2}$$
$$g^{\min} \le g(x) \le g^{\max} \tag{3}$$
$$u^{\min} \le u \le u^{\max} \tag{4}$$

where,

$$f(x) = P_{loss}(x) \tag{5}$$

x is a set of algebraic variables which include voltage magnitude and angles. $h(x)$, $g(x)$ and u are a set of equality constraints, inequality constraints, and, control variables varying between maximum ($u^{\max}$) and minimum ($u^{\min}$) value, as defined in (6) ,and (7),(8),(9) respectively. $P_{loss}(x)$ is the total active power losses in the entire offshore grid, including machines, converters, cables and transformers.

$$h(x) = \begin{cases} P_g^j - P_l^j - \sum_{j=1}^{Nb} P_{inj}^j = 0 \\ Q_g^j - Q_l^j - \sum_{j=1}^{Nb} Q_{inj}^j = 0 \end{cases} \tag{6}$$

$h(x)$ represents active and reactive power balance equations at jth bus. P_g^j, P_l^j are active power generation and load at bus j. Q_g^j, Q_l^j are reactive power generation and load at bus j . P_{inj}^j, Q_{inj}^j are active and reactive power injection from adjacent nodes at bus j . N_b is the number of buses.

$$V_j^{\min} \le V_j \le V_j^{\max} \tag{7}$$
$$\max\left(\left|I_{i1}\right|, \left|I_{i2}\right|\right) \le I_{\max} \tag{8}$$

where,

V_j, $V_j^{\min}$, $V_j^{\max}$ are actual voltage , minimum and maximum voltage limits at the jth bus. I_{i1} and I_{i2} are current measurements at the two respective terminals of a branch and $I_{\max}$ is the value of maximum design current of the branch.

$$Q_{gj}^{\min} \le Q_{gj} \le Q_{gj}^{\max}$$
$$P_{gj}^{\min} \le P_{gj} \le P_{gj}^{\max} \tag{9}$$

Q_{gj} , $Q_{gj}^{\min}$, $Q_{gj}^{\max}$ are actual reactive power generation, minimum and maximum allowed limit. P_{gj} , $P_{gj}^{\min}$, $P_{gj}^{\max}$ are actual active power generation, and corresponding minimum and maximum allowed limit.

The optimization problem (1-9) is solved through Interior Point Method (IPM). Due to its fast convergence and ease of handling inequality constraints using logarithmic barrier functions, IPM is considered as an efficient method [24].

B. Selection of Voltage Control Zone and Pilot Bus

For efficient and effective voltage control, AC buses in a system with close voltage coupling can be grouped together to form a single voltage control zone. Voltage control zones should be sufficiently decoupled from one another, each zone having sufficient reactive power resources to control the voltage within its boundaries with minimal reactive power influence from other neighboring voltage control zones. A set of buses within close electrical distance are grouped together to form a single voltage control zone. Electrical distances are calculated using the $\partial V / \partial Q$ sensitivities; they reflect the propagation of voltage variations caused by reactive power injections at other selected busses. The $\partial V / \partial Q$ sensitivities can be calculated from the Jacobian matrix with $\partial Q / \partial V$ elements. The related attenuation constants are obtained by dividing elements of each column of $\partial V / \partial Q$ matrix by the diagonal element as defined in (10).

$$\alpha_{ij} = \left[\frac{\partial V_i / \partial Q_j}{\partial V_j / \partial Q_j} \right] \tag{10}$$

Where, α_{ij} is the attenuation constant between buses i and j . The electrical distance between buses i and j can be calculated as given in (11) [25].

$$D_{ij} = -\log(\alpha_{ij}.\alpha_{ji}) \tag{11}$$

Function D_{ij} represents a real mathematical distance between the two buses. The matrix of electrical distances is then normalized by dividing each element by the maximum value of electrical distance matrix as obtained by using (11). The elements of electrical distance matrix are real mathematical numbers representing voltage coupling between any two buses. Furthermore, it is important to mention that electrical distance values between any two buses does not represent the electrical impedance between the two buses, rather they are entirely two different parameters. A detailed account of electrical distance and voltage control zone formation is provided in [25]. Since the offshore AC grid is relatively small in comparison to the main grid, therefore the offshore AC grid is treated as a single voltage control zone in this research work.

A Pilot bus is selected in the offshore AC voltage control zone, such that the voltage control at the selected bus has the highest influence on the voltages of the other buses in that zone. It has to be noted that since all the buses of a given zone are strongly coupled, the voltage profile of this zone can be smoothly maintained by controlling the voltage at the Pilot bus, reduces the control problem complexity. The Pilot bus can be selected on various factors such as its electrical distance based centrality, the highest short circuit capacity, or in some cases a selected load bus. In this research work, the bus with highest short circuit capacity has been selected as the Pilot bus. A complete short circuit analysis of the offshore AC grid has been carried out and the 155 KV bus (AC_TRF_WF) was identified as the bus with the highest short circuit capacity, hence, selected as Pilot bus for this study.

The pilot bus selection seems obvious for the WPP cluster configuration shown in Fig. 1. However, there is a growing interest in setting up many offshore WPPs in the close vicinity in the future, where more number of WPPs are likely to be interconnected to a common offshore AC network and the power is transmitted to the shore through multiple HVDC converters (Multi-infeed HVDC system) [26]. In such cases, it is unlikely to have an intuitive Pilot bus, rather the pilot bus needs to be selected from multiple candidate buses, and the methodology presented in this paper can be applied to identify the actual pilot bus.

C. Steady state Operation of CVCS

Based on the wind forecast, the optimal voltage at the Pilot bus, evaluated from the optimization routine for a given operating condition, is fed in as voltage reference value to the CVCS. Alternatively, an offline 'Reference Voltage Lookup Table' can be constructed taking into account the set of the most probable (and optimized) operating states, used in the real time operation as shown in Fig. 3. Though the first approach is more accurate as the optimal reference voltage is calculated based on the latest wind forecast, the second approach reduces computational burden by avoiding continuous running of the optimization routine for each operating condition, delivering good and reliable set points yet. For a given WPP power output, the corresponding optimal reference voltage at the Pilot bus (V_{ref}^{pilot}) is transmitted to the cluster voltage controller, that generates the required reactive power set point ($Q_{ref}^{cluster}$) for the WPP cluster. The *WPP Cluster Dispatcher* distributes this reactive power set point to each WPP within its cluster based on their respective participation factors. Finally the *WPP Dispatcher* distributes the reactive power set points of a WPP to all of its WTs. The mathematical model for the reactive power dispatch within the WPP dispatcher is given in (12).

$$Q_{ref}^{WT_i^j} = \frac{PF_{WT_i^j}}{PF_{WPP^j}} * \frac{Q_{av}^{WT_i^j}}{Q_{av}^{WPP^j}} * Q_{ref}^{WPP^j}$$

$$Q_{av}^{WPP^j} = \sum_{i=1}^{n} Q_{av}^{WT_i^j} \ with : Q_{av}^{WT_i^j} = \sqrt{(S_{Gen}^{WT_i^j})^2 - (P_{av}^{WT_i^j})^2} \quad (12)$$

$$PF_{WT_i^j} = \frac{dU_{pilotbus}}{dQ_i^j}, PF_{WPP^j} = \frac{\sum_{i=1}^{n} PF_{WT_i^j}}{n}$$

The reactive power reference for the ith WT of the jth WPP ($Q_{ref}^{WT_i^j}$) is formulated as the proportional distribution of the WPP reactive power reference ($Q_{ref}^{WPP^j}$) based on the ratio of the participation factors and the available reactive power , where $P_{av}^{WT_i^j}$, $Q_{av}^{WT_i^j}$,and $S_{Gen}^{WT_i^j}$ are the available active and reactive powers and the MVA rating of the ith wind turbine; $Q_{av}^{WPP^j}$ is the total available reactive power of the jth WPP, $PF_{WT_i^j}$ and PF_{WPP^j} are the participation factors of the ith wind turbine in the jth WPP, and total j^{th} WPP respectively . Similarly, the mathematical model for the reactive power dispatch at WPP cluster level is given in (13).

$$Q_{ref}^{WPP^j} = \frac{PF_{WPP^j}}{PF_{cluster}} * \frac{Q_{av}^{WPP^j}}{Q_{av}^{cluster}} * Q_{ref}^{cluster}$$

$$Q_{av}^{cluster} = \sum_{j=1}^{k} Q_{av}^{WPP^j} \quad (13)$$

$$PF_{cluster} = \frac{\sum_{j=1}^{k} PF_{WPP^j}}{k}$$

The reactive power reference for each WPP ($Q_{ref}^{WPP^j}$) is formulated as the proportional distribution of the WPP cluster reactive power reference ($Q_{ref}^{cluster}$) based on the ratio of participation factors and available reactive power margin. $PF_{cluster}$ is the participation factor of the WPP cluster, and $Q_{av}^{cluster}$ is the total available reactive power of the WPP cluster. Therefore, during steady state operation, for any unacceptable voltage deviation at the Pilot bus, all the WTs in WPP cluster are controlled to generate/consume additional reactive power based on the set points generated by the proposed CVCS. The reactive power controller at the WT level is shown in Fig. 4.
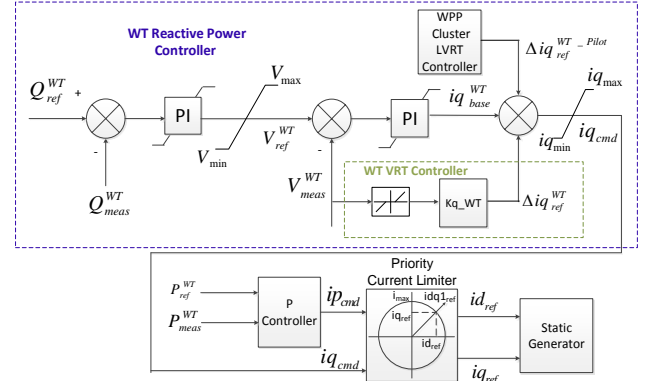

Fig. 4. WT reactive power controller

Based on corresponding reactive power set point from CVCS, the outer WT reactive power controller generates voltage reference to the WT, which then generates corresponding base reactive current reference signal (iq_{base}^{WT}) for wind generator. The Δiq_{ref}^{WT} from WT VRT controller and $\Delta iq_{ref}^{WT_i^j - Pilot}$ from the cluster CVCS are added to iq_{base}^{WT} to generate reactive current reference to the WT (iq_{cmd}). The Active Power Controller (*P Controller*) generates active current reference (ip_{cmd}). The active/reactive power priority from the WT during dynamical condition can be set by the *Priority Current Limiter*.

D. Dynamic Operation of CVCS

A dynamic event, such as short circuit fault may result in voltage ride through issues in the offshore AC grid. As per grid code regulations [5],[6], WPPs are expected to support the grid by contributing additional reactive power during and after a dynamic voltage event in the offshore AC grid for better voltage recovery of the grid. Hence, a VRT controller has been implemented at WT level, as shown in Fig.4, which generates an additional reactive current reference (Δiq_{ref}^{WT}) whose value depends on the voltage deviation from the allowed dead band (normally 0.05 to 0.1 pu) at the WT

137

terminal. Such WT VRT controller may be sufficient for a single WPP connected to offshore grid, where a voltage deviation due to a fault is expected to be observed by most of the WTs, contributing to the fault current. Instead, in a WPP cluster if more than one WPP gets connected to the same offshore grid, a fault within one of the WPPs may not be observed with same sensitivity by the WTs of the neighboring WPPs having a sufficient reactive power margin that otherwise can be used to improve, the voltage dip during the fault, and post fault voltage recovery. Therefore, to improve the voltage profile within the offshore AC grid, an additional cluster level controller 'WPP Cluster VRT Controller' is augmented with the proposed CVCS as shown in Fig. 3. The WPP Cluster VRT Controller sends additional reactive current reference signals to all WTs in the cluster, based on the voltage deviations observed at the Pilot bus during a fault in the offshore grid. The mathematical model for the WPP cluster VRT reactive current dispatch is given in (14).

$$\Delta iq_{ref}^{WPP^j} = \frac{PF_{WPP^j}}{PF_{cluster}} * \frac{Q_{av}^{WPP^j}}{Q_{av}^{cluster}} * \Delta iq_{ref}^{cluster} \qquad (14)$$

The VRT reactive current reference for each WPP ($\Delta iq_{ref}^{WPP^j}$) is formulated as the proportional distribution of the WPP cluster VRT reactive current reference ($\Delta iq_{ref}^{cluster}$) based on the ratio of participation factors and available reactive power of each WPP. Similarly, the mathematical model for the VRT reactive current dispatch at the WPP level is given in (15).

$$\Delta iq_{ref}^{WT_i^j - Pilot} = \frac{PF_{WT_i^j}}{PF_{WPPi}} * \frac{Q_{av}^{WT_i^j}}{Q_{av}^{WPP^j}} * \Delta iq_{ref}^{WPP^j} \qquad (15)$$

The VRT reactive current reference for i^{th} WT of jth WPP ($\Delta iq_{ref}^{WT_i^j - Pilot}$) is formulated as a proportional distribution of the $\Delta iq_{ref}^{WPP^j}$, based on the ratio of the participation factors and the available reactive power margin of each WT. Similar to the WPP VRT controller, the 'HVDC Converter VRT Controller' also sends an additional reactive current reference (Δiq_{HVDC}) to the HVDC converter, further enhancing the overall dynamic voltage profile of the offshore AC grid during dynamical events.

IV. SIMULATIONS RESULTS AND DISCUSSION

A. Steady State Operation

The reactive power reference generated by the CVCS is distributed among the WPPs based on their available reactive power and PFs as discussed in Section- III.
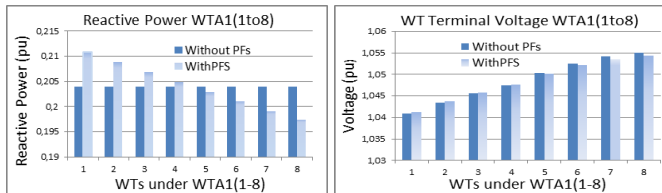
Fig. 5. (a). Reactive power   (b). Voltage of WTA1(1-8)

For an identical operating point, reactive power output and voltage at the terminals of WTA1 (1-8), with and without considering PFs, is shown in Fig. 5. It can be observed that PFs ensure lesser reactive power contribution from the WTs

farther from the collector substation (WTA1(8)) compared to the closer ones (WTA1(1)); hence, the voltage at terminals of WTA1(8) is less compared to the case without taking into account the PFs. Thus, use of PFs increase effectiveness and efficiency of the proposed CVCS by prioritizing the effective wind turbines having more influence on voltage control.

Active power losses in the offshore grid with and without CVCS are shown in Fig. 6. In the latter case, it is assumed that each WPP is in voltage control mode controlling voltage at the low voltage side of the transformer at the WPP collector substation, while WTs are in reactive power control. It can be observed from Fig. 6 that losses are relatively low with the proposed CVCS with more visible difference for higher outputs. Therefore, CVCS driven loss reduction in the offshore grid will accordingly improve the annual revenue of a WPP cluster.
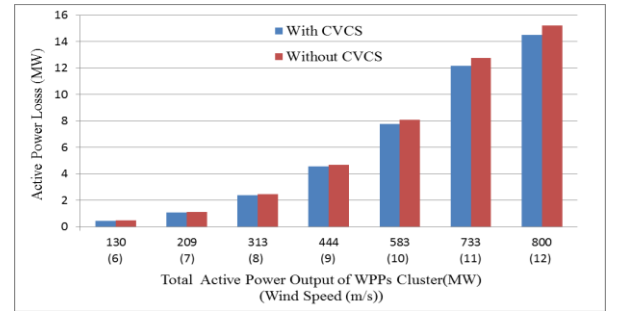
Fig. 6. Active power loss Vs active power output of WPP cluster

Due to effective and efficient utilization of the available reactive power, the proposed CVCS also improves the voltage stability margin of the offshore grid. Fig. 7 shows the PV curves at the 155 kV Pilot bus and A1B1 collector bus with and without CVCS in place. It can be observed that the Pilot bus voltage stability margin is significantly increased from 1566 MW without CVCS to 2488 MW with CVCS. A similar trend can be observed at the collector bus A1B1 where the stability margin has improved from 1641 to 2160 MW with the effect of CVCS. Hence, the proposed CVCS alleviates the overall stability margin of the offshore grid.
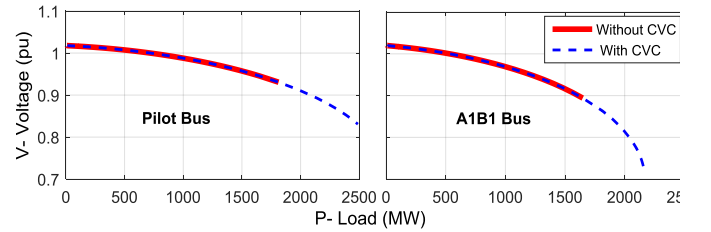
Fig. 7. PV curves of pilot bus and A1B1 collector bus

B. Dynamic Operation

In this section, the response of the investigated cluster for short circuit faults at different locations in the offshore AC grid, namely the collector cable, WT terminal and export cable, are investigated. The dynamic reactive power support from WTs in the WPP cluster with CVCS for such faults is also studied, highlighting the effectiveness of the proposed CVCS for a better voltage ride through capability of the WTs.

1). Collector Cable Fault:

A fault at collector cable is applied at the connection point

138

of WTA1 (5) of WPP- A1B1 during time t=5s having duration of 150ms. The terminal voltage, reactive power output and reactive current measurements of various WTs within WPP cluster are shown in Fig. 8, Fig. 9, & Fig. 10 respectively.
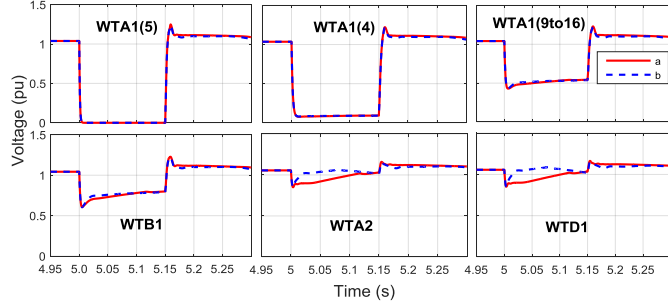

Fig. 8. Voltage at WT terminals for collector cable fault at WTA1(5)
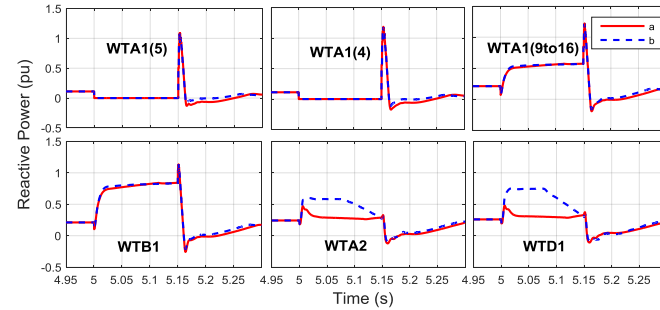a. with WT local VRT control b. with WT local VRT and WPP cluster level supplemented VRT control

Fig. 9. Reactive power at WT terminals for collector cable fault at WTA1 (5). a. WT local VRT control b. WT local VRT and WPP cluster level supplemented VRT control

The voltage at the faulted WT terminal (WTA1 (5)) and at the other WT terminal buses those are connected to the faulted collector cable, i.e. WTA1(2) to WTA1(8) drops into significantly low values (near to zero) (with voltage at WTA1(4) shown in the Fig. 8). The terminal voltage at the WTs connected to cables other than the faulted cable, however, connected to the same winding of the substation transformer, i.e. WTA1 (9 to 16) within the WPP –A1B1, drops about 50% of its nominal values. The voltage at other WTs connected to the second low voltage winding of the substation transformer (WPP-A1B1), i.e. WTB1, drops around 75% of its rated value. The voltage at WTs in other WPPs, A2B2, C1D1, and C2D2, drops around 85% of its rated value. Terminal voltage responses at WTA2 and WTD1 shown in Fig. 8 represent the behavior of WTs in the non-faulted WPPs. The voltage profile at these WTs in parallel to voltage profile of offshore WPP cluster is improved by generating/consuming additional reactive power from those WTs during the dynamic conditions, as shown in Fig. 9. Such improvement in the voltage profile is achieved by supplying an additional reactive current reference ($\Delta iq_{ref}^{WT-Pilot}$) from the WPP VRT controller of the CVCS to each WT, while Pilot bus voltage deviates from the acceptable margin. During faults, the WPP cluster VRT controller sends current references ($\Delta iq_{ref}^{WT-Pilot}$) to all WTs in the cluster, including the WTs in the faulted WPP, as shown in Fig.10.

However, the reactive power output and hence the voltage profile at WT terminal of the faulted WPP cannot be further improved due to saturation of reactive current reference from the WT VRT controller of such WTs (Δiq_{ref}^{WT}). Hence, the $\Delta iq_{ref}^{WT-Pilot}$ at these WTs does not change the total reactive current reference to the WT (iq_{cmd}) any further. However, as the Δiq_{ref}^{WT} of the WTs in the non-faulted WPPs is less than 1 pu, the $\Delta iq_{ref}^{WT-Pilot}$ from the WPP cluster VRT controller leads to additional reactive power generation from such WTs , resulting in an improved voltage profile of the offshore AC grid by utilizing otherwise unused reactive power reserve in the WPP cluster.
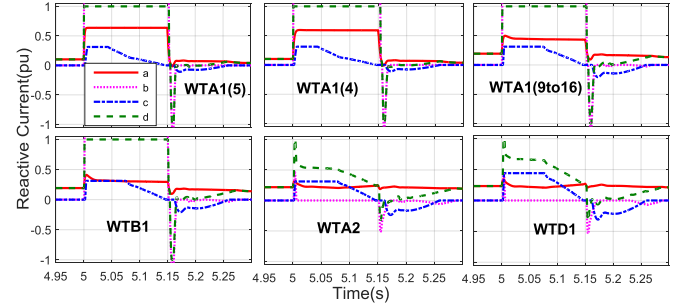

Fig. 10. Reactive current at WT terminals for collector cable fault at WTA1 (5) including the VRT from WT and WPP cluster

a. iq_{base}^{WT} b. Δiq_{ref}^{WT} c. $\Delta iq_{ref}^{WT-Pilot}$ d. iq_{cmd}

As discussed in Section III D, the 'HVDC Converter VRT Controller' also generates an additional reactive current reference for the HVDC converter (Δiq_{HVDC}), which generates/consumes reactive power based on the voltage deviation at the Pilot bus. The effectiveness of the CVCS augmented VRT controller from WPP cluster and HVDC converter, on the Pilot bus voltage, representing the voltage of the offshore WPP cluster, is shown in Fig. 11.
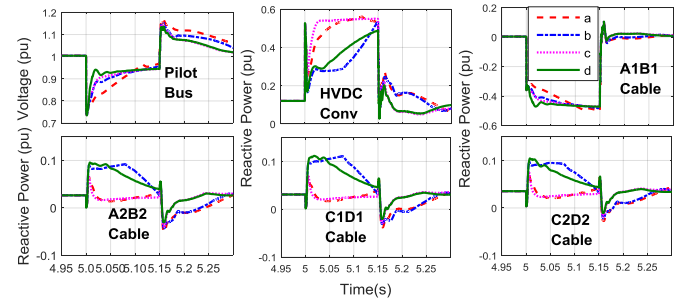
Fig. 11. Voltage at pilot bus and reactive power from HVDC converter and WPPs. a). WT local VRT control, b). VRT control from WT and WPPs cluster, c). VRT control from WT and HVDC converter, d). VRT control from WT, WPP and HVDC converter

The reactive power contribution from the HVDC converter and measured reactive power in the WPPs export cables at the Pilot bus is also shown in Fig.11. The HVDC converter and the WPP cluster share dynamic reactive power leading to improved voltage profile in the offshore grid. The proposed CVCS therefore, improves VRT capability of WTs by supplying/consuming additional reactive power from the WPP and HVDC converter during under/over voltage events upon recognizing their network.

However, it is important to compare the performance of the proposed CVCS with the traditional WPP and WT control methods. The traditional control method at WPP level is one

of the three control modes: (1) reactive power, (2) voltage, and (3) power factor, and the same control methods can be applied at the WT level as well [17]-[19]. Voltage control at WPP and WT will result in an effective voltage control during steady state and dynamic conditions [17]. Hence, the performance of the proposed CVCS is compared with the two traditional control methods of the WPP, such as, (1) Voltage control at WPP and WT level (2) Voltage control at WT alone by simulating a collector cable fault at WTA1(5). The voltage of the pilot bus for the three control methods is shown in Fig. 12. It can be observed that the voltage profile of the offshore AC grid is improved with the proposed CVCS during the fault and also after the fault clearance compared to other traditional control methods.

Fig. 12. Pilot bus voltage for collector cable fault at WTA1(5)
a). voltage control at WT alone, b). voltage control at WT and WPP, c). proposed CVCS

2) WT Terminal Fault.

A fault is applied at the WT terminals i.e. at the low voltage side of the WT transformer of WTA1 (5) under WPP-A1B1 at t= 5 s for 150 ms duration. The terminal voltage, reactive power output and reactive current measurements of the WTs within the WPP cluster are shown in Fig. 13, Fig. 14, and Fig. 15 respectively. It can be observed that the voltages at the faulted WT (WTA1(5)), WTs in the rest of the faulted collector cable, and WTA1(9-16) drops to almost zero %, 80% and 92% respectively. The rest of the WTs in the WPP A1B1 and all other WPPs are not significantly affected. The increase in the reactive power output of the WTs, shown in Fig. 14, is due to the increase in base reactive reference current (iq_{base}^{WT}), shown in Fig. 15. The reason is the cluster voltage controller sends an increased reactive power reference to the WTs when the Pilot bus voltage deviates from the reference value. However, the Pilot bus voltage does not deviate from the dead band (+/- 0.05 pu); hence, the WPP cluster VRT controller does not generate an additional reactive current reference. The VRT controller at the WTs in the faulted collector cable (WTA1(5) and WTA1(4)) senses the fault and generates additional reactive current reference.
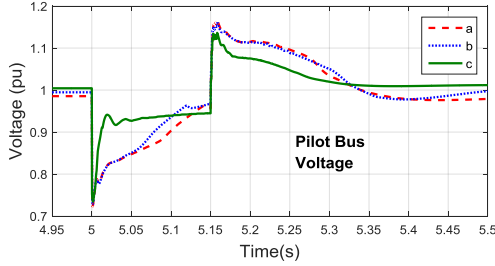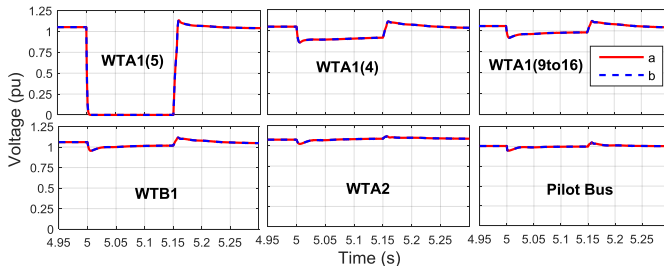

Fig 13. Voltage at WT terminals for WT terminal fault at WTA1 (5)
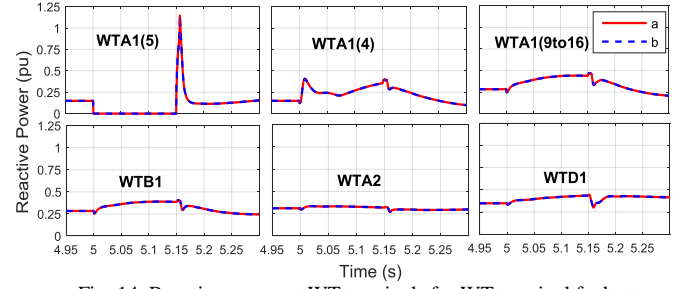a). WT local VRT control, b). VRT control from WT and WPP cluster

Fig. 14. Reactive power at WT terminals for WT terminal fault at WTA1 (5). a). WT VRT alone, b). VRT from WT and WPP cluster.
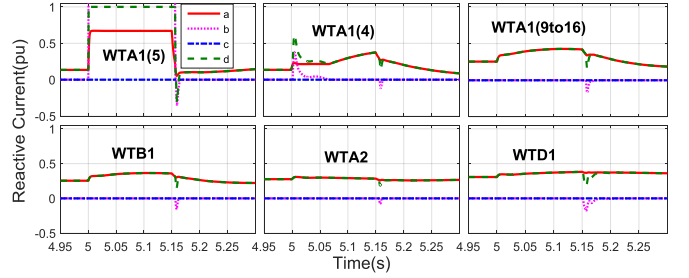

Fig. 15. WT reactive current for WT terminal fault at WTA1 (5) including the VRT from WT and WPP cluster. a). iq_{base}^{WT} ,b). Δiq_{ref}^{WT} , c). $\Delta iq_{ref}^{WT-Pilot}$ d). iq_{cmd}

3) Export Cable Fault

The fault at the export cable A1B1 is applied at A1B1 collector substation side with fault impedance of 2 Ω at t= 5 s for a duration of 150 ms. As seen from Fig. 16, the voltage at all the WPP collector substation buses, A1B1, A2B2, C1D1, and C2D2 (only A1B1 and C2D2 are shown), and the Pilot bus falls to lower values, hence, the voltage at all the WT terminals in the WPP cluster is also decreased. The reactive power and reactive current from WTA2 and WTD1 are shown Fig. 17 and Fig. 18 respectively, while the response of the rest of the WTs is similar. The CVCS cluster voltage controller sends an increased reactive power reference to all WTs within the cluster, which increases iq_{base}^{WT} during the fault. However, the reactive current references from WPP cluster VRT controller ($\Delta iq_{ref}^{WT-Pilot}$) and WT VRT controller (Δiq_{ref}^{WT}) further enhances the total reactive current reference to WT. The magnitude of Δiq_{ref}^{WT} overshoots 1 pu during the fault and falls to less than -1 pu following the fault clearance. Hence, the overall VRT capability of WPP does not change due to WPP VRT controller. However, if the export cable fault is not severe the dynamic reactive current reference provided by the proposed CVCS scheme improves the dynamic voltage profile of the offshore AC grid compared to the case without CVCS.
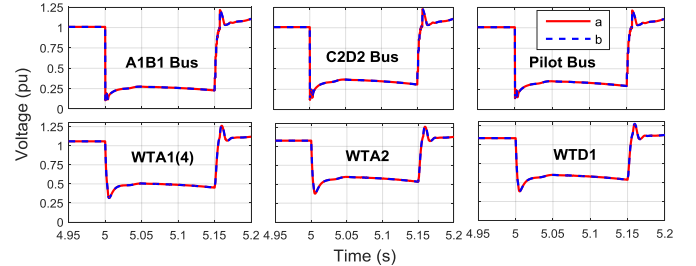

Fig. 16. Voltage at WT terminals for export cable fault at A1B1 collector substation. A). WT local VRT control, b). VRT control from WT and WPP Cluster
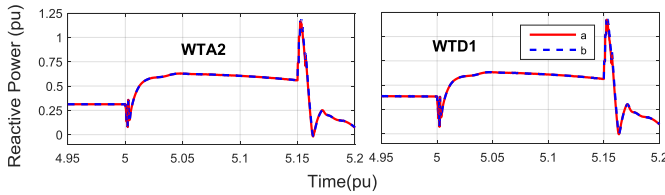
Fig. 17. WT Reactive power output for export cable fault.
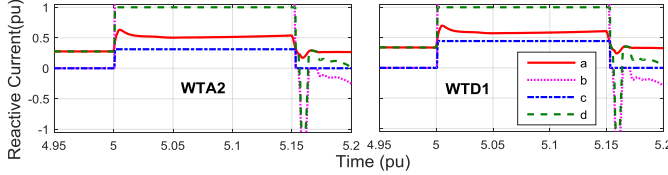a). WT VRT alone, b). VRT from WT and WPP cluster

Fig. 18. WT reactive current including the VRT from WT and WPP cluster.

a). iq_{base}^{WT} ,b). Δiq_{ref}^{WT} , c). $\Delta iq_{ref}^{WT-Pilot}$, d). iq_{cmd}

VI.   CONCLUSIONS

A coordinated voltage control scheme for an offshore AC grid with cluster of OWPPs, connected to HVDC system is proposed in this paper. The proposed CVC scheme improves both the steady state voltage profile (while minimizing the losses) and voltage ride through capability of the offshore grid. The effectiveness of the proposed CVC scheme to provide dynamic reactive power support has been demonstrated through faults applied at different locations of the offshore AC grid. The proposed CVCS considers the network sensitivity and therefore effectively and efficiently utilizes the available reactive power sources. It has also been shown that the proposed CVCS improves the voltage stability margin of the offshore AC grid. The voltage is controlled at the Pilot bus, whose reference is generated by an optimization algorithm aiming at minimum active power losses in the offshore AC grid, by sending reactive power reference to WPPs based on their available reactive power and participation factors. Participation factors ensure proper distribution of reactive power to each WPP and WTs within WPPs based on their voltage sensitivity with respect to the Pilot bus, which avoids excessive voltage rise at WTs located far from the AC collector substation.

VII.   REFERENCES

[1]   Windspeed 2015. [Online]. Available: http://www.windspeed.eu. [Accessed: 20- Dec- 2015].

[2]   M. Aragues Penalba, O. Gomis-Bellmunt and M. Martins," Coordinated Control for an Offshore Wind Power Plant to Provide Fault Ride Through Capability", *IEEE Trans. Sustainable Energy*, vol. 5, pp. 1253-1261, Sep 2014.

[3]   Oriol Gomis-Bellmunta, J. Liang, J. Ekanayake, R. King, N. Jenkins, "Topologies of multiterminal HVDC-VSC transmission for large offshore wind farms," *Electric Power Systems Research,* vol. 81, pp, 271-281, Feb 2011.

[4]   Z. Chen, J. Guerrero and F. Blaabjerg, "A Review of the State of the Art of Power Electronics for Wind Turbines," *IEEE Trans. Power Electronics*, vol. 24, pp. 1859-1875, Aug 2009.

[5]   Tennet TSO GmbH, *Requirements for Offshore grid Connections in the grid of Tennet TSO GmbH*, Germany, Dec. 2012, pp. 1–10.

[6]   Mohseni, M. and Islam, S.M, "Review of international grid codes for wind power integration: diversity, technology and a case for global standard," *Renewable and Sustainable Energy Reviews*, vol. 16, pp.3876-3890, Aug. 2012

[7]   Tsili, M. and Papathanassiou, "S. A review of grid code technical requirements for wind farms," *IET Renew. Power Generation*, vol. 3, pp. 308–332, Sep. 2009.

[8]   Z. Rather, D. Flynn, "Voltage Dip Induced Frequency Events in Wind Integrated Power Systems," *in Proc. 2015 9th IFAC symposium*, New Delhi, India.

[9]   ENTSO- E, *Draft- The Network Code on High Voltage Direct Current Connections (NC HVDC)*, Apr 2014.

[10]   Muljadi E, Samaan N, Gevorgian V, Li J, Pasupulati S., "Different factors affecting short circuit behavior of a wind power plant," *in Proc. 2010 IEEE Industry applications society annual meeting (IAS).,* p. 1–9.

[11]   R. Irnawan, K. Srivastava and M. Reza, "Fault detection in HVDC-connected wind farm with full converter generator," *International Journal of Electrical Power & Energy Systems,* vol. 64, pp. 833-838, Jan 2015.

[12]   C. Feltes, H. Wrede, F. Koch and I. Erlich, 'Enhanced Fault Ride-Through Method for Wind Farms Connected to the grid Through VSC-Based HVDC Transmission', *IEEE Transactions on Power Systems*, vol. 24, no. 3, pp. 1537-1546, 2009.

[13]   M. Mohammadi, M. Avendano-Mora, M. Barnes, et al., "A study on fault ride-through of VSC-connected offshore wind farms," *in Proc. 2013 IEEE Power and Energy Soc. General Meeting (PES)*, pp. 1–5.

[14]   [14] B. Silva, C. Moreira, H. Leite, J.A. Peças Lopes, "Control Strategies for AC Fault Ride-Through in Multi-terminal HVDC grids," IEEE Transactions on Power Delivery, vol.29, no.1, pp.395,405, Feb. 2014

[15]   S. Chaudhary, R. Teodorescu, P. Rodriguez, P. Kjaer and A. Gole, "Negative Sequence Current Control in Wind Power Plants With VSC-HVDC Connection," *IEEE Trans. Sustainable Energy*, vol. 3, pp. 535-544, May 2012.

[16]   J. I. Marvik and H. G. Svendsen, "Analysis of grid Faults in Offshore Wind Farm with HVDC Connection," *Energy Procedia*, vol. 35, pp. 81–90, Jan. 2013.

[17]   J. Fortmann, Wilch, M., F. Koch and I. Erlich, "A novel centralised wind farm controller utilising voltage control capability of wind turbines," *in Proc. 2008 IEEE Power System Computational Conference*, pp 1-8.

[18]   B. Karthikeya and R. Schutt, "Overview of Wind Park Control Strategies," *IEEE Trans. Sustainable Energy*, vol. 5, pp. 416-422, Jan 2014.

[19]   A. Hansen, P. Sørensen, F. Iov, and F. Blaabjerg, "Centralized power control of windfarms with doubly fed induction generators," *Renewable Energy*, vol. 31, pp.935-951, 2006.

[20]   *ABB. XLPE Submarine Cable Systems Attachment to XLPE Land Cable Systems,* User's Guide. 2010.

[21]   E. Muljadi et al. "Equivalencing the collector system of a large wind power plant", *in Proc. 2006 IEEE Power Engineering Society General Meeting.*

[22]   E. Muljadi et al. "Method of equivalencing for a large wind power plant with multiple turbine representation,"*in Proc. 2006 IEEE Power and Energy Society General Meeting,* pp-1-8.

[23]   *IEC 61400-27, Wind Turbines Part 27- 1: Electrical simulation models for wind power generation Wind turbine*, IEC Std. (CD) 88/424/CD Apr. 2015.

[24]   X. F. Wang, Y. Song and I. Malcolm, *Modern Power Systems Analysis, Springer Science*, Business Media, LLC, 2008.

[25]   P. Lagonotte, J. C. Sabonnadiere, J. Y. Leost, and J. P. Paul, "Structural analysis of the electrical system: Application to secondary voltage control in France," *IEEE Trans. Power Syst*., vol. 4, pp. 479–486, May 1989.

[26]   Yan Liu, "The Study on Hybrid Multi-Infeed HVDC System Connecting with Offshore Wind Farm," Aalborg University, Denmark, PhD thesis, 2015.

I.   BIOGRAPHIES

Jayachandra N. Sakamuri - (M'15) has received Master of Technology in electrical engineering from the Indian Institute of Technology, Kanpur, India in 2009. He also worked on his M.Tech thesis at Technical University of Berlin, Germany during 2008.   At present, he is working on his PhD on Coordinated control of wind power plants connected in offshore HVDC Grid. Before joining, PhD, he has worked as

Scientist at Grid System R&D, ABB Ltd for 3 years and also at Crompton Greaves Ltd as a Sr. Executive (R&D). His research interests include HVDC, Offshore WPPs integration and control, high voltage switchgear design.

Zakir Hussain Rather (M'11) received Industrial PhD in Power Systems from Aalborg University Denmark, Master of Technology (M.Tech) degree in Power Systems from Indian Institute of Technology (IIT) Delhi, India and Bachelor's degree in Electrical Engineering from Jammu University, India. He has experience of more than four years in power industry including KK wind Solutions, Denmark. He was working as Senior power system researcher at Electricity Research Centre, UCD, Dublin, Ireland. He is currently working as Assistant Professor at Indian Institute of Technology Bombay (IIT), India. His areas of research interest include grid integration of renewables, microgrids, power system security and stability, wide area measurement and control.

Johan Rimez - (M'11) was born in 1977 and received the M.Sc. degree in electro-mechanical engineering at the Vrije Universiteit Brussel (VUB), Brussels, Belgium in 2000. He's currently fully employed with Elia, the Belgian Transmission System Operator as Senior Expert. While working at Elia's, he has been a Freelance PhD Researcher at the Katholieke Universiteit Leuven (K.U.Leuven) as well from 2008 to 2014 when he obtained the PhD degree. His main interests are grid perturbations and dynamics, HVDC technology and its interaction with the AC network, wind power plants and network optimization.

Müfit Altin - ('S09-M1'3) received B.Sc. and M.Sc.degrees in electrical and electronics engineering from the Middle East Technical University (METU), Ankara in 2004 and 2008, respectively. He obtained his PhD degree from the Dept. of Energy Technology, Aalborg University, Denmark, in 2012, where he was employed as a researcher under the Vestas Power Programme during his PhD. Since February 2013, he has been a postdoc researcher at the Dept. of Wind Energy, Technical University of Denmark. His research interest includes grid connection of wind power, wind power plant control, power system modelling, and power system stability analysis.

Ömer Göksu - (S'07–M'13) received B.Sc. and M.Sc. degrees in EEE from the METU, Ankara, Turkey in 2004 and 2008, and was employed in Aselsan Inc. from 2004 to 2009. He obtained his PhD degree from the Department of Energy Technology, Aalborg University, Denmark, in 2012, under the Vestas Power Programme. In 2013, he was a research associate at the University of Manchester, UK. Currently, he is with the DTU Wind Energy. He works on wind energy control and modeling, integration of power electronics to power systems, and electrical motor drives.

Nicolaos A. Cutululis (M'07) was born in 1974. He received the M.Sc. and Ph.D. degrees in automatic control from the "Dunarea de Jos" University of Galati, Galati, Romania, in 1998 and 2005, respectively. He has been with Technical University of Denmark (former Risø) since February 2005 currently as Senior Researcher His main interest lies within wind power integration and control, , including power system control and stability, dynamic modeling and control of wind turbines and wind farms in offshore environment, and wind fluctuation statistics. He is the Danish representative in IEA WIND Task 25 and is active in CIGRE working groups.

J3 Jayachandra N. Sakamuri., Altin M, Hansen A.D., Cutululis N.A., "Coordinated Frequency Control from Offshore Wind Power Plants Connected to multi terminal DC System Considering Wind Speed Variation ", IET Rene. Power Generation, Special Issue: Active Power Control of Renewable Energy Generation Systems, Available Online Aug 2016

This page would be intentionally left blank if we would not wish to inform about that.

Coordinated Frequency Control from Offshore Wind Power Plants Connected to MTDC System Considering Wind Speed Variation

Jayachandra N. Sakamuri [1*], Müfit Altin [1], Anca D. Hansen [1,] Nicolaos A. Cutululis[1]

[1] Wind Energy Dept., Technical University of Denmark (DTU), Roskilde 4000, Denmark

[*]jays@dtu.dk

Abstract: A Coordinated fast primary frequency control (FPFC) scheme from offshore wind power plants (OWPPs) integrated to a three terminal high voltage DC (HVDC) system is proposed in this paper. The impact of wind speed variation on the OWPP active power output and thus on the AC grid frequency and DC grid voltage is analyzed. The removal of active power support from OWPP after the frequency control action may result in second frequency (and DC voltage) dips. Three different methods to mitigate these secondary effects are proposed, such as, (1) Varying the droop gains of the HVDC converter (2) Releasing the active power support from OWPP with a ramp rate limiter and (3) An alternative method for the wind turbine overloading considering rotor speed. The effectiveness of the proposed control scheme is demonstrated on a wind power plant integrated into a three terminal HVDC system developed in DIgSILIENT PowerFactory. The results show that the proposed coordinated frequency control method performs effectively at different wind speeds and minimizes the secondary effects on frequency and DC voltage.

1. Introduction

During recent years, the installation of offshore wind power plants (OWPPs) into power systems has been increased and it is expected to continue in the future [1]. The increased active power flow from OWPPs combined with long distances to the shore has encouraged the use of the voltage source converter (VSC) based HVDC transmission system to transfer power to the shore due to feasibility and economic reasons [2]. Therefore, Multi Terminal DC grids (MTDC) with VSCs may become a choice for future European offshore super grid [3]. The increased penetration of HVDC connected OWPPs results in reduced power system effective inertia due to their decoupling from the onshore AC grid [4]. This necessitates OWPPs to participate in frequency control. Therefore, two methods to replicate the onshore frequency at offshore AC grid, such as (1) Communication based and (2) Coordinated Control have been proposed in the literature [5]-[8]. The first method is based on communicating the onshore frequency to the

offshore station while the second method emulates the frequency through supplementary control blocks at HVDC stations. The coordinated control scheme is chosen in this paper due to the reliability issues with communication based method. Frequency control from WPPs connected through MTDC system has been addressed by [7],[9]. The impact of wind speed on the on the frequency control from WPPs has been addressed by [9]. The gains of the frequency controller of the wind turbine are optimized for different wind speeds ensuring an improved frequency control from WPPs over the whole wind speed range in [10]. However, the impact of release of active power support after completing fast primary frequency control from WPPs on the AC grid frequency and DC grid voltage and their mitigation methods have not been addressed.

Two methods for active power support from WPPs for frequency control have been reported in [10]-[12]. In first method, WT is operated at below maximum possible power thus creating some reserve power [11]. This method is opted when the frequency support is needed for extended period of time, e.g. primary or secondary frequency control. In second method, WT is overloaded above its possible power for certain duration thus providing active power support for fast primary frequency control [10], [12]. The need for FPFC has been reported in system framework operability report by National grid [13]. The increased penetration of HVDC connected OWPPs leads to lower system inertia resulting in higher rate of change of frequency (ROCOF). Due to higher ROCOF, particularly in case of large contingency, the frequency may dip to the lower nadir limit before the primary reserves start responding to the frequency event because of the time delay they needed to respond. To avoid this problem, it is essential that other faster reserves respond to the frequency event. Hence, a need for fast primary control reserves, which can act faster than primary reserves, has been emphasized in system framework operability report [13].

Hence, a coordinated fast primary frequency control from OWPPs integrated to a three-terminal HVDC system is proposed in this paper. By using such control scheme, the onshore frequency is replicated at offshore HVDC station through supplementary control blocks implemented at onshore and offshore HVDC stations. The WPP is overloaded to produce additional power for frequency support. The impact of different wind speeds on the WPPs active power output, hence, on the power system frequency and the DC grid voltage during and after the frequency support is studied. Three methods to mitigate the impact of second frequency and DC grid voltage dips after the frequency support are proposed. The first method is varying the

droop gains of the HVDC converter based on the wind speed forecast whereas the second method is based on smooth release of active power support from WPPs with a ramp rate limiter. The final method is using an alternative way of overloading the wind turbine which considers the effect of rotor speed on the overloading power output. The effectiveness of the individual and combination of the proposed methods is investigated based on simulations on a three-terminal HVDC system developed in DIgSILIENT PowerFactory. The paper is organized as follows. Section 2 describes the modeling of the Multi-Terminal HVDC system and OWPPs. The proposed method for frequency control from WPPs is discussed in section 3. The simulation results are presented in section 4, followed by concluding remarks in section 5.

2. Power System Model

The grid layout considered in this paper consists of 2 onshore AC grids (AC grid-2 and AC grid-3) and one offshore grid (AC grid-1) with OWPPs connected all together through a 3-terminal HVDC as shown in Fig.1a. A brief description of the simulation models for the onshore AC grid, WPP and the HVDC interconnection is given below.

2.1. Onshore AC grid Model:

The onshore AC grid-2 and AC grid-3 are modelled as a lumped synchronous machine with rated power of 5000 MVA and 2000 MVA respectively. Standard models and parameters for the governor, automatic voltage regulator and power system stabilizer have been developed according to [14]. This study is using the relevant parameters based on machine MVA base given in [10].

2.2. HVDC System Model:

A Multi-terminal HVDC interconnection based on three VSCs, modelled as an AC voltage source behind reactance, is shown in Fig.1a. It is based on symmetrical monopole configuration having same voltage with opposite polarity at the converter terminals. PowerFactory's built-in converter, π-model of the cable, and standard transformer models [15] have been used in this study. A brief description of the grid layout is summarized in Table-I of Appendix.

2.2.1 Onshore HVDC Converters

The Conv-2 and Conv-3 in Fig.1a are the onshore HVDC converter stations connected to AC grid-2 and AC grid-3 respectively. They are responsible for maintaining the power balance

in the DC system by keeping the DC voltage within the acceptable limits. The control block diagram for onshore HVDC converter is shown in Fig.1b. The onshore HVDC converter control consists of two main controllers: one for active power balance control (DC voltage – active power droop) and other for reactive power control. The sharing of active power imbalance between the onshore converters depends on the active power droop constant (k_p) of the $V_{dc} - P$ droop controller. This converter also controls the reactive power at converter bus through AC voltage droop ($Q - V_{ac}$) in order to maintain the AC voltage within specified range. The current references provided by the outer controllers are then handled by an inner current controller operating in $d - q$ reference frame. A supplementary frequency-active power droop ($f_{on} - P$) controller in the outer loop d-axis is responsible for modulating active power reference (P_{ref}) proportional to the onshore frequency deviation. This controller not only allows exchange of frequency support between the two onshore AC systems but also allows OWPPs to participate in frequency control. This loop contributes to the power system frequency regulation in coordination with a DC voltage-frequency droop controller ($V_{dc} - f_{off}$) at offshore HVDC converter, as depicted in Fig.1c, and active power controller of OWPP, shown in Fig.1d.
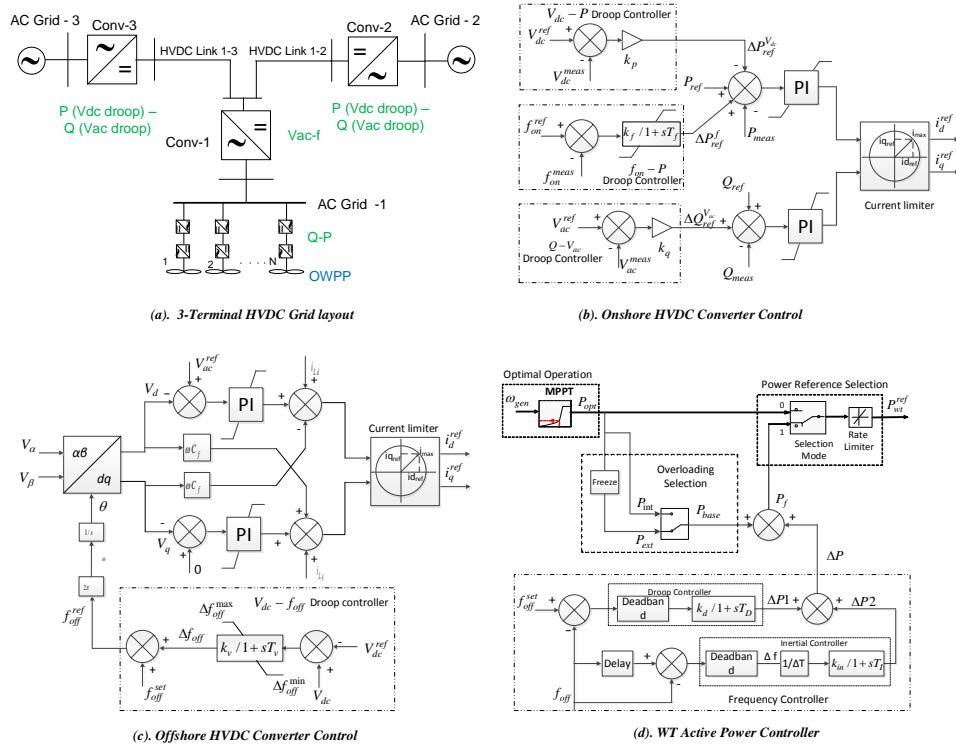

(a). 3-Terminal HVDC Grid layout

(b). Onshore HVDC Converter Control

(c). Offshore HVDC Converter Control

(d). WT Active Power Controller

Fig. 1 Coordinated frequency control scheme for an OWPP integrated to a 3-terminal HVDC system

2.2.2 Offshore HVDC Converter

The Conv-1 in Fig.1a is the offshore HVDC converter station connecting the OWPP to the MTDC system. It is responsible for controlling the voltage magnitude and frequency of the offshore AC network at the point of common connection (PCC) of the WPP, as shown in Fig.1c, and allows transferring the wind power output to the MTDC system. A DC voltage-frequency droop controller ($V_{dc} - f_{off}$) at the outer control loop changes the offshore AC grid frequency reference proportionally to the DC voltage deviation. This controller in coordination with active power controller of OWPP (Fig.1d) provides the active power support required for the frequency control of the AC grid.

2.3. Offshore Wind Power Plant Model:

The OWPP is modelled as an aggregated IEC Type-4 wind turbine (WT) based on the aggregation method given in [16]. The Type-4 WT model used in this study is based on generic approach proposed by the IEC Committee in Part 1 of IEC 61400-27 [17] for the short term power system stability studies. Additionally, this model is extended to include the dynamic features relevant for the study of the frequency control from WPPs [12]. The operation of active power controller of the WT comprising of four blocks, as shown in Fig.1d, is one of the important controller. The 'Optimal Operation' block tracks the optimal power point (P_{opt}) based on WT generator speed (ω_{gen}), thus generating maximum power point reference during normal operation. During overloading, it generates reduced power reference in proportion to ω_{gen}, particularly at below rated wind speeds. The 'Overloading Selection' block offers the option to choose from either External or Internal power reference, as described in section 3.3. The 'Frequency Controller' generates additional power reference (ΔP) to the WT based on variations in offshore frequency resulted due to coordinated frequency control action. The 'Power Reference Selection' block allows to choose between the output of the 'Optimal Operation' block (P_{opt}) during normal operation and frequency initiated power reference (P_f) during the frequency control period. The 'Rate Limiter' is used limit the rate of change of power reference to the WT. Further details of the operation of these sub blocks of WT active power controller is described in section 3.

3. Coordinated Frequency Control Scheme

In this paper, a coordinated offshore AC grid frequency modulation according to the DC grid voltage variation is proposed in order to represent the onshore AC grid frequency variations at offshore AC grid. In this method, the $f_{on} - P$ droop controller, shown in Fig.1b, modulates the active power reference (ΔP_{ref}^{f}) to the onshore HVDC converter according to the measured frequency deviation at the associated onshore AC grid. The relation between the modulated active power reference and frequency deviation is given in (1), where f_{on}^{ref} and f_{on}^{meas} are the reference and measured frequency at the onshore AC grid.

$$\Delta P_{ref}^{f} = k_f (f_{on}^{ref} - f_{on}^{meas}) \tag{1}$$

This leads to a deviation in the DC grid voltage from its initial value. Therefore, the other onshore HVDC converter inherently modulates its active power reference ($\Delta P_{ref}^{V_{dc}}$) due to $V_{dc} - P$ droop control action, thereby participates in frequency control. However, the OWPP doesn't detect the frequency event; hence mirroring onshore frequency deviation in the offshore AC network frequency is needed. The offshore HVDC converter detects this through the DC voltage variations. Therefore, the $V_{dc} - f_{off}$ droop controller at offshore HVDC converter, shown in Fig.1c, modifies the offshore AC grid frequency proportional to the DC voltage variation measured at its terminals. The relation between offshore AC grid frequency and DC voltage is given in (2),(3), where f_{off}^{set} is the offshore frequency during normal conditions and f_{off}^{ref} is the reference offshore frequency considering DC grid voltage variation.

$$f_{off}^{ref} = f_{off}^{set} + \Delta f_{off} \tag{2}$$

$$\Delta f_{off} = k_v \Delta V_{dc} \tag{3}$$

The power reference to the turbine (P_{WT}^{ref}) is then updated with the contribution ΔP from the 'frequency controller' (in Fig.1d), which consists of a combination of ΔP_1 and ΔP_2, where ΔP_1 is proportional to the frequency deviation from steady state value (Δf) and ΔP_2 is proportional to the time rate of change of frequency ($\Delta f / \Delta T$) as given in (4).

$$P_{WT}^{ref} = P_{base} + \Delta P_1 + \Delta P_2$$
$$\Delta P_1 = k_d (f_{off}^{set} - f_{off}), \Delta P_2 = k_{in} (\Delta f_{off} / \Delta T) \tag{4}$$

where, P_{base} is the base power output of 'Overloading Selection' block of WT active power controller. This value is either actual value of P_{opt} or its freezed value before overloading depending on the chosen overloading method (Internal or External) of the WT, as described in section 3.3.

In this work, short term overloading of the WT is considered for FPFC of the AC grid. Hence, the WT always operates at its optimal power output during normal operation and provides additional power above its optimal point during the FPFC period, according to the coordinated frequency control action explained before. However, the WT electrical power output depends on the magnitude and duration of this overload and also on the corresponding wind speed [12]. Above the rated wind speeds, the WT can continue to provide fixed amount of overloading power, for example 0.1pu, for extended duration by availing the aerodynamic power in the wind with the help of pitch control. However, at below rated wind speeds, if the overloading is continued for extended duration, the generator speed decreases with overloading due to difference in mechanical power input and electrical power output. The decrease in generator speed further decreases the WT output power, hit the lower speed limit and in worst cases may even lead to shutdown of the wind power plant. This phenomenon can be better understood from the overloading test performed on a typical 2 MW WT [12] at 0, 92 pu wind speed shown in Fig. 2a. During normal operating conditions (i.e. t<10s), WT output power is equal to its optimal output power (0.855pu). The overloading of the WT is initiated at t=10s by increasing its output power above its optimal value, which makes the WT generator to decelerate. The decrease in generator speed leads to the decrease of WT optimal output power subsequently reaching to zero when the speed becomes less than minimum speed (0.5 pu) at t=45s. Therefore, it is strongly recommended to limit the overloading duration to allow for the WT recovery. The results for shorter duration (10s) of overloading test on the same WT are presented in Fig.2b. The overloading of the WT is initiated at t=10s with the same magnitude as that of Fig. 2a (please note that X-Y scales are different in both figures) and released at t= 20s. It can be observed that the generator speed, hence, the optimal output power decreases with overloading, whose magnitude is same as that of Fig.2a. An abrupt change in WT output power can be observed once the overload is released at t=20s, as the WT follows the optimal value after the overloading period. The WT stars to recover and increases its output power after the overloading period and reaches to its pre-overloading operating point after few seconds.

However, the abrupt change in WT output power may cause negative impacts on associated DC grid voltage and AC grid frequency, if the overloading of the WT is initiated for FPFC of the power system. Hence, this abrupt change of the WT output power and the associated impact on the DC and AC grid should be addressed.
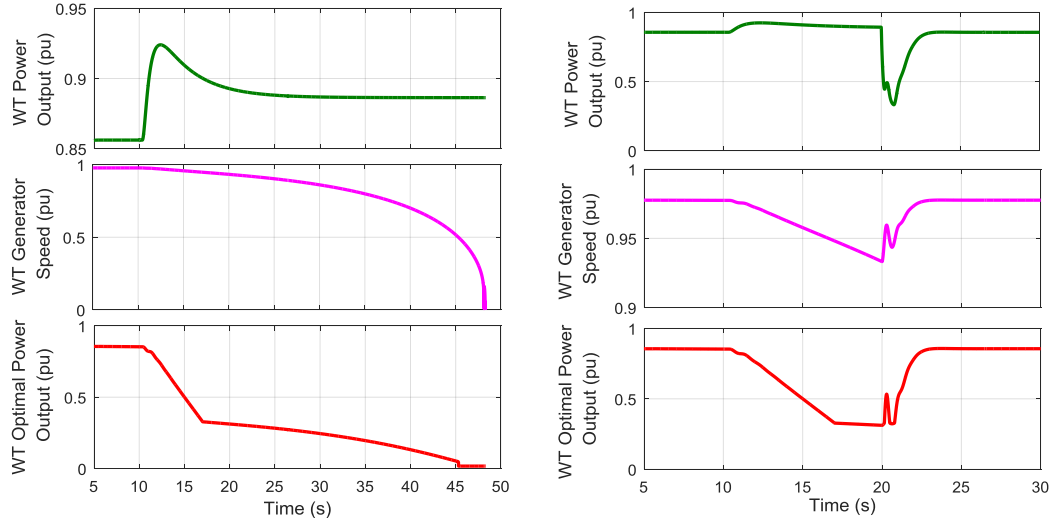

Fig. 2 (a) Extended overloading test of WT   (b): Overloading test for 10s

In this paper, three options to mitigate these impacts are investigated and presented in the following sub-sections:

- Varying the droop gains of the HVDC converter
- Releasing the active power support from OWPP with a ramp rate limiter and
- An alternative method for the wind turbine overloading considering rotor speed

These three methods are presented in sub section 3.1, 3.2, and 3.3 respectively.

3.1. Varying the droop gains of the HVDC converter

This method is based on adjusting the active power support for frequency control from the other HVDC converters in the DC grid, according to wind speed, compared to OWPP.

If the wind speed is more than the rated value, additional aerodynamic power can be availed by controlling the pitch angle during the overloading period; hence, the generator speed and WT optimal output power remain unchanged. Therefore, the WPP can take over the major share of active power support for fast primary frequency compared to the other HVDC converters in the DC grid. This can be achieved by adjusting the droop gain 'k_v' of the

'$V_{dc} - f_{off}$'droop controller of the offshore HVDC converter in Fig.1c or the droop gain 'k_d'of the frequency controller of the WPP shown in Fig.1d or combination of the both. During above rated wind speeds, overloading of a WPP can be extended until other primary/secondary frequency operating reserve in the associated AC grids is activated to take over the responsibility of frequency control, thus relieving the WPP from overloading. Since, during high wind speeds the additional power output is extracted from the aerodynamic power compared to WT kinetic energy, the release of overload on the WPP has less impact on the generator speed and WT optimal output power resulting in minimal reduction of its actual output power post-overload period. The major challenge, however, lies at below rated wind speeds where the dynamics of the WT are largely affected by the magnitude and duration of WT overload, as the additional power is supplied from the WT kinetic energy. In such cases, other AC grids connected through HVDC converters may contribute a major share of active power support for frequency control compared to the WPP thereby minimizing the overloading (for frequency control) of the WPP. This can be achieved by adjusting the droop gain 'k_p' of the $V_{dc} - P$ droop controller of the other HVDC converters in the MTDC grid. These gains can be adjusted in advance based on the available wind speed forecast. Also, this gain scheduling may be coordinated between the associated Transmission System Operators (TSOs) of the HVDC converters of the MTDC grid.

3.2. Releasing the active power support from OWPP with a ramp rate limiter

This method is based on smooth release of active power from OWPP, instead of abrupt release, by using a Ramp Rate Limiter. The Ramp Rate Limiter (RL) is used to limit the rate of rise of the power reference to the WT in case of normal and overloading conditions and also the rate of power decay after release of overload. The abrupt change in the WT output power after the overloading can be minimized by releasing the overload using a ramp rate limiter inside the 'Power Reference Selection' block of the WT active power controller shown in Fig.1d. The impact of ramp rate limiter on the WT active power output and generator speed of the WT following the release of overload can be well understood by analyzing the WT dynamics, for with and without considering RL, as shown in Fig. 3a. In both the cases, where equal overloading power magnitude (ΔP_{OL}) and overloading duration (T_{OL}) is considered, generator speed (ω_{gen}) and optimal output power (P_{opt}) decreases during the overload. It can be observed

that the magnitude and rate of power drop after overloading (ΔP_{AOL}) is predominant without the RL. The sudden power drop after the release of overloading may create negative impact on the DC grid voltage and AC grid frequency if no mitigation methods are in place. The release of WT overloading with RL results in smooth power transition and reduced magnitude of ΔP_{AOL}. This relieves the stress on the other HVDC converters. However, the inclusion of RL leads to increased recovery period T_{rec}. Hence, the selection of rate of release value is a compromise between ΔP_{AOL} and T_{rec}.

3.3. An alternative method for the wind turbine overloading considering rotor speed

In this section, an alternative method for overloading the WT for short term overloading application is proposed considering the rotor speed variations during the overload. Two different possible methods to select the base power reference (P_{base}) in the active power controller, shown in Fig.1d, for the WT overload are investigated. Two different WT overloading options for frequency control, with and without considering the impact of rotor speed, have been proposed and tested in [18]. However, constant power overloading for a fixed duration irrespective of the magnitude of frequency event and wind speed has been considered. Also, in this paper [18], there are no solid conclusions on the suitable option for the short term overload and the study is limited to one particular wind speed which did not consider the effect of overloading on the dynamics of the WT. In this paper, the two methods given in [18] are modified to consider the impact of magnitude of frequency event during the overloading period. Moreover, the impact of these two methods on the dynamics of the WT and also on the DC grid voltage and AC grid frequency during the release of overload is studied in detail and the selection of suitable method for short term overloading is proposed. These two methods differ in selecting the base power reference (P_{base}) for overloading the WT during frequency control. In Method-1, called as "External method", P_{base} is equal to the WT output power before the frequency event, i.e. freezing the value of the output of the 'Optimal Operation' block. In Method-2, called as "Internal method", P_{base} is equal to the actual output power of the 'Optimal Operation' block (P_{opt}), which decreases with overloading during frequency support at below rated wind speeds. The principle of these two methods is depicted in Fig.3b showing the frequency initiated power reference to the WT (P_f), WT optimal power, and generator speed for the same ΔP at below

rated wind speed. It can be observed that External method does not consider the impact of reduction of generator speed (hence rotor speed) and the WT optimal output power on the power reference to the wind turbine during the overload while Internal method does consider. This results in a higher frequency initiated power reference to the WT with External compared to Internal method assuming constant and equal ΔP in both methods. Therefore, the magnitude of power drop after the overload (ΔP_{AOL}) is lesser, hence lesser T_{rec} with the Internal method compared to External method. In case of above rated wind speeds, the additional energy from the wind can be utilized by changing the blade pitch angle during the overloading period, hence, generator speed and optimal power do not alter much. Hence, this study is more focused on the behavior of WT at below rated wind speeds.

It is difficult to conclude on which method is feasible, as it mainly depends on the particular application and required performance, i.e. faster and higher overloading power with the External method or shorter T_{rec} and smaller power drop (ΔP_{AOL}) after overloading with the Internal method. The impact of these two methods on the frequency and DC grid voltage is studied and also recommendations on the suitable method are made in section 4.2.3
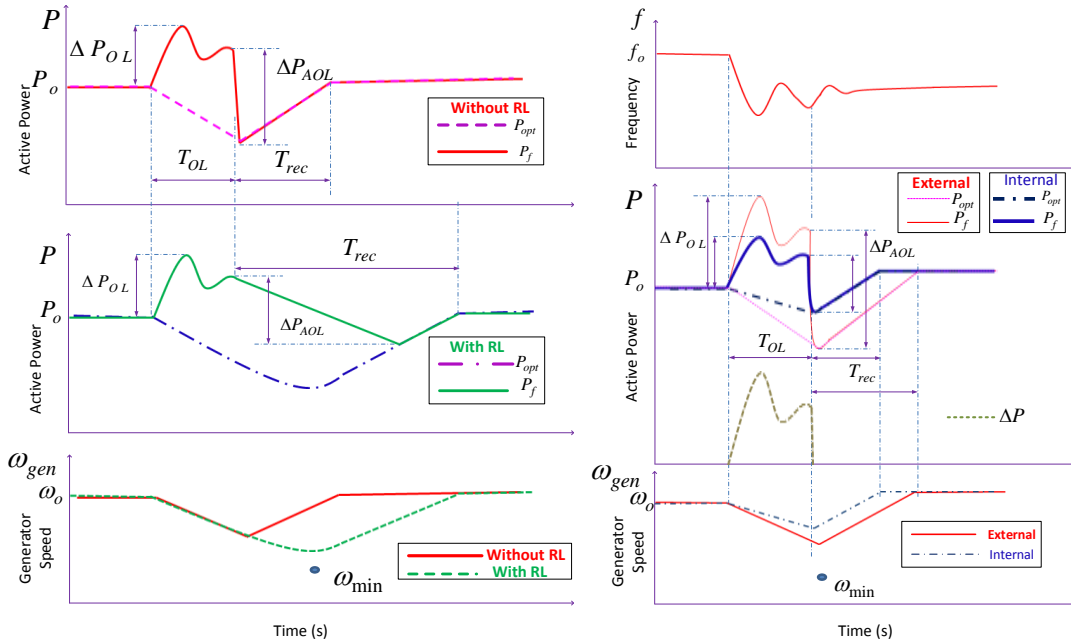

Fig 3. WT dynamics for (a) With/without WT Rate Limiter(RL) method   (b). External and Internal Overloading

4. Analysis of Simulation Results

In this section, the simulation results for the coordinated fast primary frequency control from OWPP and AC grid-2 for an under frequency event due to a 10% increase in load at AC grid-3 are presented. The study is performed at two different wind speeds. The results for above rated wind speeds (1.1 pu) are given in section 4.1, and for just below rated wind speed (0.9 pu) in section 4.2. In both cases, AC grid-2 and OWPP supply active power to AC grid-3. The magnitudes of power flow for each study case is given in Table II of Appendix. The positive sign of the active power indicates converter supplying power to the DC grid and vice versa for the negative sign. All the quantities are given in pu with the base values given in Table III of Appendix. The impact on the frequency and DC voltage due to power drop from OWPP after the release of overloading and their mitigation methods are studied.

4.1. Above Rated Wind Speed (1.1 pu):

An under frequency event is created at time, t = 10s at AC grid-3. The frequency of AC grid-3 is presented for three test cases (1) Without Coordinated Control, (2) Coordinated Control from AC grid-2 only, and (3) Coordinated Control from AC grid-2 and OWPP. The OWPP is overloaded for 10s (from t = 10s to t = 20s) to provide active power support for frequency control. The control parameters of the system under study are given in Table IV of the Appendix. External method of overloading the WT presented in section 3.3 has been used to generate the additional power reference (ΔP) and the overloading is released instantaneously (i.e. without rate limiter). The frequencies of three AC grids (including OWPP), active power and DC voltage of the three HVDC converters are given in Fig.4.
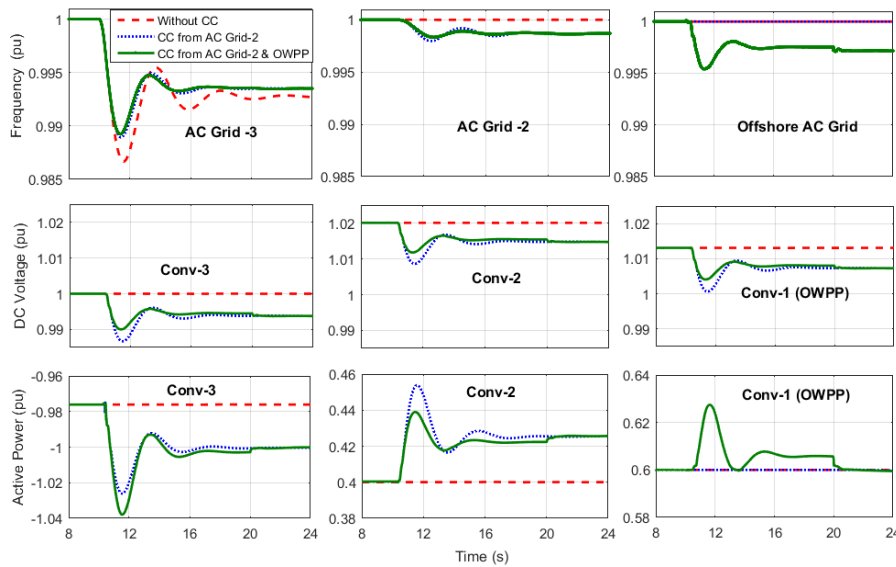
It can be observed form Fig.4 that the AC grid-3 frequency is improved with the coordinated control (CC) from AC grid-2 (dotted line) compared to without CC (dashed line). The frequency of AC grid-3 is further improved with the CC from both AC grid-2 and OWPP (solid line). It should be noted that the AC grid-2 frequency also gets affected due to its participation in the coordinated frequency control. However, the OWPP participation in frequency control together with AC grid-2 relieves the burden on the AC grid-2 thereby improving its frequency. Also, participation of OWPP in frequency control improves the DC grid voltage profile. It can also be observed that at the end of the frequency support from WPP, i.e. at t = 20s, the active power output of the OWPP reaches its pre-overloading value. The reason is because of increased aerodynamic power by changing the pitch angle which keeps the P_{opt} and generator speed (ω_{gen}) at maximum value even during the overload. This leads to minimum reduction of the WT output power after the overloading, in turn causing less impact on DC and AC grids. The WT dynamics are not shown here because they are not creating negative impact on frequency and DC voltage after release of WT overloading.

4.2. Just Below the Rated Wind Speed (0.9 pu):

The impact of overloading the WT for frequency control at just below the rated wind speed (0.9 pu) is shown in Fig.5.
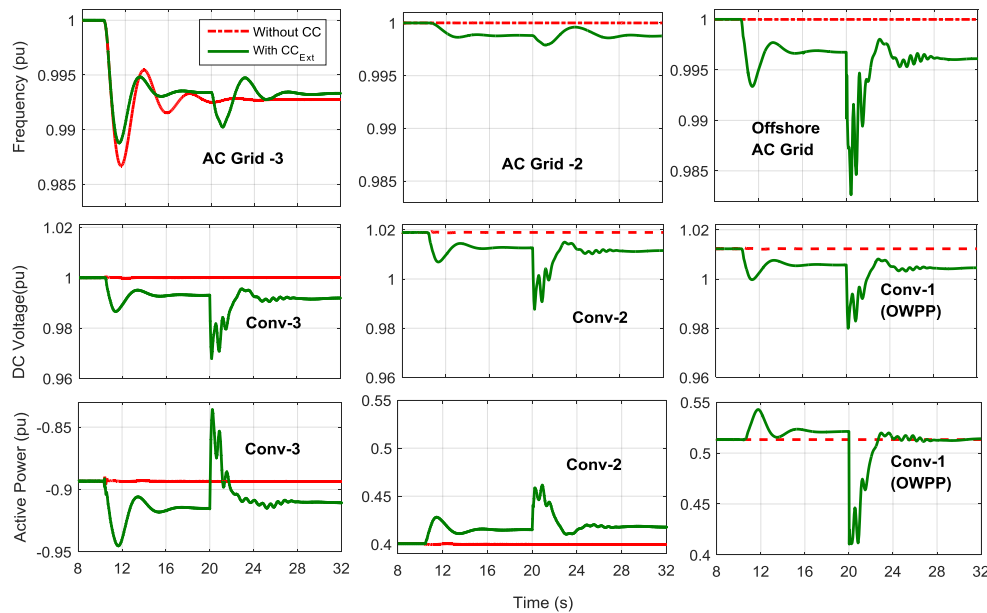
The External method of overloading the WT without the rate limiter is considered for the study as a first step. The control parameters for the study are given in Table IV of Appendix. It can be observed from Fig.5 that the frequency of AC grid-3 is improved during the overloading period (up to t= 20s). However, the output power from OWPP decreases rapidly after the release of overload, causing sudden power imbalance in the AC and DC grids, which leads to second frequency and DC voltage dips. The reason for sudden power drop from WT (hence OWPP) can be understood by its dynamics given in Fig.6. As the pitch is already at it optimal position, the decrease in WT speed due to overloading decreases the aerodynamic power and the optimal power (P_{opt}). This study indicates that there is a need for TSOs to plan for additional power reserves to balance the AC and DC grids, which involve additional costs. Hence, the impact of the three options to mitigate second frequency and DC voltage dips proposed in section 3 are investigated in the following sub sections. In all the cases, the results are compared with the standard test case given in Fig.5 and Fig.6 (External method without RL).
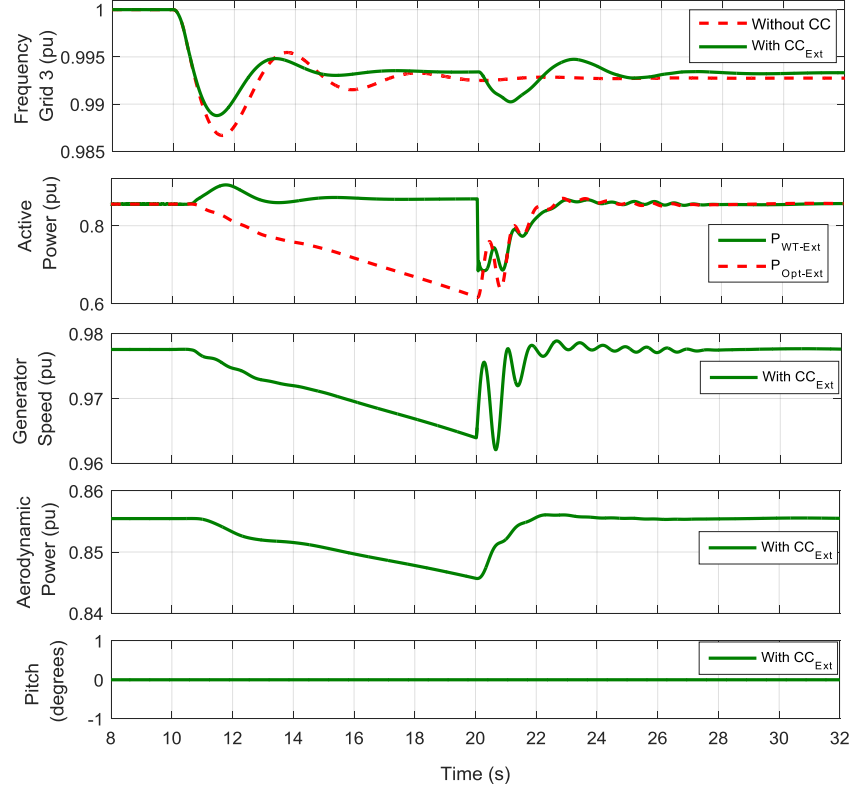
Fig. 6. AC grid-3 frequency and WT dynamics at Vw=0.9 pu- with CC from OWPP (External overloading without rate limiter).

4.2.1 *Varying the droop gains of the onshore HVDC converters*

As the active power output of the WPP drops significantly with the overloading, particularly at below rated wind speeds, the other AC grid (i.e.AC grid-2) associated to MTDC grid may take over the major share of frequency control. This can be achieved by changing the value of active power droop constant (k_p) of the $V_{dc}-P$ droop controller of HVDC Conv-2. The simulation results by varying the 'k_p'of the HVDC Conv- 2 from 2 to 8 while keeping the remaining parameters same as base case as per Table IV of Appendix is given in Fig.7. It can be observed that the problem of second dip in AC grid-3 frequency and DC grid voltage are minimized by increasing the k_p (in turn increasing the active power contribution for frequency control). In operations, the magnitude of k_p can be set in advance for, e.g. the next operating hour, based on the wind speed forecast as per the frequency control agreement between TSOs.
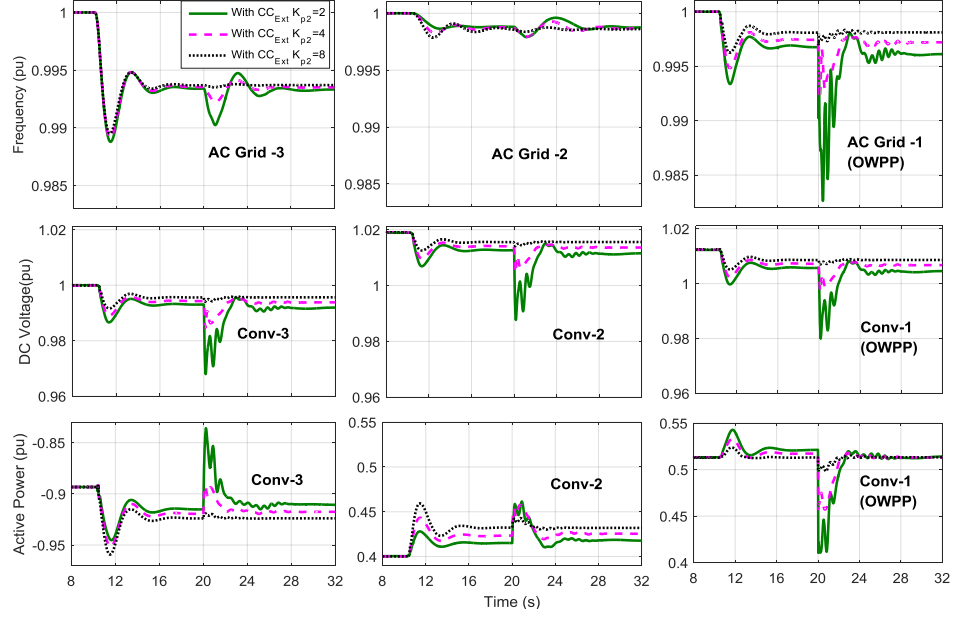
Fig. 7. Impact of varying Conv-2 droop gain on AC grid-3 frequency at wind speed Vw= 0.9 pu (WPP-External overloading without rate limiter)

One of the possible limitation of the proposed method is the inaccurate wind speed forecast may mislead the estimation of the droop gains for the onshore HVDC converters, OWPP and its associated offshore HVDC converter. Higher droop gains for offshore HVDC converter (k_v of $V_{dc} - f_{off}$ droop controller) and OWPP (k_d of frequency controller) at just below rated wind speed results in increased overloading of the OWPP, which can lead to higher power drop after the overloading period. Hence, adapting the minimum possible set of droop gains for the full range of operating wind speeds may minimize the risk. For example, the wind profile may be divided into three ranges, such as, low wind speed range (0.5 to 0.7 pu), medium wind speed range (0.7 to 1 pu) and high wind speed rage (above 1 pu) and one set of optimized droop gains for the HVDC converters and OWPP can be selected for each speed range. This is a trade-off between higher accuracy and risk.

4.2.2 Impact of ramp rate limiter while releasing WT overload

The effect of WT ramp rate limiter (with a rate of release equal to -0.02 pu/s) on the WT dynamics during the release of overload is shown in Fig.8. The results are compared with standard test case (i.e. External method without RL). It can be observed that the magnitude and rate of power reduction from the WT after the overload is small with the ramp rate limiter option, resulting in smoother WT dynamics (speed, optimal power and aerodynamic power). This leads

160

to reduced magnitude and rate of secondary frequency dip (AC grid-3) after the release of frequency support from OWPP, shown in Fig.8. The frequency of the three AC grids, DC voltage, and active power of the HVDC converters highlighting the impact of WT RL is shown in Fig.9. It can be observed that the magnitude and rate of second frequency and DC grid voltage dips are better with the RL option.
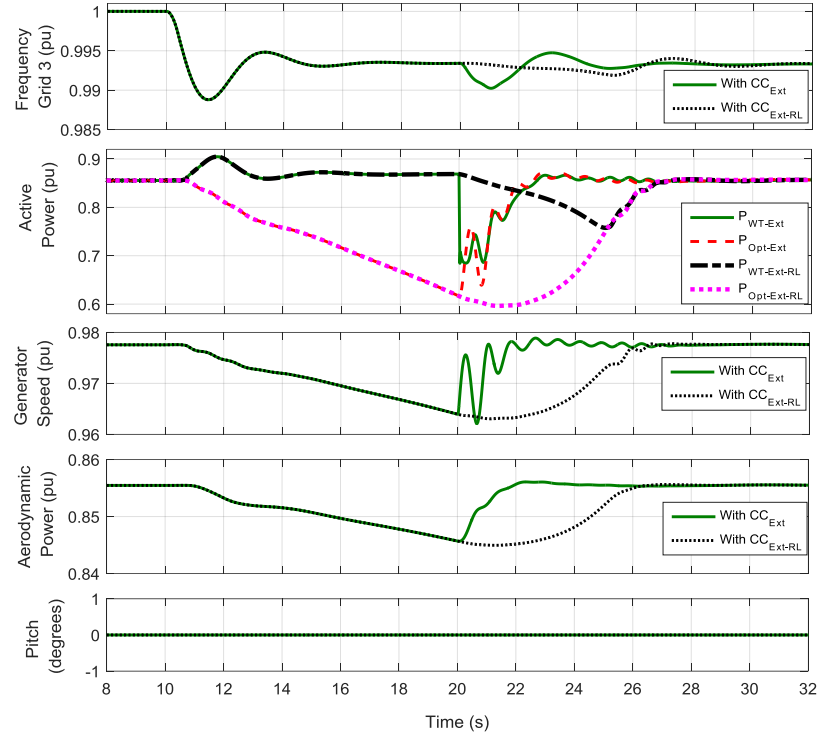
Fig. 8. Impact of Rate Limiter on WT dynamics at Vw=0.9 pu- with CC from OWPP - External overloading with (Ext-RL) and without rate limiter (Ext).

The limitation of this method is the selection of the magnitude of rate limiter itself. The higher the slope of the rate limiter, higher the power drop after overload and lower the recovery period, and vice versa. Slower recovery will reduce the stress on the mechanical parts of the WT. This also relieves the stress on the other HVDC converters in the MTDC grid, thereby minimizing the transients in the HVDC converters due to their sudden rise in output power. However, faster recovery of the WT is required to make it ready for the next frequency event. The selection of magnitude of rate limiter is a trade of between WT recovery period and rate and magnitude of power drop post-overloading period.

161
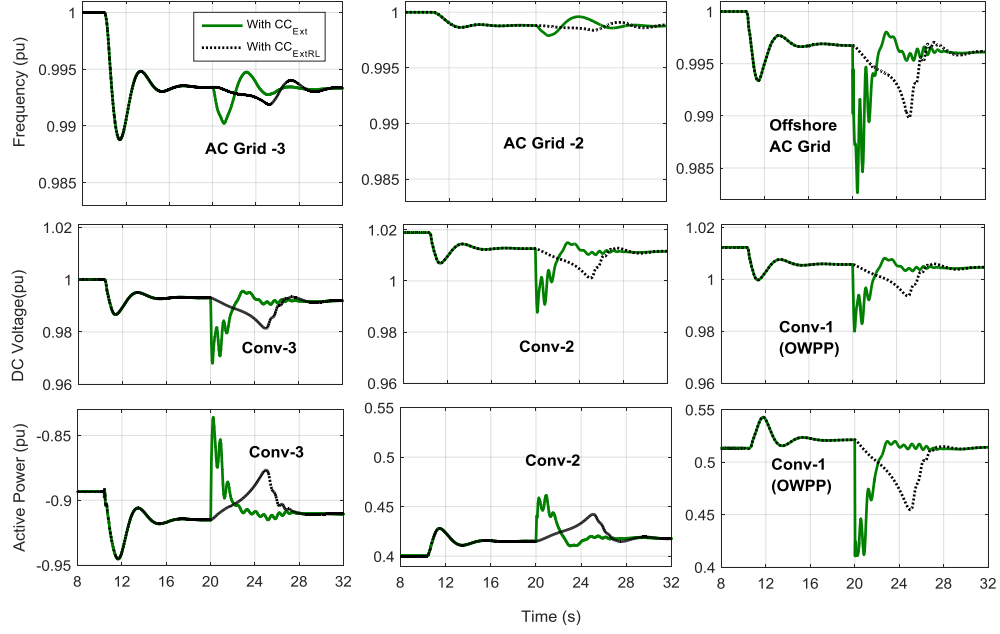
Fig. 9. Impact of Rate Limiter on AC grid-3 frequency and DC voltage - External overloading with (Ext-RL) and without rate limiter (Ext) at wind speed Vw= 0.9 pu

4.2.3 Impact of Method of Overloading the WT (Internal Vs External)

The WT dynamics and the frequency, DC voltage and active power of three terminal HVDC grid, highlighting the advantage of Internal method over External method of overloading, is shown in Fig.10 and Fig.11 respectively. As explained in section 3.3, the Internal method allows recovery of WT during the overload, which results in better dynamics of WT as shown in Fig.10. Therefore the problem of second frequency and DC voltage are minimized with Internal method compared to External method as shown in Fig.11.

Fig. 10. Impact of Method of WT overloading on WT dynamics at Vw=0.9 pu- with CC from OWPP -Internal (Int)/External (Ext) overloading without rate limiter.
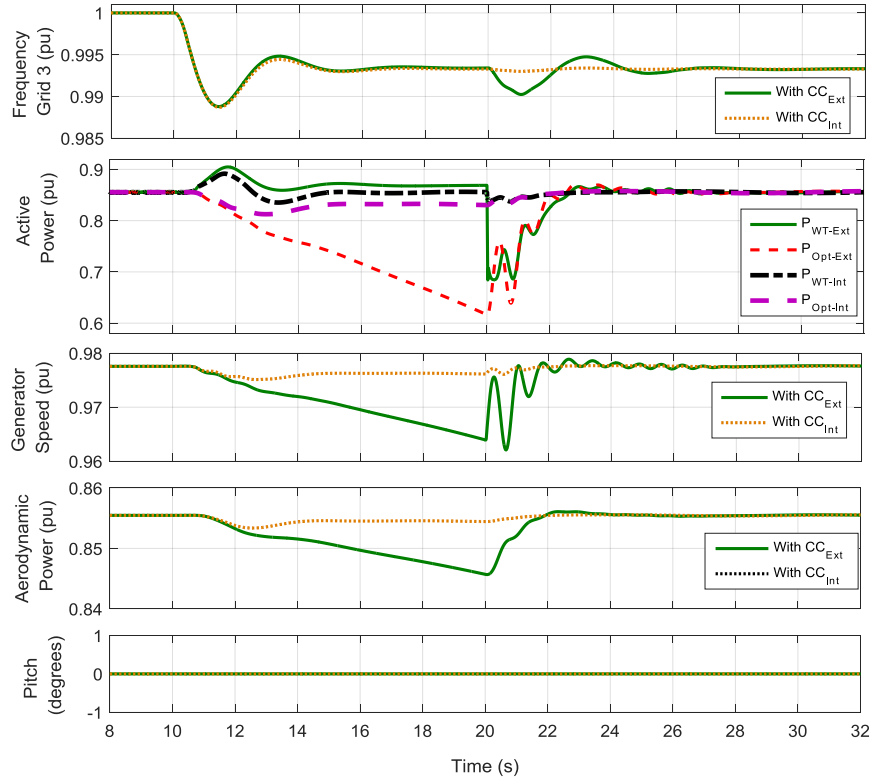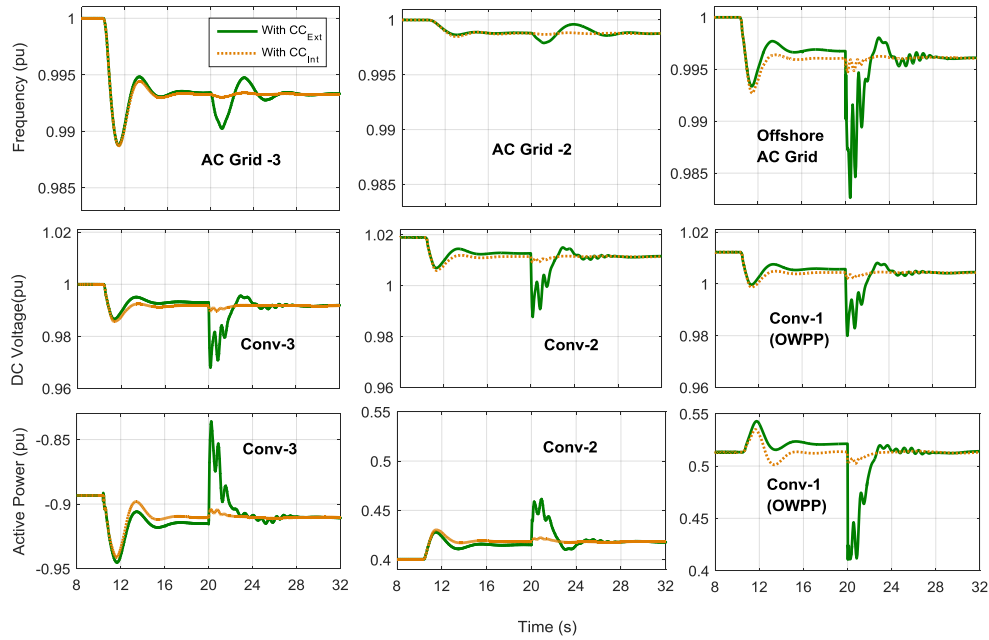

Fig. 11. Impact of Method of overloading on AC grid-3 frequency and DC voltage - Internal (Int)/External (Ext) overloading without rate limiter at wind speed Vw= 0.9 pu

The challenge lies in the selection of an overloading method with the best possible results, which actually depends on the frequency control requirement and wind speeds. For above rated wind speeds, the additional energy in the wind can be availed by changing the pitch angle during the overload, hence, the WT speed and optimal power do not alter much. Hence, there will be minimum difference between the results for Internal and External overloading methods in case of frequency control at above rate wind speeds. However, at below rated wind speeds, the selection of overloading method depends on the duration of frequency control window. The Internal method of overloading is the best option for fast primary frequency control where the overloading is limited to few seconds and the recovery of the WT starts during the overload. Moreover, this characteristic permits to yield higher kinetic energy from the WT by increasing the droop gains of OWPP, in case of Internal overloading method. Hence, Internal method provides better frequency control while minimizing the secondary effects on AC grid frequency and DC grid voltage. In case of extended frequency support (primary/secondary frequency control) and for application which involves guaranteed magnitude of power support from WT, selection of External method is suitable compared to Internal method. However, for this application, WT must have the reserve power at all wind speeds to avoid risk of the WT shutdown.

4.3. Design of controllers and stability of the test system

The onshore HVDC converter controller, shown in Fig 1b, is designed based on the references [19]- [21], while the offshore HVDC converter controller, shown in Fig 1c, is based on the references [22],[23]. All the controllers in the paper are tuned according to Internal Model Control (IMD) technique provided in [24],[25]. The DC voltage droop ($V_{dc} - P$) parameters of the test system in Fig 1a are designed according to the method proposed by [26] and the frequency droop ($f_{on} - P$) controllers are designed considering less than 2 % change in DC voltage due to frequency change. However, in actual, frequency droop parameter depends on the required active power support for frequency control of the associated AC grid, which depends on the grid code of the associated AC grid.

It would be interesting to study the stability of the proposed test system, shown in Fig.1a, including the impact of different controller (outer and inner) parameters, different droops ($V_{dc} - P$, $f_{on} - P$, and $V_{dc} - f_{off}$ of Fig.1) and WPP active power control parameters. However, detailed

theoretical analysis for such a non-linear system with multiple droops is challenging and is considered for future work.

However, an initial small signal stability analysis has been performed on the 3-terminal HVDC test system (including their associated synchronous machines and OWPP) shown in Fig.1a having the parameters in the Appendix. The corresponding Eigen values are shown in the Fig.12 below.
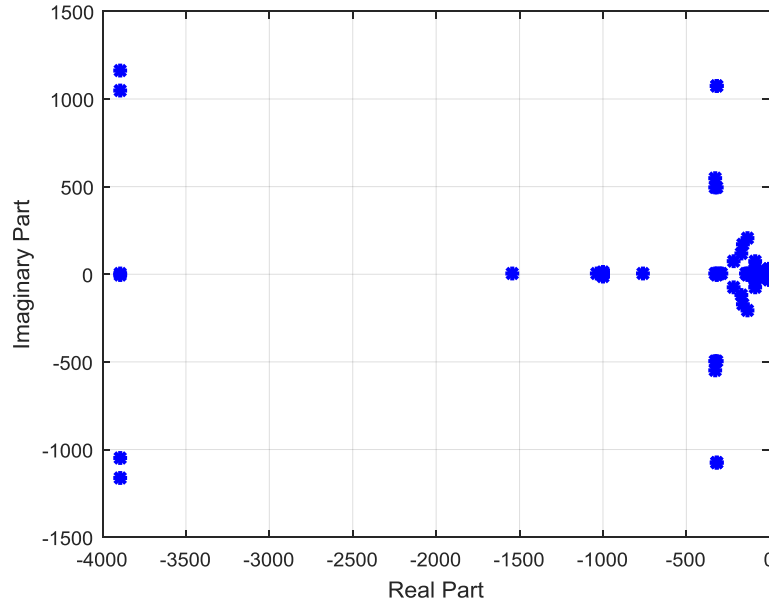
Fig.12 Eigen value pattern of the test system in Fig. 1a

It can be observed that the system is small signal stable. However, the impact of parameter sensitivities of outer (active power, AC voltage, reactive power) and inner controllers (current), different droops in the MTDC system on system stability is considered for future work.

5. Conclusions

In this paper a coordinated control scheme for fast primary frequency control from an OWPP connected to a MTDC system has been presented. The coordination is needed between onshore AC grid and OWPP to replicate the onshore frequency variations at offshore grid and to mitigate the secondary effects of OWPP participating in frequency control. The impact of wind speed on the dynamics of the wind turbine, hence on the active power output for frequency control has been investigated. The problem of second frequency (and DC voltage) dip after the

release of active power support for frequency control, particularly at below rated wind speed, is identified. Three options to mitigate these problems, such as varying the droop gains of HVDC converter, application of ramp rate limiter, alternative method of overloading the wind turbine considering rotor speed have been proposed and investigated. In the first method, the droop gains of the HVDC converter can be set in advance according to the wind speed forecast. However, the exact droop gains have to be coordinated with the associated TSO. The ramp rate limiter on the WT ensures smoother dynamics of the WT during the release of overloading which partially helps to mitigate the secondary effects on frequency and DC grid voltage. Smoother dynamics may result in reduced stress on the mechanical parts of the WT. The overloading method of the WT, which considers the variation of rotor speed and hence the actual power output during the overload, helps to minimize the secondary effects. The combination of this overloading method and the ramp rate limiter further helps to minimize the secondary effects of frequency control from offshore wind power plants and seems to be the best option if the objective is to minimize or even eliminate the second frequency dip.

6. References

[1] Windspeed 2015. [Online]. Available: http://www.windspeed.eu. [Accessed: 30- Apr- 2016].

[2] Gomis-Bellmunta, O., Liang, J., Ekanayake,J. et al.: 'Topologies of multiterminal HVDCVSC transmission for large offshore wind farms', Electr. Power Syst. Res., 2011, 81, pp. 271–281

[3] D. Van Hertem, M. Ghandhari , "Multi-terminal VSC HVDC for the European Supergrid: Obstacles," Renewable and Sustainable Energy Reviews, vol 14, pp 3156–3163, Dec 2010

[4] ENTSO- E, Draft- The Network Code on High Voltage Direct Current Connections (NC HVDC), Apr 2014.

[5] S. Nanou, S. Papathanassiou,"Evaluation of a communication-based fault ride-through scheme for offshore wind farms connected through high-voltage DC links based on voltage source converter," IET Rene. Power Generation, , pp. 1-10, Jan 2015.

[6] Y. Phulpin,"Communication-free inertia and frequency control for wind generators connected by an HVDC link," IEEE Trans on Power Systems, vol. 27, pp. 1136-1137, May 2012.

[7] Silva, B., Moreira, C.L.,Seca, L. et al.: 'Provision of inertial and primary frequency control services using offshore multiterminal HVDC network', IEEE Trans.Sustain. Energy, 2012, 3, pp. 800–808

[8] Adrià Junyent-Ferré, Yousef Pipelzadeh, Tim C. Green, "Blending HVDC-Link Energy Storage and Offshore Wind Turbine Inertia for Fast Frequency Response", IEEE Trans. on Sustainable Energy, vol. 6, pp. 1059-1066, July 2015.

[9] Sanz, I.M., Chaudhuri, B., Strbac, G. 'Inertial response from offshore wind farms connected through DC grids', IEEE Trans. Power Syst., 2015, 30, pp. 1518–1527

[10] Sakamuri, J.N., Das, K., Tielens, P. et al.: 'Improved frequency control from wind power plants considering wind speed variation'. Proc. 2016 IEEE Power System Computation Conf., June 2016

[11] K. V. Vidyanadhan and N. Senroy, " Primary Frequency Regulation by Deloaded Wind Turbines Using Variable Droop," IEEE Transactions on Power Systems, vol. 28, , pp. 837-846, May 2013.

[12] Hansen, A.D., Altin, M., Margaris, I.D. et al.: 'Analysis of short-term over production capability of variable speed wind turbines', Renew. Energy, 2014, 68, pp. 326-336

[13] National grid, System Operability Framework (SOF) 2014.

[14] P. Kundur, "Power system stability and control", 4th edition, McGraw-Hill 1994, New York.

[15] Sakamuri, J.N., Altin, M.,Hansen, A.D. et al.: 'Coordinated control scheme for ancillary services from offshore wind power plants to AC and DC grids'. Proc. 2016 IEEE PES General Meeting, July 2016

[16] E. Muljadi et al. "Method of equivalencing for a large wind power plant with multiple turbine representation," Proc. 2008 IEEE Power and Energy Society General Meeting, pp-1-8.

[17] Electrical simulation models for wind power generation Wind turbine, IEC 61400-27-1, 2015.

[18] S.Wachtel, A.Beekman, "Contribution of Wind Energy Converters with Inertia Emulation to frequency control and frequency stability in power systems," Proc. 2009 8th Wind Integration Workshop, pp.1-6

[19] T. K. Vrana, Y. Yang, D. Jovic, S. Dennetière, J. Jardini og H. Saad, "The Cigre B4 DC Grid Test System", Electra 270, pp. 10-19, October 2013.

[20] J. Beerten and R. Belmans, "Analysis of Power Sharing and Voltage Deviations in Droop-Controlled DC Grids," IEEE Transactions on Power Systems, vol. 28, no. 4, pp. 4588-4597, 2013.

[21] A. Egea-Alvarez, A. Junyent-Ferré, and O. Gomis-Bellmunt, "Active and reactive power control of grid connected distributed generation systems," in Modeling and Control of Sustainable Power Systems, L. Wang, Ed. Berlin, Germany: Springer-Verlag, 2012, ser. Green Energy and Technology, pp. 47–81.

[22] A.Yazdani and R.Iravani, "Voltage Source Converters in Power Systems". John Wiley & Sons, March 2010. ISBN: 978-0-470-52156-4.

[23] M. Delghavi and A.Yazdani, "A control strategy for islanded operation of a distributed resource (DR) unit," In Proc. 2009 IEEE Power and Energy Society General Meeting, Alberta, Canada, pp: 1-8.

[24] Lennart Harnefors and Hans-Peter Nee, "Model-based current control of ac machines using the internal model control method", IEE Transactions on Industry Applications, Vol. 34, No. 1, January/February, 1998.

[25] M. Shamsuzzoha and Moonyong Lee, "IMC-PID controller design for improved disturbance rejection of time-delayed processes", Ind. Eng. Chem. Res. Vol.46, pp-2077-2091, 2007.

[26] Rault Pierre, "Dynamic Modeling and Control of Multi-Terminal HVDC Grids " Ph.D thesis, University of Lille Nord de France, 2014.

7. Appendix

TABLE I : DESCRIPTION OF THE GRID LAYOUT IN FIG. 1

Parameter	Value	Unit
Onshore AC grid Voltage	380	kV
Offshore AC grid Voltage	155	kV
DC grid Voltage	320	kV
Converter -1 Rating	700	MVA
Converter-2 &3 Rating	1100	MVA
WPP Active Power Output	600	MW

TABLE II : POWER FLOW OF HVDC CONVERTERS

Converter	Vw=1.1 pu	Vw=0.9 pu	Unit
Conv-1 (OWPP)	600	510	MW
Conv-2	400	490	MW
Conv-3	1000	1000	MW

TABLE III : BASE VALUES FOR THE MEASUREMENTS

Parameter	Value	Unit
Base MVA, Conv-1	600	MVA
Base MVA, Conv-2	1000	MVA
Base MVA. Conv-3	1000	MVA
Base Frequency	50	Hz
Base DC grid Voltage	320	kV

TABLE IV: CONTROL PAPRAMETERS OF THE 3-TERMINAL HVDC SYSTEM

Parameter	Value	Unit
$V_{dc} - P$ droop controller gain (k_p) - Conv-2	2	pu
$V_{dc} - P$ droop controller gain (k_p) - Conv-3	4	pu
$f_{on} - P$ droop controller gain (k_f) – Conv-2	10	pu
$f_{on} - P$ droop controller gain (k_f) – Conv-3	10	pu
$V_{dc} - f_{off}$ droop controller gain (k_v)- Conv-1	0.5	pu
OWPP frequency controller gains	12	pu
Droop gain (k_d)	6	pu
Inertial gain (k_{in})		

J4 Jayachandra N. Sakamuri, Joan Sau, Eduardo Prieto, Oriol Gomis, Altin M, Hansen A.D., Cutululis N.A., "Experimental Validation of Frequency Control from Offshore Wind Power Plants in Multi Terminal DC Grid", Under Review at CIGRE Science & Engineering.

This page would be intentionally left blank if we would not wish to inform about that.

Experimental Validation of Frequency Control from Offshore Wind Power Plants in Multi-Terminal DC Grids

Jayachandra N. Sakamuri, Student *Member, IEEE*, Joan Sau-Bassols, Student Member, IEEE,
Eduardo Prieto-Araujo, Member, IEEE, Oriol Gomis-Bellmunt, Senior Member, IEEE, Anca D.
Hansen, Mufit Altin, Member, IEEE, Nicolaos A. Cutululis, Senior Member IEEE.

Abstract—This paper presents two methods for frequency control of onshore AC grids from offshore wind power plants (OWPPs) connected to a multi-terminal DC (MTDC) grid. The first method is based on communicating the onshore frequency to the OWPP and the other voltage source converters (VSCs) in the MTDC grid. The second method is based on a coordinated strategy between the VSCs in the MTDC grid, where the onshore frequency is replicated at the offshore grid using supplementary control blocks implemented locally at the VSCs of the MTDC grid. The proposed control methods are first verified through simulations on a test set up with an OWPP connected to a three-terminal DC grid using DIgSILENT PowerFactory, and then validated experimentally on a laboratory scaled three-terminal DC grid. The simulation and experimental results prove that, with the proposed control strategies, OWPPs and the VSCs in the MTDC grid can participate in frequency control and support the onshore grid frequency stability.

Index Terms—Coordinated Frequency Control, DC Voltage, Experimental Validation, HVDC, Offshore Wind Power Plants.

I. INTRODUCTION

During recent years, there has been increased penetration of offshore wind power plants (OWPPs) into the power system and this trend is expected to continue in near future [1]. Traditionally, the power output from offshore wind power plants (OWPPs) is transmitted to the shore using AC transmission system. However, voltage source converter (VSC) based high voltage DC (HVDC) technology system is considered as an optimal solution to transmit higher power over long distances due to its advantages [2],[3]. Moreover, VSC HVDC system is also being used to interconnect two

different synchronous areas [3]. The trend is also growing to interconnect OWPPs with different synchronous areas and OWPPs using VSCs to form a multi-terminal DC (MTDC) grid [3]. However, increased penetration of wind power plants (WPPs) into the power system poses several challenges to its operation and stability [3],[4]. Among them, frequency control is one of the important concerns for the transmission system operators (TSOs) [4]. In particular, increased penetration of OWPPs leads to the reduced effective inertia of the power systems and that may lead to a lower frequency nadir point, or load shedding, for a large infeed/generation loss in power systems. Therefore, fast primary frequency control reserves, which act faster than primary frequency control reserves and provide service for few seconds after the frequency event, are needed to limit the frequency nadir [5].

Another challenge with the OWPPs in the HVDC/MTDC system is that they do not respond to the frequency events in the associated onshore AC grid due to the power electronic interfaces. Hence, there are two methods proposed in the literature which make the OWPPs to participate in frequency control [6]-[9]. The first method is called 'communication based frequency control', where the OWPP and HVDC converters in the MTDC system participate in the frequency control based on the frequency signals received through communication channels from the affected onshore AC grid [6]. The method presented in [6] is limited to two terminal HVDC system and to under frequency events; therefore the impact of frequency control on DC grid cannot be identified. The second method is called as 'coordinated frequency control' which is based on a communication-less scheme, where the onshore frequency is replicated at the offshore grid through supplementary control blocks implemented locally at the VSCs in the MTDC system [7]-[9]. The coordinated frequency control from a wind power plant (WPP) in a two terminal HVDC system has been validated experimentally using a laboratory scale test set up in [10]. However, these tests are limited to under frequency events and to a point to point HVDC system. A simple power-voltage droop test on a three-terminal HVDC system has been performed on an experimental test set up in [11], [12]. However, there is no WPP model and also no frequency control issues are discussed in these papers. Also, there is no comparison between the communication based and coordinated frequency control

methods have been presented before in MTDC grid perspective.

The focus in this paper is therefore on these two frequency control methods, which are studied and compared by performing the fast primary frequency control test on an OWPP connected through a three-terminal HVDC system. The main objective is to compare these two methods and to validate the use of DC voltage as an indicator for system imbalance in the AC grid. The frequency control methods are tested both for under and over frequency events created in the test power system with the help of time domain simulations using DIgSILENT PowerFactory. Moreover, the simulation results are validated by performing the frequency control tests on a laboratory scale three-terminal DC grid test set up. The paper is organized as follows: Section II describes the traditional control methods for the MTDC system with OWPPs. The proposed methods for frequency control from OWPPs in the MTDC grid are described in Section III. The description of the laboratory scale MTDC test set up and the implementation of the proposed frequency control methods are given in Section IV. The simulation results and experimental validation for both frequency control methods are presented in Section V, followed by concluding remarks provided in Section VI.

II. MTDC GRID FOR THE STUDY AND ITS CONTROL

The three-terminal HVDC grid interconnecting two onshore (AC grid-1 and AC grid-3) and one offshore AC grids, shown in Fig. 1, is used to for the study. Root mean square (RMS) models for WPP, HVDC converters, cables, and transformers have been used for the investigation and implemented in DIgSILENT PowerFactory [13].

Fig. 1. Three-terminal HVDC grid layout

In this work, an attempt is made to prove that frequency control is possible with the two frequency control methods and in case of coordinated control the frequency event in one AC grid is replicated at other AC grid though the DC grid voltage imbalance. In case of communication based frequency control, the converters of the DC grid exchange frequency information of their associated AC grid using the dedicated communication channels, as shown in Fig.1. For the coordinated frequency control, supplementary controls at the HVDC converters are used instead of these communication channels. In the following sub sections, a brief description of the onshore and offshore HVDC converter control, OWPP control, and required additional controls needed for frequency control are given.

A. Onshore HVDC Converter

The Conv-1 and Conv-3, in Fig.1, are the onshore HVDC converters connected to the AC grid-1 and grid-3, respectively. VSCs can control active and reactive powers independently [14]. For active power control, the droop method is used to share the responsibility among the two onshore VSCs in maintaining the active power balance in the DC grid. Hence, they operate in active power control with a DC voltage droop, whose value is set by the $V_{dc} - P$ droop controller and these controllers are shown in Fig.2. Similarly, the 'Reactive Power Control Loop' in Fig.2 controls the reactive power output of the converter. The converter also has additional control loops to accommodate frequency control and the corresponding details are explained in Section III.

Fig. 2. Onshore HVDC converter control

B. Offshore HVDC Converter Control

The Conv-2, in Fig.1, is the offshore VSC connected to offshore AC grid (i.e. AC grid-2). This converter exchanges the power generated by OWPP to the DC grid by controlling the offshore AC voltage and frequency, as shown in Fig.3. The converter has additional control loops to assist frequency control, whose details are explained in Section III.

Fig. 3. Offshore HVDC converter Control

C. Offshore Wind Power Plant Model

The OWPP is modelled as an aggregated IEC Type-4 wind turbine (WT) based on the aggregation method given in [15]. The Type-4 WT model used in this study is based on generic

172

approach proposed by the IEC Committee in IEC 61400-27-1 [16] for the short term power system stability studies. Additionally, this model is extended to include the dynamic features, such as aerodynamic model, pitch control, and active power control, relevant for the study of the frequency control from WPPs [17]. The active power reference generation part of the WT active power controller is shown in Fig.4. The maximum power point tracking (MPPT) table generates optimal power reference (P_{opt}) for the WT power controller in normal operating conditions. This power reference is adjusted to be frequency initiated power reference (P_{ref}^f), which is higher or lower than P_{opt} depending on under or over frequency events, in case of frequency events. P_{ref}^f mainly depends on the modulated power reference ($\Delta P_{ref\_wpp}^f$) generated by the frequency controller depending on the selected method of the frequency control.
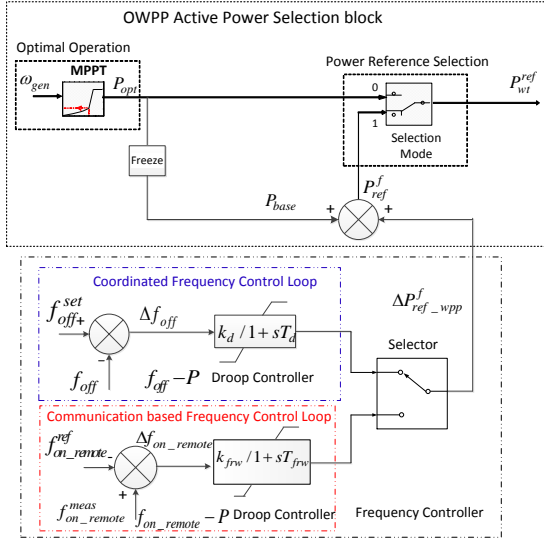

Fig. 4. Active power reference generation for WT power controller

III. FREQUENCY CONTROL METHODS

In this section, the communication based and coordinated frequency control methods are explained.

A. Communication based Frequency Control

In this method, the HVDC converters in the MTDC grid exchange the measured frequency signal of its own AC grid with each other, using the dedicated communication channels depicted in Fig.1. Any frequency event at AC grid-1 is thus communicated to both Conv-3 and OWPP at AC grid-3 and offshore AC grid, respectively. The 'Communication based Frequency Control Loop' depicted in Fig.2 and Fig.4 for Conv-3 and OWPP, generates additional power references, (ΔP_{ref}^f) and ($\Delta P_{ref\_wpp}^f$), respectively, based on the received frequency signal of onshore AC grid-1. The power contribution from Conv-3 and OWPP for frequency control can be changed by adjusting the droop gains k_{fr} and k_{frw} of the respective $f_{on\_remote} - P$ droop controller. The Conv-1

exchanges the active power to AC grid-1 from the DC grid depending on the droop gain k_p of the $V_{dc} - P$ droop controller, shown in Fig.2. In this process, the voltage droop control of the other onshore converters can affect the frequency control of the affected AC grid because the converters in the DC grid share the responsibility of balancing the DC grid by sharing the surplus/deficit power in the DC grid. For example, the Conv-3 also exchanges part of active power from the DC grid based on its droop gain k_p of the $V_{dc} - P$ droop controller. Similarly, Conv-1 and OWPP can participate in frequency control of AC grid-3, based on the received frequency signal from it through communication channels.

B. Coordinated Frequency Control

The coordinated frequency control method has been explained in detail in [9].

In this method, the onshore AC grid frequency (for grid-1 and grid-3) is replicated at offshore AC grid according to the DC voltage variation. For example, the $f_{on\_local} - P$ droop controller of the 'Coordinated Frequency Control Loop', shown in Fig.2, provides an additional active power reference (ΔP_{ref}^f) to the onshore HVDC converter according to the measured frequency deviation at the associated onshore AC grid, as given in (1), where $f_{on\_local}^{ref}$ and $f_{on\_local}^{meas}$ are the reference and measured frequency at the onshore AC grid.

$$\Delta P_{ref}^f = k_{fl}(f_{on\_local}^{ref} - f_{on\_local}^{meas}) \tag{1}$$

This leads to a deviation in the DC grid voltage from its initial value. Therefore, the other onshore HVDC converters in the MTDC grid inherently modulate its active power reference ($\Delta P_{ref}^{V_{dc}}$) due to $V_{dc} - P$ droop control action, participating in frequency control. However, the OWPP does not detect the frequency event; hence mirroring onshore frequency deviation in the offshore AC network frequency is needed. The offshore HVDC converter detects this through the DC voltage variation at Conv-2. Therefore, the $V_{dc} - f_{off}$ droop controller at offshore HVDC converter, shown in Fig.3, modifies the offshore AC grid frequency proportional to the DC voltage variation measured at its terminals as given in (2) and (3), where f_{off}^{set} is the offshore frequency during normal conditions and f_{off}^{ref} is the reference offshore frequency considering DC grid voltage variation.

$$f_{off}^{ref} = f_{off}^{set} + \Delta f_{off} \tag{2}$$

$$\Delta f_{off} = k_v \Delta V_{dc} \tag{3}$$

The power reference of the WT power controller (P_{WT}^{ref}), hence OWPP, is then updated with the contribution $\Delta P_{ref\_wpp}^f$ from the 'Coordinated Frequency Control Loop' shown in

Fig.4, according to (4).

$$P_{WT}^{ref} = P_{base} + \Delta P_{ref\_wpp}^{f}$$

$$\Delta P_{ref\_wpp}^{f} = k_d (f_{off}^{set} - f_{off}) \tag{4}$$

Where P_{base} is equal to the freezed value of P_{opt}, taken just before the frequency event.

IV. LABORATORY SCALED MTDC TEST SET UP

A frequency control test is performed on a three-terminal DC grid laboratory scaled test set up whose single line diagram is shown in Fig. 5. The main objective of performing this test is to compare the two frequency control methods and to validate the use of DC grid voltage as an equivalent AC grid frequency indicator. The three-terminal DC grid laboratory scaled test set up is composed of three cabinets, as shown in Fig. 6, and a physical emulation of the DC cables. The DC lines (1-2, 1-3 and 2-3) are modelled using the PI equivalent cable, with the values of resistance (R) and inductance (L) illustrated in Table I. The cable capacitance is included in the VSC capacitance. Each cabinet contains a three-phase 12.5 kVA transformer, the VSC, the control board and the measuring boards. The VSCs are two-level converters based on insulated-gate bipolar transistors (IGBTs) with a nominal power of 5.7 kVA. The nominal AC RMS voltage is 230 V phase to phase. The switching frequency of each converter is 20 kHz and it is controlled using a control board based on a digital signal processor (DSP) F28M35 of Texas Instruments (TI). All the converters are connected to the same AC grid of 230 V phase to phase and the behaviour of the OWPP in the AC side of Conv-2 and the frequency event in the AC grid of Conv-1 are emulated.
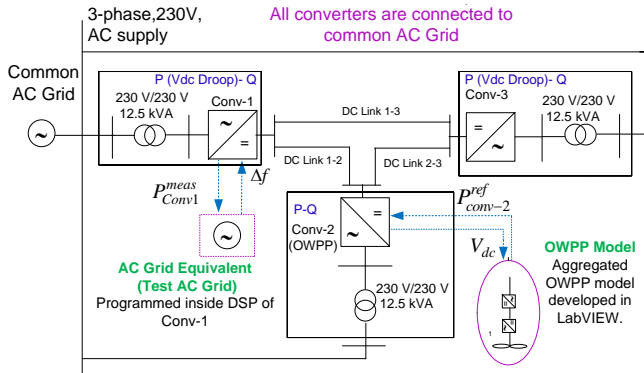

Fig. 5. Three Terminal test set up to perform frequency control test

A SCADA system is implemented in LabVIEW using the cRIO 9024 controller of National Instruments (NI) to monitor the variables of the MTDC grid and it also includes the emulation of the OWPP of Conv 2. The OWPP emulation in the cRIO 9024 is communicated with Conv 2 via the Digital to Analog Converter (DAC) and the Analog to Digital Converter (ADC) of its control board and is described in section IV.B. The emulation of the frequency event of AC grid of Conv 1 is implemented by software in the DSP of Conv. 1 and it is described in Section IV.A. The communication between converters in the case of the communication based frequency control is implemented using a Controller Area Network

(CAN) bus with period of 100 ms.

TABLE I : DESCRIPTION OF THE TEST LAYOUT IN FIG. 5

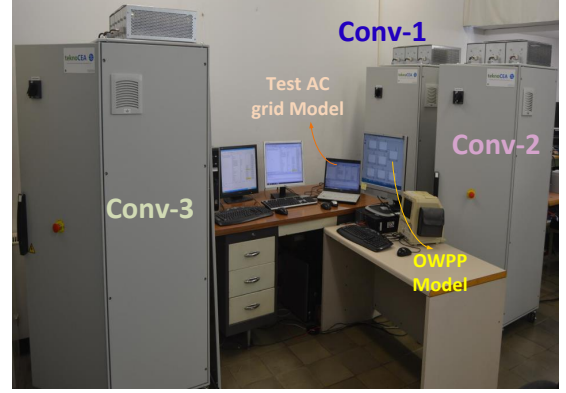| Parameter	Value	Unit
Common AC Voltage (L-L)	230	V
DC Voltage (Symmetrical Monopole)	+/- 250	V
Transformer rating (230V/230V)	12.5	kVA
Converter rating	5.7	kVA
DC line 1-2 Resistance , R12	0.22	Ω
Inductance, L12	1	mH
DC line 1-3 Resistance, R13	0.1	Ω
Inductance, L13	0.5	mH
DC line 2-3 Resistance, R23	0.44	Ω
Inductance, L23	1.5	mH
Virtual OWPP rating	2.85	kW

Fig. 6. Picture of three-terminal DC grid experimental test set up

A. AC Grid Equivalent to create Frequency Event

As it is not possible to change the frequency of the laboratory AC grid, an AC grid equivalent emulation with a dynamic frequency model (test AC grid) based on the swing equation [18], shown in Fig. 7, is implemented inside the DSP of Conv-1.
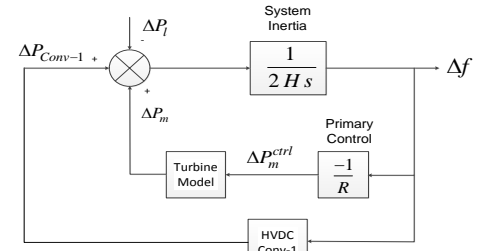
Fig. 7. AC Grid equivalent with dynamic frequency model

The change in frequency (Δf) is zero as long as there is a balance between change in mechanical power input (ΔP_m) and electrical power output (ΔP_l) of the grid. The corresponding relation between ΔP_m, ΔP_l and Δf is shown in (5), where 'H' is the inertia of the test AC grid.

$$\Delta P_m - \Delta P_l = 2H \frac{d\Delta f}{dt} \tag{5}$$

A frequency event in the test AC grid can be created by perturbing the ΔP_l. In case of coordinated frequency control, Δf is sent to the onshore HVDC Conv-1 controller (refer Fig. 2), which then provides the additional active power reference

174

(ΔP_{ref}^{f}) to the onshore HVDC converter. In case of communication based control, Δf is communicated to Conv-3 and OWPP model with a communication delay of 100 ms. In both methods, the measured change in active power output of Conv-1 due to the frequency control (ΔP_{Conv-1}) is sent to the test AC grid model, thereby participating in the frequency control of test AC grid, as given in (6).

$$\Delta P_m - \Delta P_l + \Delta P_{Conv-1} = 2H \frac{d\Delta f}{dt} \qquad (6)$$

B. Implementation of OWPP Model and Control of HVDC Converter-2

The Conv-1 and Conv-3 operate in active power control with a DC voltage droop, maintaining the power balance in the DC grid, as explained in section II.B. Nonetheless, the Conv-2 connected to OWPP operates in active and reactive power ($P-Q$) control mode instead of AC voltage and frequency control mode ($V_{ac} - f$) explained in section II.C. However, the equivalent control delays which involved in '$V_{ac} - f$' control mode, in case of coordinated frequency control, are implemented in OWPP model as shown in Fig. 8, to make the experimental implementation equivalent to its theoretical set up.

Fig. 8. OWPP model implemented in in LabVIEW (only active power reference generation part is shown here)

The HVDC Conv-2 sends the DC voltage measurement, V_{dc} to the OWPP model. The $V_{ac} - f_{off}$ droop controller changes its frequency based on the change in the DC voltage and sends the reference to the 'Coordinated Frequency Control Loop', which then generates $\Delta P_{ref\_wpp}^{f}$ according to frequency change. In case of communication based frequency control, the frequency controller of OWPP generates $\Delta P_{ref\_wpp}^{f}$ based on the test AC grid frequency, received through CAN communication channels. Finally, the OWPP model sends the active power reference to Conv-2, thereby, emulating the combined theoretical behavior of offshore HVDC converter and OWPP control, shown in Fig.3 and Fig.4.

C. Limitations of the laboratory scaled DC grid test set up

The following limitations can apply to the test system.

1. Common AC grid is being used for all the three converters; hence, it is not possible to study the impact of frequency control in one AC system on the other AC system.

2. Simulation model is considered for OWPP instead of physical implementation, where more challenges are expected.

3. The delays and difficulties for frequency measurements are ignored.

V. SIMULATION AND EXPERIMENTAL VALIDATION

The simulations of frequency control in a three-terminal DC grid, shown in Fig.5, have been performed using DIgSILIENT PowerFactory with both communication based and coordinated frequency control methods. The frequency control test is performed both for under and over frequency events created in the test AC grid, shown in Fig 6, by modifying its electrical power output (ΔP_l). The simulation results are validated with experimental results, where the tests are performed on a three-terminal test set up shown Fig 8. The results of communication based frequency control are presented in Section V.A, and the ones of the coordinated frequency control in Section V.B. In both cases, an under frequency event in the test AC grid is created by applying $\Delta P_l = 0.15$ pu and an over frequency event with $\Delta P_l = $ -0.15 pu at time t = 6s.

A. Communication based Frequency Control Method

The simulation and experimental results of communication based frequency control, both for under and over frequency events, are presented in this section. The frequency of the test AC grid is communicated to Conv-3 and OWPP with a communication delay of 100 ms. Participation of OWPP and the other converters in the MTDC grid in the frequency control is studied. The power flow and droop parameters of the 3 terminal test set up (Fig.5) used in this test are given in Table II. In normal conditions, the OWPP, hence the offshore converter (Conv-2) transfers power to DC grid whereas the onshore converters (Conv-1 and Conv-3) receive power from DC grid. The positive sign of power flow indicates power flow from DC to AC grid and vice versa for negative sign.

TABLE II : PARAMETERS OF COMMUNICATION BASED FREQUENCY CONTROL

Parameter	Unit	Under Frequency	Over Frequency
Base kVA	kVA	5700	5700
Base DC grid voltage	V	+/- 250	500
Base frequency	Hz	50	50
Power flow, Conv-1	pu	0.23	0.23
Power flow, Conv-2	pu	-0.5	-0.5
Power flow, Conv-3	pu	0.25	0.25
$V_{dc} - P$ droop gain (k_p) - Conv-1 /Conv-3	pu/pu	5/5	5/5
$f_{on\_remote} - P$ droop gain k_{frw} / k_{fr} (OWPP/Conv-3)	pu/pu	5/10	5/15

175

1) Under Frequency Event at Test AC Grid:

The simulation results of communication based frequency control for an under frequency event at test AC grid, created at time t = 6 s, are shown in Fig. 9. The test AC grid frequency, the DC voltage and active power of all three converters are presented. The corresponding experimental results are given in Fig. 10.
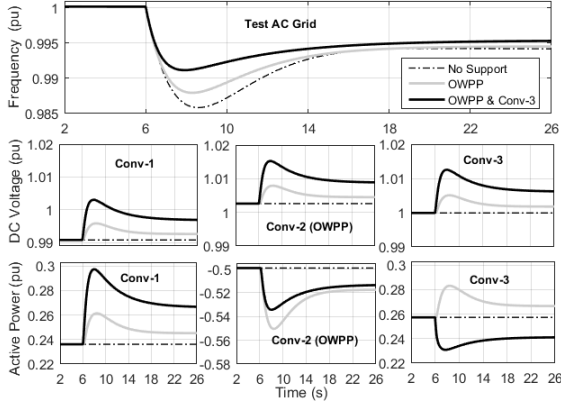
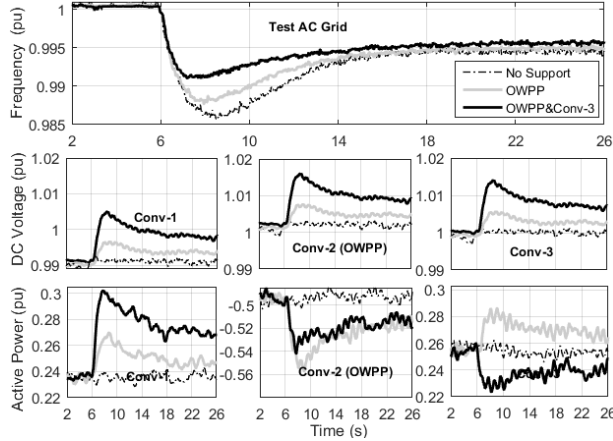Fig. 9 Communication based frequency control - Under frequency- Simulation Results

Fig.10. Communication based frequency control-Under frequency- Experimental validation of simulation results given Fig.9

It can be observed from these results that the participation of OWPP improves the frequency of test AC grid (light solid line) compared to No support from OWPP (Conv-2) and Conv-3 (dashed dotted line). It should be noticed that the increased active power support by OWPP (Conv-2) into the DC grid, because of the frequency control action, is shared by Conv-1 and Conv-3 according to their $V_{dc} - P$ droop constants.

The increased power supply into the DC grid also leads to an increase in the DC grid voltage. The participation of Conv-3 together with OWPP (dark solid line) further improves the frequency response of the test AC grid. In this case, Conv-3 participates in frequency control by reducing its power export from the DC grid due to the action of its $f_{on\_remote} - P$ droop controller. However, Conv-3 participation together with OWPP further increases the DC grid voltage.

2) Over Frequency event at test AC grid

The simulation and experimental results of the communication based over frequency test are given in Fig. 11 and Fig. 12 respectively.
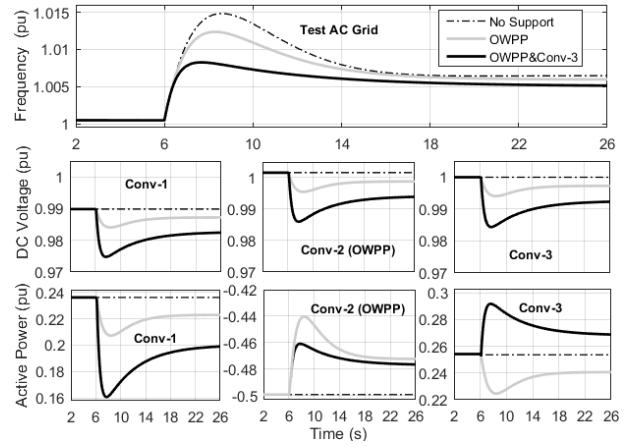
Fig. 11. Communication based frequency control- Over frequency- Simulation Results
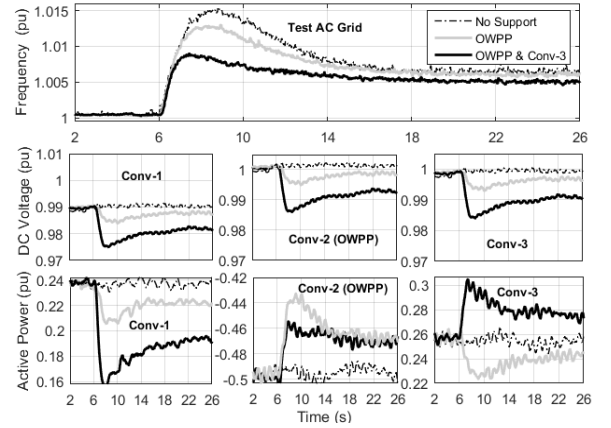
Fig. 12. Communication based frequency control- Over Frequency- Experimental validation of simulation results given in Fig. 11

From these figures, it can be observed that the participation of OWPP (Conv-2) and Conv-3 improve the frequency of test AC grid (dark solid line) compared to two other cases, i.e. participation of OWPP alone (light solid line) and No Support (dashed dotted line). In this case, OWPP (Conv-2) reduces its power input to DC grid whereas Conv-3 increases its power export from DC grid to participate in frequency control. This causes a slight reduction in DC grid voltage as can be observed from Fig.11 and 12.

It can be thus concluded that the experimental results are aligned with the simulation results, both for under and over frequency events, while using the communication based frequency control.

B. Coordinated Frequency Control Method

In this section, the simulation and experimental results of the coordinated frequency control (under and over frequency) from OWPPs and the HVDC converters of the three-terminal test DC grid are presented. A frequency event is created at test AC grid at time t = 6 s. The converters and OWPP participate in frequency control without depending on the communication channels in the DC grid. The power flow and droop parameters of the three-terminal set up (Fig. 5) used in this test are given in Table III.

1) Under Frequency event at the test AC grid

In normal conditions, the OWPP, hence the offshore

converter (Conv-2) supplies power to the DC grid, whereas the onshore converters (Conv-1 and Conv-3) receive power from the DC grid. The simulation and experimental results of the coordinated frequency control from OWPP (Conv-2) and Conv-3, for an under frequency event created at test AC grid, is shown in Fig. 13 and 14 respectively.
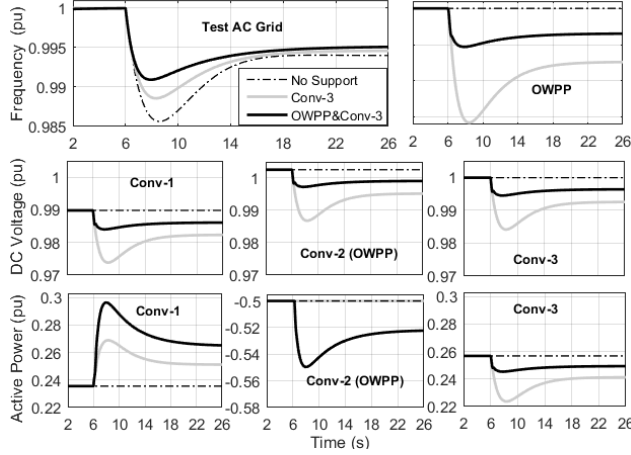

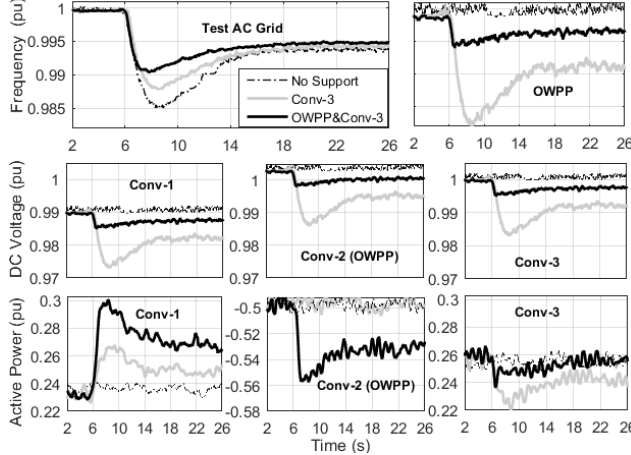Fig. 13 Coordinated frequency control- Under frequency- Simulation results

Fig. 14 Coordinated frequency control- Under frequency- Experimental validation of simulation results given in Fig.13

As explained in Section III.B, the change in frequency at the test AC grid modifies the active power reference to Conv-1, and consequently also changes the DC grid voltage. The Conv-3 changes its power output due to natural action of $V_{dc} - P$ droop controller, participating in frequency control, whereas the OWPP modulates it power output based on the measured change in frequency at OWPP model, which is modified according to DC grid voltage received from Conv-2. It can be observed from Fig. 13 and 14 that the frequency of the test AC grid is improved with the combined participation of Conv-3 and OWPP (dark solid line) compared to the other two cases, i.e. participation of Conv-3 (light solid line) alone and No support (dashed dotted line). Also, the participation of OWPP in the frequency control relieves the active power burden on Conv-3 by sharing the responsibility. It can also be observed that there is a slight decrease in the DC grid voltage due to the coordinated frequency control action for under frequency events. However, participation of the OWPP

together with the Conv-3 in frequency control minimizes the reduction in DC grid voltage.

TABLE III : PARAMETERS OF COORDINATED FREQUENCY CONTROL

Parameter	Unit	Under Frequency	Over Frequency
Base Parameters	As	per Table II	
Power flow, Conv-1	pu	0.23	0.7
Power flow, Conv-2	pu	-0.5	-0.5
Power flow, Conv-3	pu	0.25	-0.22
$V_{dc} - P$ droop gain (k_p)- Conv-1 /Conv-3	pu/pu	5/2.2	5/2.2
$f_{on\_local} - P$ gain(Conv-1)	pu/pu	10	10
$f_{off} - P$ gain (OWPP)	pu/pu	15	15

2) Over Frequency event at the test AC grid

In normal conditions, the OWPP, hence the offshore converter (Conv-2) and one of the onshore converter (Conv-3) transfers power to the DC grid whereas the other onshore converter (Conv-1) receives power from the DC grid. The simulation and experimental results of coordinated control method, for over frequency at test AC grid are given in Fig. 15 and 16, respectively.
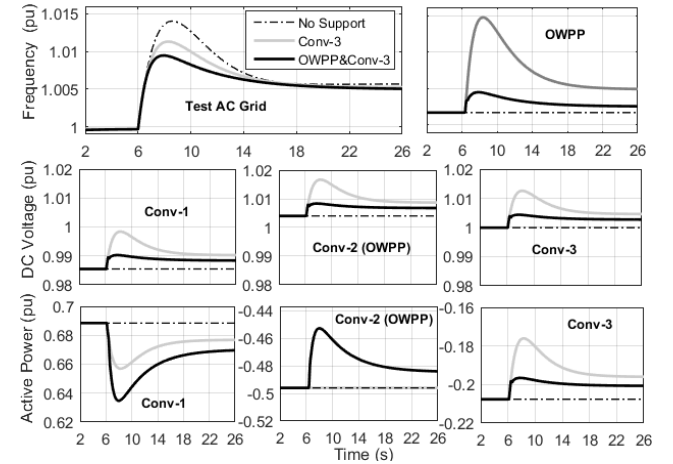

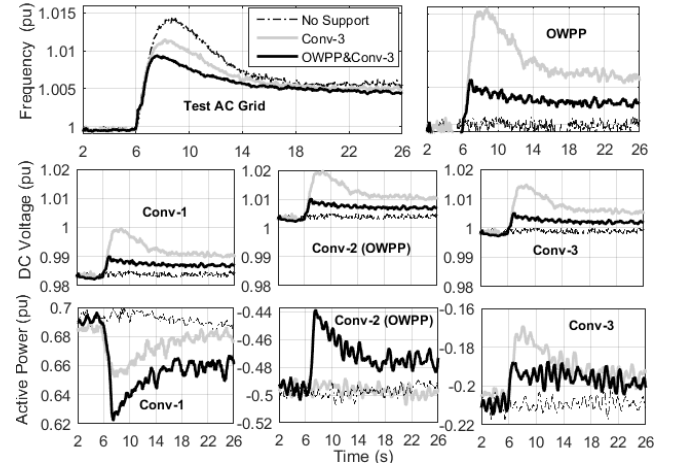Fig. 15 Coordinated frequency control- Over frequency- Simulation results

Fig. 16 Coordinated frequency control- Over frequency- Experimental validation of simulation results given in Fig.15

Similar to the previous case, participation of the OWPP along with Conv-3 improves the response of the test AC grid

frequency while relieving the burden on Conv-3 by sharing the active power support during frequency control. Also, the combined participation of the OWPP and the Conv-3 minimizes the rise in the DC voltage due to frequency control compared to the case when Conv-3 is participating alone. In case of the coordinated control method also, the experimental results are in align with simulation results, both for under and over frequency events.

C. Comparison between Frequency Control Methods

Based on the simulation results and experimental validations using the communication based and coordinated frequency control methods, the following points are worth to consider.

For communication based frequency control, there must be dedicated communication channels between each converter in the DC grid, which raises concerns on the reliability. The coordinated control, which relies on communication-less scheme, minimizes this risk. However, coordinated control increases the control complexity, particularly for frequency control of the offshore wind power plants. In case of communication based method, the increase in the number of converters participating in the frequency control can increase the risk of over/under voltage in the DC grid, depending on the under/over frequency event, during the frequency control period, as observed from Fig. 9 to 12. This risk will increase with the size of DC grid. However, in case of coordinated frequency control, the increase in the number of converters participating in frequency control can minimize the risk of over/under voltage, as observed from Fig. 13 to 16. Also, the converters operating in DC voltage droop control (Conv-3 in this case) naturally participates in frequency control with the coordinated control compared to communication based control. This feature favors the coordinated control over communication based control.

VI. CONCLUSIONS

Two methods for the fast primary frequency control, which are namely communication based control and coordinated control, from offshore wind power plants in multi terminal DC grid are presented in this paper. These control concepts are tested by performing simulations on an OWPP integrated to a three-terminal DC grid using DIgSILENT PowerFactory. Also, the simulation results are validated with experimental results, by means of a three-terminal laboratory scaled DC grid platform. The proposed frequency control methods are tested for both under and over frequency events with different power flows in the DC grid. It has been observed that the experimental results are in align with the simulation results, proving that the OWPP and HVDC converters in a MTDC grid can participate in onshore AC grid frequency control. In both methods, DC voltage acts a medium of imbalance in the associated AC grids. If the size of the DC link is small (2 or 3 converters, for example), the communication based frequency control can be preferred. However, for larger DC grids with more number of converters, the coordinated control can be preferred over communication based method, considering the reliability and dynamics of DC grid voltage.

VII. REFERENCES

[1] Windspeed 2015. [Online]. Available: http://www.windspeed.eu. [Accessed: 10- Sep- 2016].

[2] D. Van Hertem, M. Ghandhari , "Multi-terminal VSC HVDC for the European Supergrid: Obstacles," *Renewable and Sustainable Energy Reviews*, vol 14, pp 3156–3163, Dec 2010

[3] D. Van Hertem, O. Gomis-Bellmunt and J. Liang, HVDC Grids: For Offshore and Supergrid of the Future, IEEE Press Series on Power Engineering, Ed. John Wiley & Sons, 2016.

[4] ENTSO- E, Draft- The Network Code on High Voltage Direct Current Connections (NC HVDC), Apr 2014.

[5] National grid, System Operability Framework (SOF) report, 2014.

[6] L. Zeni, I. Margaris, A. Hansen, P. Sørensen and P. Kjær, "Generic Models of Wind Turbine Generators for Advanced Applications in a VSC-based Offshore HVDC Network," *in Proc. 2012 10th IET Conference on AC/DC Transmission*, Birmingham..

[7] Y. Phulpin,"Communication-free inertia and frequency control for wind generators connected by an HVDC link," IEEE Trans on Power Systems, vol. 27, pp. 1136-1137, May 2012.

[8] B. Silva, C. L. Moreira, et al., "Provision of Inertial and Primary Frequency Control Services Using Offshore Multiterminal HVDC Network", *IEEE Trans. on Sustainable Energy*, vol. 3, pp. 800-808, Oct 2012.

[9] J.N. Sakamuri, M. Altin, A. D. Hansen, N.A.Cutululis,, " Coordinated Frequency Control from Offshore Wind Power Plants Connected to MTDC System Considering Wind Speed Variation ," *IET Rene. Power Generation*, , to be published.

[10] H.Støylen, K.Uhlen, A. R. Årdal , "Laboratory Demonstration of Inertial Response from VSC-HVDC connected Wind Farms,", *in Proc. 2015 11th IET Conference on AC/DC Transmission*,

[11] R.E Torres-Olguin, A.R.Ardal, H.Støylen, K.Uhlen, et. al , "Experimental verification of a voltage droop control for grid integration of offshore wind farms using multi-terminal HVDC ,"*Energy Procedia, vol.53, 2014*

[12] Y.Li, X.Shi, B.Lio, et al , "Hardware Implementation of a Four-Terminal HVDC Test-Bed ," *in Proc. 2015 IEEE Energy Conv. Congress and Exposition pp.5363-5370*

[13] DIgSILENT GmbH, Technical Reference - PWM Converter.,2015.

[14] J. Beerten and R. Belmans, "Analysis of Power Sharing and Voltage Deviations in Droop-Controlled DC Grids," IEEE Transactions on Power Systems, vol. 28, no. 4, pp. 4588-4597, 2013.

[15] E. Muljadi et al. "Method of equivalencing for a large wind power plant with multiple turbine representation," Proc. 2008 IEEE Power and Energy Society General Meeting, pp-1-8.

[16] Electrical simulation models for wind power generation, IEC 61400-27-1, 2015.

[17] A. D. Hansen, I. Margaris, G. C. Tarnowski and F. Iov,"Simplified type 4 wind turbine modeling for future ancillary services," in *Proc. 2013 European Wind Energy Conference*, pp. 768-774.

[18] G. Anderson, Dynamics *and Control of Electric Power Systems*, Lecture Notes. Zurich: Feb 2012.

J5 Jayachandra N. Sakamuri, Joan Sau, Eduardo Prieto, Oriol Gomis, Altin M, Hansen A.D., Cutululis N.A., "Impact of Release of OWPP Kinetic Energy Support on DC voltage in MTDC Grids", Under Review at IEEE Trans on Power Delivery.

This page would be intentionally left blank if we would not wish to inform about that.

Impact of Release of Offshore Wind Power Plant Kinetic Energy Support on DC voltage in MTDC Grids

Jayachandra N. Sakamuri, Student *Member, IEEE*, Joan Sau-Bassols, Student Member, IEEE,
Eduardo Prieto-Araujo, Member, IEEE, Oriol Gomis-Bellmunt, Senior Member, IEEE, Anca D.
Hansen, Mufit Altin, Member, IEEE, Nicolaos A. Cutululis, Senior Member IEEE.

Abstract—A communication-less scheme for fast primary frequency control (FPFC) from offshore wind power plants (OWPPs) connected through multi terminal DC (MTDC) grid, considering the operation of OWPPs at different wind speeds, is presented in this paper. The kinetic energy of the OWPPs is utilized for FPFC by overloading the wind turbines (WTs). The impact of overloading WTs on their dynamics, and thus on the DC voltage in the DC grid and also on the frequency are studied considering the operation of the WTs at different wind speeds. The participation of OWPPs in FPFC by utilizing their kinetic energy is validated on an OWPP connected through a three-terminal DC grid with time domain simulations using DIgSILENT PowerFactory. Moreover, the simulation results are validated with experiment tests, performed on a laboratory scale 3-terminal DC grid. The simulation and experimental results have proved that OWPPs in MTDC grid can participate in FPFC by utilizing the kinetic energy of the WTs. However, frequency control from OWPPs depends on their WTs initial pre-overloading conditions (wind speed, mechanical limits, and control) and these conditions dictates the recovery of the WT after release of overloading (kinetic energy support), therefore creates significant impact on DC grid voltage and frequency of the associated AC grid.

Index Terms—, DC Voltage, Frequency Control, Experimental Validation, HVDC, Offshore Wind Power Plants, Wind Speed.

I. INTRODUCTION

Increased installation of offshore wind power plants (OWPPs), long transmission distance from the shore, and flexibility of power control have encouraged the use of voltage source converter (VSC) based high voltage DC transmission (HVDC) systems [1]. Multi-terminal DC (MTDC) systems seem to be also a promising technology to interconnect OWPPs with different synchronous areas [2]-[3]. However, increased penetration of wind power plants (WPPs) poses several challenges to the power system where frequency control is one of the major concerns [4]. The replacement of synchronous generators with OWPPs can pose a serious concern to the power system effective inertia, which may lead to higher rate of change of frequency (ROCOF) and low frequency nadir for a large contingency. Therefore, transmission system operators (TSOs) are imposing new grid codes which require OWPPs participation in frequency control [4], [5]. The need for fast primary frequency control (FPFC) sources, which provide active power support for few seconds after the frequency event, has also been highlighted by National Grid [6].

The OWPPs in MTDC system do not respond to the onshore frequency events due to their decoupling from the onshore AC grid because of HVDC interconnection. In general, two methods to transmit the onshore frequency events to the offshore AC grid, in a two terminal HVDC system, have been proposed [7]. In first method, the frequency of onshore AC grid is communicated to the OWPPs and other associated AC grids of the MTDC system through the dedicated communication channels. The second method, called coordinated frequency control scheme, uses the voltage of the DC link in order to communicate the frequency to OWPP and other AC grids in a coordinated manner, without using the dedicated communication channels between the converters. The coordinated frequency control scheme for primary frequency control from OWPPs in MTDC system has been proposed by [8],[9] and extended in [10]. However, in [8], it is assumed WPPs as constant power sources, while the work is restricted to primary frequency control, where the WPPs are assumed to operate in down regulation mode under normal operating conditions to create certain power reserve for frequency control. The dynamics of the WTs participating in frequency control have not been considered in [10]. The reference [9] presents inertial response from OWPP in a point to point HVDC system. There is also some basic discussion on the impact of two wind speeds on the frequency control and recovery of the WT. However, [9] does not discuss the impact of release of kinetic energy support on the dynamics of the WT (speed, pitch, aerodynamic power, active power), therefore on

181

the DC grid (as it is limited to two terminal system). The simulation of FPFC from OWPPs in MTDC system has been studied in [11]. Nevertheless, the impacts of dynamics of the WT on its active power output, therefore, on the DC voltage of DC grid and frequency have not been addressed. Moreover, the study is limited to operation of WTs at above rated wind speed, where the overloading the WT to certain extent does not affect its dynamics. The participation of WPPs in FPFC is also highlighted by [12] with focus more on frequency control at just below rated wind speed.

Considering the limited work on the impact of OWPPs participation in frequency control on the DC and AC grids, the attention in this paper is directed towards participation of OWPPs in FPFC, by utilizing their kinetic energy, considering the operation of the OWPP at different wind speeds. The ability of the OWPPs participation in frequency control is tested at three different wind speeds: (1) above rated wind speed, (2). just below rated wind speed, and (3). low wind speeds. Therefore, the main contributions of this paper are:

(1). the FPFC from OWPPs in MTDC grid is studied by utilizing the kinetic energy of WTs at different wind speeds, considering the impact of dynamics of the WTs.

(2). the impact of release of kinetic energy support from OWPPs on the DC grid voltage and frequency of the affected AC grid are studied. The possibilities for minimizing these impacts on AC and DC grids by releasing the WT overloading with a ramp rate limiter are also discussed.

(3). the coordinated frequency control method and the impact of wind speed on the FPFC and on the DC grid voltage is verified with the time domain simulations and experimental validations on an OWPP model integrated to a three-terminal DC grid test set up.

The major contributions of this paper are twofold: 1. Experimental validation of the frequency control from OWPP by utilizing its kinetic energy and 2. Investigation of the impact of release of kinetic energy support from OWPP on the DC grid voltage.

The time domain simulations for frequency control are performed on an OWPP connected through a three-terminal DC grid using DIgSILENT PowerFactory. Moreover, the frequency control scheme and the impact of wind speed are validated experimentally by performing the tests on an OWPP model integrated to a laboratory scale three-terminal DC grid. One of the main objectives of this paper is studying the impact of the kinetic energy release from OWPP on the DC voltage. In this paper, this impact on the DC gird dynamics has been studied with time domain simulations and validated using a small scale experimental platform that can reproduce the very fast dynamics of the DC voltage despite of its reduced scale. The paper is organized as follows. Section II describes the modeling of the OWPP and the 3-terminal HVDC grid, its control and the coordinated frequency control method. The description of the laboratory scaled MTDC test set up and the implementation of the frequency control method are given in section III. The simulation results and experimental validation of frequency control from OWPPs are presented in section IV,

followed by the concluding remarks provided in section V.

II. CONTROL OF THE MTDC SYSTEM AND FREQUENCY CONTROL METHOD

A three-terminal DC grid test system with an OWPP, shown in Fig.1, is considered in this paper. The test DC grid interconnects two independent onshore AC grids (AC grid-1 and AC grid-3) and one offshore AC grid having an OWPP. Root mean square (RMS) models for OWPP, VSC-HVDC converters, cables, and transformers have been used for the investigation and implemented in DIgSILENT PowerFactory[13].
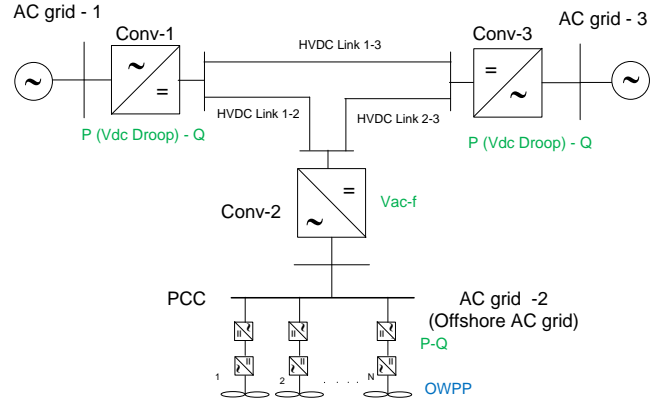

Fig. 1 Three-terminal HVDC grid layout

In the following sub sections, a brief description of the onshore and offshore HVDC converter control, OWPP control, and additional controls needed for frequency control are given.

A. Onshore HVDC Converter

The Conv-1 and Conv-3 in Fig. 1 are the onshore HVDC converters, based on VSC technology, connected to AC grid-1 and grid-3, respectively. They share the responsibility of active power balance in the DC grid; hence, they operate in active power control with a DC voltage droop [14], whose value is set by the $V_{dc} - P$ droop controller shown in Fig. 2. Similarly, they also control the reactive power supply to the respective AC grids using the 'Reactive Power Control loop'. The 'Frequency Control Loop' in Fig. 2 generates additional power reference (ΔP_{ref}^f) to the HVDC converter based on the frequency deviation measured at the respective AC grid.
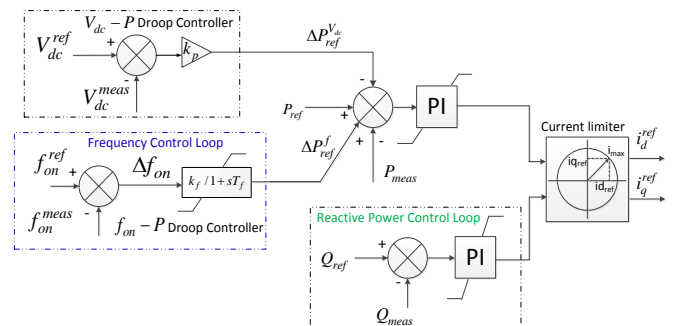

Fig. 2 Onshore HVDC converter control

B. Offshore HVDC Converter

The Conv-2 in Fig.1 is the offshore HVDC converter is also a VSC connected to the offshore AC grid (i.e. AC grid-2). The control structure of this converter is shown in Fig. 3, where the main responsibility of this converter is to control the AC voltage and frequency of the offshore AC grid and exchanging the power generated by the OWPP to the DC grid [7],[15],[16]. The 'Frequency Control Loop' of this converter changes the frequency of the offshore AC grid proportional to the DC voltage measured at its terminals. Further details of the frequency control are explained in section II. D.
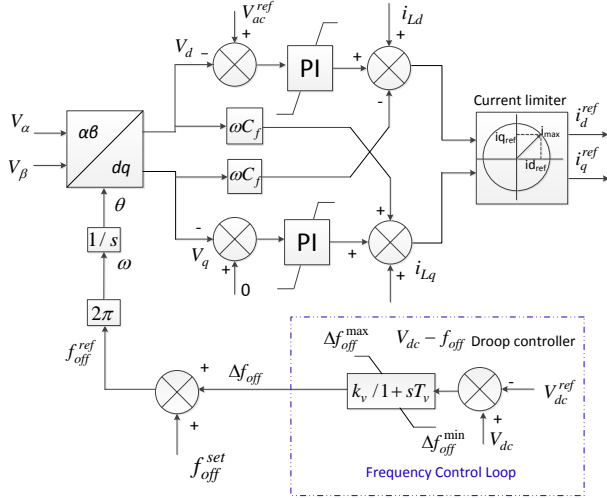
Fig.3 Offshore HVDC converter Control

C. Offshore Wind Power Plant Model

The OWPP is modelled as an aggregated IEC Type-4 wind turbine (WT) based on the aggregation method given in[17]. The Type-4 WT model used in this study is based on generic approach proposed by the IEC Committee in Part 1 of IEC 61400-27[18] for the short term power system stability studies. Additionally, this model is extended, as shown in Fig.4, to include the dynamic features, such as the aerodynamic model, pitch control, and mechanical model, relevant for the study of the frequency control from WPPs [19].
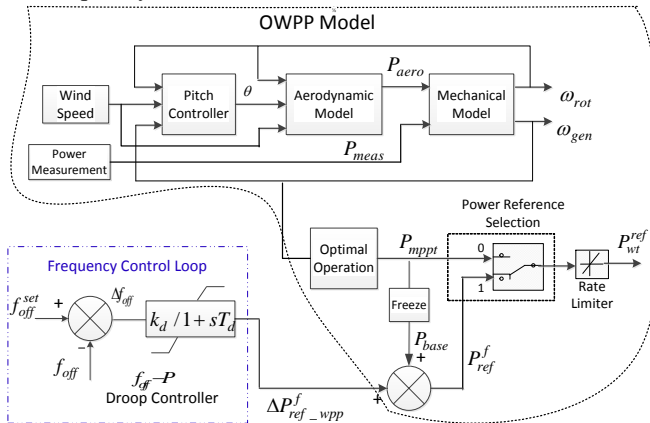
Fig. 4. WT active power reference generation.

The active power reference generation part of the active power controller of the WT is shown in Fig.4. This model generates either optimal power reference (P_{mppt}) or frequency initiated power reference (P_{ref}^f), depending on normal or frequency control operation. P_{ref}^f is a combination of P_{base}, which is equal to the magnitude of P_{mppt} before the frequency event and modulated power reference according to frequency ($\Delta P_{ref\_wpp}^f$) generated by the 'Frequency control loop'. The 'Rate Limiter' is used to limit the rate of change of power reference to the WT.

D. Coordinated Frequency Control Scheme

The brief description of coordinated frequency control scheme is explained in this section [12].

In this method, the onshore AC grid frequency is replicated at the offshore AC grid according to the DC voltage variations. For example, the $f_{on} - P$ droop controller of the 'Frequency Control Loop', shown in Fig.2, changes the active power reference (ΔP_{ref}^f) to the onshore HVDC converter according to the measured frequency deviation at the associated onshore AC grid as given in (1), where f_{on}^{ref} and f_{on}^{meas} are the reference and measured frequency at the onshore AC grid.

$$\Delta P_{ref}^f = k_f (f_{on}^{ref} - f_{on}^{meas}) \qquad (1)$$

The change in active power output of this converter results in deviation of the DC grid voltage from its initial value. Therefore, the other onshore HVDC converters in the MTDC grid inherently modulate its active power reference ($\Delta P_{ref}^{V_{dc}}$) due to $V_{dc} - P$ droop control action, thereby participating in frequency control. However, the OWPP does not detect the frequency event; hence representing the onshore frequency event in the offshore AC network frequency is needed. Therefore, the $V_{dc} - f_{off}$ droop controller at offshore HVDC converter, shown in Fig. 3, modifies the offshore AC grid frequency reference proportional to the DC voltage variation measured at its terminals as given in (2) and (3), where f_{off}^{set} is the offshore frequency during normal conditions and f_{off}^{ref} is the reference offshore frequency considering DC grid voltage variation.

$$f_{off}^{ref} = f_{off}^{set} + \Delta f_{off} \qquad (2)$$

$$\Delta f_{off} = k_v \Delta V_{dc} \qquad (3)$$

This leads to a change offshore AC grid frequency (f_{off}). The active power reference to the WT (P_{WT}^{ref}), hence OWPP, is then modified according to the change in offshore AC grid frequency from its nominal value as shown in (4). The 'Frequency Control Loop' of the WT active power generation, shown in Fig.4, generates the additional power

reference to the WT ($\Delta P_{ref\_wpp}^{f}$), according to the frequency change as shown in Fig. 4

$$P_{WT}^{ref} = P_{base} + \Delta P_{ref\_wpp}^{f}$$

$$\Delta P_{ref\_wpp}^{f} = k_d (f_{off}^{set} - f_{off}) \tag{4}$$

A. WT behavior for Kinetic Energy Support

The impact of kinetic energy release is more critical at below rated and low wind speeds, as overloading the WT at these wind speeds makes it slow down, causing drop in its active power output. In case of above rated wind speeds, the extra energy in the wind is availed by changing the pitch of the blades to bring back the WT rotational speed near to its nominal value, therefore drop in active power output is lesser compared to the case with below rated wind speed. Hence, in this paper, authors have made an attempt to study the impact of WT kinetic energy release at three wind speeds (above rated, just below rated, and low wind speeds), which represents the behavior of WT for whole wind speed range The WT behavior due to kinetic energy support is well explained in [20 and is briefly presented below. The WT power drop and recovery period after the release of overloading (for an overloading duration of 10s with a magnitude of 5% above its optimal power) at different wind speeds is given in Fig. 5 below.
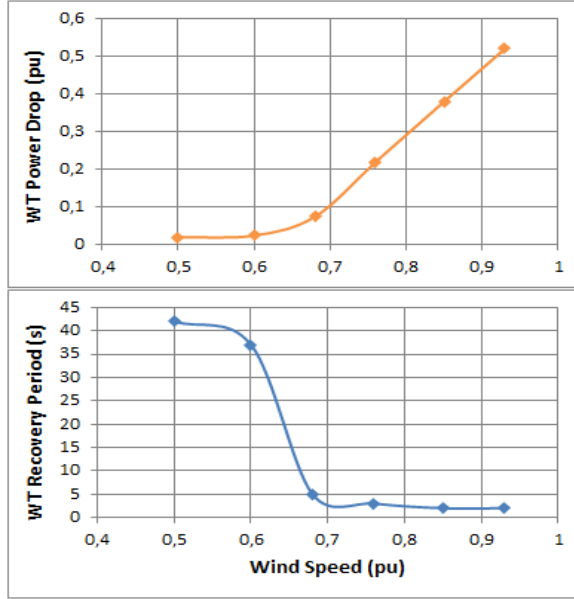
Fig.5. WT power drop and recovery period for a fixed overloading magnitude of 5% and overloading duration of 10 s.

From this figure, it can be observed that the power drop due to overloading is more severe at just below rated wind speeds compared to low wind speed range. However, WT recovers very fast at just below rated wind speeds compared to low wind speeds. Even though the recovery period is low, the higher power drop at just below rated wind speeds severely impacts the DC grid. Because, the DC grid voltage dynamics are faster, the sudden power drop from the WPP must be taken care of other converters in the DC Grid, which again may impact the associated AC grids. For above rated wind speeds,

the power drop and recovery period are minimal, hence the corresponding results are not shown in Fig.5.

III. LABORATORY SCALE MTDC TEST SET UP

The objective of laboratory scaled test set up is to validate the use of DC grid voltage as an equivalent AC grid frequency indicator and also to study the impact of wind speed on the fast primary frequency control. The frequency control test is performed on a three-terminal DC grid laboratory test set up shown in Fig. 6, whose description is given in Table 1. The three-terminal DC grid laboratory scaled test set up is composed of three cabinets, as shown in Fig. 7, and a physical emulation of the DC cables. The DC lines (1-2, 1-3 and 2-3) are modelled using the PI equivalent cable, with the values of resistance (R) and inductance (L) illustrated in Table I. The cable capacitance is included in the VSC capacitance. The DC capacitor value for each VSC, given in Table I, has been chosen to keep the time constant $\tau = W / P$ as in the simulated system [21], where $W = \frac{1}{2}CV_{dc}^{2}$ the energy in the capacitor and P is the nominal power of the converter. The obtained τ for both systems is 22.5 ms. Each cabinet contains a three-phase 12.5 kVA transformer, the VSC, the control board and the measuring boards. The VSCs are two-level converters based on insulated-gate bipolar transistors (IGBTs) with a nominal power of 5.7 kVA. The nominal AC RMS voltage is 230 V phase to phase. The switching frequency of each converter is 20 kHz and it is controlled using a control board based on a digital signal processor (DSP) F28M35 of Texas Instruments (TI). All the converters are physically connected to the same AC grid of the laboratory, which is 230 V phase-to-phase. The behaviour of the OWPP in the AC side of Conv-2 is emulated using a model implemented in LabVIEW in an external controller that receives data from the DC grid and sends the power reference to be injected by Conv-2 in the DC grid. The frequency event in the AC grid of Conv-1 is emulated considering a model of a virtual AC grid implemented in the DSP of the control board of Conv-1.
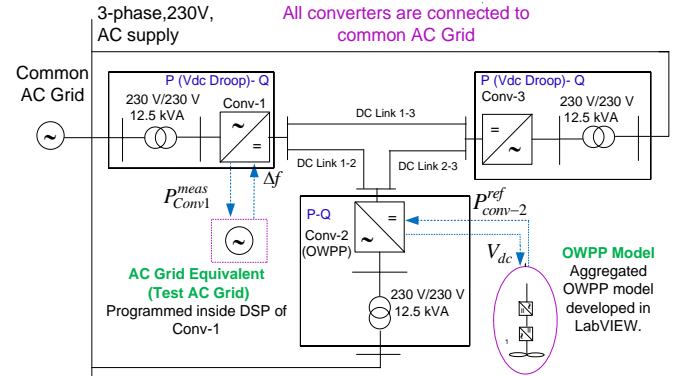

Fig. 6. 3 Terminal test set up to perform frequency control test

A SCADA system is implemented in LabVIEW using the cRIO 9024 controller of National Instruments (NI) to monitor the variables of the MTDC grid and it also includes the emulation of the OWPP of Conv 2. The OWPP emulation in the cRIO 9024 is communicated with Conv 2 via the Digital to Analog Converter (DAC) and the Analog to Digital Converter

(ADC) of its control board and is described in section IV.B. The emulation of the frequency event of AC grid of Conv 1 is implemented by software in the DSP of Conv. 1 and it is described in Section IV.A.
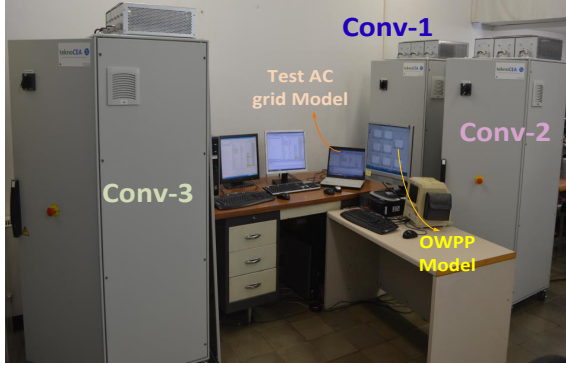

Fig. 7. Picture of the three-terminal experimental test set up

TABLE I : DESCRIPTION OF THE TEST LAYOUT IN FIG. 6

Parameter	Value
Common AC Voltage (L-L)	230 V
DC Voltage (Symmetrical Monopole)	+/- 250 V
Transformer rating (230V/230V)	12.5 kVA
Converter rating	5.7 kVA
DC line 1-2 Resistance, R12	0.22 Ω
DC line 1-2 Inductance, L12	1 mH
DC line 1-3 Resistance, R13	0.1 Ω
DC line 1-3 Inductance, L13	0.5 mH
DC line 2-3 Resistance, R23	0.44 Ω
DC line 2-3 Inductance	1.5 mH
OWPP rating	2.85 kW
VSC capacitance (C)	1020 μF

A. AC Grid Equivalent to create Frequency Event

As it is not possible to change the frequency of the laboratory AC grid, an AC grid equivalent model (test AC grid) based on the swing equation [22], is implemented in the DSP of Conv-1, as shown in Fig. 8.
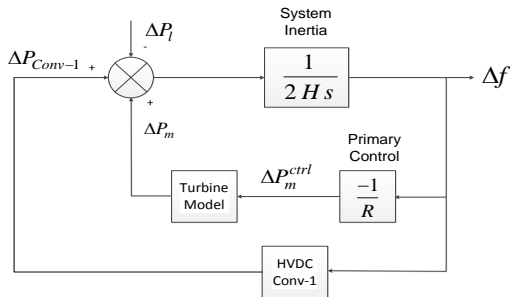
Fig. 8. AC Grid equivalent with dynamic frequency model

The change in frequency (Δf) is zero until the balance is achieved between the change in mechanical power input (ΔP_m) and electrical power output (ΔP_l) of the grid. A frequency event in the test AC grid can be created by perturbing the ΔP_l, which leads to change in Δf. This (Δf) is then sent to the onshore HVDC Conv-1 controller (refer Fig.2

and Fig.6), which changes its active power reference (ΔP_{ref}^f).

The measured variation in active power output of the Conv-1 due to frequency control (ΔP_{Conv-1}) is sent back to the test AC grid model, thereby participating in the frequency control of test AC grid.

B. Implementation of OWPP Model and Control of HVDC Converters

The Conv-1 and Conv-3 operate in active power control with a DC voltage droop, maintaining the power balance in the DC grid, as explained in section II.B. However, the Conv-2 (offshore VSC) connected to OWPP operates in active and reactive power ($P-Q$) control mode, instead of AC voltage and frequency control mode ($V_{ac}-f$) as explained in section II.C. In general, the offshore VSC is responsible for controlling the voltage and frequency of the isolated offshore AC grid. In that case, there must be an energy source representing the OWPP, synchronized to this frequency, independent of utility AC grid. However, in the present scenario, the OWPP is implemented as a simulation model sending power references to the offshore VSC which operates in P-Q control mode and is connected to the utility grid (laboratory AC grid), where it is not possible to control its frequency.

The OWPP model generates power reference to the Conv-2. The main reason for operating Conv-2 in $P-Q$ control is because the OWPP is implemented as a simulation model programmed in LabVIEW instead of the physical implementation as an isolated AC grid and it is not possible to control the frequency and AC voltage of the simulation model. However, the equivalent control delays which involved in '$V_{ac}-f$' control mode are implemented in OWPP model so as to make the coherence between theoretical and experimental set up for frequency control. The updated active power controller of the OWPP is shown in Fig. 9.
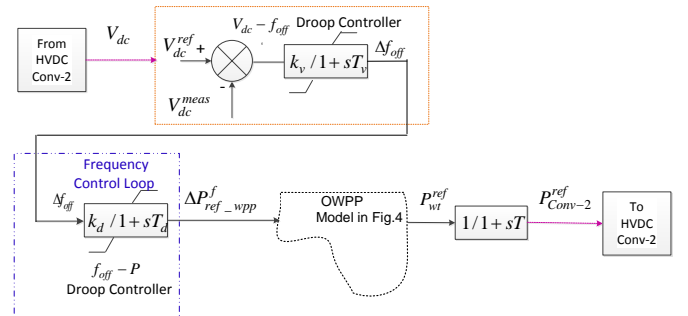

Fig. 9 OWPP model implemented in LabVIEW (only active power controller is shown here)

The HVDC Conv-2 sends the DC voltage measurement, V_{dc} to the OWPP model. The $V_{ac}-f_{off}$ droop controller changes its frequency based on the change in the DC voltage and Frequency Control Loop' generates $\Delta P_{ref\_wpp}^f$ according to the change in frequency. Finally, the OWPP model sends the

active power reference to HVDC Conv-2 (ΔP_{Conv-2}^{ref}), thereby, emulating the combined theoretical behavior of offshore HVDC converter and OWPP control, shown in Fig.3 and Fig.4.

IV. SIMULATION AND EXPERIMENTAL RESULTS

The simulation results and corresponding experimental validation of FPFC from OWPPs and other converters in a three-terminal DC grid are presented for three different wind speeds: (1) above rated wind speed (1.1 pu), (2) just below rated wind speed (0.92 pu) and (3) low wind speed (0.7 pu) in the following sub sections A, B, and C, respectively. An under frequency event is created at test AC grid, in Fig. 8, by increasing its electrical power output $\Delta P_l = 0.15$ pu at time t = 6s. In all three the test cases (A/B/C), kinetic energy of the OWPP is utilized by overloading the WT for 10 seconds after the initiation of frequency event, i.e. the kinetic energy support of the OWPP is released at time t = 16s. The impact of release of the kinetic energy support from the OWPP on the DC and AC grids is studied and possible mitigation methods are discussed. The parameters used in the study are given in Table II. It should be noted that, in normal operation, the OWPP (Conv-2) and Conv-3 send power to DC grid (- sign), whereas, Conv-1 receives from DC grid (+ sign). However, the magnitude of power output from OWPP varies according to wind speed and is given in Table II.

The DC voltage droop ($V_{dc} - P$) parameters of the test system in Fig. 6 are designed according to the methods given in [28] and the frequency droop ($f_{on} - P$) controllers are designed considering up to 2 % change in DC voltage due to frequency change.

TABLE II : PARAMETERS OF 3-TERMINAL DC GRID FOR FREQUENCY CONTROL

Parameter	Value
Conv Base kVA	5700 kVA
OWPP base kVA	2800 kVA
Base DC grid voltage	500 V
Base frequency	50 Hz
Power flow, Conv-1(A/B/C)	0.7/0.7/0.7 pu
Power flow, Conv-2(A/B/C)	-0.5/-0.42/-0.16 pu
Power flow, Conv-3(A/B/C)	-0.2/-0.28/-0.54 pu
$V_{dc} - P$ droop gain (k_p) - Conv-1 /Conv-3	5/2.2 pu
$f_{on} - P$ droop gain(Conv-1)	10 pu
$V_{dc} - f_{off}$ droop gain(Conv-3)	1 pu
$f_{off} - P$ gain (OWPP)	15 pu

A. *Frequency Control at above rated wind speed (Vw_1.1 pu)*

The simulation results and their experimental validations are discussed in this section. The results are analyzed for two time periods, (1) during the frequency control period (t = 6 to 16 s) and for the (2) post frequency control period (> t =16s). The simulation results for the frequency of test AC grid and OWPP, DC voltage and active power output of the three

converters with and without the coordinated frequency control are given in Fig. 10. The corresponding experimental test results are given in Fig. 11.
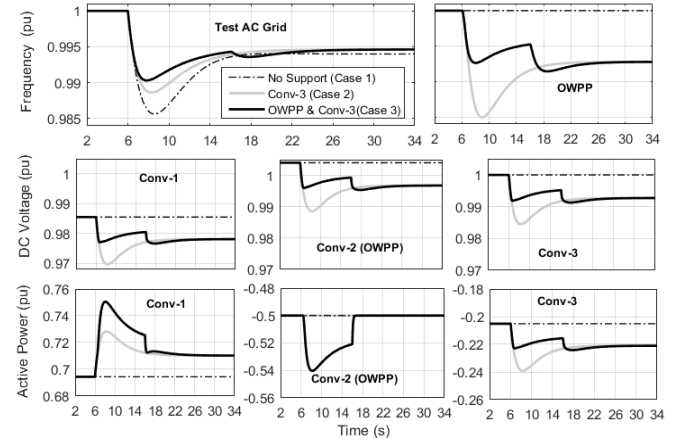

Fig. 10. Coordinated frequency control-Vw_1.1 pu - Simulation results
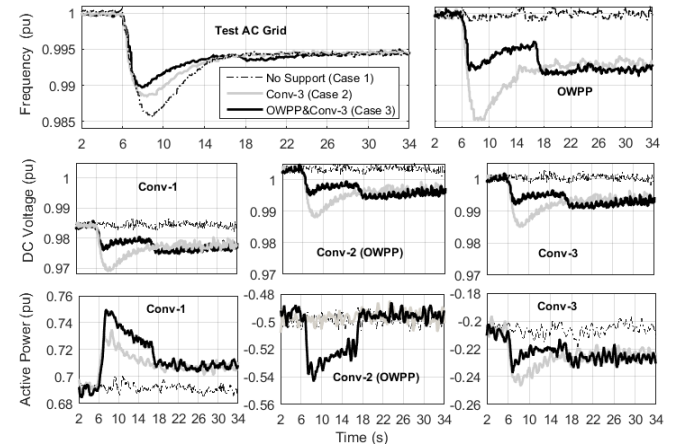

Fig. 11 Coordinated frequency control- Vw_1.1 pu - Experimental validation of simulation results given in Fig. 10.

A small dip in DC voltage of the DC grid and frequency of the test AC grid can be observed during the post frequency control period. These are consequences of releasing of kinetic energy support from the OWPP which can be well understood from the experimental results of active power output, speed, and aerodynamic power of WT shown in Fig.12. Note that the values are given in pu based on OWPP base kVA (2850 kVA). During the frequency control period, active power output of WT (P_{out}) is increased (approximately to 1.1 pu) above its optimal power output value ($P_{mppt} = 1$ pu). This results in a slight reduction in the WT speed (both rotor and generator speed). Once the reduction in WT speed is detected, the aerodynamic power of the WT is increased by changing the pitch angle. As the WT is operating at above rated wind speed, the additional power from the wind is availed to bring back the WT speed and the optimal power output to their initial values quickly. At the end of the frequency control period, the active power reference to WT is brought back to its optimal value, which results in minor drop in the WT power output. Hence, at above rated wind speed, there is a minimum impact of release of kinetic energy of the WT on DC grid voltage and frequency
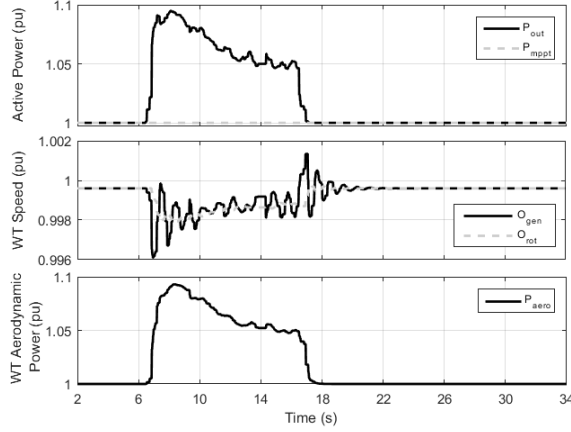
186

of the test AC grid.

Fig.12. WT Dynamics for Frequency control at Vw_1.1pu (Experiment)

B. Frequency Control at just below rated wind speed (Vw_0.93)

The behavior of the WT for overloading at just below rated speed is interesting because of its dynamics. The simulation and experimental results of frequency control (frequency, DC voltage, and active power) are given in Fig.13 and 14, respectively, and the parameters of the system for the test are given in Table II.
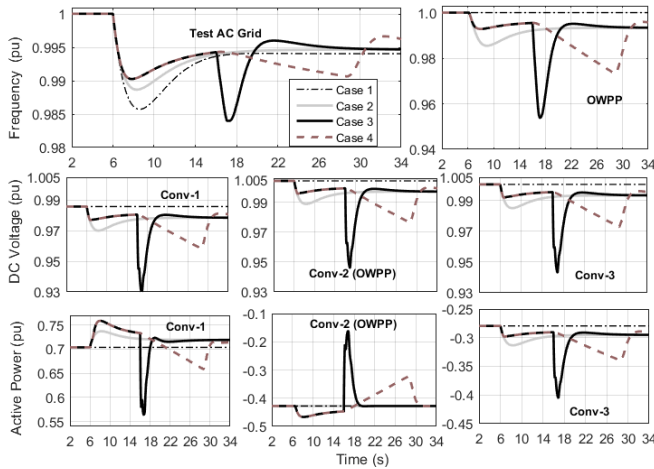

Fig. 13 Coordinated frequency control-Vw_0.92 pu - Simulation results 1). No Support, 2). Support from Conv-3 3). Support from OWPP and Conv-3 4). Support from OWPP and Conv-3 with rate limiter at WT

During the frequency control period, the results are similar to that of above rated wind speeds. The frequency of the test AC grid is improved with the participation of OWPP and Conv-3 (Case 3) compared to other two cases (Case 1 and 2). However, at end of frequency control period, there is a considerable dip in the DC voltage of the DC grid and frequency of the test AC grid, in case 3 compared to a and b. However, the magnitude secondary dips are lesser for Case 4 (overloading is released with a rate limiter) compared to Case 3, which is explained a bit later in this section. The reason for these secondary dips is due to the sudden drop in active power output after the release of kinetic energy support from the OWPP. This is understood by the simulation and experimental results of WT dynamics given in Fig. 15 and 16,

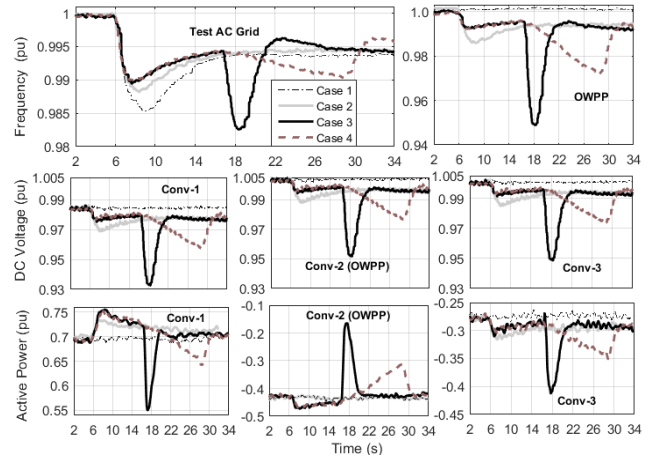respectively and note that these values are given in pu based on OWPP base kVA (2850 kVA).

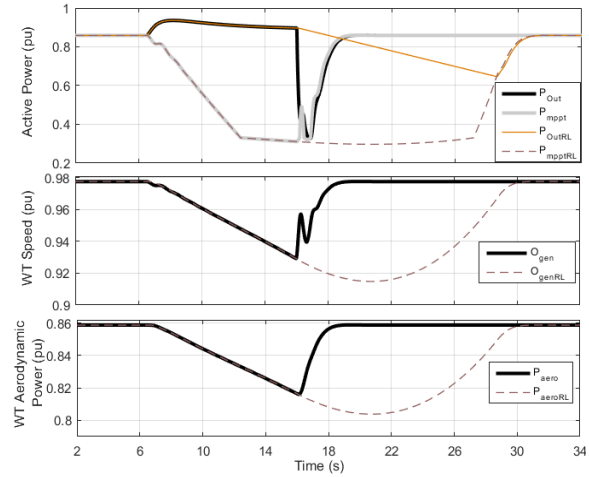Fig. 14 Coordinated frequency control- Vw_0.92 pu - Experimental validation of simulation results given in Fig. 13

Fig.15. WT Dynamics for Frequency control at Vw_0.92 pu-Simulation results

During the frequency control period, the WT power output (P_{out}) is increased above its optimal value (P_{mppt}). Hence, the WT speed (O_{gen}) starts to decrease with the progress of overloading, causing a reduction in the aerodynamic power (P_{aero}), which further reduces the P_{mppt}. The P_{aero} cannot be increased, as done in case of above rated wind speeds, because the pitch is already at its optimal position. This process is continued until the end of frequency control period which results in a considerable reduction of P_{mppt}. For prolonged frequency control period, there is a risk that WT stops producing power at some point. At the end of frequency control period, P_{out} is set back to P_{mppt}, hence results in sudden reduction of active power output of WT (0.9 pu to 0.3 pu). After that, WT starts recovering and reaches its pre-overloading operating point quickly (approximately in 2.5 s). However, the sudden drop in WT, hence OWPP power output burdens the Conv-3 because it increases its power output to maintain the balance in the DC grid.
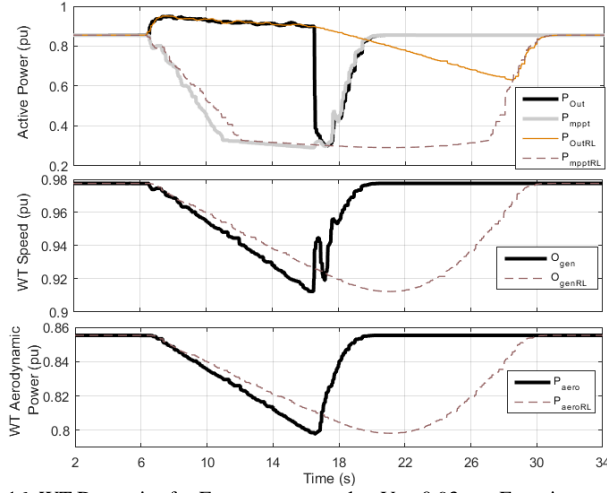
187

Fig.16. WT Dynamics for Frequency control at Vw_0.93 pu- Experimental validation of simulation results given in Fig.15

This sudden power drop from OWPP has to be avoided to avoid secondary effects on DC grid voltage and frequency of the test AC grids. One possible way is to smoothly releasing the overloading of the OWPP using a rate limiter (RL), shown in Fig.4. At the end of frequency control period, the overloading of the OWPP is released at a rate of 0.025 pu/s instead of using instantaneous release and the corresponding results are given as Case 4 in Fig. 13 and 14. It can be observed from Fig. 13 and 14 that the magnitude and rate of secondary dip in frequency an DC voltage are lesser with the rate limiter option (Case 4) compared to the case without rate limiter (Case 3). The corresponding WT dynamics are also smoother, as shown in Fig 15 and 16 with subscripts 'RL', for example, WT power output with rate limiter (P_{outRL}), optimal power output with rate limiter (P_{mpptRL}), and WT speed with rate limiter (O_{genRL}).

C. Frequency Control at lower wind speeds (Vw_0.7pu)

At 0.7 pu wind speed, the Conv-3 takes the major share (-0.54 pu) of power transfer to Conv 1 (0.7 pu) compared to Conv-2 (0.16 p u), as given in Table II. Hence, the share of OWPP participation in frequency control is also less. The simulation and experimental results of frequency control at wind speed of 0.7 pu are given in Fig.17 and 18 respectively. Similar to the previous results, the OWPP participation improves frequency during the frequency control period, and leads to secondary dip in DC grid voltage frequency of the test AC grid after the release of kinetic energy support at the end of frequency control period. The reason for this behavior is due to the reduction in WT optimal power output due to overloading as illustrated in Fig 19 and 20, similar to the behavior at just below rated wind speed depicted in section IV. B. However, the magnitude of secondary effects is lesser compare to just below rated wind speed. Also, at lower wind speeds, the recovery time of WT is much higher (around 30s) than that of just below rated wind speeds (2.5 s). Therefore, sufficient time has to be ensured before making the OWPP ready for another frequency event. The impact of rate limiter at lower wind speed is negligible because the drop in WT power output at the end of frequency control period is also less (0.015 pu, refer Fig. 19 and 20) compared to the just below rated wind speed (0.6 pu, refer Fig 15 and 16). Hence, results with rate limiter are not discussed here.
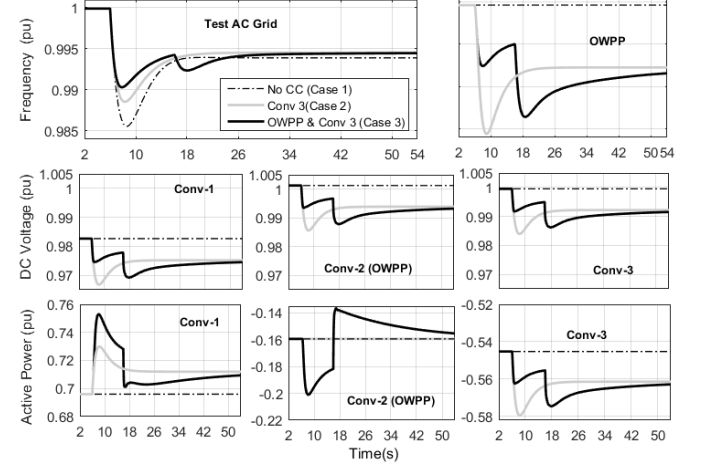

Fig. 17 Coordinated frequency control-Vw_0.7pu - Simulation results
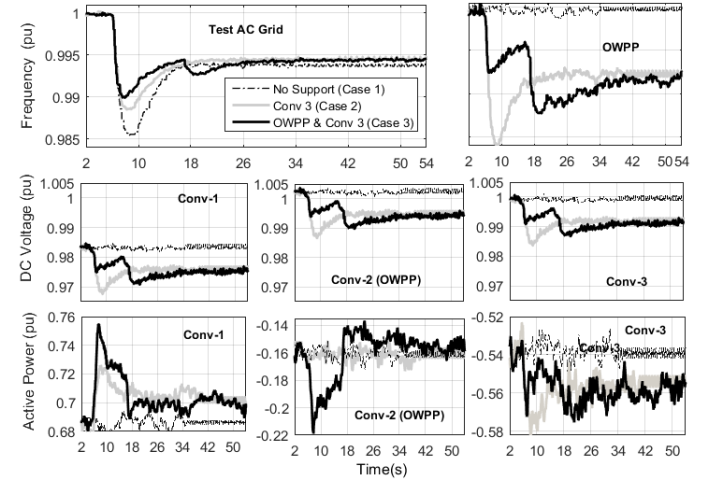

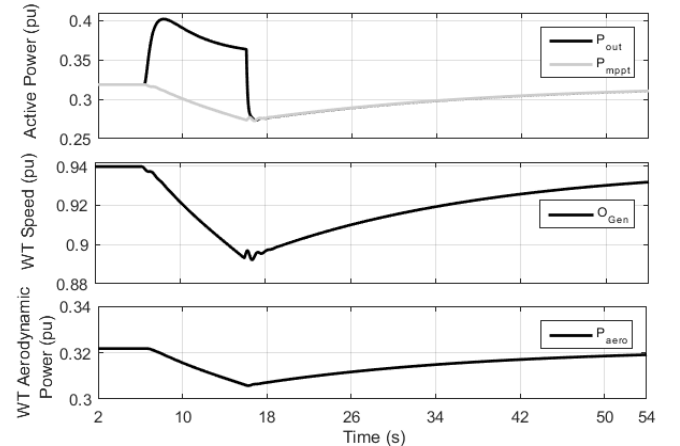Fig. 18 Coordinated frequency control- Vw_0.7 pu - Experimental validation of simulation results given in Fig.17

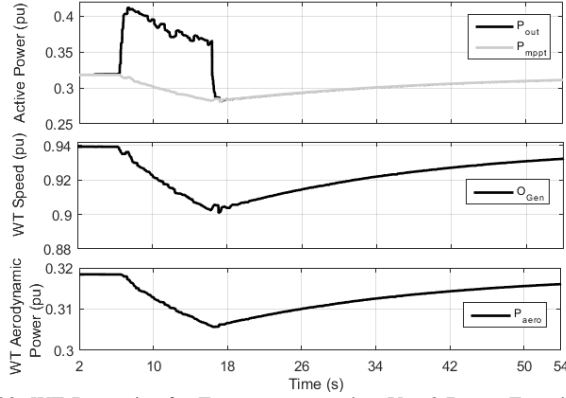Fig. 19. WT Dynamics for Frequency control at Vw_0.7 pu -Simulation results

188

Fig. 20. WT Dynamics for Frequency control at Vw_0.7 pu - Experimental validation of simulation results given in Fig.19.

D. Aggregated impact of WTs operating at different wind speeds

To study the impact of different WTs operating at different wind speeds on the frequency control, the OWPP is modelled with four WTs (WTA, WTB, WTC, and WTD) as shown in Fig. 21 below. These WTs have equal power rating (1/4ᵗʰ of the OWPP given in Table I) and are operating at different constant wind speeds, 1.1 pu, 0.93 pu, 0.8 pu, and 0.65 pu respectively. The frequency control study is performed and the corresponding active power outputs of each WT and the total WPP are shown in Fig. 22 during and after the frequency control period. It can be observed that the overall impact at WPP level is the average impact of these four WTs. The corresponding simulation results for the frequency of test AC grid and OWPP, DC voltage and active power output of the three converters l are given in Fig. 23. The frequency of the test AC grid is improved with the participation of WPP in frequency control and also there is a secondary dip in DC grid voltage and test AC grid frequency after the frequency control period, similar to the results of aggregated WPP model operating at different wind speeds presented in sections IV A, B, C".
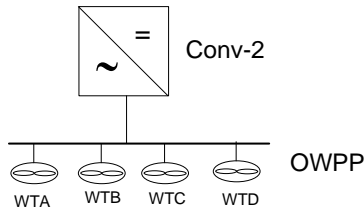

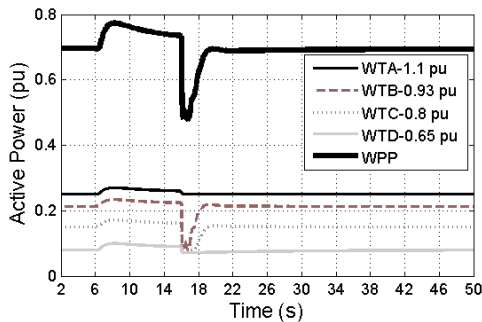Fig. 21. OWPP model with four WTs operating at different wind speeds

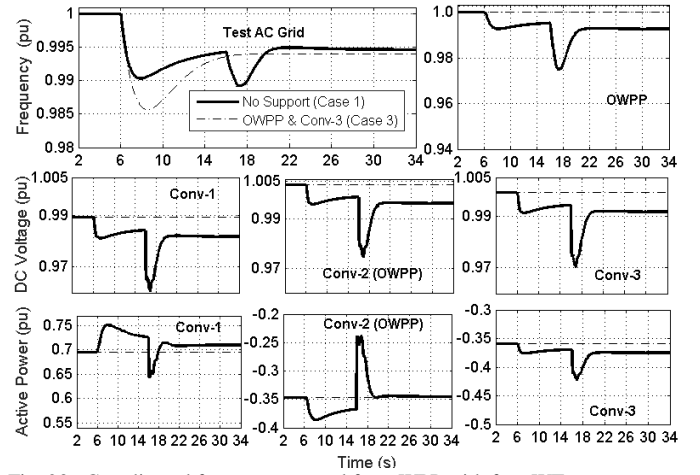Fig: 22 Active Power outputs of WTs and OWPP

Fig. 23. Coordinated frequency control from WPP with four WTs - Simulation results

E. Limitations of this study

The simulations and tests in this paper have been performed on an aggregated WPP model instead of a detailed WPP model with collector grid and WTs. This limits studying the impact of FPFC on the WTs within the WPP operating at different wind speeds. The main study in this paper has concentrated on the impact of WPP behavior for FPFC on AC and DC grids. However, it is proven by few studies that aggregation of WPP can be used for active, reactive power control, FRT control, instead of detailed WPP model, without losing much accuracy in results [23]-[26]. In case of studies related to the oscillation modes inside the HVDC connected WPPs; detailed modeling of WPPs may be necessary and is considered as potential future work. However, the oscillatory modes can be avoided by a proper design and they are irrelevant for the frequency control studies discussed in this paper.

The frequency control study in this paper has been performed on a WPP simulation model integrated to three-terminal DC grid laboratory test set up instead of testing on a real/actual WPP. However, the simulation models used in this study are verified IEC models, where few models have been validated with field tests [27]. The frequency control tests on actual WTs/WPP integrated to MTDC grid can be considered as potential future work, where the impact of FPFC and kinetic energy support on the mechanical parts of the WT can also be studied.

The other limitation of the implemented test setup is that all the converters in the DC grid are connected to common utility AC grid. As it is not possible to change the utility frequency, the impact of participation of a converter in the frequency control on its associated AC grid frequency is not visible. However, in actual practice, AC grid-1 and Ac gri-3 are two separate AC grids. Participation of frequency control of one AC grid (AC grid-1) will affect the other grid frequency, which depends on the magnitude of participation and characteristics (inertia and power reserves) of that AC grid. The magnitude of participation of a particular AC grid in the frequency control of other AC grid could be set by the system operators of the AC grids, and the DC grid operator.

V. CONCLUSIONS

In this paper, a coordinated frequency control scheme for fast primary frequency control from offshore wind power plants and HVDC converters in the MTDC grid has been presented, considering the operation of the wind power plant at different wind speeds. Kinetic energy of the wind turbines has been utilized to avail the extra energy for few seconds after the frequency event. The proposed frequency control method is tested on an OWPP connected through a three-terminal DC grid with time domain simulations using DIgSILENT PowerFactory. The simulation results are validated experimentally by performing the test on a laboratory scale DC grid test set up, at different wind speeds. The simulation and experimental results prove that the OWPPs and the other converters in a MTDC grid can participate in frequency control without depending on communication channels between the converters in the DC grid and the DC voltage can be used to transmit the frequency of the affected AC grid between the other AC grids. However, wind speeds play a major role on frequency control. In case of above rated wind speeds, the additional aerodynamic power can be utilized by changing the pitch angle to get the additional energy during the frequency control period. In this case, WT dynamics are smoother and secondary DC voltage and frequency dips due to the release of kinetic energy support from OWPP are reasonable. However, at just below rated wind speed, overloading the wind turbine results in a faster reduction in WT output power, causing significant secondary dips in frequency and DC voltage at the end of frequency control period. Limiting the rate of power release can smoothen the WT dynamics to some extent and minimizes the secondary effects. At lower wind speed, secondary DC voltage and frequency dips are minimal due to less share in the active power output from OWPP compared to the other converters in the DC grid. However, the recovery time after releasing the overloading is longer, thus sufficient time has to be ensured to make the OWPP ready for another frequency event.

VI. REFERENCES

[11] Windspeed 2015. [Online]. Available: http://www.windspeed.eu. [Accessed: 10- Sep- 2016].

[12] D. Van Hertem, M. Ghandhari , "Multi-terminal VSC HVDC for the European Supergrid: Obstacles," *Renewable and Sustainable Energy Reviews*, vol 14, pp 3156–3163, Dec 2010

[13] D. Van Hertem, O. Gomis-Bellmunt and J. Liang, HVDC Grids: For Offshore and Supergrid of the Future, IEEE Press Series on Power Engineering, Ed. John Wiley & Sons, 2016.

[14] ENTSO- E, Draft- The Network Code on High Voltage Direct Current Connections (NC HVDC), Apr 2014.

[15] Requirements for Offshore Grid Connections in the Grid of TenneT TSO GmbH, TenneT TSO GmbH, Bayreuth Germany, December 2012.

[16] National grid, System Operability Framework (SOF) report, 2014.

[17] L. Zeni, I. Margaris, A. Hansen, P. Sørensen and P. Kjær, "Generic Models of Wind Turbine Generators for Advanced Applications in a VSC-based Offshore HVDC Network," *in Proc. 2012 10th IET Conference on AC/DC Transmission*, Birmingham.

[18] Y. Phulpin,"Communication-free inertia and frequency control for wind generators connected by an HVDC link," IEEE Trans on Power Systems, vol. 27, pp. 1136-1137, May 2012.

[19] Y. Pipelzadeh, B. Chaudhuri, T. C. Green, "Inertial response from remote offshore wind farms connected through VSC-HVDC links: A Communication-less scheme", *2012 IEEE Power and Energy Society General Meeting*, pp. 1-6, July 2012.

[20] B. Silva, C. L. Moreira, et al., "Provision of Inertial and Primary Frequency Control Services Using Offshore Multiterminal HVDC Network", *IEEE Trans. on Sustainable Energy*, vol. 3, pp. 800-808, Oct 2012.

[21] A. Junyent-Ferre, Y. Pipelzadeh and T. C. Green, "Blending HVDC-link energy storage and offshore wind turbine inertia for fast frequency response", IEEE Trans. Sustain. *Energy*, vol. 6, no. 3, pp. 1059-1066, Jul. 2015.

[22] J.N. Sakamuri, M. Altin, A. D. Hansen, N.A.Cutululis,, " Coordinated Frequency Control from Offshore Wind Power Plants Connected to MTDC System Considering Wind Speed Variation ," *IET Rene. Power Generation*, to be published.

[23] DIgSILENT GmbH, Technical Reference - PWM Converter.,2015.

[24] J. Beerten and R. Belmans, "Analysis of Power Sharing and Voltage Deviations in Droop-Controlled DC Grids," IEEE Transactions on Power Systems, vol. 28, no. 4, pp. 4588-4597, 2013.

[25] A.Yazdani, R. Iravani, " Voltage-sourced converters in power systems: Modeling, Control, and Applications" (JohnWiley & Sons, 2010), ISBN: 978-0-470-52156-4

[26] M. Delghavi and A.Yazdani, "A control strategy for islanded operation of a distributed resource (DR) unit," In Proc. 2009 IEEE Power and Energy Society General Meeting, Alberta, Canada, pp: 1-8.

[27] E. Muljadi et al. "Method of equivalencing for a large wind power plant with multiple turbine representation," Proc. 2008 IEEE Power and Energy Society General Meeting, pp-1-8.

[28] Electrical simulation models for wind power generation Wind turbine, IEC 61400-27-1, 2015.

[29] A. D. Hansen, I. Margaris, G. C. Tarnowski and F. Iov,"Simplified type 4 wind turbine modeling for future ancillary services," in *Proc. 2013 European Wind Energy Conference*, pp. 768-774.

[30] A.D.Hansen, M .Altin, I. D.Margaris, et al," Analysis of the short-term overproduction capability of variable speed wind turbines", Renewable Energy, vol.68, pp.326–336.

[31] A. Egea-Alvarez, F. Bianchi, A. Junyent-Ferré, G. Gross and O. Gomis-Bellmunt, "Voltage Control of Multiterminal VSC-HVDC Transmission Systems for Offshore Wind Power Plants: Design and Implementation in a Scaled Platform," IEEE Trans. Ind. Electron., vol 60, no. 6, pp. 2381-2391, Jun. 2013.

[32] G. Anderson, Dynamics and Control of Electric Power Systems, Lecture Notes. Zurich: Feb 2012.

[33] M. Altin O. Goksu A. Hansen P. Sorensen "Aggregated wind power plant models consisting of IEC wind turbine models" *in Proc. IEEE PowerTe*ch, pp. 1-5, Jun. 2015

[34] A.D. Hansen, M. Altin, and N.A. Cutululis, "Modelling of wind power plant controller, wind speed time series, aggregation and sample results", DTU Wind Energy. E, no. 0080, 38p, 2015,

[35] A. D. Hansen, , N. A. Cutululis, and M. Altin, "Methods for Representations of Wind Power Plants for Active Power Studies, " *12th International Workshop on Large-Scale Integration of Wind Power into Power Systems as well as on Transmission Networks for Offshore Wind Power*, 2013

[36] P.E. Sørensen, P. E., P. Pinson, N.A. Cutululis, et al, " Power fluctuations from large wind farms - Final report", DTU Wind Energy, R; No. 1711(EN)).

[37] O.Goksu, M .Altin, J.Fortmann, P.Sorensen, " Field validation of IEC 61400-27-1 wind generation Type 3 model with plant power factor controller", IEEE Trans. Energy Convers. Pp. 1170-1178, March 2016.

[38] Pierre, R.: 'Dynamic modeling and control of multi-terminal HVDC grids'. PhD thesis, University of Lille Nord de France, 2014